REGULATION OF *C. ELEGANS* EPIDERMAL GROWTH FACTOR RECEPTOR SIGNALING AND TRAFFICKING BY RABS, ARFS AND MOTORS

By

Olga Skorobogata

Faculty of Medicine,

Department of Anatomy and Cell Biology,

McGill University, Montreal, Quebec, Canada

December 2015

A thesis submitted to McGill University in partial fulfilment of the requirements for the degree of Doctor of Philosophy

TABLE OF CONTENTS

ABSTRACT

A highly conserved Epidermal Growth Factor Receptor (EGFR) signaling pathway specifies vulval cell fate induction during *C. elegans* development. LET-23 EGFR has to be present on the basolateral membrane of the polarized vulval precursor cells (VPCs) in order to engage and transmit EGF signal. In mammals, EGFR also localizes to basolateral membranes of epithelial cells. Excessive activation of the EGFR signaling pathway has been implicated in cancer and a majority of cancers originate from epithelial cells. Thus, *C. elegans* VPCs provide a unique *in vivo* model to study EGFR signaling and localization in polarized epithelium.

We conducted a genetic screen for essential regulators of EGFR signalling and identified mutations in the *agef-1* and *dhc-1,* which code for an Arf GTPase guanine nucleotide exchange factor and the heavy chain of the dynein minus-end microtubule motor protein, respectively.

A partial loss-of-function mutation in *agef-1* enhances EGFR signaling in sensitized backgrounds as well as leads to secretory defects in multiple tissues. Additionally, *agef-1* mutant animals have enlarged late endosomes/lysosomes in the coelomocytes. These phenotypes suggest that both secretory and endocytic trafficking pathways are affected in *agef-1* mutants. We found that AGEF-1 functions with two Arf GTPases and the AP-1 clathrin adaptor complex to negatively regulate EGFR signaling by antagonizing the basolateral localization of the receptor. Taken together with the recently described role of the AP-1 adaptor in the maintenance of epithelial polarity, AGEF-1 might regulate LET-23 EGFR signaling via multiple mechanisms: directly by antagonizing basolateral localization of the receptor and indirectly by maintaining epithelial polarity in the VPCs. A human homolog of AGEF-1 is mutated in numerous cancer cell lines supporting a tumor suppressive function in humans. Our recent data indicate that a small GTPase RAB-10 is required for multiple *agef-1* phenotypes, including negatively regulating LET-23 EGFR signaling in the vulva and affecting the size of late endosomes. This effect is specific to RAB-10 and suggests that AGEF-1 and RAB-10 might function closely in an antagonistic manner.

dhc-1(vh22) animals are small and temperature sensitive, with increased embryonic lethality due cell division defects at a restrictive temperature of 20°C. Loss of *dhc-1* results in increased LET-23 EGFR signaling in sensitized backgrounds suggesting that DHC-1 is a negative regulator of EGFR signaling. LET-23::GFP accumulates in plasma membrane proximal foci of the VPCs in *dhc-1* mutants suggesting that dynein functions at an early step of EGFR endosomal trafficking. Moreover, a late endosomal GTPase RAB-7 also antagonises LET-23 EGFR signaling

and its loss leads to LET-23::GFP accumulation in cytoplasmic foci. Given the ability of mammalian Rab7 to engage dynein to promote late endosome trafficking towards the lysosome, it is possible that RAB-7 and DHC-1 might function together at a later step of EGFR trafficking for degradation. Our recent findings identify ZEN-4 KIF23, a kinesin plus-end directed microtubule motor, as a suppressor of *dhc-1(vh22)* and a positive regulator of LET-23 EGFR signaling in the vulva. Our data indicate that ZEN-4 kinesin is likely to regulate EGFR signaling by its role in epithelial polarity rather than by movement of EGFR-containing vesicles along the microtubule track opposite dynein.

Understanding how these genes regulate EGFR signaling and trafficking in *C. elegans* will inform our understanding of EGFR signaling in human epithelial cells with a potential of uncovering novel tumor suppressors that could serve as therapeutic targets for the treatment of malignancies.

RESUMÉ

Chez *C. elegans* une voie de signalisation EGFR/Ras/MAPK, qui est très conservée, est responsable pour la spécification du destin des cellules de la vulve. LET-23 EGFR doit être présent sur la membrane basolatérale des cellules précurseurs vulvaires (CPVs) afin d'engager et de transmettre le signal EGF. Chez les mammifères, l'EGFR localise également à membranes basolatérale des cellules épithéliales. Activation excessive de la voie de signalisation de l'EGFR a été impliquée dans le cancer et une majorité des cancers proviennent des cellules épithéliales. Ainsi, CPVs de *C. elegans* offrent un modèle unique *in vivo* pour étudier la signalisation et la localisation de l'EGFR dans l'épithélium polarisé.

Nous avons mené une étude génétique pour trouver des régulateurs essentiels de la signalisation d'EGFR et nous avons identifié des mutations dans *agef-1* et *dhc-1*, qui code pour un facteur d'échange de nucléotide guanine (GEF) des protéines G Arf et une chaîne lourde de complexe motrice dynéine qui se dirige vers l'extrémité négative des microtubules, respectivement.

Une mutation dans *agef-1* représente une perte partielle de fonction qui cause l'amélioration de la signalisation d'EGFR ainsi que des défauts de sécrétion dans plusieurs tissus. En outre, *agef-1* a d'énormes endosomes tardifs/lysosomes dans les coelomocytes. Ces phénotypes suggèrent que la sécrétion et le trafic vésiculaire sont affectés dans le mutant. Nous avons constaté qu'AGEF-1 fonctionne avec deux protéines G Arf et le complexe AP-1, un adaptateur de clathrine, pour réguler négativement la signalisation d'EGFR. Cet effet est atteint par l'opposition de la localisation basolatérale du récepteur. Le rôle de l'adaptateur AP-1 dans le maintien de la polarité épithéliale a été récemment décrit, donc AGEF-1 peut réguler la signalisation LET-23 EGFR en utilisant de mécanismes multiples: directement en antagonisant la localisation basolatérale du récepteur et indirectement par le maintien de la polarité épithéliale dans les CPVs. Un homologue humain d'AGEF-1 est muté dans de nombreuses lignées de cellules cancéreuses ce qui est favorable à sa fonction comme le suppresseur de tumeur chez les mammifères. Nos données récentes indiquent qu'une protéine G RAB-10 est nécessaire pour plusieurs phénotypes chez *agef-1*, y compris la régulation négative de la signalisation de LET-23 EGFR dans la vulve et régulation de la taille des endosomes tardifs. Ces effets sont spécifiques à RAB-10 ce qui suggère qu'AGEF-1 et RAB-10 sont intimement reliés en fonctionnant de façon antagoniste.

Les animaux *dhc-1(vh22)* sont petits et sensibles à la température, c'est-à-dire que la létalité embryonnaire augmente à une température restrictive de 20°C en raison de défauts de la division cellulaire. Perte de DHC-1 cause l'augmentation de la signalisation de LET-23 EGFR suggérant que DHC-1 est un régulateur négatif de la signalisation d'EGFR. LET-23::GFP accumule dans les structures proches de la membrane plasmique de CPVs en animaux *dhc-1*, ce qui suggère que dynéine fonction à une étape précoce du trafic vésiculaire de l'EGFR. En outre, une protéine G RAB-7 antagonise également la signalisation de LET-23 EGFR et sa perte mène à l'accumulation de LET-23::GFP dans les structures cytoplasmique. Vu que Rab7 mammifère est capable à engager dynein pour promouvoir le trafic des endosomes vers le lysosome, il est possible que RAB-7 et DHC-1 puissent fonctionner ensemble à une étape précédente la dégradation d'EGFR. Nos récents résultats indiquent que ZEN-4 KIF23, une protéine motrice kinésine qui se déplace en direction de pôle positif des microtubules, est un suppresseur de *dhc-1(vh22)* et un régulateur positif de la signalisation de LET-23 EGFR dans la vulve. Nos données indiquent que ZEN-4 kinésine peut réguler la signalisation d'EGFR grâce à son rôle dans la polarité épithéliale plutôt qu'à cause de son implication dans le mouvement de vésicules contenant EGFR le long de microtubules en face de dynein.

Mieux comprendre comment ces gènes régulent la signalisation et le trafic de LET-23 EGFR chez *C. elegans* informera notre compréhension de la signalisation d'EGFR dans les cellules épithéliales humaines. Ce qui a un potentiel de découvrir de nouveaux gènes suppresseurs de tumeur qui pourraient servir de cibles thérapeutiques pour le traitement des malignités.

ACKNOWLEDGEMENTS

I would like to thank my supervisor, Dr. Christian Rocheleau, for taking me aboard as an undergraduate summer student to perform a genetic screen, which gave me enough starting material and ground for research to include into both Master's and Doctoral theses. Thank you for your continuous guidance and support during these past seven years, and for always being available to help with valuable discussions and advice. I am grateful for the positive learning environment that you provided me with and that allowed me to grow as a scientist.

Many thanks to my lab mates, current and past, for keeping a friendly and warm atmosphere in the lab that made it a pleasure to come to the bench each morning and to carry on with my research. Thank you to Kim, Icten, Fiona, Preston, Mideum, Jassy and Jung Hwa for finding ways to have some fun and keep up the spirits when the research was not going that well. A special thank you to our research assistant, Jung Hwa Seo, for always supporting me and making sure time and again that new and terrifying techniques were not that tough in the end.

I would also like to thank all the members of the PPL laboratory for always sharing their equipment and reagents, and for being great neighbours. PPL journal clubs have been invaluable in developing my expertise for critical analysis of the literature. Thank you to Dr. Stéphane Laporte, Dr. Louise Larose, Dr. Barry Posner, Dr. Simon Wing and Dr. Christian Rocheleau for great discussions during PPL journal clubs. Thank you to Dr. Stéphane Laporte for allowing me to use his confocal microscopes, to Dr. Eugénie Goupil and Dr. Min Fu for taking their time to train me and always being there to help with imaging.

I would like to thank the Montreal *C. elegans* community for being a great and supportive audience during our monthly meetings, and for always being eager to share their expertise. Thank

you to Dr. Richard Roy and Shaolin Li for sharing their RNAi library and being accommodative during my numerous trips to the Stuart Biology building.

Finally, I would like thank my family for continuous and strong support during my graduate studies. I am eternally grateful to my husband Maksim, who has been encouraging me every step of the way and guiding me towards becoming a scientist since the very beginning. Thank you for pushing me out of my comfort zone and opening the doors to interdisciplinary research for me. Many thanks to my parents-in-law, Oleksandr and Tetyana, who have been supportive throughout graduate school. Your support helped me to become the person that I am today. Last, but not least, thank you to my children, Alexander and Anastasia, you bring sunshine and happiness to my life every single day.

CONTRIBUTIONS OF AUTHORS

This thesis is written in a manuscript-based form in accordance with the Graduate and Postdoctoral Studies of McGill University thesis guidelines for thesis preparation. It consists of an introduction presenting a comprehensive review of literature, two manuscripts, which are listed below with the contributions of authors, followed by a chapter presenting unpublished follow-up data related to the two manuscripts. Finally, the discussion including the contribution of the presented research to our greater scientific understanding and a reference list conclude the thesis.

Skorobogata O, Escobar-Restrepo JM, Rocheleau CE (2014) An AGEF-1/Arf GTPase/AP-1 Ensemble Antagonizes LET-23 EGFR Basolateral Localization and Signaling during *C. elegans* Vulva Induction. PLoS Genet 10(10): e1004728. doi:10.1371/journal.pgen.1004728

In this study, I have designed and performed all the experiments included in the manuscript, analyzed the data and wrote the manuscript. Escobar-Restrepo JM shared *zhIs038* and *zhIs035* strains expressing LET-23::GFP that I have used to study the role of AGEF-1 and AP-1 on the LET-23 EGFR localization in the VPCs. Rocheleau CE designed the study, analyzed the data and wrote the manuscript.

Skorobogata O*, Meng J* and Rocheleau CE. Dynein-mediated trafficking negatively regulates LET-23 EGFR signaling. * These authors contributed equally. **Under review – Molecular Biology of the Cell**.

In this study my contribution was seventy percent. I have identified and cloned the *dhc-1(vh22)* mutant, performed RNAi experiments to confirm the identity of the mutation, as well as conducted genetic epistasis experiments and live animal imaging to determine the effect of various mutant

background mutations on LET-23 EGFR localization in the VPCs. I have also designed the experiments, analyzed the data and wrote the manuscript. Meng J was an undergraduate student/casual employee in the Rocheleau lab working under my co-supervision. Meng J performed complementation tests using two known alleles of *dhc-1*, *or195* and *or352*, and rescue with DHC-1::GFP transgene, performed VPC-specific RNAi experiments and scored double-mutants between *lin-2(e1309)* and different alleles of *dhc-1*. Rocheleau CE designed the study, analyzed the data and wrote the manuscript.

LIST OF FIGURES

NOMENCLATURE

In this thesis *C. elegans* genes and proteins have been designated using accepted genetic nomenclature (described in Horvitz et al., 1979; Riddle et al., 1997). Below is a brief summary of the rules:

- Gene names are given by three or four italicized letters, a hyphen, and an Arabic number; e.g. *agef-1.* Gene name could refer to the phenotype originally detected and/or phenotype most easily scored; e.g. lethal for *let-60* (LEThal). Alternatively, gene name could refer to the predicted protein product based on the sequence similarity; e.g. Arf GEF in case of *agef-1*.

- Gene name could be followed by an italicized Roman numeral indicating the linkage group (i.e. chromosome) to which this gene maps; e.g. *agef-1 I.*

- Each mutation has a unique allelic designation, which consists of one or two italicized letters and an Arabic number; e.g. *vh4*, *e1309.*

- When both gene and mutation names are used, gene name is followed by mutation name in the parenthesis; e.g. *agef-1(vh4).*

- The protein product of the gene is referred to by the gene name in non-italic capital letters; e.g. AGEF-1 is a protein coded by *agef-1.*

- Phenotypes could be described in words, e.g. dumpy uncoordinated, or non-italicized three letter abbreviation with the first letter capitalized can be used, e.g. Dpy Unc.

- Genotypes of the animals carrying multiple mutations are written by listing the mutations sequentially according the left-right order on the genetic map. Five autosomes are designated *I, II, III, IV* and *V*, *X* is the X chromosome; linkage groups are separated by semicolons and are written

in order; e.g. *unc-101(sy108) agef-1(vh4) I; lin-2(e1309) X*, in this example both *unc-101* and *agef-1* are on chromosome *I* with *unc-101* to the left of *agef-1*, whereas *lin-2* in on *X*.

- Transgenes consisting of multiple or single copies of exogenous DNA could be integrated into the genome or transmitted as large extrachromosomal arrays. Integrated transgenes are designated by the laboratory allele name, followed by *Is* and an Arabic number, all italicized. Extrachromosomal arrays are written in italicized letters consisting of the laboratory allele name, followed by *Ex* and an Arabic number. Both *Is* and *Ex* could be followed by the brackets containing molecular information describing the transgene; e.g. *vhEx7[Plin-31::ARF-1.2::GFP + Pttx-3::GFP]*.
- Strain names are written in non-italicized letters and consist of two upper case letters followed by a number. Strain name prefix differs from the allele name prefix; both represent the laboratory of origin. For example, QR512 *agef-1(vh4) I*; *lin-2(e1309) X* is a stain constructed in the Rocheleau laboratory (strain prefix is QR, mutation prefix is *vh*).

LIST OF ABBREVIATIONS

AC: Anchor Cell

AEE: Apical Early Endosome

AP: Adaptor Protein

APPL: ADAPTOR protein, Phosphotyrosine interaction, PH domain, Leucine-zipper containing

AR: Amphiregulin

ARE: Apical Recycling Endosome

Arf: ADP-Ribosylation Factor

BEE: Basolateral Early Endosome

BTC: Betacellulin

CCV: Clathrin Coated Vesicle

CID: CASK Interacting Domain

CIE: Clathrin-Independent Endocytosis

CME: Clathrin-Mediated Endocytosis

CNK-1: Connector Enhancer of Ksr

CRE: Common Recycling Endosome

DAG: Diacylglycerol

DIC: Differential Interference Contrast

DlgA: Discs-Large A

EEA1: Early Endosome Antigen 1

EGF: Epidermal Growth Factor

EGFR: Epidermal Growth Factor Receptor

Egl: Egg-Laying Defective

EPR: epiregulin

EPS-8: EGFR Substrate Protein-8

ESCRT: Endosomal Sorting Complex Required for Transport

GAP: GTPase Activating Proteins

GCK-1: Germinal Center Kinase

GEF: guanine nucleotide exchange factor

GPI-APs: Glycosylphosphatidylinositol Anchored Proteins

Grb2: Growth Factor Receptor-Bound Protein 2

GTPases: Guanosine Tri Phosphatases

HB-EGF: Heparin-binding EGF

Hrs: Hepatocyte Growth Factor-Regulated Tyrosine Kinase Substrate

ILV: Intraluminal Vesicles

JAMs: Junctional Adhesion Molecules

KSR-1: Kinase Suppressor of Ras

LDLR: Low Density Lipoprotein Receptor

LIP-1: Lateral Signal Induced Phosphatase 1

MAGUK: Membrane-Associated Guanylate Kinase

MAPK: Mitogen Activated Protein Kinase

MDCK: Madin-Darby Canine Kidney epithelial cells

Muv: Multivulva

MVBs: Multivesicular Bodies

PDZ: PSD-95, Discs Large, ZO-1

PI3K: Phosphatidylinositol 3-Kinase

PIP3: Phosphatidylinositol 3,4,5-Triphosphate

PLCγ: Phospholipase Cγ

PKC: Protein Kinase C

PKD: Polycystic Kidney Disease

PTB: Phosphotyrosine Binding

RILP: Rab-Interacting Lysosomal Protein

RNAi: RNA interference

RTK: Receptor Tyrosine Kinase

SH2: Src Homology 2

SH3: Src Homology 3

siRNA: small interfering RNA

SOS: Son of Sevenless

STAT: Signal Transducers and Activators of Transcription

SynMuv: Synthetic Multivulva

TfR: Transferrin Receptor

TGFα: Transforming Growth Factor-α

TGN: Trans-Golgi Network

TKB: Tyrosine Kinase Binding

TKD: Tyrosine Kinase Domain

Tsg101: Tumor Susceptibility Gene 101

Ub: Ubiquitin

UBDs: Ubiquitin-Binding Domains

VPCs: Vulval Precursor Cells

Vps24: Vacuolar Protein Sorting 24

VSVG: Vesicular Stomatitis Virus G Protein

Vul: Vulvaless

CHAPTER 1: INTRODUCTION – LITERATURE REVIEW

1.1. Epidermal Growth Factor Receptor (EGFR) signaling pathway

1.1.1. ErbB receptor tyrosine kinase (RTK) family

EGFR (ErbB1/HER1) belongs to the family of ErbB receptors, which also includes ErbB2/Neu/HER2, ErbB3/HER3 and ErbB4/HER4. ErbB receptors share the same domain composition, which is represented by an extracellular ligand-binding domain, single span transmembrane region and an intracellular tyrosine kinase domain (Figure 1) (Hynes et al., 2001b). This family of RTKs is expressed in multiple tissues of epithelial, mesenchymal and neuronal origin, where they promote various processes such as cell proliferation, differentiation, migration, growth and survival. Depending on the ligand binding the receptor, ErbB family members are capable of homo- or heterodimerization, with the exception of ErbB2, for which a specific ligand has not been found thus preventing it from homodimerization (Klapper et al., 1999). Soluble forms of receptors have been identified as well, these lack a transmembrane and cytoplasmic regions and are produced by alternative splicing at the mRNA level or at the cell surface by proteolytic cleavage referred to as ectodomain shedding (Chen and Hung, 2015).

A number of peptide ligands that are able to bind ErbB family of RTKs have been described (Goffin and Zbuk, 2013) (Figure 1). Some of the ligands are capable of binding one type of the ErbB receptor only such as epidermal growth factor (EGF), transforming growth factor-α (TGFα) and amphiregulin (AR) that bind specifically ErbB1. Whereas others possess dual specificity, for example, heparin-binding EGF (HB-EGF), betacellulin (BTC) and epiregulin (EPR) are able to bind both ErbB1 and ErbB4 (Hynes et al., 2001a). Activation of RTKs is achieved through dimerization. Upon hetero- or homodimerization of the receptors, the intrinsic tyrosine kinase activity of the intracellular domain becomes activated leading to autophosphorylation on specific tyrosine residues, which serve as docking sites for signaling molecules involved in signal

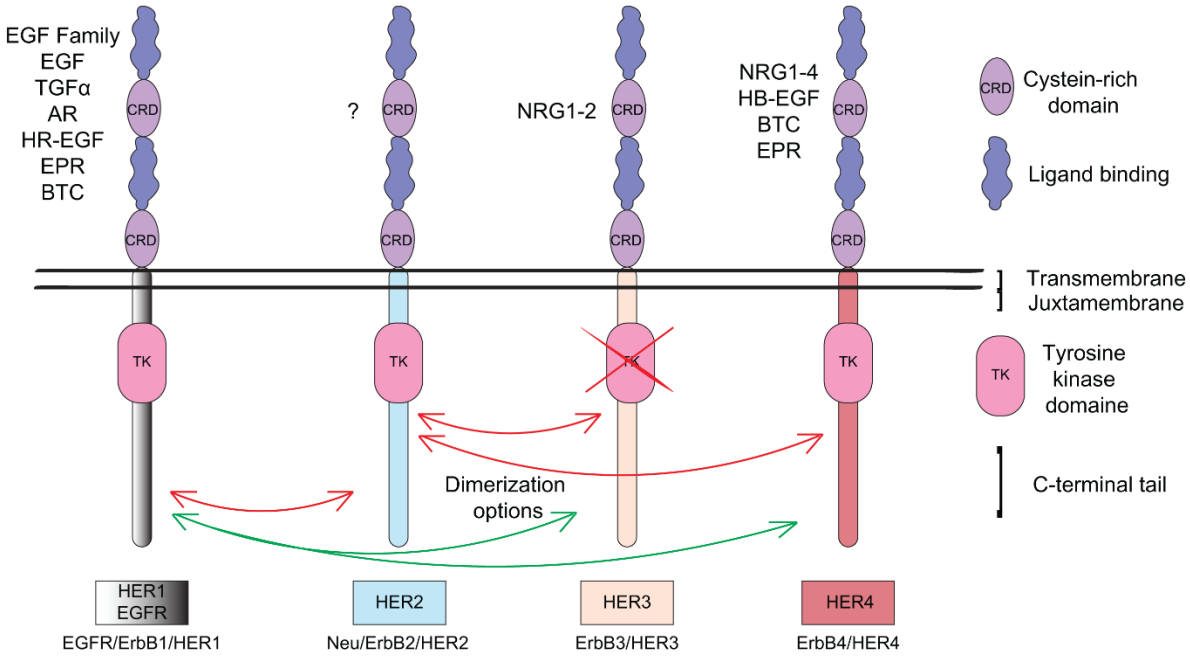

Figure 1. ErbB family of receptor tyrosine kinases (RTKs).

Schematic representation of the ErbB family of RTKs showing the receptor domain composition as well as known ligands and dimerization capabilities. No ligand has been found thus far for the ErbB2 receptor and it appears that it is mainly involved in heterodimer formation. ErbB3 does not have tyrosine kinase activity. Various ligands capable of binding these RTKs are indicated to the left of the relevant receptor.

transduction. This ultimately results in changes in target gene expression. Moreover, heterodimerization brings on signaling diversity as the signaling output from heterodimers is not represented simply by the sum of properties of the two monomers, but rather leads to new signaling characteristics (Olayioye et al., 2000).

1.1.2. EGFR signaling pathway

Dimerization of the EGFR is driven by the receptor itself without a contribution of the ligand to the dimerization interface (Garrett et al., 2002). Ligand binds simultaneously to two sites on the same receptor molecule, without crosslinking two separate receptor molecules, in the 2:2 ratio resulting in a conformational change that exposes a previously occluded dimerization site and allows for dimerization to occur (Figure 2A) (Lemmon and Schlessinger, 2010). It has been proposed that both monomers and dimers of EGFR are present on the cell surface in equilibrium. Ligand binding induces conformational changes that stabilize the active dimer conformation and activate phosphotyrosine kinase activity of the cytoplasmic portion of the receptor leading to phosphorylation of multiple tyrosine residues (Schlessinger, 2000). Intracellular tyrosine kinase domains (TKDs) of the EGFR, similar to other RTKs, consist of an N-lobe and a C-lobe and are *cis*-autoinhibited through specific intramolecular interactions (Figure 2B) (Lemmon and Schlessinger, 2010). Upon dimerization of the EGFR, the C-lobe of one TKD named "Activator" makes a directed contact with the N-lobe of another TKD named "Receiver", which leads to release of autoinhibition within the Receiver TKD and autophosphorylation of its C-terminal tyrosine residues resulting in the active configuration of the receiver kinase (Zhang et al., 2006). Thus, both intracellular TKDs within the dimer become active. In contrast to the activation of the majority of RTKs (Hubbard, 2004), EGFR does not require *trans*-phosphorylation of its activation loop within

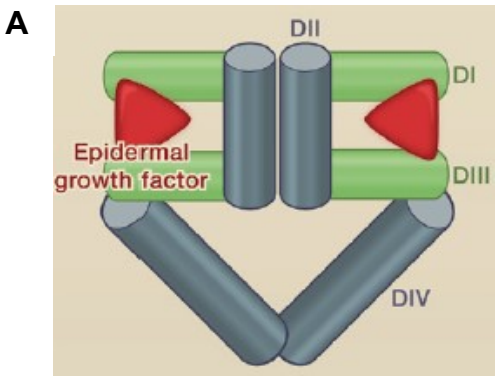

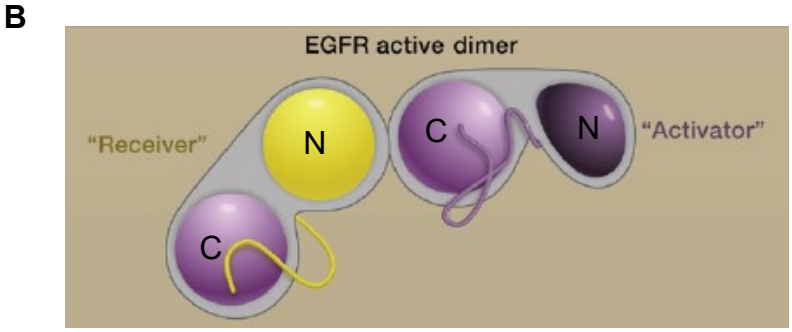

(Adapted from Lemmon and Schlessinger, 2010)

Figure 2. Activation of the EGFR.

(A) Ligand binds two sites (DI and DIII) of a single molecule of EGFR leading to 2:2 ligand:receptor ratio. Dimerization is entirely receptor-driven and ligand is not involved in the formation of the dimerization interface between two EGFR molecules. The conformational change achieved by the ligand exposes the previously hidden DII dimerization interface promoting dimerization of the receptor molecules. (B) Each TKD of the EGFR consists of an N-lobe and a C-lobe. The TKD of EGFR is activated by a direct contact of the C-lobe of the "Activator" TKD and the N-lobe of the "Receiver" TKD. This results in the release of autoinhibition within the activation loop of the "Receiver" TKD.

the TKD since it has been shown that mutations of the conserved tyrosine residue within this activation loop does not prevent activation of the EGFR present on the lipid vesicles (Zhang et al., 2006).

The following downstream signaling pathways are activated by ligand binding to EGFR: Ras/mitogen activated protein kinase (MAPK), phosphatidylinositol 3-kinase (PI3K)/Akt, phospholipase Cγ (PLCγ)/protein kinase C (PKC) and signal transducers and activators of transcription (STAT) pathways. The Ras/MAPK pathway regulates cell proliferation and survival. In this pathway, the phosphotyrosine-binding adaptors SHC and Grb2 serve as a link between the phosphorylated receptor and a guanine nucleotide exchange factor (GEF) Son of sevenless homolog (SOS) (Batzer et al., 1994). SOS in turn activates a small GTPase Ras and leads to activation of a linear kinase cascade consisting of Raf/MEK/Erk (Figure 3) (Gaestel, 2006). Activated phospho-Erk1/2 then translocates to the nucleus, where it phosphorylates various transcription factors to modulate their activity (Yarden and Shilo, 2007).

The PI3K/Akt signaling pathway is involved in cell growth, migration and resistance to apoptosis. PI3K is a heterodimeric kinase consisting of a regulatory subunit, p85, and a catalytic subunit, p110, that produces a second messenger phosphatidylinositol 3,4,5-triphosphate (PIP3) on the membrane, which in turn recruits a serine/threonine kinase Akt and results in its activation leading to a biological response (Vivanco and Sawyers, 2002). This pathway is activated mainly upon heterodimerization of EGFR with HER3 since EGFR itself lacks pYXXM (pY – phosphotyrosine, M – methionine) docking sites for the regulatory subunit of PI3K whereas these sites are abundant on HER3 (Prigent and Gullick, 1994). Alternatively, an adaptor protein Gab1 (Grb2-associated adaptor binder-1) could link EGFR with the p85 regulatory subunit (Mattoon et al., 2004).

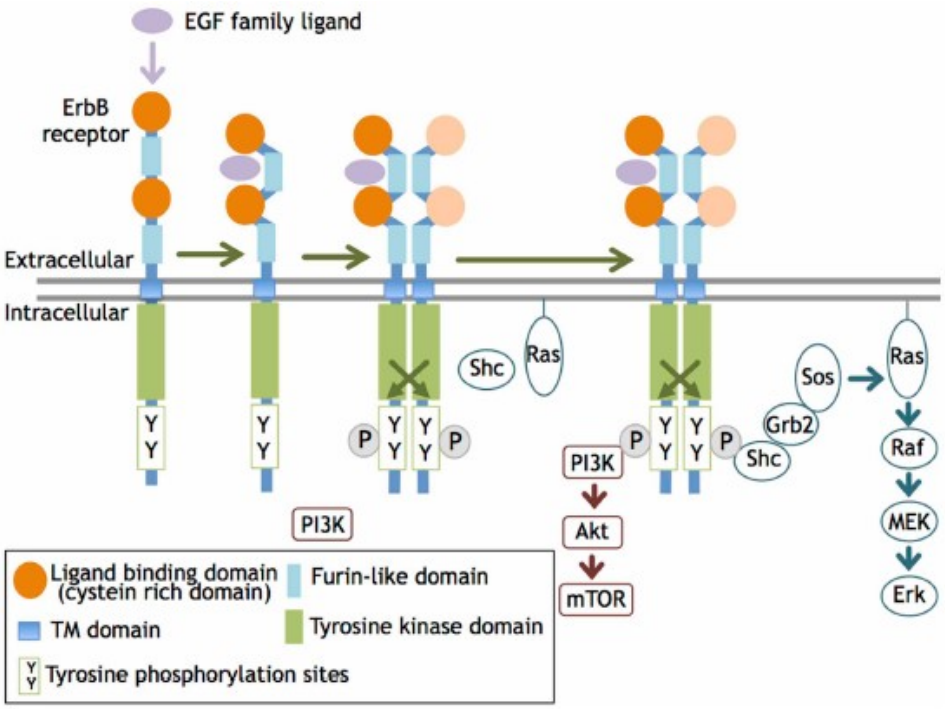

(From Iwakura and Nawa, 2013)

Figure 3. Dimerization and signal propagation of ErbB receptors.

Ligand binding to the receptor induces dimerization and activation of the intrinsic tyrosine kinase activity leading to transphosphorylation on certain tyrosine residues in the cytoplasmic portion of the receptor allowing for recruitment of adaptors/effectors and signal propagation. The two main signal transduction pathways activated upon ErbB receptor activation are Ras/MAPK and PI3K/Akt pathways.

The PLCγ/PKC pathway is involved in cell migration and division. PLCγ interacts directly with the activated EGFR and hydrolyses phosphatidylinositol 4,5-biphosphate present abundantly on the plasma membrane to produce diacylglycerol (DAG), a co-factor in PKC activation, and inositol 1,3,5-triphosphate involved in the intracellular calcium release. PKC then phosphorylates and activates Raf-1 kinase leading to MEK1 and MEK2 as well as Erk1/2 activation (Scaltriti and Baselga, 2006).

STATs can directly interact with activated EGFR via their Src homology 2 (SH2) domain. This interaction leads to phosphorylation of STAT by EGFR, dimerization, activation and translocation to the nucleus, where STATs could bind to target sequences within gene promoters and regulate gene expression (Haura et al., 2005). Of great importance to the pathogenesis of malignancy is the STAT3 protein, which when activated leads to production of Bcl2 family members, regulators of apoptosis, increasing cell survival (Real et al., 2002).

1.1.3. Endocytic trafficking and EGFR signaling

Upon EGFR activation, it is endocytosed into the early endosomes via clathrin-mediated endocytosis (CME) and clathrin-independent endocytosis (CIE) (Sorkin and von Zastrow, 2009). It has been proposed that the internalization and movement within the endocytic pathway regulates EGFR signaling output (Tomas et al., 2014b). Depending on the localization of the activated EGFR within the degradative pathway, its binding partners vary resulting in formation of novel signal transduction complexes.

1.1.3.1. Receptor internalization and ubiquitination

The first study to uncover key components of the endocytosis and lysosomal degradation of the activated EGFR has proposed that its sole purpose is signal attenuation (Carpenter and

Cohen, 1979). However, a later study (Cohen and Fava, 1985) discovered EGF/EGFR complexes as well as active EGFR present in the isolated intracellular vesicles of epidermoid carcinoma cells suggesting a more complex and physiologically relevant role of endocytosis on the signaling pathway.

Two studies have reported that the majority of the response to EGFR activation in terms of MAPK activation and transcription occurs while the receptor is signaling from the cell surface (Brankatschk et al., 2012; Sousa et al., 2012). Sousa and colleagues have blocked endocytosis by depleting the small GTPase dynamin, which is responsible for pinching off of the endocytic vesicles from the plasma membrane during both CME and CIE, to show that this leads to increased EGFR phosphorylation and ubiquitination, but has no effect on the Erk phosphorylation (Sousa et al., 2012). In the study by Brankatschk et al. the authors depleted HeLa cells of endosomal sorting complex required for transport (ESCRT) components, which promote formation of the multivesicular bodies containing endocytosed EGFR, however this did not lead to increased EGF-induced transcriptional response (Brankatschk et al., 2012).

Depending on the concentration of the ligand activating EGFR and the type of endocytosis, the fate of the endocytosed receptor changes (Figure 4). For example, it has been shown in HeLa cells that a low physiological concentration (≥1-2 ng/ml) of the EGF ligand promotes rapid CME of the EGFR followed by recycling of the majority of the receptor pool and prolonged signaling response (Sigismund et al., 2008). In contrast, stimulation with a high concentration of the EGF leads to ubiquitination of the receptor and CIE of the EGFR with subsequent degradation of the receptor in the lysosomal compartment (Sigismund et al., 2005). It has been proposed that in the physiological situation, EGFR is endocytosed via CME, however once the clathrin machinery

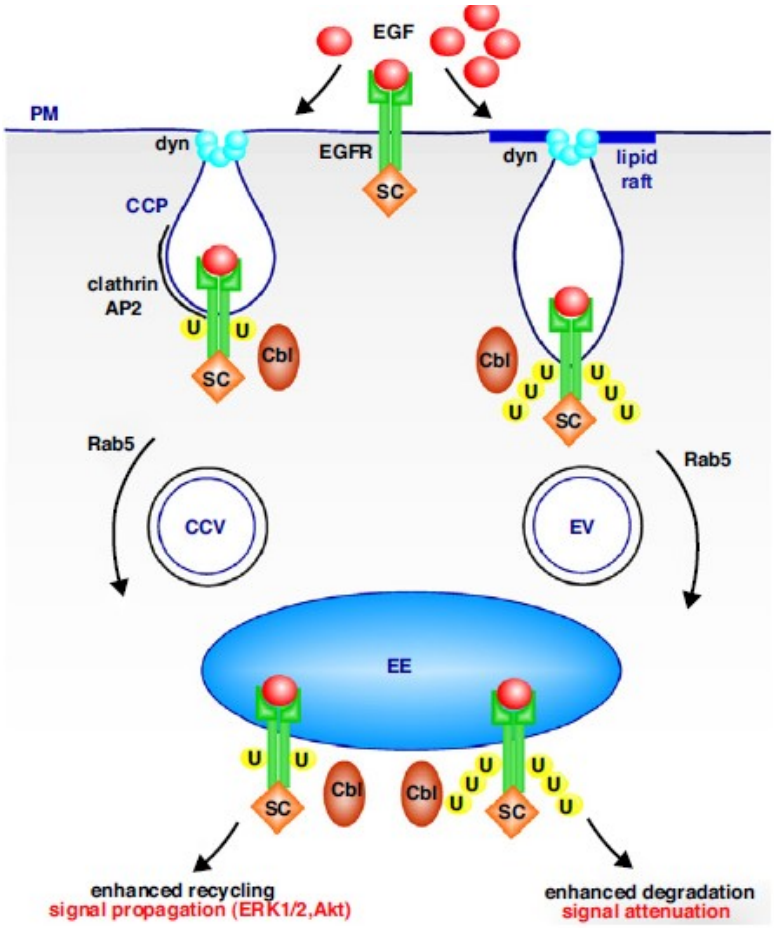

(From Platta and Stenmark, 2011)

Figure 4. Fate of the EGFR depending on EGF ligand concentration.

At low EGF concentration (left), the EGFR is endocytosed via CME through clathrin-coated pits; at stimulation with high EGF concentrations (right), clathrin-independent mechanism is involved. The receptor is continuously ubiquitinated, however in case of high ligand concentration ubiquitination is more pronounced. The clathrin-dependent route results in increased receptor recycling and signal propagation, whereas CIE promotes EGFR degradation and signal attenuation. SC, signaling cascade; CCV, clathrin-coated vesicle; EV, endocytic vesicle; PM, plasma membrane; dyn, dynamin; U, ubiquitin moiety.

saturates, CIE becomes involved to control the strength of the signaling output (Tomas et al., 2014a). Depending on the nature of the ligand binding EGFR, its

trafficking and signaling vary as well. For example, it has been shown in Hep-2 human laryngeal epithelial carcinoma cells that EGFR stimulation with HB-EGF and BTC results in continuous receptor phosphorylation and ubiquitination with consequent receptor degradation; whereas stimulation with TGF-α promotes decreased levels of EGFR phosphorylation and ubiquitination leading to complete receptor recycling (Roepstorff et al., 2009). Moreover, the ability of the ligand to stay bound to the receptor at lower pH correlates with degradation of the receptor. HB-EGF, BTC and EGF stay bound to the EGFR in the acidic environment of endosomes ending in receptor degradation, whereas TGF-α/EGFR complexes dissociate and the receptor is recycled back to the plasma membrane (Ebner and Derynck, 1991; Roepstorff et al., 2009).

EGFR activation results in transphosphorylation of tyrosine residues in the carboxy-terminal portion of the receptor as well as phosphorylation and recruitment of adaptor proteins, which not only promote signal propagation to downstream components of the signal transduction cascade, but also play a role in the receptor internalization and result in ubiquitination of the EGFR. A growth factor receptor-bound protein 2 (Grb2) is recruited to activated EGFR via its SH2 domain. Mutations of the two binding sites for Grb2 within EGFR, Y1068 and Y1086, led to decreased EGFR internalization in porcine aortic endothelial (PAE) cells and overexpression of Grb2, which either entirely lacks or carries inactivating mutations in the SH3 domain, dramatically decreased EGFR endocytosis in PAE and HeLa cells (Jiang et al., 2003). Thus, Grb2 has dual roles on signaling, which contribute to opposite effects on the signaling outcome. On one hand, it recruits a Ras GEF SOS via its SH3 domain to promote signaling; on the other hand, it promotes internalization of the activated EGFR. Another strong evidence of the latter function comes from

the experiments where knock-down of Grb2 by siRNA in PAE and HeLa cells specifically reduced internalization of the EGFR (Jiang et al., 2003). Moreover, Grb2-EGFR complexes localize to clathrin-coated pits and Grb2 is necessary for EGFR recruitment to these structures (Johannessen et al., 2006; Stang et al., 2004).

Cbl, a RING finger-containing E3 ubiquitin ligase, is one of the main interacting partners of Grb2, which is recruited via the SH3 domain to active EGFR in order to ubiquitinate lysine residues within the kinase domain of EGFR (Huang et al., 2006). Additionally Cbl can directly bind EGFR via its tyrosine kinase binding (TKB) domain that interacts with the phosphorylated Y1045 residue of the receptor (Levkowitz et al., 1999). Cbl promotes ubiquitination of the receptor by recruiting E2 ubiquitin conjugating enzymes (Umebayashi et al., 2008). Six distinct lysine (K) residues within the kinase domain of EGFR can be ubiquitinated, as has been determined by mass spectrometry (Huang et al., 2006). EGFR could be polyubiquitinated, with the poly-ubiquitin chains linked mainly through K63 of ubiquitin (Ub) or monoubiquitinated (Huang et al., 2006). It has been proposed that polyubiquitination of EGFR with short K63-linked chains but not monoubiquitination increases interaction of the ubiquitinated EGFR with adaptors involved in endocytic sorting of the activated receptor to the lysosome (Huang et al., 2013). Cbl-mediated ubiquitination of EGFR is essential for lysosomal targeting and degradation of the receptor, but it is not necessary for the internalization of the receptor since ubiquitination-deficient EGFR (poly-lysine to arginine mutant) was still endocytosed at a level similar to wild-type, however the turnover of the receptor was impaired (Huang et al., 2006). The latter is further supported by findings that EGFR lacking the Y1045 residue, which is involved in Cbl recruitment, is weakly ubiquitinated, however its internalization is not impaired (Jiang et al., 2003).

1.1.3.2. Early endocytic compartment and multivesicular body formation

Upon endocytosis, clathrin-coated vesicles lose their coat and fuse with early endosomes. It has been shown that activated EGFR can activate Rab5a, an early endosomal Rab GTPase, to promote endocytosis of the receptor (Barbieri et al., 2000). Some of the signaling appears to be specific to early endosomes and thus has a potential to change the signaling output. (Sorkin and von Zastrow, 2009). An example of such a specific signaling complex is the one containing active EGFR, Rab5 and two homologs of Rab5 effectors, APPL1 and APPL2 (adaptor protein, phosphotyrosine interaction, PH domain, leucine-zipper containing), which functions as an intermediate in signal propagation between the plasma membrane and the nucleus (Miaczynska et al., 2004). In cultured HeLa cells, APPL-containing endosomes have been shown to be important for Erk1/2 and Akt activation (Zoncu et al., 2009). This complex has a role *in vivo* as well since it has been shown that in the developing zebrafish embryo APPL1 is required for Akt activation and a pool of Akt has been transiently found on early endosomes (Schenck et al., 2008). Moreover, the internalized receptor present on the early endosomes is still accessible to signal to downstream targets (Sigismund et al., 2008).

EGF does not dissociate from the receptor in the early endosomes since pH of this compartment is only mildly acidic (pH 6.0-6.5) (Sorkin et al., 1988), which preserves dimerized phosphorylated EGFR that is still interacting with Grb2 and Cbl on early endosomes (Galperin et al., 2004; Sorkin and Carpenter, 1991). Upon maturation of the early endosome, the receptor can be either recycled back to the plasma membrane or accumulate in the intraluminal vesicles (ILV) of multivesicular bodies (MVB) on their way towards the lysosome. The equilibrium between these two pathways balances the signaling from endosomes and then of the recycled receptor from the plasma membrane with signal attenuation following receptor degradation. Two distinct

pathways of EGF-EGFR complex recycling have been reported (Sorkin et al., 1991). The rapid recycling pathway has been proposed to originate from limiting membranes of the MVBs, whereas slow recycling is likely to occur through the Rab11-positive late recycling compartment (Sorkin and Goh, 2008). It has been shown that a short isoform of Eps15 (EGFR pathway substrate 15), an endocytic adaptor promoting clathrin-mediated endocytosis, is involved in the recycling of EGFR through Rab11-positive recycling endosomes (Chi et al., 2011). Additionally, the dimerization partner of the EGFR is important in determining the fate of the endocytosed receptor. Homodimerization of EGFR leads mainly to degradation of the receptor dimers, whereas EGFR heterodimers are not as effective in Cbl recruitment and evade degradation (Peschard and Park, 2003). For example, a number of tumors such as breast, ovary, prostate and brain overexpress HER2/ErbB2, which form heterodimers with EGFR, and recruit Cbl at a reduced rate. These heterodimers are internalized at a slower rate and are recycled faster leading to potentiation of EGFR signaling outputs (Peschard and Park, 2003).

Ubiquitinated EGFR is believed to interact with the ESCRT–0 components Hrs (hepatocyte growth factor-regulated tyrosine kinase substrate) and STAM1/2 through their ubiquitin-binding domains (UBDs) (Fisher et al., 2003). Hrs depletion by siRNA has been shown to prevent degradation of the EGFR, promote its accumulation on EEA1 (early endosome antigen 1)-positive early endosomes and increase recycling of the receptor (Malerod et al., 2007; Raiborg et al., 2008). Several models exist explaining how ESCRT-0 is involved in the formation of ILVs. One of them, a conveyer belt model of ESCRT assembly, proposes that Hrs recognizes ubiquitinated cargo and hands it over in sequence from ESCRT-I to ESCRT-II and –III, all of which contain UBDs, thus ESCRT-0 complex remains peripheral to the site of ILV formation (Hurley and Emr, 2006). Another model, a concentric circle model of ESCRT assembly, suggests that the ESCRT-0

recognizes cargo via UBDs and promotes recruitment of ESCRT-I and –II leading to the assembly of a super-complex above the cargo, which then recruits ESCRT-III to form ILVs (Nickerson et al., 2007). The concentric circle model places ESCRT-0 in the epicenter of ILV formation proposing that it has to be released prior to pinching off of the membrane.

Depletion of the ESCRT-I component, Tsg101, has been shown to prevent EGFR sorting into ILVs and cause its accumulation on the structurally deformed early endosomes suggesting that ESCRT-I might be involved in both cargo recognition and recruitment of the components required for membrane deformation during the process of MVB formation (Doyotte et al., 2005). Similarly, depletion of an ESCRT-III component, Vps24, prevents degradation of the EGFR (Bache et al., 2006). However, whereas Tsg101 knock-down resulted in sustained activation of the MAPK signaling pathway, loss of Vps24 did not have such an effect. Additionally, EGFR accumulated in non-acidified early endosomes in Tsg101 depleted cells, whereas Vps24 knock-down resulted in receptor accumulation within small MVBs (Bache et al., 2006). Thus, it has been proposed that EGFR loses its ability to signal to downstream targets once it is entrapped in the ILVs of the MVBs and that this is the "point of no return" in terms of signal transduction, where removing the function of the proteins involved in the endocytic trafficking past the step of ILVs formation will not have an effect on the strength of EGFR signaling, and that degradation of the receptor is not required to terminate signaling (Bache et al., 2006). Thus, the ESCRT complexes could be referred as early, ESCRT-0 and –I, and late, ESCRT-II and –III. Depleting cells of "early" ESCRT components leads to increased MAPK signaling potentially due to increased recycling of the EGFR to the plasma membrane, whereas loss of "late" ESCRTs does not cause sustained MAPK activation (Raiborg et al., 2008; Wittinger et al., 2011). In contrast, in *Drosophila*, not

only ESCRT-0 and –I, but also ESCRT-II and –III are involved in regulation of the receptor signaling (Vaccari et al., 2009).

1.1.3.3. Late endocytic compartment and degradation

The role of the ESCRT machinery in EGFR degradation is widely accepted. The receptor included in the ILVs of the MVBs is then targeted for fusion with the lysosome. Upon maturation, the early endosome loses Rab5 and acquires Rab7 in a mechanism known as Rab conversion (Rink et al., 2005). There is growing evidence for the role of a small GTPase Rab7 in the degradation of the EGFR. It has been shown in HeLa cells that overexpressing a dominant-negative mutant of Rab7 slows the degradation of EGF/EGFR complexes and stalls them in the late endosomes, whereas an activated mutant of Rab7 accelerates degradation of these complexes (Ceresa and Bahr, 2006). These findings provide evidence for a role of Rab7 in the trafficking of EGFR from late endosomes to the lysosome for degradation. Moreover, two of the Rab7 interacting proteins, XAPC7 (a proteasome α-subunit) and RILP (Rab-interacting lysosomal protein) have been shown to inhibit EGFR endocytic trafficking by overexpression (Cantalupo et al., 2001; Dong et al., 2004). Even though loss of Rab7 function has been shown to prevent the degradation of the EGFR and lead to receptor accumulation in the late endosomes, the effect of this loss on the signaling output is not known. Our work in *C. elegans* demonstrates genetically that loss of Rab7 results in increased EGFR signaling during vulva development (Skorobogata and Rocheleau, 2012). In addition, the receptor accumulates in cytoplasmic foci in *rab-7* mutants suggesting that signaling is still possible from this compartment (Chapter 3 and Skorobogata and Rocheleau, 2012).

Even though the late endocytic compartment is believed to be mainly involved in signal attenuation by promoting degradation of the EGFR in the lysosome, there is evidence for its role in modulation of the signaling output. Proper Erk activation requires signaling from the late

endosome during embryogenesis and tissue homeostasis using p14 and MP1 (MEK1 partner) adaptors, which recruit MEK1 to the late endosome and promote Erk1/2 nuclear translocation (Teis et al., 2006). Lu and colleagues have demonstrated that EGFR promotes K-Ras recruitment to the endosomal membranes in a clathrin-dependent manner, which is later transported to late endosomal and lysosomal membranes. K-Ras remains associated with phosphorylated Raf1 on the late endosomes/lysosomes, where it is able to interact with MEK1 present on the same membranes as a part of the p14/MP1/MEK1 complex leading to Erk1/2 activation (Figure 5) (Lu et al., 2009).

1.1.4. EGFR trafficking and cancer

It is widely accepted that EGFR signaling plays an underlying role in the pathogenesis of cancer as it promotes survival, tumor growth and metastasis. Activating mutations in EGFR have been linked to various types of malignancies such as ovarian cancer, glioblastoma and lung cancer, and EGFR overexpression is associated with poor prognosis and lower therapeutic responsiveness to treatments (Lafky et al., 2008; Lee et al., 2006a; Paez et al., 2004). Moreover, failure to downregulate the receptor within the endocytic pathway also leads to increased EGFR signaling and cancer (Bache et al., 2004; Polo et al., 2004). Overexpression and certain mutations in the extracellular portion of the EGFR could promote increased dimerization of the receptor and lead to activation (Shan et al., 2012).

A number of EGFR mutants found in the glioblastomas have been described that lack binding sites required for interaction with Cbl upon EGFR activation resulting in defects in ubiquitination and degradation, resulting in prolonged signal transduction (Roepstorff et al., 2008). The best studied EGFR variant is EGFRvIII, it was initially found in glioblastoma, and later in other tumor types such as breast cancer, lung cancer and prostate cancer (Ge et al., 2002; Okamoto et al., 2003; Olapade-Olaopa et al., 2000; Sugawa et al., 1990). EGFRvIII is characterized by a

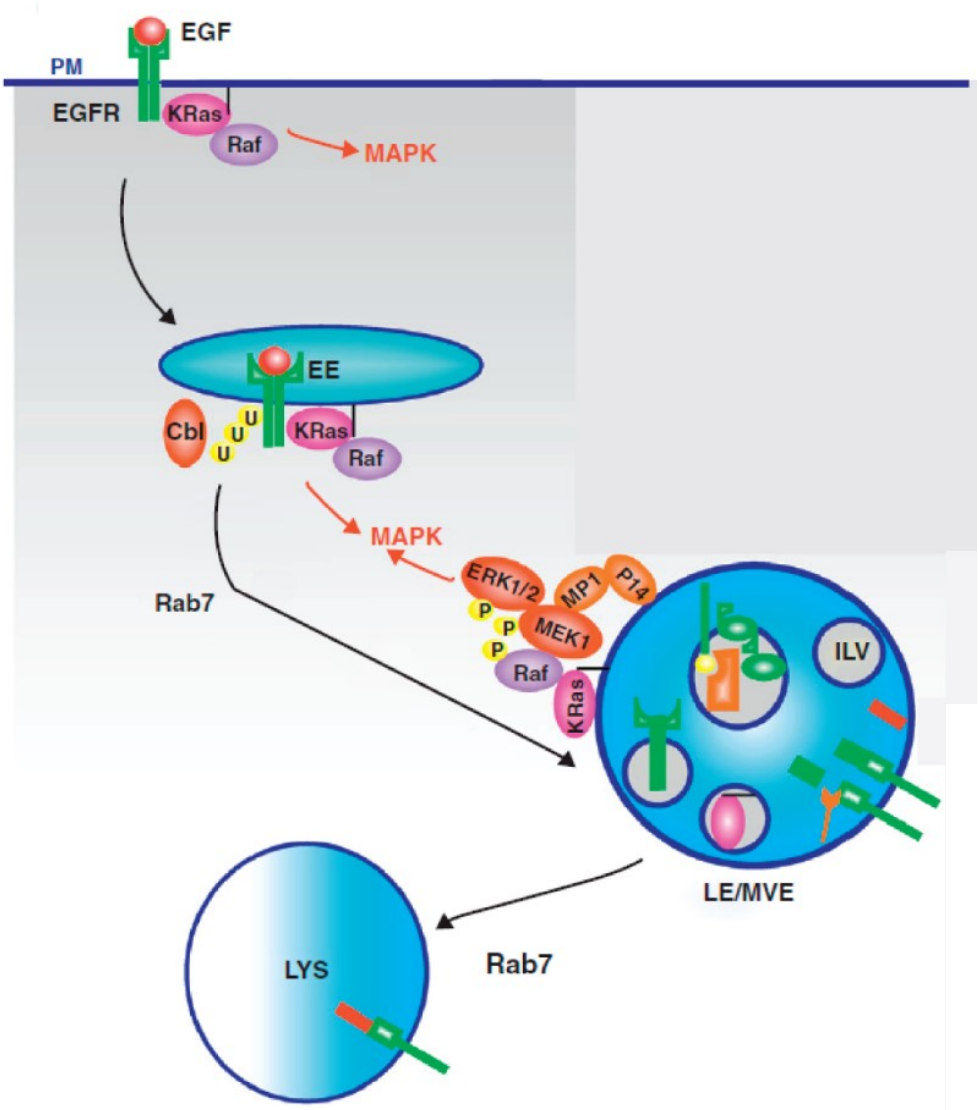

(Adapted from Platta and Stenmark, 2011)

Figure 5. EGFR signaling from the late endosome.

Schematic representation of EGFR signaling from the late endosome (LE)/multivesicular endosome (MVE). EGFR recruits KRas and active Raf to the endosomal membrane. Once the endosome matures from an early to late endosome, with EGFR now in the ILVs, adaptors p14 and MP1 recruit MEK1 to the LE membrane hosting KRas and phospho-Raf, which allows for Erk1/2 activation and signal propagation. (Continued on the next page)

deletion in the extracellular portion of the receptor, which produces a receptor unable to bind ligands, but that remains constitutively active and signals through Ras-Erk1/2 and PI3K-Akt (Kuan et al., 2001; Roepstorff et al., 2008). EGFRvIII could be downregulated when Cbl is overexpressed (Davies et al., 2006). However, it has been demonstrated that in the case of endogenous Cbl levels, EGFRvIII is not efficiently ubiquitinated, escapes degradation, and is instead recycled back to the plasma mebrane (Grandal et al., 2007). Even though EGFRvIII is able to bind Cbl via Grb2, virtually no ubiquitination of the mutant EGFR could be detected, and it has been proposed that hypo-phosphorylation of this variant on the Y1045 residue, a direct Cbl binding site, contributes to defective ubiquitination (Grandal et al., 2007; Han et al., 2006). Additionally, several mutations in the machinery involved in the EGFR endocytic downregulation have been linked to tumorigenesis, these include Cbl, Tsg101 (ESCRT-I component) and Vps25 (ESCRT-II component) (Roepstorff et al., 2008). Alternatively, genes modulating trafficking of the EGFR have been identified as oncogenes. One such example of an oncogene is Vav2, a Rho GTPase GEF, which plays a role in cell adhesion, motility and proliferative response to growth factor signaling, has been demonstrated to slow down the internalization and degradation of the EGFR by interaction with endosome-associated proteins, which results in increased Erk and Akt phosphorylation (Thalappilly et al., 2010).

Since mutations in EGFR cause overexpression of the receptor in 40% of glioblastomas, 75% of colorectal cancer and 20% of non-small-cell lung cancer, a number of therapies aim at targeting the receptor itself (Gazdar, 2009; Goldstein and Armin, 2001; Hatanpaa et al., 2010). Two different types of compounds acting on EGFR have been used to date: monoclonal antibodies to the extracellular portion of EGFR (mAb, e.g. Cetuximab) and low molecular weight tyrosine kinase inhibitors (e.g. Gefitinib) (Tomas et al., 2014b). Cetuximab is a monoclonal antibody that

targets the EGFR-ligand binding region thus preventing its stimulation with endogenous ligand, the receptor-antibody complexes are internalized leading to downregulation of EGFR expression (Regad, 2015; Tomas et al., 2014b). Gefitinib is a specific EGFR tyrosine kinase inhibitor, and has been used in the treatment of non-small-cell lung cancer (Regad, 2015). It has been proposed that Gefitinib, which is effective in the treatment of some but not other patients, promotes EGFR degradation in the lysosome in patients responsive to treatment, and leads to suppression of endocytosis in patients resistant to therapy (Nishimura et al., 2007). Moreover, EGFR is believed to enter the nucleus to promote non-homologous end-joining double-strand DNA break repair following ionizing radiation treatment, which could increase cell survival (Tomas et al., 2014b). Thus, further studies aimed at finding molecular targets involved in promoting EGFR internalization and degradation may potentiate anti-cancer treatment in patients with tumors resistant to conventional chemotherapy.

1.2. EGFR signaling in *Caenorhabditis elegans*

1.2.1. Overview of the EGFR signaling pathway and its role in nematode development

Out of 33 predicted *C. elegans* RTKs, two receptors LET-23, a homolog of EGFR, and EGL-15, a Fibroblast Growth Factor (FGF) receptor homolog, have been shown to signal mainly through LET-60 Ras (Aroian et al., 1994; DeVore et al., 1995; Sundaram, 2013). To date, only one LET-23 EGFR ligand has been identified in *C. elegans*, a LIN-3 EGF-related protein (Hill and Sternberg, 1992). The canonical Ras signaling pathway is conserved in *C. elegans* (Figure 6). EGF stimulation leads to EGFR dimerization and activation through autophosphorylation (Lemmon and Schlessinger, 2010), which recruits the adaptor protein Grb2 and a Ras GEF Sos leading to activation of Ras (Karnoub and Weinberg, 2008). This in turn results in the activation of the kinase

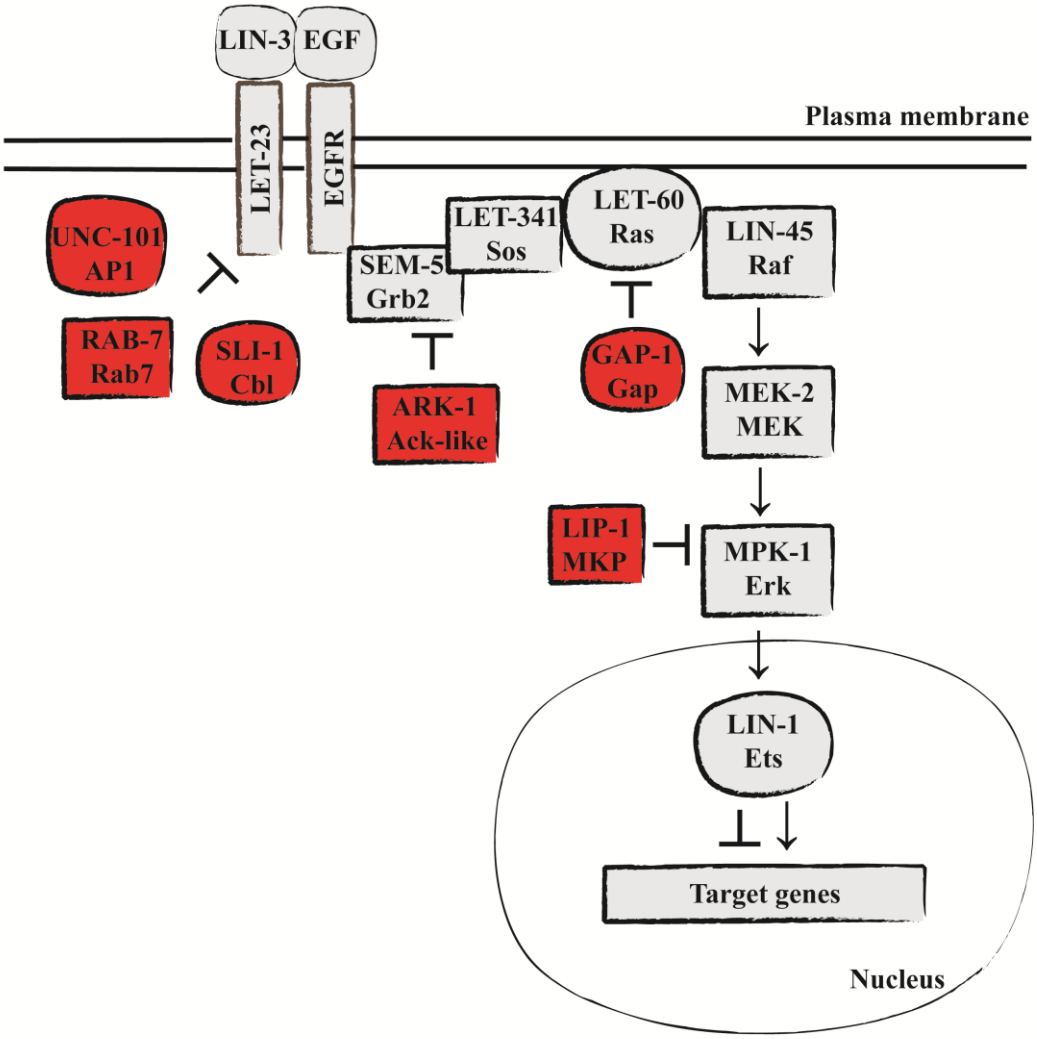

Figure 6. *C. elegans* canonical LET-23 EGFR signaling pathway.

Diagram of the canonical LET-23 EGFR signaling cascade. The core components of the pathway are in gray, the negative regulators of the signaling are shown in red. Names of the *C. elegans* proteins are on top, names of the human homologs are on the bottom.

cascade consisting of Raf/Mek/Erk (Udell et al., 2011). Activated Erk then translocates to the nucleus and phosphorylates its targets leading to modulation in gene expression (Wortzel and Seger, 2011).

Several alternative signaling pathways utilizing components of the EGFR/Ras/MAPK cascade exist as well (Sundaram, 2013). Unknown receptors may stimulate Ras/MAPK signaling, for example MPK-1 Erk promotes multiple aspects during gonad development, however it is not known which upstream receptor promotes this signaling (Lee et al., 2007). Additionally, LET-60 Ras can function independently of MPK-1 Erk by effector switching. For example, activation of LET-60 Ras may act through RGL-1, a homolog of the mammalian guanine nucleotide exchange factor Ral GEF, and Ral GTPase during cell fate specification in development, where the gradient of inductive LIN-3 EGF-like ligand is proposed to promote Ras effector switch (Zand et al., 2011). In contrast to known mammalian Ras effectors, the evidence of LET-60 Ras acting through PI3K has not yet been found (Sundaram, 2013). However, alternative putative Ras effectors capable of interaction with activated Ras have been identified, these are PLC-1 PLCε and AFD-1 AF-6 (Shibatohge et al., 1998; Watari et al., 1998). Finally, LET-23 EGFR may stimulate other Ras-independent pathways such as synaptic vesicle release involved in feeding and locomotion in a PLCγ and DAG-dependent manner (Van Buskirk and Sternberg, 2007).

In the nematode, LET-23 EGFR signaling through LET-60 Ras/MPK-1 Erk is involved in a number of developmental pathways. One of these pathways determines excretory duct cell fate and differentiation. The excretory duct cell is part of a tubular network involved in osmoregulation and in the nematode plays a role analogous to the mammalian renal system (Nelson et al., 1983; Nelson and Riddle, 1984). Loss-of-function mutations in *let-60 Ras* result in larval lethality, where animals fill up with waste fluid and have a characteristics rod-like phenotype due to lack of

excretory duct cell (Abdus-Saboor et al., 2011; Yochem et al., 1997). Duct cell fate determination represents a sole pathway regulated by Ras/Erk signaling, which is essential for animal viability as determined by a genetic mosaic analysis of the *let-60 Ras* gene (Yochem et al., 1997).

Another developmental pathway involving LET-23 EGFR/LET-60 Ras/MPK-1 Erk promotes P12 vs. P11 ectoblast cell fate. P11 and P12 ectoblasts are two neighbouring cells located in the posterior part of the animal and giving rise to hypodermal and neuronal descendants (Sulston and Horvitz, 1977). A conserved EGFR signaling pathway promotes specialization of the P12 fate, whereas decreased Ras signaling leads to P12 to P11 transition resulting in two P11 cells, and alternatively increased Ras signaling, promotes P11 to P12 cell fate transformation leading to two P12 cells being formed (Jiang and Sternberg, 1998).

Finally, vulval cell fate specification (discussed in detail below) is determined by LET-23 EGFR signaling through Ras. The inductive EGF signal is secreted by the anchor cell (AC) of the gonad to promote vulval cell fates. Ras signaling through Raf/MEK/Erk promotes the primary (1º) vulval fate, whereas Ras signaling through Ral GEF in conjunction with Notch signaling promotes the secondary (2º) vulval fate (Chen and Greenwald, 2004; Simske and Kim, 1995; Zand et al., 2011). Mutants with decreased Ras signaling have a Vulvaless (Vul) phenotype, whereas increased Ras signaling leads to a Multivulva (Muv) phenotype.

1.2.2. Vulva induction in *C. elegans*

C. elegans vulva induction serves as a paradigm of LET-23 EGFR signaling. Six multipotent vulval precursor cells (VPCs), P3.p through P8.p are polarized epithelial cells located in the ventral hypodermis (Figure 7). Vulval induction begins at the early L3 larval stage. In wild-type animals P6.p acquires the 1º vulval cell fate, neighbouring P5.p and P7.p become 2º vulval

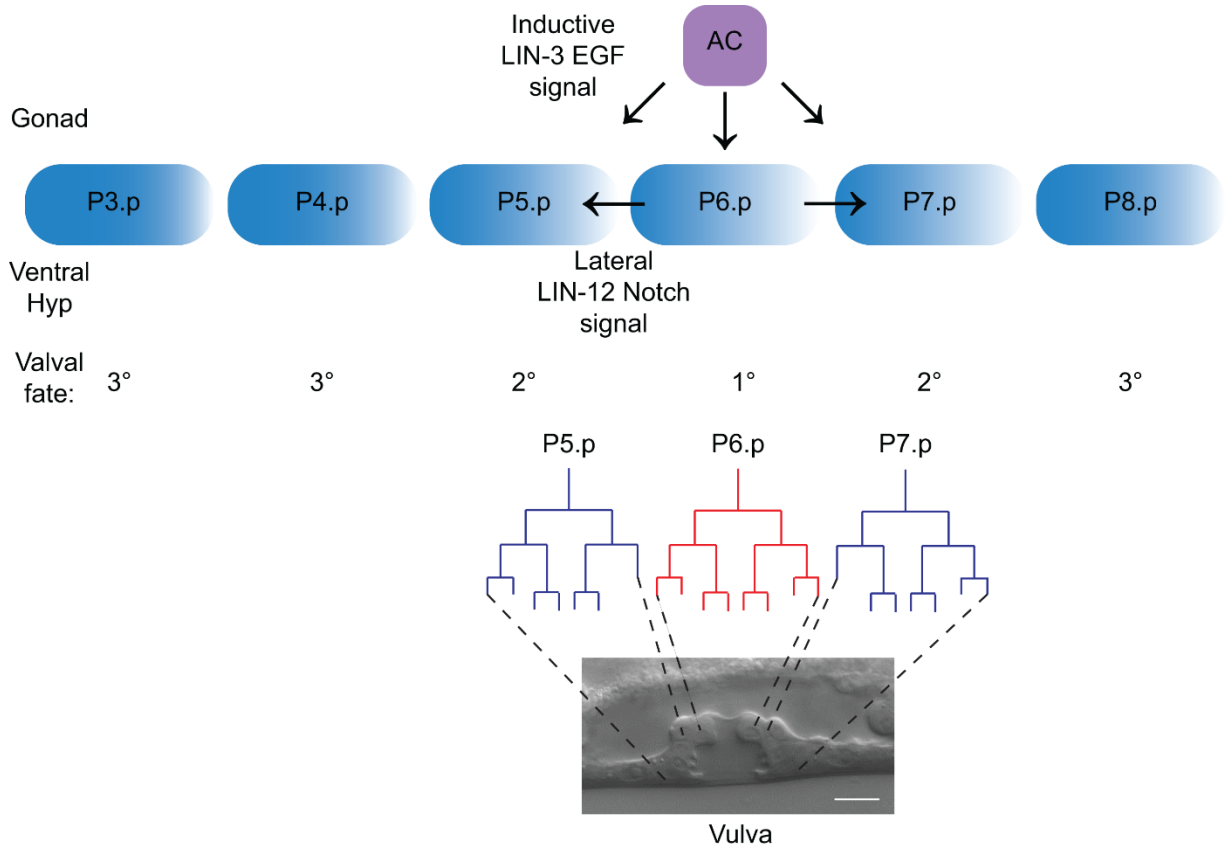

Figure 7. VPC induction in *C. elegans.*

Schematic representation of the six VPCs (P3.p-P8.p). The apical membrane of the VPCs is facing the ventral hypodermis (Hyp), whereas the basolateral membrane is facing the gonad. The anchor cell (AC) of the gonad secretes the inductive LIN-3 EGF ligand, which activates LET-23 EGFR on the P6.p due to proximity leading to a 1º vulval fate as well as lateral LIN-12 Notch signaling to the neighbouring P5.p and P7.p, which acquire the 2º vulval fates. The remaining P3.p, P4.p and P8.p become 3º non-vulval cells and fuse with the underlying Hyp7. P5.p – P7.p give rise to 22 cells of the wild-type vulva, schematic representation of the vulval cell lineages is shown. DIC image of the vulva in early L4 larva. Bar, 5 µm.

cells, and the remaining P3.p, P4.p and P8.p divide once and fuse with the Hyp7 hypodermis (P3.p divides 50% of the time and the other 50 % of the time, it fuses with the Hyp7 during L2 larval stage). Any of the 6 VPCs are competent to produce vulva as has been shown by laser ablation experiments (Kimble, 1981; Sternberg and Horvitz, 1982; Sulston and White, 1980). For example, in a scenario, where P6.p is ablated, P5.p may adopt a 1º fate and P4.p a 2º fate or P7.p may become the 1º and P8.p a 2º fate (Kimble, 1981; Sternberg and Horvitz, 1982). Alternatively, ablation of the AC prior to L3 stage leads to all six VPCs becoming 3º non-vulval cells (Kimble, 1981). Whereas ablating all 6 VPCs did not result in P2.p or P9.p acquiring vulval cell fates suggesting that only P3.p-P6.p are competent to produce vulva thus forming the "vulval competence group" (Sternberg and Horvitz, 1982).

There is a 3º-3º-2º-1º -2º -3º pattern of VPC induction, which could be explained by a number of factors. P6.p is the closest cell to the AC, which produces the inductive LIN-3 EGF ligand, and thus LET-23 EGFR is activated more strongly on P6.p and to a lesser extent on P5.p and P7.p. Activated Ras signaling within P6.p leads to a lateral LIN-12 Notch signaling to P5.p and P7.p. EGFR and Notch signaling pathways have inhibitory effects on each other: Notch signaling in P5.p and P7.p promotes activation of the negative regulators of EGFR signaling (will be discussed later) as well as downregulation of the LET-23 EGFR receptor within these VPCs (Stetak et al., 2006), whereas EGFR signaling in the P6.p downregulates LIN-12 Notch receptor and upregulates DSL-1/DSL Notch ligand expression (Chen and Greenwald, 2004; Shaye and Greenwald, 2002). Additionally, LET-23 EGFR activates Ral GEF in the P5.p and P7.p (Zand et al., 2011). It is believed that these signaling pathways coordinate to promote a specific pattern of VPC induction by using a graded LIN-3 EGF signal and lateral LIN-12 Notch signaling via the DSL-1 ligand. A combination of antagonistic LET-23 EGFR and LIN-12 Notch signaling

promotes the 1º and inhibits the 2º fate in P6.p as well as activates the 2º and suppresses the 1º vulval fate in P5.p and P7.p (Figure 8), the remaining P3.p, P4.p and P8.p become 3º non-vulval cells.

Two nuclear targets of LET-23 EGFR acting through Raf/MEK/Erk involved in vulval induction are LIN-31, a winged helix (WH)-like transcription factor, and LIN-1, an Ets domain containing transcription factor. Both LIN-31 and LIN-1 can be phosphorylated by MPK-1 Erk, phosphorylation of LIN-31 disrupts the complex between LIN-31 and LIN-1, whereas inactivating mutations in *lin-31* and *lin-1* lead to excessive induction (Beitel et al., 1995; Tan et al., 1998).

In wild type animals 3 of the VPCs give rise to 22 cells of the hermaphrodite vulva. Mutations leading to decreased Ras signaling cause less than 3 VPCs being induced and a Vul phenotype. These animals fail to produce vulva and are egg-laying defective (Egl), they accumulate eggs within the uterus, which then hatch internally leading to a bag-of-worms phenotype. Alternatively, activating mutations within the Ras signaling pathway lead to excessive induction and a Muv phenotype.

1.2.3. Regulators of the LET-23 EGFR signaling

C. elegans offers a simple system for the identification of the key components of the signaling pathways involved in biological processes. Forward genetic screens have been performed to identify the core components of the LET-23 EGFR/LET-60 Ras/MPK-1 Erk signaling pathway involved in vulval induction through studying mutants with Vul and Muv phenotypes (Ferguson and Horvitz, 1985). Many of the regulators of the EGFR signaling pathway have been identified in forward or reverse genetic screens in sensitized genetic backgrounds (Figure 6). These regulators do not have pronounced phenotypes when singly mutated, but in the sensitized backgrounds may lead to robust phenotypes (Sundaram, 2013).

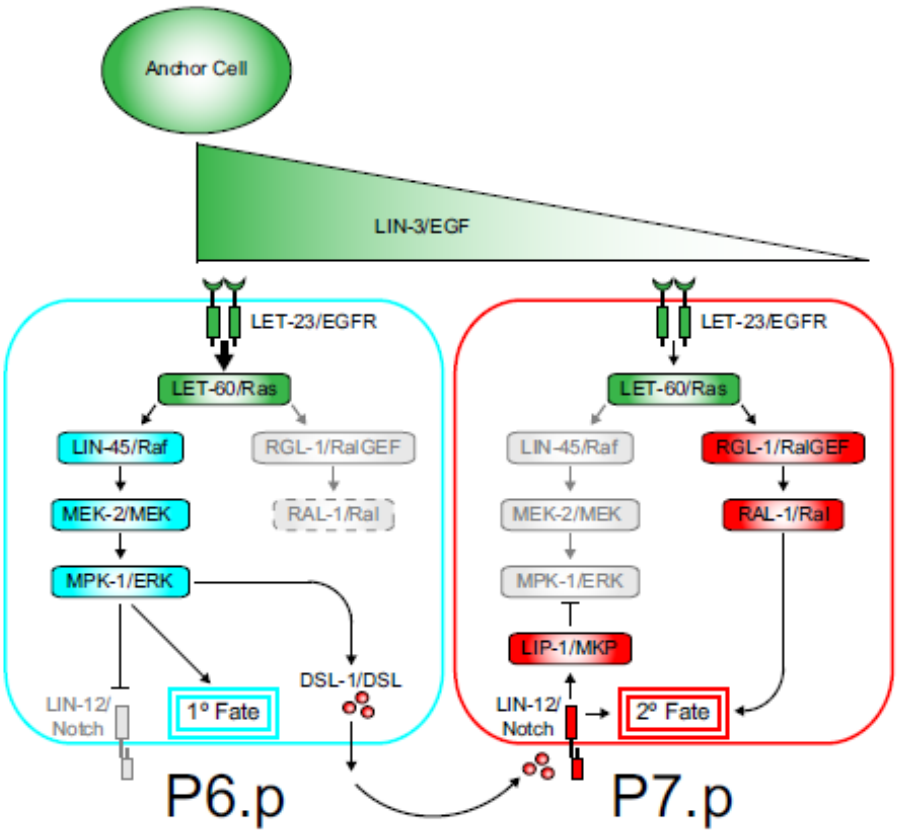

(From Zand et al., 2011)

Figure 8. Opposing vulval cell fates through LET-23 EGFR and LIN-12 Notch signaling.

The AC secretes an inductive LIN-3 EGF signal and is located above P6.p, thus LET-23 EGFR becomes engaged and the Ras signaling pathway gets activated more strongly on P6.p due to a higher ligand concentration compared to the neighbouring P5.p and P7.p cells. Ras signaling through Raf/MEK/Erk promotes the 1º fate in P6.p, activates lateral LIN-12 Notch signaling in P5.p and P7.p and leads to upregulation of DSL-1 DSL ligand and downregulation of LIN-12 Notch receptor in P6.p. LIN-12 Notch signaling in P5.p and P7.p downregulates Ras signaling through Raf/MEK/Erk by activation of LIP-1/MKP phosphatase. Additionally, low levels of LIN-3 EGF activating LET-23 EGFR on the P5.p and P7.p are proposed to result in Ras effector switching and signaling through Ral GEF, which together with LIN-12 Notch signaling promotes the 2º vulval fate in these VPCs.

1.2.3.1. Regulators of LIN-3 EGF ligand

One of the ways to regulate ligand involves restriction of its expression. LIN-3 EGF expression is restricted to the AC during vulval induction (Hill and Sternberg, 1992), in the descendants of the primary VPC P6.p during uterine development (Chang and Sternberg, 1999) and in the excretory canal cell in the process of excretory duct development (Abdus-Saboor et al., 2011). There are three sets of transcriptional regulators that function redundantly to inhibit LIN-3 EGF transcription; these are called SynMuv (Synthetic Multivulva) A, B and C. SynMuv A and B genes most of the time produce Muv phenotype when double-mutants are made between the two groups, whereas mutations in the genes from the same group usually do not have a Muv phenotype suggesting that genes belonging to the same group function together within the same complex, whereas genes from group A and B are most likely to function in parallel to each other (Fay and Yochem, 2007). Class C genes belong to the Tip60/NuA4-like histone acetyltransferase complex (Ceol and Horvitz, 2004), whereas SynMuv A genes include components of the THAP domain transcriptional repressors (Davison et al., 2005; Davison et al., 2011) and SynMuv B genes include a large number of transcriptional repressors such as the nucleosome remodeling and histone deacetylase (NuRD) complex components (Lu and Horvitz, 1998) and DRM (DP, Rb, Myb) transcriptional regulator subunits (Harrison et al., 2006). It has been shown that SynMuv A and SynMuv B genes function redundantly to suppress the expression of LIN-3 EGF by the Hyp7 hypodermis to limit ligand production to the AC (Cui et al., 2006; Myers and Greenwald, 2005).

Additional means of ligand regulation comes from ligand processing. *C. elegans* LIN-3 EGF, like other EGF family ligands, is produced as a transmembrane protein, which has to be proteolytically cleaved in order for the ligand to be secreted (Hill and Sternberg, 1992). For example, a Rhomboid homolog ROM-1 has been implicated in cleavage of the long LIN-3 EGF

isoform to promote signaling to the VPCs located more distally in respect to the AC (Dutt et al., 2004).

1.2.3.2. Regulators acting on the LET-23 EGFR

In order for the inductive LIN-3 EGF signal to occur, the LET-23 EGFR receptor has to be available on the basolateral membrane of the VPCs. The complex of three PDZ domain-containing proteins, LIN-2 Cask, LIN-7 Mint and LIN-10 Veli, positively effects EGFR signaling in the VPCs by promoting basolateral targeting of the LET-23 EGFR (Kaech et al., 1998; Simske and Kim, 1995; Whitfield et al., 1999). Another positive regulator of the signaling is the EGFR substrate protein-8 (EPS-8) that stabilizes basolateral membrane localization of LET-23 EGFR in the primary VPC by means of interaction with LIN-2/-7/-10 complex, which allows for inductive signal to occur in the primary cell lineage, whereas lower levels of EPS-8 in the neighboring secondary VPCs lead to decreased levels of LET-23 EGFR available on the basolateral membrane and thus secondary vulval cell fate (Stetak et al., 2006). Additionally, we have recently demonstrated (described in Chapter 2) that the small GTPases ARF-1.2 Arf1 and ARF-3 Arf3 as well as AGEF-1, a homolog of Big1/2 Arf GEF, function together with clathrin adaptor UNC-101 AP-1μ1 to negatively regulate LET-23 EGFR signaling during vulva induction by antagonizing basolateral targeting of the receptor in the primary VPC descendants (Skorobogata et al., 2014).

A number of negative regulators of Ras/MAPK signaling that act at the level of the receptor have been described, these are believed to promote endocytic trafficking of the LET-23 EGFR based on mammalian data. Among those are SLI-1, a homolog of an E3 ubiquitin ligase c-Cbl (Jongeward et al., 1995; Yoon et al., 1995), ARK-1, an Ack-related nonreceptor tyrosine kinase (Hopper et al., 2000), subunits of the clathrin adaptors UNC-101 AP-1μ1 and DPY-23 AP-2μ2 (Lee et al., 1994; Yoo et al., 2004), a small GTPase RAB-7 Rab7 and components of the

ESCRT-0 and ESCRT-1 complexes (Skorobogata and Rocheleau, 2012), as well as DHC-1, a heavy chain of the dynein microtubule motor (see Chapter 3). As mentioned earlier, these negative regulators do not show any vulval phenotypes when singly mutated, but are capable to modulate vulva induction in the sensitized backgrounds, and double-mutants between negative regulators functioning in parallel to each other lead to a synthetic Muv phenotype.

Additionally, tyrosine phosphatases may de-phosphorylate activated LET-23 EGFR to downregulate signaling. DEP-1, a homolog of mammalian tumor suppressor Density Enhanced Phosphatase-1, has been shown to have antagonistic role on the EGFR signaling in the secondary VPCs in conjunction with Notch signaling to promote secondary vulval fate (Berset et al., 2005).

1.2.3.3. Regulators of LET-60 Ras

LET-60 Ras belongs to the family of small GTPases, which can cycle between an inactive GDP-bound form and an active GTP-bound form. GEFs regulate the status of the GTPases by promoting the release of GDP and subsequent binding of GTP, whereas GAPs (GTPase activating proteins) activate the intrinsic GTPase activity of the small GTPase leading to hydrolysis of GTP (Cherfils and Zeghouf, 2013). LET-341 Sos is a putative LET-60 Ras GEF and is required in a number of developmental events controlled by Ras signaling, however there is a possibility that another yet unidentified LET-60 Ras GEF exists (Chang et al., 2000). Three putative LET-60 Ras GAPs have been identified, GAP-1, GAP-2 and GAP-3, they have redundant function and have been implicated in developmental events in different tissues. For example, GAP-1 negatively regulates LET-23 EGFR signaling during vulva induction in the VPCs and P12 fate specification, whereas GAP-3 functions predominantly in the gonad during meiotic progression (Hajnal et al., 1997; Stetak et al., 2008).

An additional level of LET-60 Ras regulation comes from regulation of *let-60 Ras* mRNA levels by *mir-84* and *let-7*, belonging to a family of *let-7* microRNAs. Both microRNAs act by directly binding to the 3' UTR of *let-60 Ras* mRNA to lower Ras levels, a mechanism conserved in the mammals for the regulation of *Ras* levels (Johnson et al., 2005).

1.2.3.4. Regulators of Raf-MEK-Erk cascade

Positive regulation of the kinase cascade is achieved by scaffold proteins. KSR-1 (Kinase Suppressor of Ras) (Sundaram and Han, 1995), KSR-2 (Ohmachi et al., 2002). CNK-1 (Connector enhancer of Ksr) (Rocheleau et al., 2005) and SOC-2 (Sieburth et al., 1998) do not seem have any direct enzymatic activity on the kinases, but rather form complexes with the kinases in order to bring together core components of the cascade. For example, KSR-1 and KSR-2 are individually required only for specific aspects of gonad development, in addition they have redundant functions during the majority of Ras-mediated developmental events such as excretory system, hermaphrodite vulva and male spicule development (Ohmachi et al., 2002). Double-, but not single-mutants for KSR proteins, have decreased levels of MPK-1 Erk phosphorylation and have been proposed to function downstream of activated Raf and upstream of MEK/Erk (Ohmachi et al., 2002; Rocheleau et al., 2005). The other two scaffolds are not individually required during developmental events, CNK-1 is placed upstream of Raf activation by phosphorylation (Rocheleau et al., 2005), whereas SOC-2 functions upstream of the removal of Raf inhibitory phosphorylation (Yoder et al., 2004). Moreover, the functions of scaffold proteins in *C. elegans* are in agreement with mammalian studies (Li et al., 2000; Muller et al., 2001; Yao et al., 2000).

Negative regulation of the kinase cascade signaling comes from de-phosphorylation of activated MPK-1 Erk or binding to MPK-1 Erk. MAP kinase phosphatase LIP-1 (lateral signal induced phosphatase-1), a homolog of human Mkp3/Pyst1, decreases the level of MPK-1 Erk

activity both in somatic cells and germline (Berset et al., 2001; Lee et al., 2006b). GCK-1 (Germinal Center Kinase) binds to MPK-1 Erk in the germline to prevent its activation (Schouest et al., 2009). Alternatively, GLA-3 is a zinc-finger-containing protein, which acts in the germline to negatively regulate MAPK signaling by binding to MPK-1 Erk without affecting its phosphorylation status (Kritikou et al., 2006).

1.3. Endocytic trafficking and polarity

1.3.1. Polarized epithelial cells

Epithelial cells are organized into sheets to form skin as well as the lining of major organs such as lungs, stomach and kidneys to perform multiple physiological functions. Tissues composed of epithelial cells provide a barrier and serve as protection from the environmental factors. They are also involved in nutrient absorption and play a role in secretion among other functions (Bryant and Mostov, 2008).

Asymmetric organization of plasma membrane underlies cell polarity (Orlando and Guo, 2009). The plasma membrane of polarized epithelial cells is divided into distinct basolateral and apical domains, which are separated by tight junctions (Caplan, 1997). Tight junctions localize at the border of apical and basolateral membranes and prevent the redistribution of proteins and lipids between the two domains. Additionally, tight junctions, which are multiprotein complexes that include three major transmembrane protein families, occludins, claudins and junctional adhesion molecules (JAMs), form a continuous barrier to control the movement of solutes across epithelium (Anderson and Van Itallie, 2009).

The basolateral membrane comprises desmosomes, gap junctions and adherence junctions, providing means of communication with neighbouring cells as well as contacts with the basement

membrane, a sheet of extracellular matrix providing separation of epithelial tissue from the underlying cells and connective tissue (Cao et al., 2012). The apical membrane contacts the external environment and possesses specific features such as microvilli and the primary cilium. Due to usually harsh conditions of external environments, such as for example the lumen of the digestive tract, the apical membrane has to be constructed in a way to withstand these conditions and retain integrity. The differential lipid composition between the apical and basolateral membranes provides such specificity, where sphingolipids are enriched apically and together with cholesterol form lipid rafts that are capable of providing protection (Simons and van Meer, 1988).

The integrity of the polarized epithelium is ensured by the establishment and the maintenance of polarity. The first step in establishing polarity is sensing of the cues within the extracellular matrix involving integrins, dystroglycan and proteoglycan molecules to define the basal pole and orient the cell's polarity (Cao et al., 2012). Three protein complexes, PAR, Crumbs and Scribble promote establishment of polarity by redistribution within the cell with PAR and Crumbs promoting apical polarity and Scribble promoting basolateral polarity (Bryant and Mostov, 2008). Apical and basolateral polarity complexes are mutually exclusive and, once in place, exclude each other (Watari et al., 1998). The cytoskeletal rearrangements along the axis of polarity take place in addition to redistribution of polarity complexes. Following this process, the microtubules run along the apico-basal axis of polarity with the minus end close to the nucleus at the apical surface of the cell accompanied by the overall increase in the stability of microtubules (Li and Gundersen, 2008). Additionally, short microtubules running along apical and basal surface are also present (Musch, 2004). Furthermore, actin also re-organizes with horizontal filaments running along the apical membrane, where it organizes into apical microvilli and terminal web by

interactions with ezrins and villins, and with actin filaments being organized by E-cadherin localized along the lateral membrane (Cao et al., 2012).

1.3.2. Trafficking routes in the polarized cells

In order for polarity to be established and maintained in the polarized epithelial cells, the proteins and lipids specific for apical and basolateral membranes have to be delivered appropriately (Figure 9). The trans-Golgi network (TGN) is considered to be the primary sorting station for newly synthesized proteins and lipids, where distinct types of carriers are produced to be targeted to endosomes, lysosomes, cell surface or secretory granules (Folsch et al., 2009). On the way to the appropriate plasma membrane in the biosynthetic pathway, this newly synthesized cargo is packaged into carrier vesicles and can be either directly targeted to the cell surface from the TGN or transit through one or multiple endocytic compartments (Stoops and Caplan, 2014). Polarized epithelial cells possess specialized types of endocytic compartments consistent with the need for a more precise targeting required to achieve and maintain polarity. Non-polarized cells have only one type of early endosome, whereas polarized cells have distinct apical and basolateral early endosomes (AEE and BEE, respectively) (Sheff et al., 2002). Additionally, whereas non-polarized cells have one juxtanuclear recycling endosome, which is positive for transferrin receptor (TfR) and a small GTPase Rab11, there are at least two distinct types of recycling endosomes in polarized cells (Taguchi, 2013). The common recycling endosome (CRE) in polarized cells is Rab11-negative and receives cargo from AEE and BEE (Brown et al., 2000; Sheff et al., 1999). The second type of recycling endosome present in polarized cells is the apical recycling endosome (ARE), this compartment is represented by a subapical tubular network, contains Rab11 and receives cargo transcytosed from the basolateral membrane as well as some of the apically recycling proteins (Apodaca et al., 1994; Brown et al., 2000). Most of the experiments involving

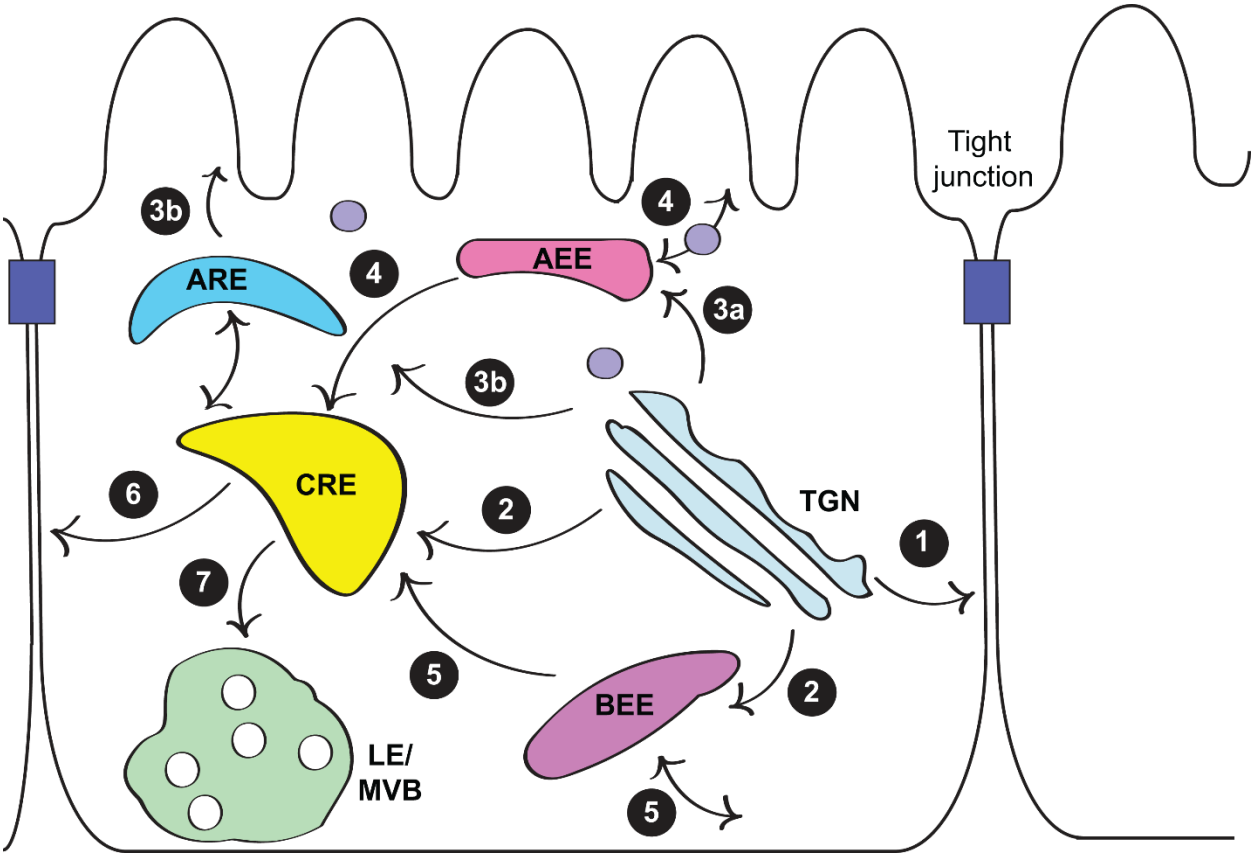

Figure 9. Biosynthetic and endocytic routes in polarized epithelial cells.

Newly synthesized basolateral proteins could reach their destination either directly from the TGN (1) or through endosomes (2). The biosynthetic route for apical cargo traffic from TGN through apical early endosome (AEE) (3a) or apical recycling endosome (ARE) (3b) prior to delivery to the cell surface. Endocytosed apical and basolateral cargo traverse AEE (4) or basolateral early endosome (BEE) (5), respectively before either being recycled back to the plasma membrane via the common recycling endosome (CRE) (6), using the same signals as the biosynthetic route, or forwarded for degradation (7).

studies of the trafficking in polarized epithelial cells have been carried out in Madin-Darby Canine Kidney Epithelial cells (MDCK). These would be presented below to describe the biosynthetic and endocytic trafficking routes to basolateral and apical membranes.

1.3.2.1. Basolateral sorting signals and trafficking routes

Basolateral sorting signals of integral membrane proteins are found within the cytoplasmic tail of the protein and are similar to those that promote rapid endocytosis and sorting to the lysosome and lysosome-related organelles (Traub and Bonifacino, 2013). The most common basolateral sorting signals are di-leucine (D/ExxxLL) and tyrosine-based motifs (NPxY or YxxØ, where x is any amino acid and Ø is a bulky hydrophobic amino acid) (Hunziker and Fumey, 1994; Hunziker et al., 1991; Matter et al., 1992). Additionally, monoleucine basolateral sorting motifs have also been identified in some proteins such as stem cell factor and CD147 (Deora et al., 2004; Wehrle-Haller and Imhof, 2001). Mutations in these motifs prevent basolateral sorting and lead to apical mislocalization of the cargo. For example, mutation in the targeting peptide motif of the low density lipoprotein receptor (LDLR) underlies a human disease, familial hypercholesterolemia–Turku variant. Mutant LDLR is missorted to the apical instead of the basolateral surface of the MDCK and hepatic epithelial cells, which results in decreased basolateral endocytosis of LDL and failure to clear cholesterol from the circulating blood leading to hypercholesterolemia (Koivisto et al., 2001).

Components of the cellular trafficking machinery, including heterotetrameric clathrin adaptor protein (AP) complexes, recognize these motifs within the cargo's cytosol-facing regions, interact directly with these sequences and promote incorporation of the cargo into nascent vesicles. Golgi-localized AP-1B, expressed specifically in a subset of polarized epithelial cells, AP-1A and AP-4 are involved in cargo sorting from the Golgi. Other members of the multimeric adaptors,

plasma membrane-localized AP-2 and endosomal AP-3 are involved in endocytosis and trafficking to the lysosome, respectively (Bonifacino, 2014). The AP complexes have to be recruited to the Golgi to promote formation of cargo-containing vesicles. Members of the ADP-ribosylation factor (Arf) family of small GTPases, Arf1 and Arf3, recruit AP-1 and AP-4 to the TGN membranes. These Arfs serve as binary switches for coat formation, where in the active GTP-bound conformation, they promote AP recruitment to the membranes and coat assembly, whereas in the inactive GDP-bound form they promote coat disassembly (Bonifacino and Lippincott-Schwartz, 2003). Thus, regulators of Arf activation status control assembly and disassembly of the AP-containing coats. Arf GEFs, such as Sec7 domain containing BIG1/2, activate Arfs by promoting release of GDP and binding of GTP, whereas GAPs, such as ARAP1, promote hydrolysis of the GTP by Arfs and lead to inactivation (Donaldson et al., 2005).

While AP-1A is found ubiquitously, AP-1B is epithelia-specific. AP-1A and B share large β and γ subunits, as well as small σ1 subunits, and have unique μ1A and μ1B medium subunits, which provide specificity to AP-1A and B function in terms of cargo recognition to produce distinct populations of carriers (Folsch et al., 1999). Moreover, AP-1B is found only in a subset of epithelial cells such as kidney distal and intestinal epithelial cells, but not in other epithelial cells (i.e. kidney proximal cells) or other polarized cell types such as hepatocytes and neurons (Bonifacino, 2014). The differential roles of AP-1A and AP-1B in cargo sorting were first observed in two kidney cell lines. The MDCK cell line, derived from kidney distal tubule cells, and the LLC-PK1 cell line, derived from kidney proximal tubule cells, can both be grown as columnar monolayer, but they sort the same cargo to different plasma membrane domains (Folsch et al., 1999). MDCK cells, which express the μ1B isoform, target TfR and LDLR basolaterally, whereas LLC-PK1 cells, which express only the μ1A isoform, deliver the same cargo apically

(Folsch et al., 1999). Interestingly, expression of μ1B subunit in LLC-PK1 cells redirects TfR and LDLR to the basolateral surface of the cells without any effect on the other apically-targeted cargo demonstrating an important role of the μ1 subunit in basolateral cargo sorting (Folsch et al., 1999). Consistent with the role of AP-1 in basolateral protein targeting, the clathrin coat was also shown to be required for biosynthetic delivery and recycling of cargo to the basolateral membrane of polarized epithelial cells (Deborde et al., 2008).

Both AP-1A and AP-1B have been shown to localize to TGN as well as CRE and to co-localize with each other, additionally they show preferential interactions with some cargo (Guo et al., 2013). It has been proposed that AP-1B allows for more efficient delivery of some cargo to the basolateral membrane as well as to expand the repertoire of cargo targeted basolaterally in cells expressing the μ1B subunit. Indeed, AP-1B has been shown to bind some cargo with higher affinity compared to AP-1A. For example, AP-1B binds sorting signals contained within LDLR with five-fold higher affinity compared to AP-1A (Guo et al., 2013). Cargo targeted by AP-1 from the TGN to the basolateral membrane is delivered either directly to the plasma membrane or may traffic through CRE or BEE (Folsch et al., 2009). Additionally, non-conventional adaptors could also be involved in biosynthetic cargo sorting. In such a way syndecan-1 is targeted to the basolateral membrane of MDCK cells, this distribution has been shown to depend on syndecan-1 PDZ (PSD-95, discs large, ZO-1) domain interaction with a yet unidentified cytosolic PDZ domain-containing protein, and this localization is mediated by targeting rather than retention of syndecan-1 at the basolateral membrane (Maday et al., 2008).

The role of AP-1 in basolateral cargo sorting still remains to be fully elucidated. There are multiple models that could explain AP-1 function. Some studies have demonstrated that AP-1 and clathrin are not required to strictly deliver basolateral cargo, but rather to exclude basolaterally-

targeted proteins from proteins destined to the apical membrane (Carvajal-Gonzalez et al., 2012; Deborde et al., 2008). Thus, AP-1 could function to exclude basolateral cargo from apical carriers by incorporating them into clathrin coated vesicles (CCV), or it could remove basolateral cargo from the apical carriers and re-direct these proteins to the proper membrane (Bonifacino, 2014). Finally, AP-1 could promote formation of the specialized domain at the TGN/CRE, where basolateral cargo would be segregated away from the sites of apical carrier formation (Bonifacino, 2014).

1.3.2.2. Apical cargo sorting

In contrast to conserved cytosolic peptide sequences targeting cargo basolaterally, apical sorting signals are more diverse and can be located in the cytoplasmic, transmembrane or extracellular regions of the protein (Stoops and Caplan, 2014). The nature of the apical sorting signals could be based on amino acids, lipids or carbohydrates. One of the first apical targeting signals to be identified comes from the discovery that endogenous glycosylphosphatidylinositol anchored proteins (GPI-APs) are localized to the apical membrane of polarized MDCK cells (Lisanti et al., 1988). Further studies showed that attachment of the GPI anchor to a basolateral antigen or a secreted protein leads to incorporation into apical surface of polarized epithelial cells (Lisanti et al., 1989). Moreover, the proteins containing this extracellular lipid attachment tend to oligomerize and cluster into detergent-resistant membrane domains that lack basolaterally targeted proteins, which is consistent with the idea that lipid rafts play an important role in apical cargo targeting (Brown and Rose, 1992; Paladino et al., 2004; van Meer and Simons, 1988). It has been proposed that GPI-APs incorporate into these microdomains due to their affinity for glycosphingolipid-enriched rafts, which form vesicles destined for the apical membrane (Stoops and Caplan, 2014).

N-glycans and O-glycans, carbohydrate modifications, represent a second group of apical sorting signals. Removal of N-glycans or O-glycans leads to loss of polarized distribution of apical erythropoietin and neurotrophin receptor, respectively (Kitagawa et al., 1994; Yeaman et al., 1997). Furthermore, addition of the N-glycan to normally non-glycosylated growth hormone results in its apical secretion rather than being secreted without polarity (Scheiffele et al., 1995). It appears that N-glycans are recessive to basolateral sorting signals since many of the basolaterally targeted proteins are N-glycosylated, but become targeted to the apical membrane only following the removal of the cytosolic basolateral sorting signal; it has been proposed that this basolateral signal may have a higher affinity to its sorting machinery compared to exoplasmic N-glycans (Fiedler and Simons, 1995). Lectins have been described as the sorting receptors that promote clustering of N-glycosylated proteins to apical carriers (Delacour et al., 2009). Alternatively, N-glycans are viewed not as sorting signals but rather as structural components that allow for efficient protein folding and prevent aggregation thus promoting interactions of other regulatory sequences with apical sorting receptors or lipid domains (Rodriguez-Boulan and Gonzalez, 1999).

Additionally, sequences found in the transmembrane regions have been implicated in the apical sorting of proteins such as the α subunit of gastric H, K- adenosine triphosphatase (ATPase) protein, influenza virus hemagglutinin and neuraminidase (Barman and Nayak, 2000; Dunbar et al., 2000; Lin et al., 1998). All major classes of apical targeting sequences have been implicated in clustering of the cargo into detergent-resistant microdomains (Stoops and Caplan, 2014). However, the role of lipid raft association on apical cargo delivery is contradictory since exclusion of the proteins from the lipid rafts either by removing transmembrane sequences required for this association or mild depletion of cells of cholesterol to prevent GPI-APs from raft association still resulted in apical delivery of the cargo in question (Lipardi et al., 2000; Tall et al., 2003). In their

review Rodriguez-Boulan et al. have proposed that apical sorting sequences promote cargo association with small lipid rafts, which are further clustered into big apical sorting platforms and that any feature of the protein that promotes oligomerization could promote apical targeting (Rodriguez-Boulan et al., 2005).

1.3.2.3. Endosomes as sorting stations

Endosomes serve as major sorting stations during both endocytic and biosynthetic events aimed at protein, lipid and solute trafficking. In the biosynthetic route some of the basolateral cargo is delivered to CRE prior to reaching its destination, where AP-1 is involved in further sorting to the basolateral membrane. AEE and BEE accept cargo endocytosed in an AP-2-dependent manner from apical and basolateral membranes, respectively (Sheff et al., 2002). This cargo is then either directly sent back to the cell surface via a fast recycling route, targeted for lysosomal degradation, or for a slow recycling, passed on to the CRE (Stoops and Caplan, 2014). At the CRE the same signals that are used for sorting in the biosynthetic pathway are used to sort cargo either back to the appropriate membrane domains, or to the ARE (Stoops and Caplan, 2014). AREs have a cup-like shape, are localized to the subapical compartment, are positive for the Rab11 GTPase (Lapierre et al., 2003) and its interactor, the Myosin Vb (Myo Vb) motor (Lapierre et al., 2001). Moreover, their importance in establishment and maintenance of polarity *in vivo* has been shown (Winter et al., 2012). Mutations in Myo Vb gene lead to microvillus inclusion disease, a lethal congenital disorder characterized by failure to produce mature apical membranes in enterocytes (Ruemmele et al., 2010). The ARE is viewed as an important apical sorting station, however there is evidence that some basolateral cargo such as E-cadherin could pass through ARE prior to basolateral delivery (Lock and Stow, 2005). The ARE as well as the TGN cluster around the subapical centrosome in a microtubule-dependent manner (Musch, 2004).

Multiple pathways through the endosomal system have been observed for the biosynthetic delivery of cargo targeted to the apical surface. The role of the AEE and ARE in the apical delivery of the newly synthesized raft-dependent and raft-independent proteins have been demonstrated by selectively disrupting function of either compartment (Cresawn et al., 2007; Mattila et al., 2009). Disrupting the function of the ARE by overexpression of dominant-negative Myo Vb motor resulted in perturbation in apical delivery of non-raft associated endolyn, but had no effect of the apical trafficking of raft-dependent influenza hemagglutinin, whereas horseradish peroxidase-dependent ablation of AEE disrupted influenza hemagglutinin but not endolyn apical delivery (Cresawn et al., 2007). Additionally, proteins relying on glycan-dependent apical targeting signals transit through the ARE, this has been demonstrated through inactivation of the ARE exit by overexpression of the Myo Vb tail, which disrupted delivery of heavily glycosylated MUC1 to the apical surface, whereas treatment with horseradish peroxidase to inhibit the function of the AEE had no effect on MUC1 apical delivery (Mattila et al., 2009).

Moreover, there is evidence that in addition to cargo being sorted to different types of endosomal compartments, there exist subdomains within the same endosome that facilitate cargo sorting (Miaczynska and Zerial, 2002). Immuno-electron microscopy was used to show that continuous endosomal membranes are compartmentalized, where recycling endosomes contain distinct Rab4 and Rab11 positive domains and early endosomes have Rab4 and Rab5 domains (Sonnichsen et al., 2000). This theory of lateral segregation is further supported by accumulation of the cargo destined for lysosomal degradation in the spherical part of the early endosome, whereas recycling cargo is segregated into the tubular domains of the early endosome (Mayor et al., 1993).

Interestingly, MVBs, which normally play a role in cargo delivery to the lysosome for degradation, could fuse directly with the apical and basolateral membranes to release apical and basal exosomes (Lakkaraju and Rodriguez-Boulan, 2008). Finally, the CRE has a role in sorting of cargo undergoing transcytosis from the apical to the basolateral membrane or from the basolateral to the apical membrane, away from the cargo that has to be recycled back to the appropriate membrane following endocytosis (Musch, 2004).

1.3.2.4. Cargo transport to the plasma membrane

In order to maintain epithelial polarity, the cargo sorted at the TGN and CRE or endocytosed from the plasma membrane needs to be delivered to the apical or basolateral membranes. For this, sorting events must be synchronized with the transport of the cargo-containing vesicles. These events are coordinated by Rab proteins as well as components of microtubule and actin cytoskeleton.

Disruption of microtubules with pharmacological agents have been shown to preferentially inhibit apical cargo delivery (Musch, 2004). These observations are not surprising given the microtubule structure in polarized MDCK and Caco-2 (human intestinal) cells, where the majority of microtubules run along the apico-basal polarity axis with their minus end oriented towards apical membrane and their plus end directed towards the basolateral membrane in addition to a stable subcortical network of horizontal microtubules (Bacallao et al., 1989; Gilbert et al., 1991). Consistently, microtubule motors such as dynein and several kinesins, which include KIFC3, KIF5B, KIF1A and KIF16B, have been implicated in apical carrier delivery (Rodriguez-Boulan and Macara, 2014). For example, cytoplasmic dynein, a minus end-directed microtubule motor, has been shown to interact with the C-terminal of rhodopsin via dynein light chain, and to promote targeting of rhodopsin to the apical membrane of MDCK cells (Tai et al., 1999). Another minus

end-directed motor KIFC3 is involved in the apical delivery of influenza hemagglutinin (Noda et al., 2001). Interestingly, some cargo relies on different motors for membrane delivery in non-polarized and polarized MDCK cells. This is the case for p75-neurotrophin receptor, which relies on KIF5B for the delivery to the apical membrane of polarized MDCK cells, but uses KIF1A and KIF1Bβ for post-Golgi trafficking in non-polarized MDCK cells (Xue et al., 2010).

In contrast to the critical role of microtubules and microtubule motors in apical cargo delivery, basolateral carriers rely extensively on the actin cytoskeleton. Myosin 2 and myosin VI actin motors are required for basolateral delivery of vesicular stomatitis virus G protein (VSVG) and tyrosine motif-containing proteins, respectively (Au et al., 2007; Musch et al., 1997). Basolateral vesicle carriers fuse with the plasma membrane exclusively in the upper third portion of the lateral membrane in close proximity to tight junctions, a location consistent with the t-SNARE syntaxin-4 localization in polarized MDCK cells (Kreitzer et al., 2003). Basolateral fusion sites and lateral localization of syntaxin-4 do not depend on the polarization status of microtubules, whereas their dependence on actin cytoskeleton and its regulators (such as Cdc42) has been demonstrated (Rodriguez-Boulan et al., 2005). Disruption of actin cytoskeleton by Latrunculin B treatment led to defects in basolateral cargo recycling and delivery of basolaterally-endocytosed cargo to the apical membrane (Durrbach et al., 2000; Sheff et al., 2002). Moreover, loss of Cdc42 function by overexpression of the dominant-negative form leads to selective inhibition of basolateral membrane traffic within both biosynthetic and endocytic pathways, but has no effect on apical cargo polarized distribution (Cohen et al., 2001; Kroschewski et al., 1999).

1.4. EGFR distribution in polarized epithelial cells

In polarized epithelial cells EGFR distribution is restricted mainly to the basolateral membranes. For example, in polarized MDCK cells more than 90% of the total EGFR is found on the basolateral surface (Singh et al., 2013). This polarized distribution of EGFR in the MDCK cells have been shown to depend on two basolateral sequences within its juxtamembrane domain, which contains a conserved basolateral leucine-based targeting motif as well as a polyproline-containing region (He et al., 2002). The dileucine-based motif is recognized by the AP-1B adaptor representing one of the mechanisms for the basolateral EGFR targeting, whereas the polyproline-containing region is involved in an AP-1B-independent constitutive basolateral trafficking route for which an adaptor is yet to be identified (Ryan et al., 2010). Loss of polarized distribution of membrane proteins including EGFR underlies a number of disorders. In polycystic kidney disease (PKD) a number of basolaterally localized cargos such as EGFR, Na^+ K^+-ATPase and Na^+ K^+ $2Cl^-$ symporter are mistargeted to the apical membranes of the renal tubule epithelia (Wilson, 2011). It has been proposed that in PKD, mislocalization of EGFR is responsible for the severity of the disease due to enhancement of cysts as a result of increased EGFR signaling activity as well as for its effect on the molecular network involved in tubule formation during development in pre-PKD kidney (Cotton et al., 2013; Wilson, 2011).

C. elegans provides an excellent model for studying polarized epithelia *in vivo*. Moreover, the importance of polarized distribution of EGFR *in vivo* comes from studies in this nematode. As mentioned earlier, VPCs are polarized epithelial cells, which form the vulva, an egg-laying apparatus of the worm, as a result of synchronized EGFR and Notch signaling. LET-23 EGFR is localized to both apical and basolateral membranes of the VPCs (Figure 10). During vulval induction, the AC in the overlying gonad secretes a LIN-3 EGF-like ligand to induce LET-23

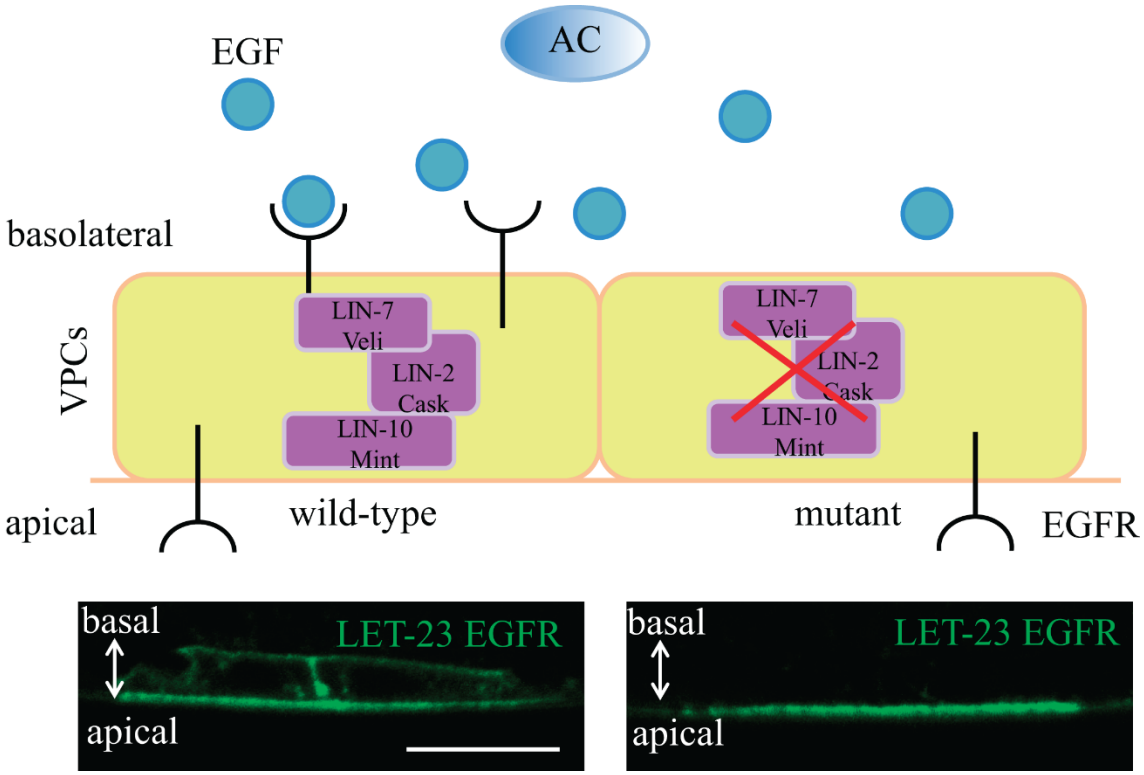

Figure 10. LET-23 EGFR localization in the VPCs.

LET-23 EGFR is localized to both basolateral and apical membranes of the VPCs. Its basolateral localization is required in order to receive an inductive LIN-3 EGF signal coming from the AC. A tripartite complex consisting of LIN-2 Cask/LIN-7 Veli/LIN-10 Mint is required for basolateral LET-23 EGFR localization. Mutations in either component of this complex result in a Vul phenotype due to loss of basolateral LET-23 EGFR and inability to receive LIN-3 EGF signal. Confocal images of the P6.p descendants demonstrate the localization of GFP-tagged LET-23 EGFR in live animals at the early L3 larval stage. Note that the receptor is localized both apically and basolaterally in the wild-type animals (left image) and becomes apical only in the *lin-2(e1309)* mutant (right image). Apical and basolateral membranes are shown with arrows, the apical membrane is oriented towards the bottom of the image and the basolateral membrane is facing upwards. Bar, 5 µm.

EGFR specifically on the basolateral membrane of the proximal P6.p to promote primary vulval fate. It has been shown that a tripartite complex consisting of LIN-2 Cask/LIN-7 Veli/LIN-10 Mint is required for the basolateral LET-23 EGFR localization in the VPCs (Kaech et al., 1998; Whitfield et al., 1999).

LIN-7 contains a single PDZ (PSD 95, a postsynaptic density protein; Dlg (*Drosophila* Disc large); and ZO-1) domain, which is involved in protein-protein interactions with other PDZ domain-containing proteins and C-terminal parts of proteins (Kim, 1997). LIN-2 encodes a homolog of mammalian Lin2/Cask, which belongs to the family of membrane-associated guanylate kinases (MAGUKs) that also includes PSD-95 and disc-large A (DlgA) (LaConte and Mukherjee, 2013). PSD-95 binds C-terminal tail of the NR2 subunit of the NMDA receptor as well as Shaker-type K^+ channels and is believed to play a role in either the localization of the ion channel subunits to the plasma membrane or in their clustering at the plasma membrane (Sheng, 1996). Both mammalian and fly DlgA binds the C-terminus of the Shaker-type K^+ channels and has been shown to function in the neuro-muscular junction synaptic localization and clustering of Shaker channels in *Drosophila* (Rafael et al., 1998; Tejedor et al., 1997). LIN-2 contains a CaM kinase domain, a PDZ domain, an SH3 domain and a guanylate kinase domain (Kaech et al., 1998). LIN-10, a Mint (Munc18-interacting) homolog, has a CID (CASK interacting domain) domain, a PTB (phosphotyrosine binding) domain and two PDZ domains (Kaech et al., 1998).

Animals mutant for LIN-2, LIN-7 or LIN-10 are Vul due to failure in vulval induction as a result of exclusively apical localization of LET-23 EGFR in the VPCs, where the receptor is unable to receive the inductive paracrine LIN-3 EGF signal (Kaech et al., 1998; Simske et al., 1996; Whitfield et al., 1999). It has been shown that LIN-7 interacts with the C-terminus of the

LET-23 EGFR via its PDZ domain. The LIN-7 L27 domain, which is N-terminal to the PDZ domain, binds the region of LIN-2 between its CaM kinase and PDZ domains, and that CaM kinase domain of LIN-2 binds to CID domain of LIN-10 (Kaech et al., 1998). Thus, LIN-2/7/10 form a ternary complex, where LIN-2 interacts with both LIN-7 and LIN-10, and LIN-7 in turn binds LET-23 EGFR, and this complex is required for the basolateral localization of LET-23 EGFR in the *C. elegans* VPCs. EPS-8 has been shown to associate with LIN-2 to promote retention of the LET-23 EGFR on the basolateral surface of the primary VPC (Stetak et al., 2006).

Similar complexes exist in mammals as well. For example, Mint1 and Veli binding to CASK to form a tripartite complex involved in synaptic vesicle exocytosis in the rat brain (Butz et al., 1998). Furthermore, the role of the same complex has been shown in trafficking of the Kir2.2 inward rectifier potassium channels in the rat brain (Leonoudakis et al., 2004). Moreover, when expressed in the polarized MDCK cells, Kir2.2 is targeted to the basolateral membrane, a process dependent on CASK-containing complex (Leonoudakis et al., 2004). Together these findings provide a basis for the role of CASK, Mint and Veli proteins in polarized targeting of receptors and channels to the cell surface. It has been proposed that the ability of Mint to interact with microtubules via the KIF17 motor and with the Munc-18 docking machinery leads to synaptic delivery of the NMDA receptor subunit NR2B in the neuronal dendrites (Setou et al., 2000), by analogy, the above tripartite complex could play a role in basolateral cargo targeting. Moreover, the localization of mammalian CASK to the basolateral membrane of various polarized epithelial cells and its ability to interact with syndecan-2, which could bind extracellular matrix, and actin-binding protein 4.1, is considered to allow CASK to act as a scaffold at the plasma membrane and promote signal transduction cascades (Cohen et al., 1998). Additionally, three different mammalian Lin7 Veli isoforms have been shown to be expressed in various regions of the kidney,

with a potential to regulate basolateral cargo localization (Olsen et al., 2005). Finally, all four human ErbB receptors are expressed basolaterally in the polarized epithelial cells and this localization is mediated by human Lin7 with the PDZ domain involved in the stabilization at the basolateral surface and kinase interacting domain (KID) playing a role in the targeting of the receptor to the basolateral membrane (Shelly et al., 2003).

Given that a large number of epithelial-derived tumors overexpress EGFR and the receptor has a polarized distribution with most of the EGFR localized to basolateral membranes, further understanding of the mechanisms involved in targeted distribution of the receptor is required to identify novel targets for anti-cancer therapies.

1.5. Rationale and objectives

Our previous work demonstrated that a small GTPase RAB-7 antagonizes LET-23 EGFR signaling during *C. elegans* vulva induction (Skorobogata and Rocheleau, 2012). However, RAB-7 has never been found in previous screens for negative regulators of Ras signaling. *rab-7(ok511)* mutants are maternal effect embryonic lethal, where homozygous *rab-7* mutants coming from heterozygous mothers are viable, they do not have any progeny themselves and lay dead eggs only. Thus, it is possible that the previous screens have selected for viable mutants only. We have developed a strategy, where a recovery of potentially lethal mutants is possible (Figure 11). The goal of the screen was to identify novel negative regulators of EGFR signaling, which may play a role in the receptor trafficking and potentially function with RAB-7. The screen was performed in the Vul *lin-2(e1309)* background. The hermaphrodites were mutagenized with EMS (ethyl methanesulfonate) and allowed to have progeny, which would carry any new mutations in a heterozygous form. The F1 generation was then transferred to individual plates and its progeny

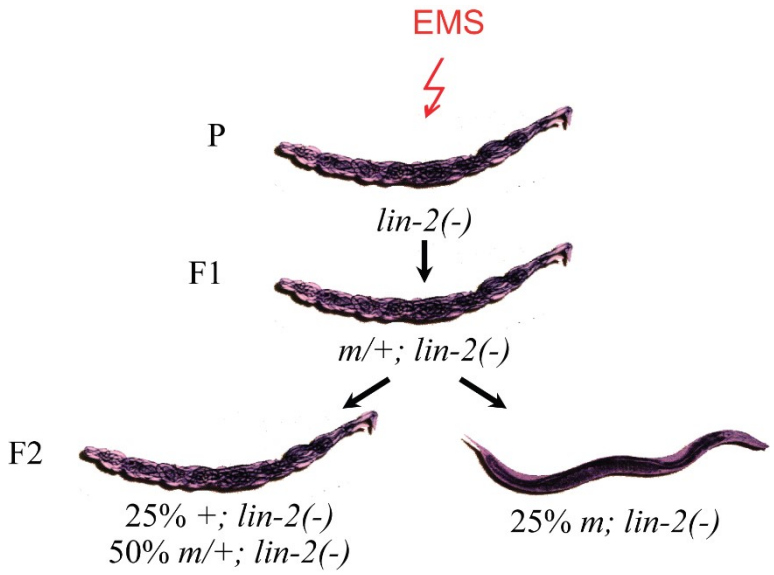

Figure 11. Strategy for the clonal forward genetic screen to uncover novel negative regulators of LET-23 EGFR signaling.

lin-2(e1309) Vul animals were mutagenized with EMS. The F1 progeny, heterozygous for the new mutation, were plated individually and the F2 progeny were screened for the suppression of the Vul phenotype (i.e. presence of egglayers). Suppressed animals (homozygous for the mutation of interest) were isolated along with about 4 non-suppressed siblings (50% of these animals are expected to carry the mutation of interest in a heterozygous form) to allow for the propagation of the potentially lethal mutations. Only mutants that were both able to suppress the *lin-2* Vul phenotype and had unique phenotypes, which were not previously described for the known negative regulators of LET-23 EGFR signaling, were kept. Two out of seven suppressors identified were further pursued due to presence of high degree of suppression and trafficking-related phenotypes.

was screened for the suppression of the Vul phenotype by looking for animals able to lay eggs. The suppressed animals (homozygous for mutation) were then isolated along with their siblings (some of which would be heterozygous for the mutation of interest) to allow for the recovery of lethal mutations. The screen led to identification of seven suppressors of the *lin-2(e1309)* Vul phenotype, two of which had the strongest level of suppression and phenotypes consistent with trafficking defects. The objectives of my thesis were to determine the identity of these genes, to place the mutants within the LET-23 EGFR/LET-60 Ras signaling pathway and to characterize the mechanisms, which underlie the ability of these negative regulators to antagonize signaling.

CHAPTER 2: An AGEF-1/Arf GTPase/AP-1 Ensemble Antagonizes LET-23 EGFR Basolateral Localization and Signaling during *C. elegans* Vulva Induction

Olga Skorobogata, Juan M. Escobar-Restrepo, Christian E. Rocheleau

Reproduced from *PLoS Genetics*. 2014 10(10): e1004728.

doi:10.1371/journal.pgen.1004728

PREFACE

The *vh4* mutant had the highest level of suppression of the *lin-2(-)* Vul phenotype among the mutants that we have identified in the genetic screen for the negative regulators of the EGFR/Ras/MAPK signaling during vulval induction. Additionally, its partial embryonic lethality, dumpy body and uncoordinated movement phenotypes distinguished it from the already known suppressors of Ras signaling. Moreover, the enlarged vesicles present in macrophage-like cells suggested a presence of a trafficking defect. Thus, this mutant was chosen for further characterization. We have cloned this gene and determined that it codes for AGEF-1, a homolog of the mammalian BIG1/2 Arf GEFs. The involvement of BIG1/2 in regulating the strength of EGFR signaling has not been previously demonstrated. However, following the publication of our study, BIG1/2 were found by whole-genome sequencing to be mutated in multiple cancer cell lines, thus making our discovery relevant to human disease and further supporting the role for AGEF-1 BIG1/2 as a negative regulator of EGFR signaling.

ABSTRACT

LET-23 Epidermal Growth Factor Receptor (EGFR) signaling specifies the vulval cell fates during *C. elegans* larval development. LET-23 EGFR localization on the basolateral membrane of the vulval precursor cells (VPCs) is required to engage the LIN-3 EGF-like inductive signal. The LIN-2 Cask/LIN-7 Veli/LIN-10 Mint (LIN-2/7/10) complex binds LET-23 EGFR, is required for its basolateral membrane localization, and therefore, vulva induction. Besides the LIN-2/7/10 complex, the trafficking pathways that regulate LET-23 EGFR localization have not been defined. Here we identify *vh4,* a hypomorphic allele of *agef-1,* as a strong suppressor of the *lin-2* mutant Vulvaless (Vul) phenotype. AGEF-1 is homologous to the mammalian BIG1 and BIG2 Arf GTPase guanine nucleotide exchange factors (GEFs), which regulate secretory traffic between the Trans-Golgi network, endosomes and the plasma membrane via activation of Arf GTPases and recruitment of the AP-1 clathrin adaptor complex. Consistent with a role in trafficking we show that AGEF-1 is required for protein secretion and that AGEF-1 and the AP-1 complex regulate endosome size in coelomocytes. The AP-1 complex has previously been implicated in negative regulation of LET-23 EGFR, however the mechanism was not known. Our genetic data indicate that AGEF-1 is a strong negative regulator of LET-23 EGFR signaling that functions in the VPCs at the level of the receptor. In line with AGEF-1 being an Arf GEF, we identify the ARF-1.2 and ARF-3 GTPases as also negatively regulating signaling. We find that the *agef-1(vh4)* mutation results in increased LET-23 EGFR on the basolateral membrane in both wild-type and *lin-2* mutant animals. Furthermore, *unc-101(RNAi)*, a component of the AP-1 complex, increased LET-23 EGFR on the basolateral membrane in *lin-2* and *agef-1(vh4); lin-2* mutant animals. Thus, an AGEF-1/Arf GTPase/AP-1 ensemble functions opposite the LIN-2/7/10 complex to antagonize LET-23 EGFR basolateral membrane localization and signaling.

INTRODUCTION

C. elegans vulval cell induction requires a highly conserved Epidermal Growth Factor Receptor (EGFR)/ Ras GTPase/ Mitogen Activated Protein Kinase (MAPK) signaling pathway providing an *in vivo* model in which to study signaling in a polarized epithelia (Sternberg, 2005; Sundaram, 2013). During larval development, an equivalence group of six vulval precursor cells (VPCs), P3.p-P8.p, have the potential to be induced to generate the vulva. The anchor cell in the overlying gonad secretes the LIN-3 EGF-like ligand, inducing the closest VPC, P6.p, to adopt the primary vulval fate, and a combination of graded LIN-3 EGF signal and lateral signaling by LIN-12 Notch specifies the neighboring VPCs, P5.p and P7.p, to adopt the secondary vulval fate. Together P5.p-P7.p generate the 22 nuclei of the mature vulva, eight cells from the primary cell and seven from each of the secondary cells. The remaining VPCs, P3.p, P4.p, and P8.p, divide once and fuse with the surrounding hypodermal syncytium (50% of the time P3.p fuses prior to dividing) and thus adopt a tertiary non-vulval fate. Inhibition of LET-23 EGFR signaling causes a Vulvaless (Vul) phenotype in which less than the normal three VPCs are induced. Conversely, increased LET-23 EGFR signaling causes a Multivulva (Muv) phenotype in which greater than three VPCs are induced.

LET-23 EGFR localizes to both the apical and basolateral membranes of the VPCs, though, it is the basolateral localization that is thought to engage LIN-3 EGF and induce vulva induction (Haag et al., 2014; Kaech et al., 1998; Whitfield et al., 1999). A tripartite complex of proteins, LIN-2 Cask, LIN-7 Veli, and LIN-10 Mint (LIN-2/7/10), interacts with the C-terminal tail of LET-23 EGFR and is required for its basolateral localization (Kaech et al., 1998; Whitfield et al., 1999). Mutations in any component of the complex, or the *let-23(sy1)* mutation, which deletes the last six amino acids of LET-23 EGFR that are required for its interaction with LIN-7, result in LET-23

EGFR localizing only to the apical membrane and a strong Vul phenotype (Aroian et al., 1994; Aroian and Sternberg, 1991; Ferguson and Horvitz, 1985; Kaech et al., 1998; Whitfield et al., 1999). The Vul phenotype of *lin-2/7/10* mutants or the *let-23(sy1)* mutant are easily suppressed to a wild-type or even a Muv phenotype by loss of negative regulators of LET-23 EGFR signaling such as *sli-1 Cbl, gap-1 RasGAP, rab-7 GTPase,* and *unc-101 AP-1μ* (Haag et al., 2014; Hajnal et al., 1997; Jongeward et al., 1995; Lee et al., 1994; Skorobogata and Rocheleau, 2012). Thus far, no suppressors of the *lin-2/7/10* mutant Vul phenotype have been shown to restore LET-23 EGFR to the basolateral membrane.

UNC-101 and APM-1 are two μ1 subunits for the AP-1 adaptor protein complex, which function redundantly to antagonize vulva cell induction (Lee et al., 1994; Shim et al., 2000). In mammals, AP-1 localizes to the *trans*-Golgi network (TGN) and endosomes, promotes formation of clathrin-coated vesicles, and is involved in regulated secretion from the TGN. (Braulke and Bonifacino, 2009; Gonzalez and Rodriguez-Boulan, 2009; Robinson, 2004). In epithelial cells, AP-1 sorts cargo, including EGFR, to the basolateral membrane, which would be inconsistent with AP-1 antagonizing signaling (Bonifacino, 2014; Ryan et al., 2010). The small GTPase, Arf1, recruits AP-1 to the TGN and thus facilitates the formation of clathrin-coated vesicles (Robinson, 2004; Stamnes and Rothman, 1993; Traub et al., 1993). BIG1 and BIG2 are Sec7 domain containing guanine nucleotide exchange factors (GEFs) for class I Arf GTPases (Morinaga et al., 1996; Togawa et al., 1999), and are required for recruitment of AP-1 to the TGN and endosomes (Ishizaki et al., 2008; Manolea et al., 2008). To date, neither Arf1 nor the BIG1/2 GEFs have been implicated in EGFR/Ras/MAPK signaling.

Here we identify *C. elegans* AGEF-1, a homolog of yeast Sec7p and the mammalian BIG1 and BIG2 Arf GEFs, as negatively regulating EGFR/Ras/MAPK-mediated vulva induction. We

show that AGEF-1 regulates protein secretion in multiple tissues, regulates polarized localization of the SID-2 transmembrane protein in the intestine, and regulates the size of late endosomes/lysosomes with the AP-1 complex in the macrophage/scavenger cell-like coelomocytes. Genetic epistasis places AGEF-1 upstream or in parallel to LET-23 EGFR. We find that the ARF-1.2 and ARF-3 GTPases also negatively regulate LET-23 EGFR signaling. Moreover, our genetics are consistent with AGEF-1 BIG1/2, ARF-1.2 Arf1 and UNC-101 AP-1μ1 functioning together in preventing ectopic vulva induction. It has been 20 years since UNC-101 was identified as a negative regulator of LET-23 EGFR signaling, however its mechanism of action has remained an enigma (Lee et al., 1994). Contrary to the role of AP-1 in basolateral sorting in mammalian cells, we demonstrate that AGEF-1 BIG1/2 and UNC-101 AP-1μ1 antagonize the basolateral membrane localization of LET-23 EGFR in the VPCs. Thus, the AGEF-1/Arf GTPase/AP-1 ensemble antagonizes LET-23 EGFR-mediated vulva induction via regulation of LET-23 EGFR membrane localization.

MATERIALS AND METHODS

Strains and alleles

General methods for the handling and culturing of *C. elegans* were as previously described (Brenner, 1974). *C. elegans* Bristol strain N2 is the wild-type parent for all the strains used in this study; *E. coli* stain HB101 was used as a food source. The Hawaiian strain CB4856 was used for SNP mapping. All experiments were performed at 20°C. Information on the genes and alleles used in this work can be found on WormBase (www.wormbase.org) and are available through Caenorhabditis Genetics Center (www.cbs.umn.edu/cgc) unless otherwise noted in the strain list (Table S1).

lin-2(e1309) suppressor screen

lin-2(e1309) L4 hermaphrodites were mutagenized as previously described (Brenner, 1974). F1 progeny (*m/+; lin-2*) were transferred to individual plates. Due to the strong Vul phenotype of *lin-2(e1309)* animals, the self-progeny hatch internally (Ferguson and Horvitz, 1985) . F2 progeny were screened at the adult stage in order to identify plates that had a large number of eggs and egg-layers, additional preference was given to plates that had Muv, embryonic lethality, or dumpy phenotypes, similar to the *rab-7(ok511)* mutant. Progeny of a total of 2430 F1 animals (4860 haploid genomes) were screened and two *lin-2 (e1309)* suppressor mutants that are dumpy and partly embryonic lethal were identified, *vh4* and *vh22*.

Genetic mapping and cloning of *agef-1(vh4)*

Single nucleotide polymorphism (SNP) mapping was used to place *vh4* to the right arm of chromosome I (Davis et al., 2005). Chromosome mapping showed linkage of *vh4* to SNPs at 13 (F58D5), 14 (T06G6) and 26 (Y105E8B) map units (m.u.). Interval mapping using two sets of recombinants, 141 animals in total, was conducted using the following SNPs: *pkP1133* at 17.4 m.u (A/T Bristol/CB4856, RFLP DraI); *pkP1134* at 18.95 m.u. (T/C Bristol/CB4856, RFLP AflIII); *haw14061* at 19.51 m.u. (T/C Bristol/CB4856, sequencing); *haw14137* at 20.65 m.u. (T/A Bristol/CB4856, sequencing); *haw14164* at 21.04 m.u. (C/T Bristol/CB4856, sequencing); *CE1-248* at 21.97 m.u. (T/A Bristol/CB4856, sequencing); *CE1-220* at 23.16 m.u. (A/G Bristol/CB4856, sequencing); *pkP1071* at 23.4 m.u. (C/T Bristol/CB4856, RFLP EcoRI). In the course of interval mapping the following predicted sequencing SNPs were confirmed: *haw14061* and *haw14137* as T/C and T/A Bristol/CB4856, respectively. Genomic DNA from *vh4* and *vh22* was isolated and submitted to Genome Quebec for Illumina sequencing. Within the defined map region, the *agef-1* gene was the only gene carrying a non-synonymous mutation unique to the *vh4* strain.

RNA interference

RNAi feeding was performed essentially as previously described (Kamath et al., 2001) using the *unc-101* (I-6G20), *agef-1* (I-6L22), *arf-1.2* (III-3A13), and *arf-3* (IV-4E13) clones from Ahringer RNAi library (Geneservice, Cambridge, United Kingdom). Clones were verified by DNA sequencing. To avoid embryonic and larval lethal phenotypes, synchronized L1 larvae were placed on RNAi plates and scored for vulva induction when the animals reached L4 stage 36-48 hours

later.

Microscopy and phenotype analysis

General methods for live animal imaging using Nomarski differential interference contrast (DIC) microscopy were as previously described (Sulston and Horvitz, 1977). Animals were analyzed on an Axio Zeiss A1 Imager compound microscope (Zeiss, Oberkochen, Germany) and images were captured using an Axio Cam MRm camera and AxioVision software (Zeiss, Oberkochen, Germany). Muv and Vul phenotypes were scored by counting the numbers of vulval and non-vulval descendants of P3.p-P8.p in L4 stage larvae as described previously (Skorobogata and Rocheleau, 2012). Fisher's exact test (www.graphpad.com/quickcalcs) was used for statistical analysis of the vulval phenotypes. Comparison of GFP intensities wild-type and *agef-1(vh4)* was performed using identical exposure times for conditions being compared. Fiji image processing tool was used to measure intensities in raw images; any adjustments to contrast/brightness were for presentation purposes and were performed after analysis (Schindelin et al., 2012). Tissue/organ of interest was outlined using the free hand selection tool followed by measurement of the average pixel intensity. Images selected for figures are representative of the mean value for average pixel intensity for the group. Statistical analysis and graphing was done using Prism 5 (GraphPad Software, Inc., La Jolla, CA).

Confocal analysis was performed using a Zeiss LSM-510 Meta laser scanning microscope with 63X oil immersion lens (Zeiss, Oberkochen, Germany) in a single-track mode using a 488 nm excitation for GFP. Images were captured using ZEN 2009 Image software (Zeiss, Oberkochen, Germany). Animals at the L4 larval stage were selected for visualization of endocytic/secretory compartments in the coelomocytes. Images selected for figures are representative of the mean value for the largest vesicle diameter for the group. Statistical analysis

and graphing was done using Prism 5 (GraphPad Software, Inc., La Jolla, CA). Confocal analysis of *zhIs038* transgene-carrying animals was performed at early L3 larval stage using the Zeiss LSM-510 Meta laser scanning microscope. Confocal analysis of *zhIs035* was performed using the Zeiss Axio Observer Z1 LSM-780 laser scanning microscope with 63X oil immersion lens (Zeiss, Oberkochen, Germany) in a single-track mode using an Argon multiline laser with 488 nm excitation for GFP. Images were captured using ZEN 2010 Image software (Zeiss, Oberkochen, Germany). The apical and basal LET-23::GFP intensities were measured using Fiji by drawing a line through the center of the nucleus in the DIC channel and transferring the selection into the GFP channel to prevent bias.

Plasmid and transgenic construction

arf-1.2 was amplified by PCR from wild-type cDNA using the primers 5'-CATAAGAATAGTCGACATGGGAAACGTGTTCGGCAGC-3' (forward) and 5'-GATTCTGATTACCGGTTCAGATCTATTCTTGAGCT-3' (reverse) containing SalI and AgeI cut sites, respectively. The PCR product was cloned into pEGFP-N1 plasmid using SalI 639 and AgeI 666 sites. *arf-1.2::GFP* was digested using SalI and NotI and subcloned into the p255 *lin-31* promoter plasmid. Transgenic animals were generated by DNA microinjection (Berkowitz et al., 2008) of the *Plin-31::ARF-1.2::GFP* plasmid and a marker plasmid *Pttx-3::GFP* at a concentration of 50 ng/µl of each into N2 animals using maxiprep quality DNA. Two of three lines were used for this study, *vhEx7* and *vhEx8*. Rescue of *agef-1(vh4)* and *arf-1.2(ok796)* mediated suppression of the *lin-2(e1309)* Vul phenotype was scored in animals expressing ARF-1.2::GFP in the VPCs.

Phylogenetic analysis

Analysis of the Arf GTPases was performed using MAFFT version 7 multiple alignment program for amino acid or nucleotide sequences online (http://mafft.cbrc.jp) (Katoh et al., 2002). Input sequences were human NP_001649.1 (Arf1), NP_001650.1 (Arf3), NP_001651.1 (Arf4), NP_001653.1 (Arf5), AAV38671.1 (Arf6), NP_001168.1 (Arl1) and *C. elegans* NP_501242.1 (ARF-1.1), NP_498235.1 (ARF-1.2), NP_501336.1 (ARF-3), NP_503011.1 (ARF-6), NP_495816.1 (ARL-1). Phylogenetic tree was constructed and visualized using Archaeopteryx (Han and Zmasek, 2009; Zmasek and Eddy, 2001).

RESULTS

Identification of *agef-1(vh4)* as a suppressor of the *lin-2(e1309)* Vul phenotype

We previously reported that *rab-7(ok511),* a maternal effect embryonic lethal mutant, strongly suppresses the *lin-2(e1309)* Vul phenotype (Skorobogata and Rocheleau, 2012). To identify new candidate regulators of LET-23 EGFR trafficking and signaling we conducted a clonal screen for essential suppressors of *lin-2(e1309)* (see Materials and Methods). In this screen we identified *vh4* as a strong suppressor of the *lin-2(e1309)* Vul phenotype (Figure 12A-D; Table 1, lines 1-4). The *vh4* mutation can suppress the 100% Vul phenotype of *lin-2(e1309)* to 20% Vul, and 30% Muv. In a *lin-2(+)* background, however, *vh4* mutant animals have 100% wild-type vulva induction. Consistent with a potential role in vesicular trafficking, the coelomocytes (macrophage-like scavenger cells) of *vh4* mutants accumulate abnormally large vesicular structures (Figure 12E, F). Additionally, *vh4* mutants have a dumpy body morphology, uncoordinated movement and ~50 percent embryonic lethality (Figure 12G, H).

To determine the molecular identity of *vh4*, we used a single nucleotide polymorphism (SNP) mapping strategy (Davis et al., 2005). Genome-wide mapping located *vh4* to the right arm of chromosome I, and interval mapping placed *vh4* in a 2.75 map unit region between SNPs *haw14137* and *pkP1071* at positions 20.65 and 23.4 map units, respectively (Figure 13A). We further refined the genomic interval by complementation with chromosomal deficiencies *dxDf2* and *eDf3*. *vh4* failed to complement the large deficiency *dxDf2*, but complemented the small *eDf3*, indicating that *vh4* lies in a 0.9 map unit region (20.65 – 21.51) containing 27 genes. We found that one obvious candidate, *vps-28*, was an RNAi suppressor of the *lin-2* Vul phenotype (Skorobogata and Rocheleau, 2012). However, *vh4* complemented the *vps-28(tm3767)* deletion allele and no lesion in the *vps-28* coding sequence of *vh4* animals was detected by DNA sequencing

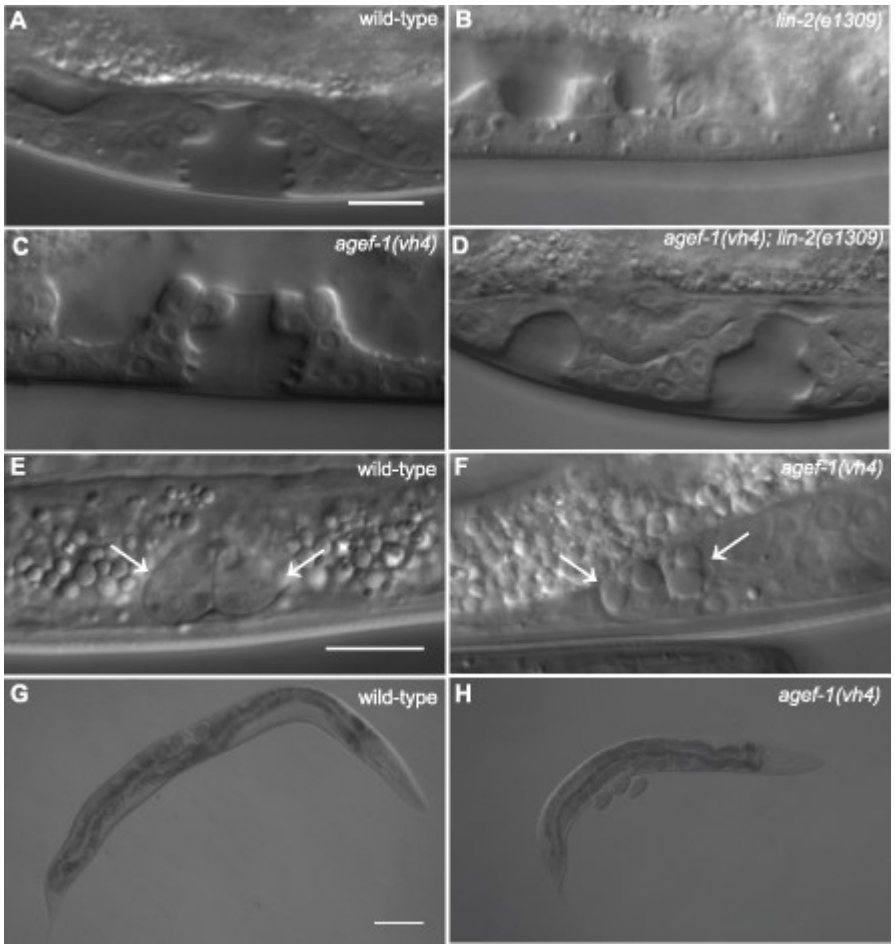

Figure 12. *agef-1(vh4)* suppresses the *lin-2(e1309)* Vul phenotype, has large vesicles in coelomocytes and a dumpy body morphology.

(A-D*)* Representative Differential Interference Contrast (DIC) images of vulvas of wild-type, *lin-2(e1309)*, *agef-1(vh4)* and *agef-1(vh4); lin-2(e1309)* L4 stage larvae. The *lin-2(e1309)* larva lacks a vulva while *agef-1(vh4); lin-2(e1309)* has a second vulval invagination and hence is Muv. *agef-1(vh4)* single mutants have a wild-type vulva. Bar, 10 µm. (E, F) DIC images of coelomocyte pairs (white arrows) of wild-type and *agef-1(vh4)* L4 larvae. *agef-1(vh4)* coelomocytes have enlarge vesicles as compared to wild-type. Bar, 10 µm. (G, H) DIC images of adult wild-type and *agef-1(vh4)* animals; *agef-1(vh4)* mutants have a smaller body length compared to wild-type. Bar, 100 µm.

Table 1. AGEF-1 is a negative regulator of EGFR/Ras/MAPK signaling during vulva induction

	GENOTYPE	Muv, %	Vul, %	AVG. # of VPCs INDUCED	VPCs INDUCED, %					
					P3.p	P4.p	P5.p	P6.p	P7.p	P8.p
1	wild-type	0	0	3.0	0	0	100	100	100	0
2	*agef-1(vh4)*	0	0	3.0	0	0	100	100	100	0
3	*lin-2(e1309)*	0	100	0.31	0	1	6	13	11	0
4	*agef-1(vh4); lin-2(e1309)*	30***	20****	3.0****	0	15	90****	98****	88****	6
5	*agef-1(vh4); lin-2(e1309); vhEx7*	5*	90****	1.69****	0	2	43***	77**	41***	5
6	*agef-1(vh4); lin-2(e1309); vhEx8*	4*	61**	2.07****	0	0	61**	93	50**	2
7	*agef-1(RNAi); lin-2(e1309)*	0	90	0.93***	0	3	25*	38*	28	0
8	*zhIs035; lin-2(e1309)*	0	0****	3.0****	0	0	100****	100****	100****	0
9	*zhIs038; lin-2(e1309)*	8	12****	2.96****	0	4	100****	96****	96****	0
10	*let-60(n1046)*	65	0	3.55	33	15	100	100	100	8
11	*agef-1(vh4); let-60(n1046)*	88**	0	4.04	19	51**	100	100	100	34
12	*let-23(sy1)*	0	100	0.14	0	0	9	0	5	0
13	*agef-1(vh4); let-23(sy1)*	4	48****	2.3****	0	4	66****	90****	64****	5
14	*let-23(sy97)*	0	93	0.4	0	0	14	16	10	0
15	*agef-1(vh4); let-23(sy97)*	0	96	0.24	0	0	7	11	6	0
16	*lin-3(e1417)*	0	98	0.72	0	0	13	48	11	0
17	*agef-1(vh4); lin-3(e1417)*	0	76**	1.54****	0	0	38**	78***	36**	2
18	*sli-1(sy143)*	0	0	3.0	0	0	100	100	100	0
19	*agef-1(vh4); sli-1(sy143)*	59****	0	3.42***	0	0	98	100	100	44****
20	*unc-101(sy108)*	0	0	3.0	0	0	100	100	100	0

21	*unc-101(RNAi) agef-1(vh4)*	43****	0	3.38***	0	1	100	100	100	37****
22	*unc-101(sy108) agef-1(RNAi)*	54****	0	3.34**	0	12*	100	100	100	22**
23	*arf-1.2(ok796)*	0	0	3.0	0	0	100	100	100	0
24	*unc-101(sy108); arf-1.2(ok796)*	50****	0	3.35***	0	0	100	100	100	35***
25	*agef-1(vh4); arf-1.2(ok796)*	63****	5	3.29**	0	0	94	94	94	34****

Statistical analysis was performed using Fisher's exact test (www.graphpad.com/quickcalcs) comparing each double mutant with the single mutant on the line above with the following exceptions: lines 5 and 6 were compared to line 4, lines 7, 8 and 9 were compared to line 3, and lines 19, 21, 22, 24, and 25 were compared to line 2. *P<0.05; **P<0.01; ***P<0.001; ****P<0.0001.

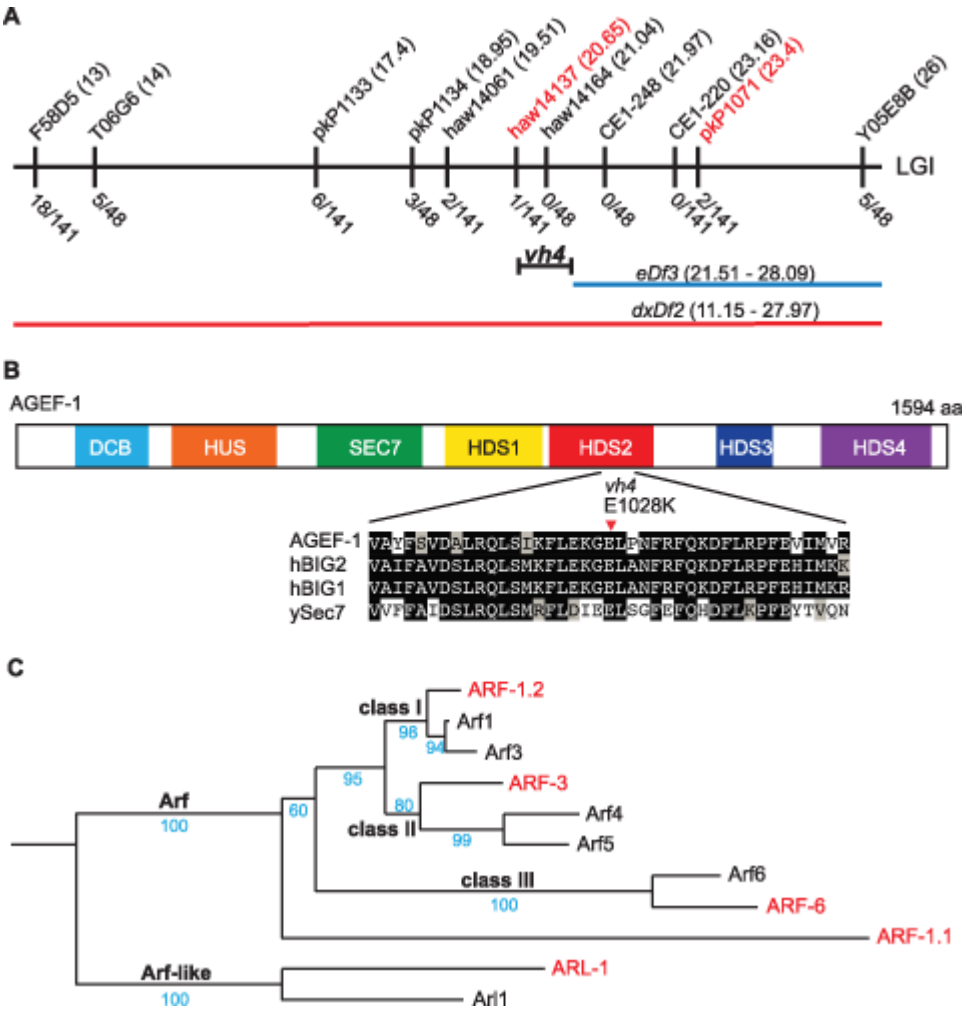

Figure 13. *vh4* is a missense mutation in *agef-1* and homology between *C. elegans* and human Arf GTPases.

(A) Schematic representation of the right end of chromosome I (LGI). The SNPs used for interval mapping are indicated on top with their chromosomal locations (map units). The number of recombinant animals positive for the Hawaiian SNP out of the total number of animals tested for each SNP is indicated below. The two chromosomal deficiencies used for mapping are *dxDf2* and *eDf3* shown in red and blue, respectively. A bracket indicates the 0.9 map unit interval between the *haw14137* SNP and the left end of *eDf3* to which *vh4* maps. (B) Homology domains of the AGEF-1 protein that are common with the human BIG1 and BIG2 proteins and *S. cerevisiae* Sec7 Arf GEFs: Dimerization Cyclophilin Binding (DCB), Homology Upstream of Sec7 (HUS),

catalytic GEF domain (SEC7), Homology Downstream of Sec7 (HDS1-4). HDS1-4 are not homologous to each other. Below shows the alignment of the sequences around the amino acid E1028 which is substituted for a Lysine (K) in *agef-1(vh4)*. E1028 is conserved in the human and yeast homologs. Amino acid (aa) identities are highlighted in black and similarities in grey. (C) A phylogenetic tree showing the evolutionary relationship between the four *C. elegans* Arf GTPases and the three classes of human Arf GTPases as well as the closely related Arl1 GTPases. The human and *C. elegans* Arfs are depicted in black and red, respectively. Bootstraps are shown in blue.

suggesting that *vh4* is not an allele of *vps-28*. Whole genome sequencing revealed a homozygous G to A transition at position 3082 in exon 11 of the *agef-1* gene (AAA TTT TTG GAA AAG GGA **G**AA CTT CCG AAT TTC CGA TTT) that corresponds to a glutamate to lysine substitution in a conserved region of the predicted AGEF-1 protein (Figure 13B). Consistent with *vh4* being a mutation in *agef-1*, we find that *agef-1(RNAi)* suppresses the severity of the *lin-2* Vul phenotype (Table 1, lines 3 and 7) and *agef-1(vh4)* mutant oocytes have defects in CAV-1 body formation as previously seen with *agef-1(RNAi)* (Figure S1J-M) (Sato et al., 2006). Finally, *agef-1(vh4)* fails to complement two deletion alleles, *agef-1(ok1736)* and *agef-1(tm1693)*, resulting in a strong embryonic lethal phenotype. These data indicate that *vh4* is a hypomorphic allele of *agef-1*.

The coelomocytes of *agef-1(vh4)* mutants have enlarged late endosomes/lysosomes

To determine the identity of the large vesicles in *agef-1(vh4)* coelomocytes, we used GFP tagged endosomal and Golgi proteins. Since the vesicles are presumably in flux, we measured the diameter of the largest GFP-positive vesicle per coelomocyte. We found a modest, but significant increase in the size of vesicles positive for the early endosomal 2xFYVE::GFP and the pan-endosomal RME-8::GFP markers in *agef-1(vh4)* animals as compared to wild-type (Figure 14A-C and Figure S2A-C). However, the large vesicles in *agef-1(vh4)* coelomocytes visible by DIC optics correspond to LMP-1::GFP, a marker for late endosomes/lysosomes (Figure 14D-F). This finding corroborates a concurrent study identifying large LMP-1 positive vesicles in the coelomocytes of *agef-1(RNAi)* animals (Tang et al., 2012). LMP-1 is a transmembrane protein, whose mammalian homolog, Lamp1, can transit from Golgi via the plasma membrane and endosomes to the lysosome (Saftig and Klumperman, 2009). Therefore, we assessed the morphology of the Golgi in *agef-1(vh4)* mutants using a mannosidase II::GFP marker. While there

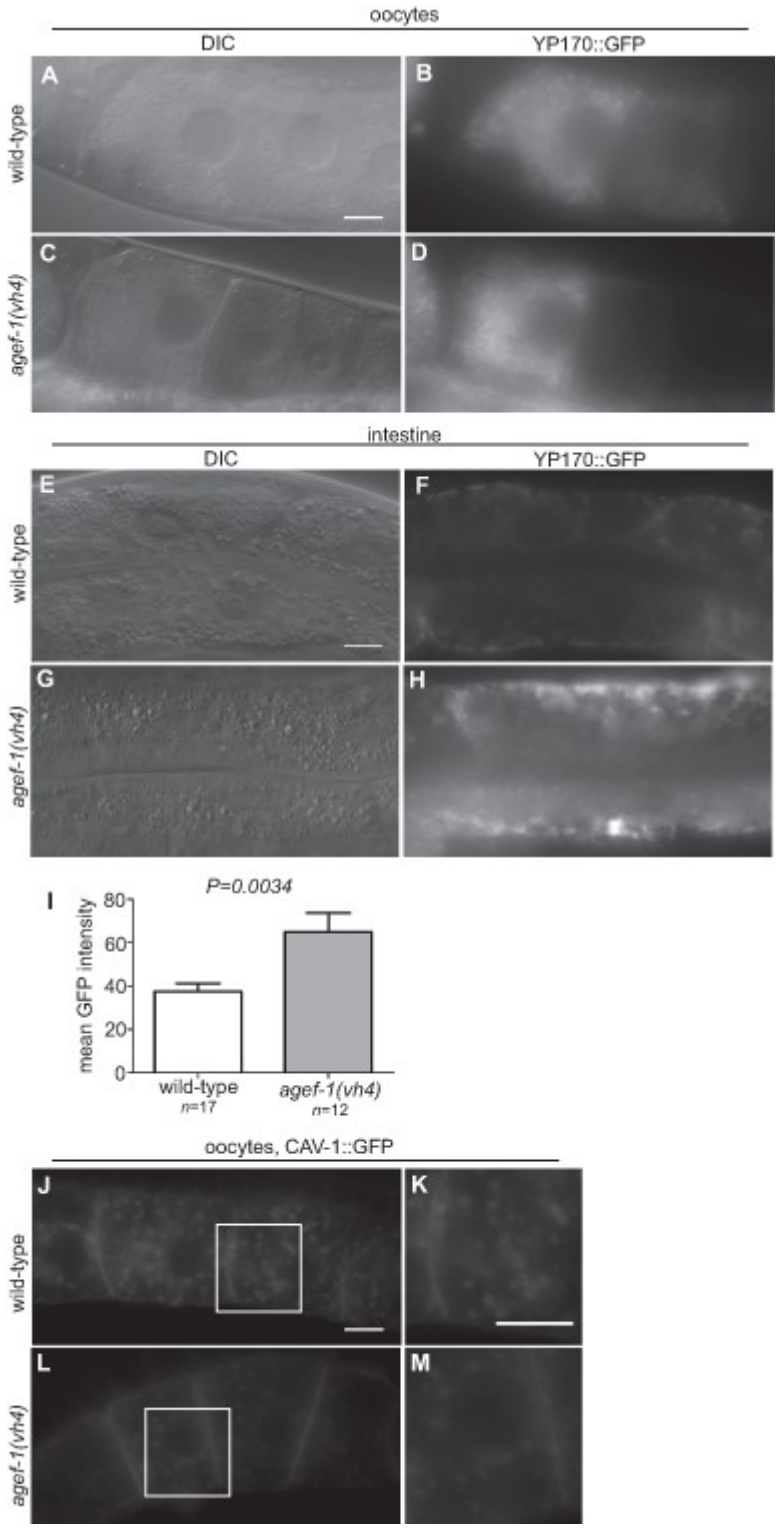

Figure S1. *agef-1(vh4)* animals are defective in Yolk secretion from the intestine and CAV-1 body formation in oocytes.

(A-D) DIC and corresponding epifluorescent images (55ms exposure time) of the oocytes of wild-type and *agef-1(vh4)* animals expressing YP170::GFP. (E-H) Representative DIC and corresponding epifluorescent images (50ms exposure time) of the intestine of wild-type and *agef-1(vh4)* animals expressing YP170::GFP. (I) Quantification of the mean YP170::GFP pixel intensity in the intestine. Statistical analysis was performed as described in Figure 15. (J-M) Epifluorescent images (80ms exposure time) of wild-type and *agef-1(vh4)* oocytes expressing CAV-1::GFP. The areas outlined with white squares in (J) and (L) are enlarged in (K) and (M), respectively. CAV-1::GFP forms ring-like structures, CAV-1 bodies, in wild-type animals (J, K), which are largely absent from *agef-1(vh4)* mutant oocytes (L, M). All bars, 10 μm.

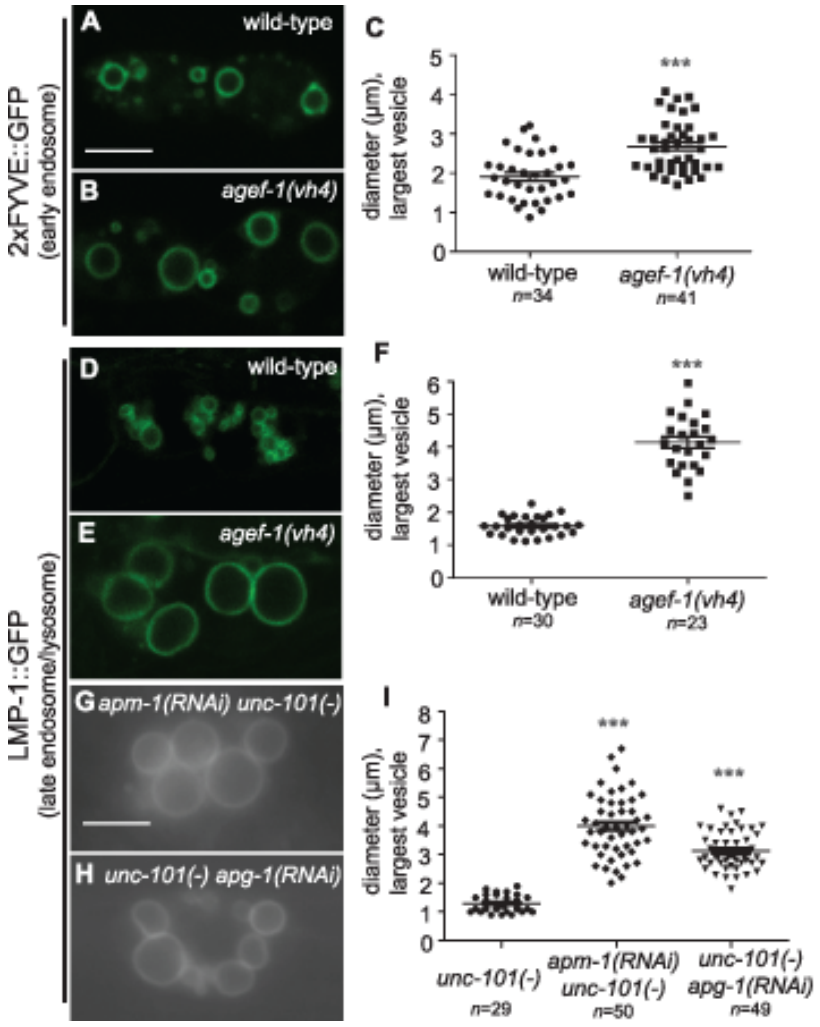

Figure 14. AGEF-1 and the AP-1 complex regulate the size of late endosomes/lysosomes in coelomocytes.

(A, B) Confocal images of the coelomocytes of wild-type and *agef-1(vh4)* L4 larvae expressing the early endosomal marker 2xFYVE::GFP. (C) Quantification of the diameter of the largest 2xFYVE::GFP-positive vesicle per coelomocyte in wild-type and *agef-1(vh4)*. (D, E) Confocal images of the coelomocytes of wild-type and *agef-1(vh4)* L4 larvae expressing the late endosomal/lysosomal marker LMP-1::GFP. (F) Quantification of the diameter of the largest LMP-1::GFP-positive vesicle per coelomocyte in wild-type and *agef-1(vh4)*. (G, H) Epifluorescent images of the coelomocytes of *apm-1(RNAi) unc-101(sy108)* and *unc-101(sy108) apg-1(RNAi)* L4

larvae. (I) Quantification of the diameter of the largest LMP-1::GFP-positive vesicle per coelomocyte upon depletion of multiple AP-1 subunits.. Prism 5 (GraphPad Software, Inc., La Jolla, CA) was used for statistical analysis; unpaired t-test was performed to compare changes in the vesicle size. *** $P<0.001$. Shown is the mean vesicle size plus standard error of the mean. All bars, 5 µm.

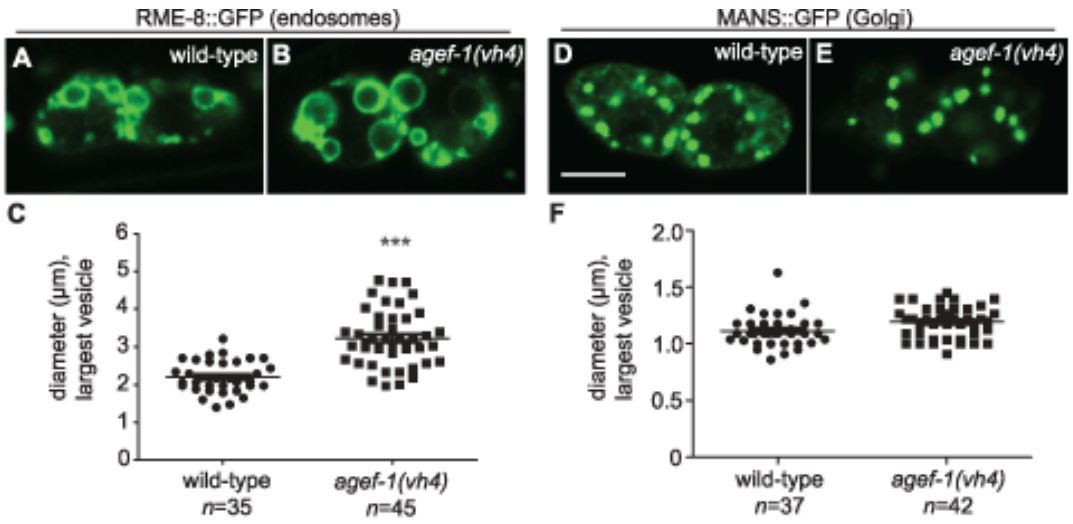

Figure S2. *agef-1(vh4)* mutants have enlarged endosomal compartments.

Representative confocal images of wild-type (A, D) and *agef-1(vh4)* (B, E) coelomocytes expressing either RME-8::GFP endosomal or MANS::GFP Golgi markers. (C, F) Quantification of the diameter of the largest GFP-positives structures demonstrate an increase in the size of endosomes outlined by RME-8::GFP. Statistical analysis is the same as in Figure 14. Bar, 5 µm.

might be a slight increase in the size of the Golgi mini-stacks, they were distinct from the large LMP-1::GFP positive vesicles seen by DIC (Figure S2D-F). Of note, the mannosidase II::GFP strands that appear to interconnect the Golgi mini-stacks in wild-type (30/37 coelomocytes) were largely absent in *agef-1(vh4)* mutants (6/42 coelomocytes are interconnected). These data show that *agef-1(vh4)* disrupts endosome and Golgi morphology and possibly trafficking.

The body wall muscle cells and intestinal cells of *agef-1(vh4)* mutants have defects in protein secretion

To test if *agef-1(vh4)* coelomocytes have an endocytosis defect we analyzed the internalization of a signal secreted GFP (ssGFP) that is expressed in body wall muscle cells, secreted into the pseudocoelom, and endocytosed by the coelomocytes (Fares and Greenwald, 2001). We found less ssGFP in the coelomocytes of *agef-1(vh4)* animals as compared to wild-type (Figure 15A-E). However, we did not detect a significant accumulation of ssGFP in the pseudocoelom of *agef-1(vh4)* mutants as would be expected for an endocytosis defect. Rather there was a clear accumulation of ssGFP in the body wall muscle cells of *agef-1(vh4)* animals as compared to wild-type (Figure 15F-J). While this does not rule out a potential endocytosis defect in *agef-1(vh4)* coelomocytes, it does indicate that *agef-1(vh4)* mutants have a secretion defect in the body wall muscle cells.

We also analyzed a Yolk::GFP fusion (YP170::GFP) that is secreted from the intestine, and internalized by maturing oocytes (Grant and Hirsh, 1999). We did not detect a difference in the uptake of YP170::GFP by oocytes (Figure S1A-D), however YP170::GFP levels in the intestine were higher in *agef-1(vh4)* animals than in wild-type (Figure S1E-I). An independent study also

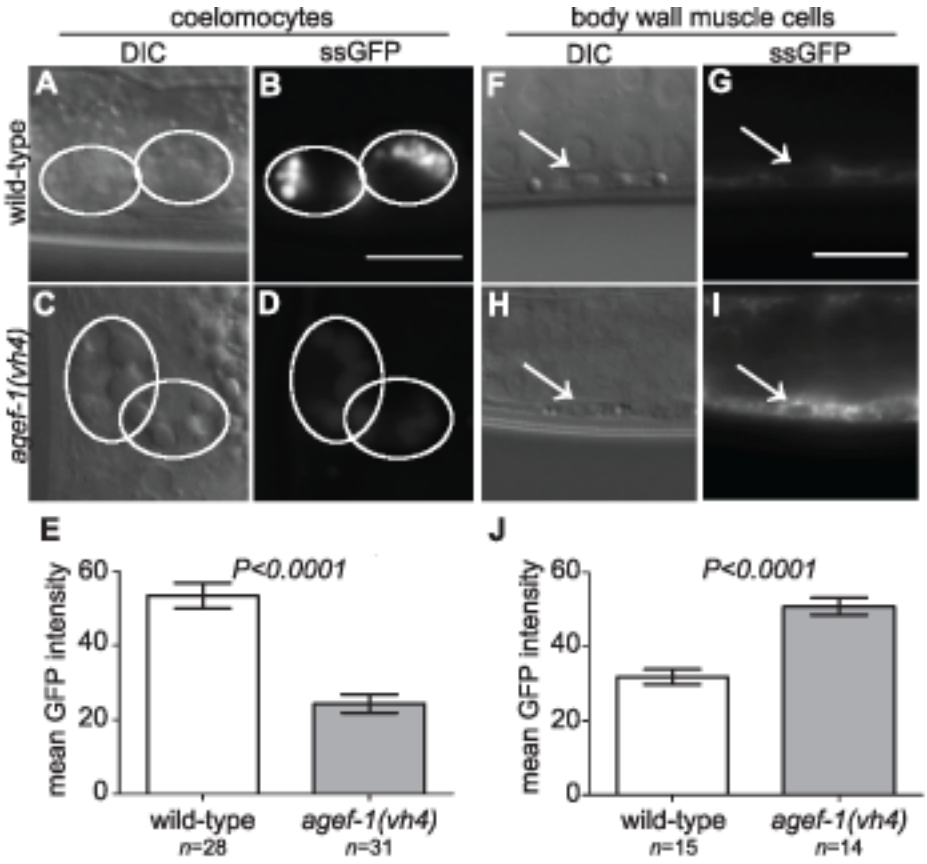

Figure 15. Secretion defect from the body wall muscle cells in *agef-1(vh4)* mutants.

(A-D) Representative DIC and epifluorescent images of ssGFP in the coelomocytes of wild-type and *agef-1(vh4)* mutants. Coelomocytes are outlined with white circles. (E) Quantification of mean ssGFP pixel intensity in the coelomocytes. Images were acquired at an exposure time of 25 ms. (F-I) Representative DIC and epifluorescent images of wild-type and *agef-1(vh4)* body wall muscle cells expressing ssGFP. Arrows indicate nuclei of the muscle cells. (J) Quantification of mean ssGFP pixel intensity in the body wall muscle cells. Images were acquired at an exposure time of 100 ms. Prism 5 (GraphPad Software, Inc., La Jolla, CA) was used for statistical analysis; unpaired t-test was performed to compare mean GFP intensities and standard error of the mean between wild-type and *agef-1(vh4)* animals. All bars, 10 µm.

found impaired secretion of yolk in *agef-1(RNAi)* animals (Ackema et al., 2013). Thus, *agef-1(vh4)* mutants have impaired protein secretion from both body wall muscle and intestinal cells.

AGEF-1 antagonizes signaling upstream or in parallel to LET-23 EGFR

To understand the role of AGEF-1 in the LET-23 EGFR/ LET-60 Ras signaling pathway, we made double mutants with *agef-1* and several mutations in core components of the pathway. A gain of function mutation in *let-60 ras (n1046)* causes a Muv phenotype that can be enhanced by loss of a negative regulator of the pathway (Berset et al., 2005; Hopper et al., 2000; Kritikou et al., 2006; Skorobogata and Rocheleau, 2012). *agef-1(vh4)* significantly enhances the Muv phenotype of *let-60(n1046),* consistent with AGEF-1 being a negative regulator of signaling (Table 1, lines 10-11). We performed epistasis analysis to determine at which step of the pathway AGEF-1 functions. We found that *agef-1(vh4)* strongly suppresses the Vul phenotype of the *let-23(sy1)* mutant (Table 1, lines 12-13). The *sy1* allele truncates the last six amino acids of LET-23 EGFR that are required for its interaction with the LIN-2/7/10 complex, and thus behaves identically to mutations in components of this complex (Aroian et al., 1994; Kaech et al., 1998). However, *agef-1(vh4)* fails to suppress the Vul phenotype of the *let-23(sy97)* allele that results in a more severe truncation of LET-23 EGFR that blocks signaling to the LET-60 Ras (Table 1, lines 14-15) (Aroian and Sternberg, 1991). We next tested if *agef-1(vh4)* can suppress the Vul phenotype of *lin-3(e1417)*, a strong hypomorphic allele of *lin-3 EGF* (Hwang and Sternberg, 2004). We found that *agef-1(vh4)* partially suppressed the *lin-3(e1417)* Vul phenotype (Table 1, lines 16-17). These data are consistent with AGEF-1 antagonizing signaling upstream or in parallel to LET-23 EGFR.

SLI-1 Cbl, a putative E3-ubiquitin ligase, and UNC-101 AP-1μ are negative regulators of LET-23 EGFR signaling that also function at the level of LET-23 EGFR (Jongeward et al., 1995; Lee et al., 1994; Yoon et al., 1995). Like *agef-1(vh4),* mutations in *sli-1 Cbl* and *unc-101 AP-1μ* do not cause a vulval phenotype alone, but double mutants cause a synergistic Muv phenotype. Therefore, we tested if *agef-1(vh4)* is Muv in combination with strong loss-of-function alleles of *sli-1 Cbl* and *unc-101 AP-1μ.* We found that *agef-1(vh4); sli-1(sy143)* animals are strongly Muv, suggesting that AGEF-1 might function in parallel to SLI-1 Cbl (Table 1, lines 18-19). We were unable to identify *unc-101(sy108) agef-1(vh4)* double mutants segregating from *unc-101(sy108) agef-1(vh4)/unc-101(sy108)* mothers suggesting that they are zygotic lethal. Thus, we fed L1 larvae RNAi and found that both *unc-101(RNAi) agef-1(vh4)* and *unc-101(sy108) agef-1(RNAi)* animals have a strong Muv phenotype (Table 1, lines 20-22). Since there are two AP-1μ genes, *unc-101* and *apm-1*, that are functionally redundant, we cannot conclude whether AGEF-1 functions in parallel to UNC-101, or whether they function together; we favor the later, see below. However, the strong genetic interactions of *agef-1(vh4)* and mutations in *sli-1* and *unc-101* further support AGEF-1 functioning at the level of LET-23 EGFR to negatively regulate signaling.

ARF-1.2 and ARF-3 antagonize LET-23 EGFR signaling

The identification of a putative Arf GEF as a negative regulator of LET-23 EGFR signaling suggests that one or more of the four *C. elegans* Arf GTPases might also regulate LET-23 EGFR signaling. The mammalian Arf GTPases have been placed in three classes based on homology (Kahn et al., 2006). To gain a better understanding of the relationship of the *C. elegans* and human Arf GTPases we undertook a phylogenetic analysis (Figure 13C). From this we conclude that *C. elegans* ARF-1.2 is homologous to Class I Arfs; ARF-3 is related to both Class I and II Arfs, but

clusters with the Class II; ARF-6 is a homolog of the Class III Arf, whereas ARF-1.1 appears to be a Caenorhabiditis specific Arf GTPase that is distinct from the Arf-like Arl GTPases (Figure 13C). We used RNAi and deletion mutants to test each *arf* gene for suppression of the *lin-2(e1309)* Vul phenotype. RNAi of either *arf-1.2* or *arf-3* partially suppressed of the *lin-2(e1309)* Vul phenotype (Table 2, lines 1-3). The *arf-1.2(ok796)* deletion mutant was a much more potent suppressor of the *lin-2(e1309)* Vul phenotype consistent with RNAi being less effective in the VPCs (Skorobogata and Rocheleau, 2012; this study) (Table 2, lines 4-5). The *arf-3(tm1877)* deletion is zygotic lethal and did not permit analysis. However, *arf-3(RNAi)* into *arf-1.2(ok796); lin-2(e1309)* animals led to an even stronger suppression of the Vul phenotype comparable to that of *agef-1(vh4); lin-2(e1309)* (Table 2, line 8). Neither the *arf-6(tm1447)* nor the *arf-1.1(ok1840)* deletions were able to suppress the *lin-2(e1309)* Vul phenotype (Table 2, lines 9-12). These data suggest that ARF-1.2 and ARF-3 function in a partly redundant manner, possibly with AGEF-1, to antagonize LET-23 EGFR signaling.

ARF-1.2 and AGEF-1 antagonize LET-23 EGFR signaling in the VPCs

To test if *arf-1.2* was required in the VPCs we generated two transgenic extrachromosomal arrays, *vhEx7* and *vhEx8,* expressing ARF-1.2::GFP under the control of the VPC-specific promoter, *lin-31* (Tan et al., 1998). Both transgenic lines were able to strongly rescue *arf-1.2(ok796)* suppression of the *lin-2(e1309)* Vul phenotype (Table 2, lines 6-7). Thus, ARF-1.2 functions in the VPCs to negatively regulate LET-23 EGFR signaling. We next tested whether VPC-specific overexpression of ARF-1.2::GFP can revert the suppression of Vul phenotype in *agef-1(vh4); lin-2(e1309).* Both lines, *vhEx7* and *vhEx8*, led to a more severe Vul phenotype when expressed in *agef-1(vh4); lin-2(e1309)* animals (Table 1, lines 5-6). This suggests that AGEF-1

Table 2. Class I and II Arf mutants suppress the *lin-2(e1309)* Vul phenotype

	GENOTYPE	Muv%	Vul%	AVG. # of VPCs INDUCED	VPCs INDUCED, %					
					P3.p	P4.p	P5.p	P6.p	P7.p	P8.p
1	*lin-2(e1309)*	0	100	0.31	0	1	6	13	11	0
2	*arf-1.2(RNAi); lin-2(e1309)*	0	95	0.73**	0	0	18	30	25	0
3	*arf-3(RNAi); lin-2(e1309)*	0	85*	0.79**	0	1	25*	23	30	0
4	*arf-1.2(ok796)*	0	0	3.0	0	0	100	100	100	0
5	*arf-1.2(ok796); lin-2(e1309)*	20***	52****	2.66****	0	30**	85****	100****	51***	0
6	*arf-1.2(ok796); lin-2(e1309); vhEx7*	0*	90**	1.48****	0	0**	38***	70***	40	0
7	*arf-1.2(ok796); lin-2(e1309); vhEx8*	0	100**	1.38****	0	0*	33***	67**	38	0
8	*arf-1.2(ok796); arf-3(RNAi); lin-2(e1309)*	34****	25****	2.97****	0	23*	89****	98****	72****	16*
9	*arf-6 (tm1447)*	0	0	3.0	0	5	100	100	95	0
10	*arf-6(tm1447); lin-2(e1309)*	0	94	0.4	0	0	16	13	11	0
11	*arf-1.1(ok1840)*	0	0	3.0	0	0	100	100	100	0
12	*arf-1.1(ok1840); lin-2(e1309)*	0	97	0.37	0	1	11	17	7	0

Statistical analysis was performed as described above. All mutant combinations with *lin-2(e1309)* were compared to *lin-2(e1309)* single mutants except for *arf-1.2(ok796); lin-2(e1309); vhEx7* and *arf-1.2(ok796); lin-2(e1309); vhEx8*, which were compared to *arf-1.2(ok796); lin-2(e1309)*. *P<0.05; **P<0.01; ***P<0.001; ****P<0.0001.

functions in the VPCs through ARF-1.2 to antagonize LET-23 EGFR signaling.

AGEF-1, ARF-1.2, and UNC-101 AP-1*μ* cooperate to repress ectopic vulva induction

Having observed a strong Muv phenotype in *unc-101(RNAi) agef-1(vh4)* and *unc-101(sy108) agef-1(RNAi)* doubles (Table 1, lines 21-22), we hypothesized that *arf-1.2(ok796)* would have similar interactions. Indeed, both *unc-101(sy108); arf-1.2(ok796)* and *agef-1(vh4); arf-1.2(ok796)* animals have a strong Muv phenotype (Table 1, lines 24-25). Given that *agef-1(vh4)* is a weak hypomorphic allele and ARF-1.2 and UNC-101 AP-1μ are each functionally redundant with ARF-3 and APM-1 AP-1μ, respectively; these data are consistent with AGEF-1, ARF-1.2 and UNC-101 AP-1μ functioning together to negatively regulate LET-23 EGFR signaling.

AGEF-1 and UNC-101 have shared phenotypes in coelomocytes and the intestine

If AGEF-1, the ARF GTPases and the AP-1 complex function together, we expect that they will have shared phenotypes. We tested whether the ARFs and the AP-1 complex regulate the size of vesicles in coelomocytes as does AGEF-1. While *unc-101(sy108)* mutants do not have large vesicles, further depletion of the AP-1 complex by RNAi of *apm-1 AP-1μ* or *apg-1 AP-1γ* in the *unc-101(sy108)* background resulted in enlarged LMP-1::GFP vesicles in the coelomocytes (Figure 14G-I). Consistent with previous studies, we found no evidence for *arf-1.2* or *arf-3* in regulating the size of vesicles in the coelomocytes (Tang et al., 2012), nor do deletions in *arf-1.1* or *arf-6*. The complement of ARF GTPases that function with AGEF-1 and AP-1 in coelomocytes

remains to be determined.

The AP-1 complex has recently been shown to restrict both apical and basolateral membrane protein localization in the *C. elegans* intestine (Shafaq-Zadah et al., 2012; Zhang et al., 2012). Similarly, we found that the apically localized SID-2 transmembrane protein (Winston et al., 2007), was mislocalized to the cytoplasm and basolateral membranes in *agef-1(vh4)* mutants (Figure S3A-D), suggesting that AGEF-1 and AP-1 might function together to regulate polarized localization of membrane proteins in the intestine.

AGEF-1 and UNC-101 antagonize LET-23 EGFR basolateral localization

The role of AGEF-1 in restricting SID-2::GFP on the apical membrane suggests that AGEF-1, the ARF GTPases and the AP-1 complex might restrict LET-23 EGFR to the apical membrane in the VPCs. To test this hypothesis we made use of two transgenic strains expressing a LET-23 EGFR GFP fusion (*zhIs035* and *zhIs038*) that mimic the localization of endogenous LET-23 EGFR as seen by antibody staining (Haag et al., 2014). In wild-type animals, LET-23::GFP localizes to both the apical and basolateral membranes of P6.p and in the *lin-2(e1309)* animals LET-23::GFP localizes strictly to the apical membrane (Figure 16A, C and Figure S4A, C). At the Pn.px stage, some basolateral, or lateral only localization is seen in *lin-2(e1309)* animals. Despite the lack of basolateral localization at the Pn.p stage, we find that the LET-23::GFP transgenes fully rescue the *lin-2(e1309)* Vul phenotype (Table 1, lines 8 and 9), suggesting that the levels of LET-23 EGFR at the basolateral membrane required for VPC induction are below the level of detection. Similarly, the *gaIs27* LET-23::GFP transgene, that is only detectable by immunostaining with anti-GFP antibody, suppressed the *lin-2(e1309)* egg-laying defective phenotype (Skorobogata and

Rocheleau, 2012).

To determine if AGEF-1 regulates LET-23 EGFR localization we compared the ratio of basolateral versus apical localization of LET-23::GFP in the P6.p cell of wild-type and *agef-1(vh4)* animals (Table 3). In wild-type, the average basal/apical intensity of LET-23::GFP in P6.p was 0.49 for *zhIs035* and 0.65 for *zhIs038.* In *agef-1(vh4)* animals, the average basal/apical intensity of LET-23::GFP in the P6.p cell is 0.79 for *zhIs035* and 0.93 for *zhIs038* reflecting a decrease in apical intensity and an increase in basolateral intensity. We also found LET-23::GFP is present on the basolateral membrane of the intestinal cells in *agef-1(vh4)* animals whereas we did not see this in wild-type by confocal microscopy (Figure S3E-H). Therefore, AGEF-1 represses basolateral localization of LET-23::GFP in the VPCs and intestinal cells.

We next tested if *agef-1(vh4)* could restore the basolateral localization of LET-23::GFP in *lin-2(1309)* animals. We found that ~40% of *agef-1(vh4); lin-2(e1309)* animals with *zhIs035* have weak basolateral membrane localization of LET-23::GFP in P6.p compared to 9% in *lin-2(e1309)* animals (Figure 16C-D, G). Similarly, at the P6.px stage, we see an increase in the number of animals with basolateral localization of LET-23::GFP in *agef-1(vh4); lin-2(e1309)* as compared to *lin-2(e1309)* single mutants (Figure 16C'-D', G'). No basolateral LET-23::GFP was seen with *agef-1(vh4); lin-2(e1309)* animals with the lower expressing *zhIs038* (Figure S4C'-D', F'). Since *agef-1(vh4)* is a weak hypomorphic mutation, we tested if knocking down the AP-1 complex via *unc-101(RNAi)* can further restore basolateral localization of LET-23 EGFR in *agef-1(vh4); lin-2(e1309)* mutants. We found that *unc-101(RNAi) agef-1(vh4); lin-2(e1309)* animals with either *zhIs035* or *zhIs038* had an increase in basolateral membrane localization of LET-23::GFP in both the intensity and the number of animals (Figure 16F-G' and Figure S4E, F). *unc-101(RNAi); lin-2(e1309)* animals only showed mild restoration of LET-23::GFP using the *zhIs035* transgene

(Figure 16E, E', G and G'). The restoration of LET-23 EGFR on the basolateral membrane in *agef-1(vh4); lin-2(e1309)*, *unc-101(RNAi); lin-2(e1309)* and *unc-101(RNAi) agef-1(vh4); lin-2(e1309)* animals suggests that AGEF-1 and UNC-101 AP-1μ negatively regulate LET-23 EGFR signaling by limiting basolateral membrane localization.

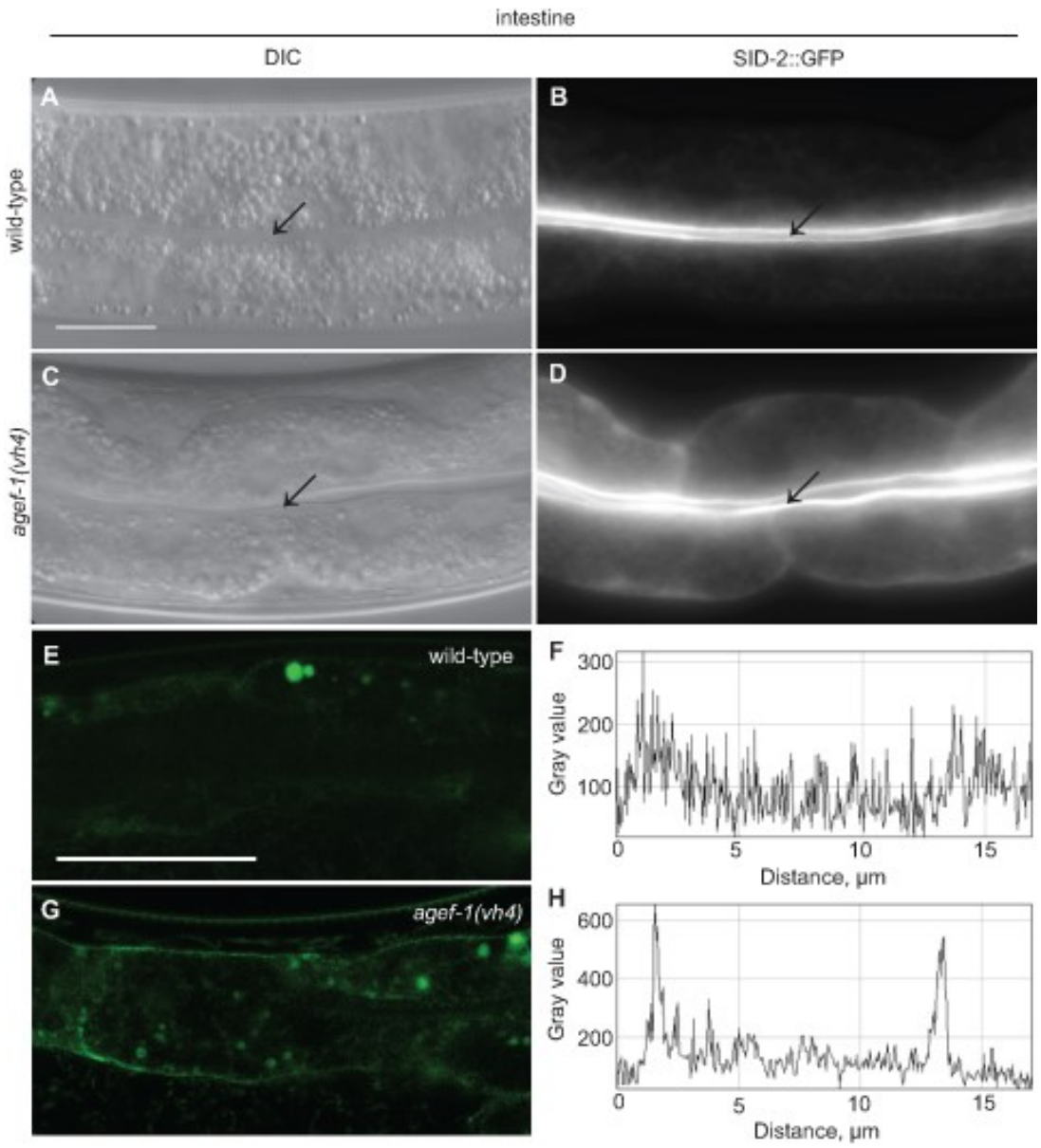

Figure S3. AGEF-1 antagonizes basolateral localization of SID-2::GFP and LET-23::GFP in the intestine.

(A-D) Representative DIC and epifluorescent images of the intestine of wild-type and *agef-1(vh4)* animals expressing SID-2::GFP. The arrows mark the intestinal lumen corresponding to the apical membrane of the intestinal cells. Note that in wild-type animals SID-2::GFP expression is restricted to the apical membrane, whereas in *agef-1(vh4)* mutants SID-2::GFP is localized to both

apical and basolateral membranes. (E, G) Confocal images of the intestine of wild-type and *agef-1(vh4)* animals carrying the *zhIs035* transgene. LET-23::GFP is present on the basolateral membrane of intestinal cells in *agef-1(vh4)* mutants, but is not detected in wild-type animals. (F, H) Graphs indicate the fluorescent intensity along a line drawn across the intestine in wild-type and *agef-1(vh4)* animals. The two distinct intensity peaks observed in (H) mark LET-23::GFP on the basolateral membrane in (G). All bars, 20 μm.

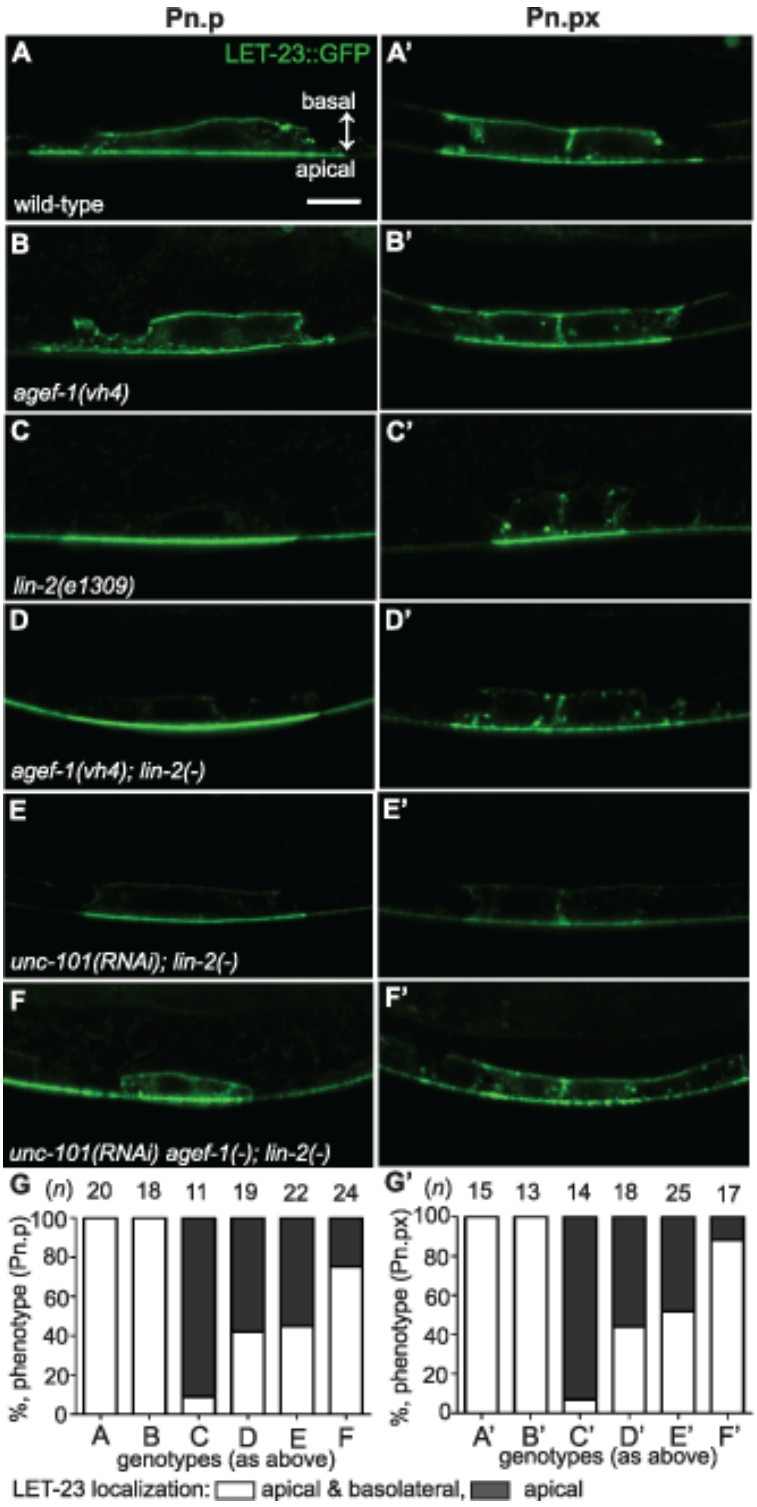

Figure 16. AGEF-1 and UNC-101 AP-1μ antagonize basolateral localization of LET-23 EGFR. (Figure legend is on the next page)

(A-F') Representative confocal images of LET-23::GFP localization in P6.p (A-F) and P6.px (A'-F') vulval cells of *zhIs035* transgene-carrying animals. (A-B') The LET-23::GFP is localized to both apical and basolateral membranes in wild-type and *agef-1(vh4)* animals. (C, C') The basolateral receptor localization is lost in *lin-2(e1309)* mutants. (D, D') *agef-1(vh4); lin-2(e1309)* mutants with faint LET-23::GFP expression on the basolateral membrane of P6.p and P6.px. (E, E') *unc-101(RNAi); lin-2(e1309)* animals with faint LET-23::GFP expression on the basolateral membrane of P6.p and P6.px. (F, F') *unc-101(RNAi)* in *agef-1(vh4); lin-2(e1309)* mutants results in more LET-23::GFP on the basolateral membranes. (G, G') Percent animals with LET-23::GFP on both the basolateral and apical membranes or apical only localization. Because some animals have no or little basolateral membrane localization, basolateral localization of LET-23::GFP in the P6.p and P6.px cells was determined by measuring the intensity at the basal membrane versus background. If the GFP intensity on the basal membrane was twice that of the background the cell was considered to have basolateral membrane localization.

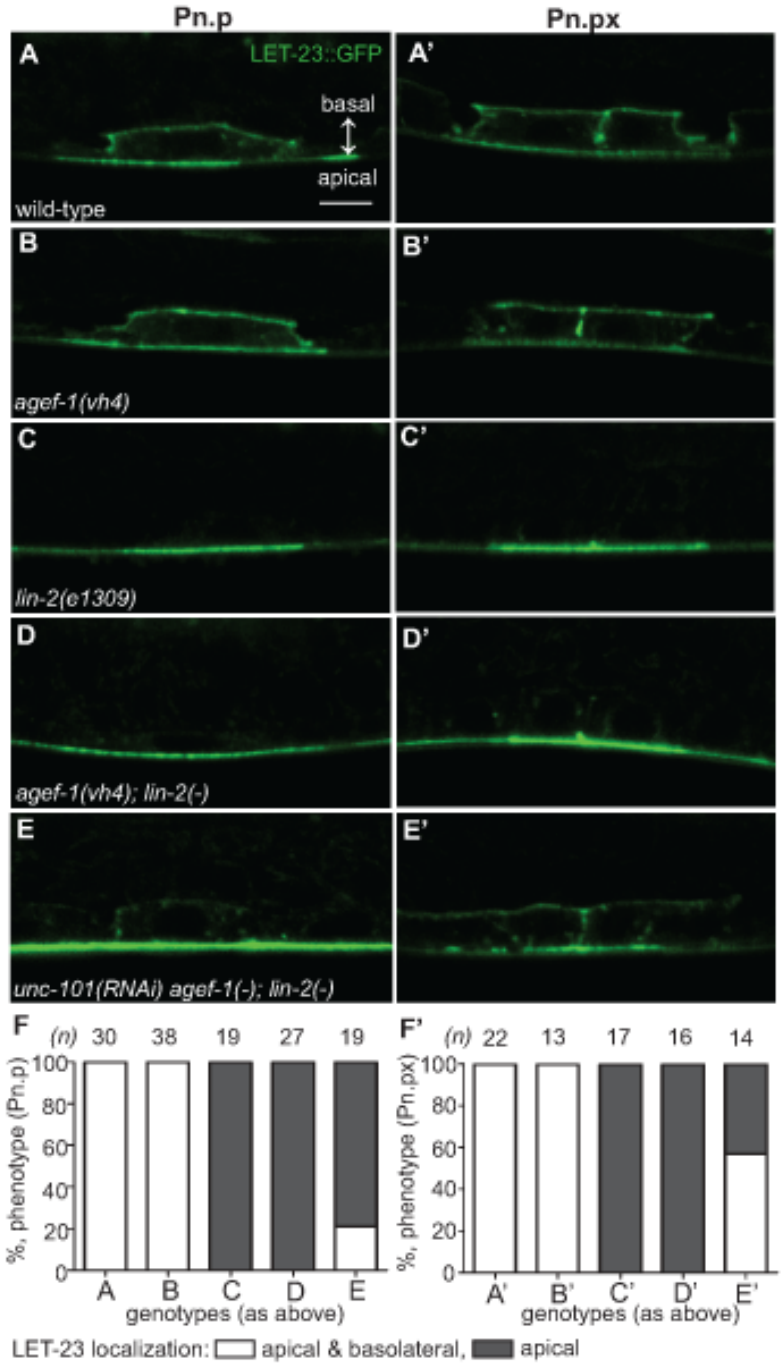

Figure S4. AGEF-1 and UNC-101 AP-1μ antagonize basolateral localization of LET-23 EGFR. (Figure legend is on the next page)

(A-E') Confocal images of *zhIs038* LET-23::GFP in the P6.p (A-E) and P6.px (A'-E') cells. (A-B') Both wild-type and *agef-1(vh4)* animals express LET-23::GFP on both the basolateral and apical membranes. (C, C') Basolateral localization is lost in *lin-2(e1309)* mutants. (D, D') *agef-1(vh4); lin-2(e1309)* double mutants do not have detectable basolateral LET-23::GFP. (E, E') *unc-101(RNAi)* in *agef-1(vh4); lin-2(e1309)* background results in faint basolateral LET-23::GFP accumulation. (F, F') Quantification of LET-23::GFP localization in P6.p and P6.px cells. Bar, 5 μm.

Table 3. AGEF-1 antagonizes basal membrane localization of LET-23 EGFR in P6.p

Genotypes	Avg. Basal Intensity	Avg. Apical Intensity	Avg. Basal/Apical Intensity	*n*
zhIs035	1385	2826	0.49	20
agef-1(vh4) zhIs035	1548	1959	0.79	18
zhIs038	1199	1844	0.65	30
agef-1(vh4); zhIs038	1277	1373	0.93	38

DISCUSSION

Regulators of LET-23 EGFR trafficking are likely required for viability, as is the case for the RAB-7 GTPase (Skorobogata and Rocheleau, 2012). In a screen for essential negative regulators of LET-23 EGFR-mediated vulva induction we identified a hypomorphic allele in the *agef-1* gene. AGEF-1 is the *C. elegans* homolog of the yeast Sec7p and human BIG1 and BIG2 Arf GEFs, which function with class I Arf GTPases and the AP-1 complex to regulate cargo sorting and trafficking from the TGN (Casanova, 2007). We demonstrate that AGEF-1 regulates protein secretion, polarized protein localization, and late endosome/lysosome morphology. We show that AGEF-1 antagonizes signaling in the VPCs, upstream or in parallel to LET-23 EGFR, and that the class I/II Arf GTPases, ARF-1.2 and ARF-3, also negatively regulate signaling. Our genetic and phenotypic data are consistent with AGEF-1, the ARF-1.2 and ARF-3 GTPases, and the AP-1 complex together preventing ectopic vulva induction. The AGEF-1/Arf GTPase/AP-1 ensemble antagonizes the basolateral membrane localization of LET-23 EGFR in the VPCs; and hence, LET-23 EGFR-mediated vulva induction.

The clonal screen for suppressors of the *lin-2(e1309)* Vul phenotype was initially aimed at identifying maternal effect lethal mutants, like *rab-7(ok511).* Instead, we identified two strong suppressors of *lin-2(e1309)* with partial embryonic lethal phenotypes, *agef-1(vh4)* and *vh22* (J. Meng, O.S. and C.E.R., unpublished data); which we currently believe function independently of each other and *rab-7*. The *agef-1* deletion alleles are zygotic lethal and RNAi in the VPCs with *agef-1, arf-1.2* and *rab-7* has proven less effective than their corresponding genetic mutations (Skorobogata and Rocheleau, 2012; this study). Therefore, the *agef-1(vh4)* mutation, being a recessive partial loss-of-function allele, provides a unique tool to study the function of *agef-1,* particularly in tissues refractory to RNAi such as the VPCs and neurons.

The *agef-1(vh4)* lesion changes a conserved negatively charged Glutamic Acid in the HDS2 domain to a positively charged Lysine. Collectively, the HDS2, HDS3, and HDS4 domains of yeast Sec7p have been shown to have an autoinhibitory function (Richardson et al., 2012). However, the specific function of the HDS2 domain is not known. Given the recessive nature of the *agef-1(vh4)* allele, it suggests that the HDS2 domain has a positive role in promoting AGEF-1 function.

Consistent with yeast Sec7p and human BIG1/BIG2 functioning in the secretory pathway, we found that *agef-1(vh4)* animals had defects in secretion of ssGFP from body wall muscles and Yolk::GFP from the intestine. Similar yolk secretion defects were recently reported for *agef-1(RNAi)* (Ackema et al., 2013). We found that *agef-1(vh4)* coelomocytes accumulated enlarged LMP-1::GFP positive late endosomes/lysosomes. Independently, Tang *et al.* (2012) found that *agef-1(RNAi)* also caused enlargement of LMP-1::GFP vesicles and proposed a role for AGEF-1 in late endosome to lysosome trafficking, however, they did not find a defect in lysosome acidification or protein degradation. We do not know the reason for the enlarged late endosomes/lysosomes, but it could reflect a defect in retrograde transport from late endosomes to the Golgi as has been shown for knockdown of BIG1 and BIG2 or the AP-1 complex in mammalian cells (Ishizaki et al., 2008). Consistent with this idea, we found that knockdown of the AP-1 complex also induced enlarged LMP-1::GFP vesicles. Tang *et al.* (2012) also reported that ssGFP accumulated in the pseudocoelom suggesting an uptake defect in the coelomocytes. We found that *agef-1(vh4)* mutants accumulated ssGFP in the body wall muscles rather than the pseudocoelom; thus the reduced ssGFP in coelomocytes could be explained by reduced secretion from the body wall muscles. However, we cannot rule out an uptake defect in the coelomocytes

as well. Perhaps these discrepancies reflect a difference in reducing the levels of *agef-1* by RNAi versus the *vh4* missense mutation.

Our genetic analysis with *agef-1(vh4)* indicate that AGEF-1 is a potent negative regulator of LET-23 EGFR-mediated vulva induction. Similar to other negative regulators, *agef-1* enhanced the Muv phenotype of the gain-of-function Ras mutant, *let-60(n1046),* and was a potent suppressor the Vul phenotypes of *lin-2(e1309)* and *let-23(sy1)* mutations, restoring vulva induction and even inducing a Muv phenotype. However, *agef-1(vh4)* failed to suppress a strong *let-23(sy97)* allele similar to *sli-1* and *unc-101* mutations and consistent with a role for AGEF-1 upstream or in parallel to LET-23 EGFR. In accordance with AGEF-1 being an Arf GEF, we found that ARF-1.2 and ARF-3, Class I/II Arf GTPases, also negatively regulate LET-23 EGFR signaling. The *arf-1.2(ok796)* deletion allele was a less potent suppressor of the *lin-2(e1309)* Vul phenotype as compared to the *agef-1(vh4)* mutant. However, *arf-3(RNAi)* in *arf-1.2(ok796); lin-2(e1309)* doubles showed suppression comparable to that in *agef-1(vh4); lin-2(e1309)* mutants. Therefore, ARF-1.2 and ARF-3 appear to function in a partly redundant manner during vulva development. Furthermore, expression of an ARF-1.2::GFP fusion in the VPCs rescued the suppressed Vul phenotype of both *arf-1.2(ok796); lin-2(e1309)* and *agef-1(vh4); lin-2(e1309)* animals indicating that ARF-1.2 antagonizes signaling in the VPCs likely downstream of AGEF-1.

In mammalian cells, the BIG1/BIG2 proteins and Arf1 recruit the AP-1 adaptor protein complex to the TGN and endosomes (Robinson, 2004; Stamnes and Rothman, 1993; Traub et al., 1993). Both of the *C. elegans* AP-1μ subunits, *unc-101* and *apm-1*, negatively regulate LET-23 EGFR mediated vulva development (Lee et al., 1994; Shim et al., 2000). In fact, *apm-1(RNAi) unc-101(sy108)* animals had a Muv phenotype, indicating that UNC-101 and APM-1 are functionally redundant during vulva induction, thus revealing a role for the AP-1 complex in

inhibiting ectopic vulva induction (Shim et al., 2000). Our findings that various double-mutant combinations between *agef-1(vh4)*, *arf-1.2(ok796)* and *unc-101(sy108) AP-1μ* result in a synergistic Muv phenotype are consistent with AGEF-1, the Arfs and AP-1 functioning together to inhibit ectopic vulva induction. However, we cannot conclude whether they function in parallel pathways or in a common pathway due to the fact that *agef-1(vh4)* is not a null allele and the *unc-101(sy108)* and *arf-1.2(ok796)* mutations, while severe loss-of-function or null alleles, function in a partly redundant manner with *apm-1* and *arf-3,* respectively. We favor a model whereby AGEF-1, the Arfs, and AP-1 function in a common pathway since this is most consistent with data from yeast and mammals, and that loss of AGEF-1 and components of the AP-1 complex have similar phenotypes in coelomocytes and the intestine. While synergistic genetic interactions are typically more indicative of genes in parallel pathways, we interpret that no single mutation in the AGEF-1/Arf/AP-1 pathway is sufficient to increase LET-23 EGFR signaling above a threshold necessary for ectopic induction. It is only when the activity of the AGEF-1/Arf/AP-1 pathway is further compromised by two mutations that LET-23 EGFR signaling increases above a threshold to induce a synergistic Muv phenotype. It is important to note that the AGEF-1/Arf/AP-1 pathway is essential, and only animals that survive to the fourth larval stage can be scored for vulva induction phenotypes. Thus, LET-23 EGFR signaling and localization phenotypes would likely be more severe if we were able to assess true null mutations in the VPCs only.

In polarized epithelial cells, the AP-1 complex mediates sorting and polarized distribution of transmembrane proteins, including EGFR, and thus the AGEF-1/Arf GTPase/AP-1 ensemble could regulate signaling via LET-23 EGFR localization. In the P6.p cell, we showed that the localization of LET-23 EGFR is altered in *agef-1(vh4)* animals using two transgenic lines (*zhIs035* and *zhIs038)* expressing LET-23::GFP (Haag et al., 2014). In wild-type animals, LET-23::GFP is

present on both the apical and basolateral domains, however the average levels of LET-23:GFP on the apical membrane are double (*zhIs035)* or close to double (*zhIs038)* that on the basolateral membrane (Figure 17A). In *agef-1(vh4)* animals there was a redistribution of LET-23::GFP from apical to basolateral membrane bringing the average intensities closer to equal, suggesting that AGEF-1 either promotes apical localization or antagonizes basolateral localization of the receptor (Figure 17A, B). In the *lin-2(e1309)* background, LET-23::GFP is apical only (Figure 17C). In the more highly expressed line, *zhIs035*, we see some lateral only or faint basolateral in the P6.p descendants, P6.pa and P6.pp of *lin-2(e1309)* larvae. In the *zhIs035* line, *agef-1(vh4)* partially restores LET-23::GFP on the basolateral membrane in *lin-2(e1309)* larvae. RNAi of *unc-101* also partially restores basolateral localization and enhances the effect of *agef-1(vh4)* such that we see increased levels of LET-23::GFP, with both lines, in *lin-2(e1309)* larvae (Figure 17D). Therefore, AGEF-1 and UNC-101 AP-1μ cooperate to antagonize LET-23 EGFR basolateral localization and thus provide a mechanism by which these genes/proteins antagonize LET-23 EGFR signaling. Despite the lack of basolateral localization of LET-23::GFP in *lin-2* mutant animals, the two LET-23::GFP transgenes used in this study rescued the *lin-2(e1309)* Vul phenotype, suggesting that the levels of receptor required for VPC induction are below detection. Therefore, the modest amount of LET-23::GFP restored to the basolateral membrane in *agef-1(vh4); lin-2(e1309)* or *unc-101(RNAi); lin-2(e1309)* could be more than sufficient to explain the strong restoration of VPC induction in these double mutants.

Our findings that an AGEF-1/Arf GTPase/AP-1 ensemble antagonizes the basolateral localization of LET-23 EGFR is contradictory to the established role of the mammalian AP-1A and AP-1B complexes in sorting transmembrane proteins to the basolateral membrane through the specific binding of basolateral sorting motifs in the cytoplasmic tail (Bonifacino, 2014) . In fact,

the AP-1B complex promotes the basolateral localization of EGFR in MDCK cells (Ryan et al., 2010). LET-23 EGFR does have several putative AP-1 sorting motifs, and thus could be a direct target for AP-1 regulation, but this would imply that AP-1 is impeding basolateral localization. A precedent for AP-1 having an antagonistic role in protein sorting or secretion has been found with the yeast Chs3p and Fus1p proteins, which rely on the exomer for secretion (Barfield et al., 2009; Wang et al., 2006). In the absence of exomer, Chs3p and Fus1p are retained internally in an AP-1 dependent manner (Barfield et al., 2009; Starr et al., 2012; Valdivia et al., 2002). An analogous situation whereby the LIN-2/7/10 complex sorts/maintains LET-23 EGFR localization on the basolateral membrane and the AGEF-1/Arf/AP-1 pathway plays an antagonistic role could exist.

Recent studies in *C. elegans* and mice have shown that both basolateral and apical membrane cargos are mislocalized in the absence of the AP-1 complex (Hase et al., 2013; Shafaq-Zadah et al., 2012; Zhang et al., 2012), suggesting that the AP-1 complex is required to maintain the polarity of the epithelial cells (reviewed in Bonifacino, 2014). Similarly, we find that *agef-1(vh4)* mutants mislocalized the SID-2 protein to the basolateral membranes, which is strictly apical in wild-type animals. Therefore, AGEF-1 might function with AP-1 to maintain polarity in the intestinal epithelia and by extension the AGEF-1/Arf GTPase/AP-1 ensemble could indirectly regulate LET-23 EGFR localization via maintenance of VPC polarity.

In summary, an AGEF-1/Arf GTPase/AP-1 ensemble functions opposite the LIN-2/7/10 complex to regulate apical versus basolateral localization of LET-23 EGFR in the VPCs, thus explaining how the it negatively regulates LET-23 EGFR-mediated vulva induction. We don't yet know whether the AGEF-1/Arf GTPase/AP-1 ensemble directly regulates LET-23 EGFR sorting and localization or whether it is indirect via maintenance of VPC polarity. Further studies will be

required to sort out the mechanisms by which the AGEF-1/ARF GTPase/AP-1 ensemble regulates LET-23 EGFR localization.

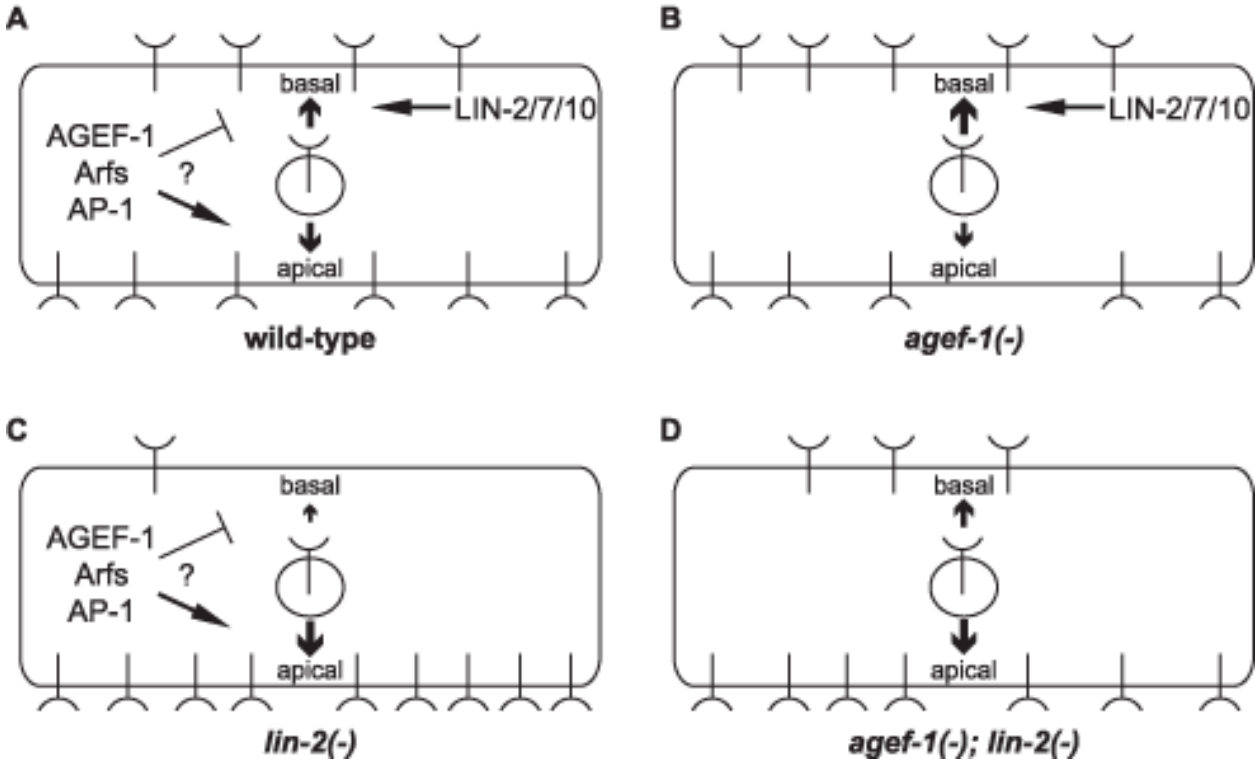

Figure 17. Model of LET-23 EGFR regulation by AGEF-1/Arf/AP-1 and LIN-2/7/10.

(A) LET-23 EGFR is localized to both basal and apical membranes in the VPCs of wild-type animals. The LIN-2/7/10 complex promotes the basal localization while the AGEF-1/Arf/AP-1 ensemble either inhibits basal or promotes apical localization. (B) In an *agef-1(-)* background, there is more LET-23 EGFR on the basal and less apical. (C) In a *lin-2(-)* background, most all of the LET-23 EGFR is apical with presumably residue LET-23 EGFR at the basal membrane, but not enough to induce vulva cell fates. (D) In an *agef-1(-); lin-2(-)* background, the loss of AGEF-1 partially restores LET-23 EGFR to the basal membrane sufficient to induce vulva cell fates.

Table S1. Strain list

CB1309 *lin-2(e1309) X*

CB1417 *lin-3(e1417) IV*

CB2769 *eDf3/eDf24 I*

CB4856 (Hawaiian mapping strain)

DH1033 *sqt-1(sc103) II; bIs1[Pvit-2::VIT-2::GFP; rol-6(su1006)] X*

DH1336 *bIs34[Prme-8::GFP::RME-8; rol-6]*

FX01447 *arf-6 (tm1447) IV* (Shohei Mitani, Tokyo Women's Medical University)

FX01693 *agef-1(tm1693)/+ I* (Shohei Mitani, Tokyo Women's Medical University)

FX03767 *vps-28(tm3767)/+ I* (Shohei Mitani, Tokyo Women's Medical University)

FX12006 *arf-3(tm1877)/nT1 IV* (Shohei Mitani, Tokyo Women's Medical University)

GS1912 *arIs37[pmyo-3::ssGFP; dpy-20(+)] I; dpy-20(e1282) IV*

HC722 *qtIs5[SID-2::C-GFP]; sid-2(gk505) III* (Craig Hunter, Harvard University)

MT2124 *let-60(n1046) IV*

N2 (Bristol wild-type parent strain)

NP822 *unc-119(ed3) III*; *cdIs54[pcc-1::MANS::GFP; unc-119(+)]*

NP941 *unc-119(ed3) III*; *cdIs85 [pcc-1::2xFYVE::GFP + unc-119(+) + Pmyo-2::GFP]*

PS80 *let-23(sy1) unc-4(e120) II*

PS295 *let-23(sy97) unc-4(e120)/mnC1[dpy-10(e128) unc-152(e444)] II*

PS529 *unc-101(sy108) I*

PS2728 *sli-1(sy143) X*

QR180 *agef-1(vh4) I* (this study)

QR201 *agef-1(vh4) I*; *bIs1[Pvit-2::VIT-2::GFP; rol-6(su1006)] X* (this study)

QR202 *agef-1(vh4) I*; *pwIs50[Plmp-1::LMP-1::GFP + Cbr-unc-119(+)]* (this study)

QR252 *agef-1(vh4) I; pwIs28(Ppie-1::CAV-1::GFP)* (this study)

QR268 *arf-1.2(ok796) III; lin-2(e1309) X* (this study)

QR269 *agef-1(vh4) I*; *bIs34[Prme-8::GFP::RME-8; rol-6]* (this study)

QR277 *agef-1(vh4) I; lin-3(e1417) IV* (this study)

QR293 *agef-1(vh4) I; let-23(sy97) unc-4(e120)/mIn1 II* (this study)

QR297 *agef-1(vh4) I; let-60(n1046) IV* (this study)

QR301 *agef-1(vh4) I*; *qtIs5(SID-2::C-GFP)* (this study)

QR307 *agef-1(vh4) I; let-23(sy1) unc-4(e120) II* (this study)

QR324 *agef-1(vh4) I*; *cdIs54[pcc-1::MANS::GFP; unc-119(+); myo2::GFP]* (this study)

QR325 *arf-1.1* and F45E4.7(ok1840) *IV; lin-2(e1309) X* (this study)

QR326 *agef-1(vh4) I*; *cdIs85 [pcc-1::2xFYVE::GFP + unc-119(+) + Pmyo-2::GFP]* (this study)

QR339 *agef-1(vh4) I; sli-1(sy143) X* (this study)

QR344 *arIs37[pmyo-3::ssGFP; dpy-20(+)] agef-1(vh4) I* (this study)

QR347 *arf-6(tm1447) IV; lin-2(e1309) X* (this study)

QR356 *agef-1(vh4) I; arf-1.2(ok796)/hT2 III* (this study)

QR357 *unc-101(sy108) I; arf-1.2(ok796) III* (this study)

QR382 *arf-1.2(ok796) III; lin-2(e1309) X; vhEx7[Plin-31::ARF-1.2::GFP + Pttx-3::GFP]* (this study)

QR383 *arf-1.2(ok796) III; lin-2(e1309) X*; *vhEx8[Plin-31::ARF-1.2::GFP + Pttx-3::GFP]* (this study)

QR401 *unc-101(sy108) I*; *pwIs50[Plmp-1::LMP-1::GFP + Cbr-unc-119(+)]* (this study)

QR403 *agef-1(vh4) I; lin-2(e1309) X; vhEx7[Plin-31::ARF-1.2::GFP + Pttx-3::GFP]* (this study)

QR404 *agef-1(vh4) I; lin-2(e1309) X; vhEx8[Plin-31::ARF-1.2::GFP + Pttx-3::GFP]* (this study)

QR475 *agef-1(vh4) I; zhIs038[Plet-23::LET-23::GFP; unc-119(+)] IV* (this study)

QR476 *zhIs038[Plet-23::LET-23::GFP; unc-119(+)]; lin-2(e1309) X* (this study)

QR477 *agef-1(vh4) I; zhIs038[Plet-23::LET-23::GFP; unc-119(+)] IV; lin-2(e1309) X* (this study)

QR479 *zhIs035[Plet-23::LET-23::GFP; unc-119(+)] agef-1(vh4) I* (this study)

QR480 *zhIs035[Plet-23::LET-23::GFP; unc-119(+)] I; lin-2(e1309) X* (this study)

QR512 *agef-1(vh4) I; lin-2(e1309) X* (this study)

QR513 *zhIs035[Plet-23::LET-23::GFP; unc-119(+)] agef-1(vh4) I; lin-2(e1309) X* (this study)

RB1535 *arf-1.1 and F45E4.7(ok1840) IV*

RT258 *unc-119(ed3) III; pwIs50[Plmp-1::LMP-1::GFP + Cbr-unc-119(+)]*

RT688 *unc-119(ed3) III*; *pwIs28[Ppie-1::CAV-1::GFP + unc-119(+)]*

SL536 *dxDf2/spe-9(eb19) unc-101(m1)* I

VC567 *arf-1.2(ok796) III*

VC1286 *agef-1(ok1736)/hIn1[unc-101(sy241)] I*

zhIs035[Plet-23::LET-23::GFP; unc-119(+)] I (Alex Hajnal, University of Zurich)

zhIs038[Plet-23::LET-23::GFP; unc-119(+)] III (Alex Hajnal, University of Zurich)

CHAPTER 3: Dynein-mediated trafficking negatively regulates LET-23 EGFR signaling

Olga Skorobogata*, Jassy Meng * and Christian E. Rocheleau

* These authors contributed equally

Reproduced with permission from O Skorobogata, J Meng and CE Rocheleau. 2015.

Under review – Molecular Biology of the Cell.

PREFACE

The second mutant identified in the screen for suppressors of the *lin-2(-)* Vul phenotype that showed a high level of suppression, small body size, temperature-sensitive embryonic lethality and multinucleated embryo phenotype was *vh22*. The following study aimed at cloning the gene, placing *vh22* within the Ras signaling pathway and elucidating the mechanism by which it regulates the strength of signaling using genetic and cell biological approaches. Our finding that *vh22* is an allele of *dhc-1*, a component of the cytoplasmic dynein complex, which is involved in cargo trafficking along the microtubule cytoskeleton was an exciting discovery. Since it has been shown that in mammals Rab7 is able to couple dynein and promote late endosome fusion with the lysosome, not only did we identify a gene, whose product is involved in vesicular trafficking, but it also has a potential to work closely with Rab7 in addition to being a negative regulator of Ras signaling.

ABSTRACT

Epidermal Growth Factor Receptor (EGFR) signaling is essential for animal development and increased signaling underlies many human cancers. Identifying the genes and cellular processes that regulate EGFR signaling *in vivo* will help elucidate how this pathway can become inappropriately activated. *Caenorhabditis elegans* vulva development provides an *in vivo* model to genetically dissect EGFR signaling. Here we identified a mutation in *dhc-1*, the heavy chain of the cytoplasmic dynein minus-end directed microtubule motor, in a genetic screen for regulators of EGFR signaling. Despite the many cellular functions of dynein, DHC-1 is a strong negative regulator of EGFR signaling during vulva induction. DHC-1 is required in the signal-receiving cell, genetically functions upstream or in parallel to LET-23 EGFR. LET-23 EGFR accumulates in cytoplasmic foci in *dhc-1* mutants consistent with mammalian cell studies whereby dynein has been shown to regulate late endosome trafficking of EGFR with the Rab7 GTPase. However, we found different distributions of LET-23 EGFR foci in *rab-7* versus *dhc-1* mutants, suggesting that dynein functions at an earlier step of LET-23 EGFR trafficking to the lysosome than RAB-7. Our results demonstrate an *in vivo* role for dynein in limiting LET-23 EGFR signaling via endosomal trafficking.

INTRODUCTION

Epidermal Growth Factor Receptor (EGFR) signaling regulates many cellular processes, most notably cell proliferation in mammalian cells (Normanno et al., 2006). Thus, it is not surprising that EGFR and family members are overexpressed in many human cancers. Lysosomal degradation is an important mechanism to turnover activated EGFR receptors (Sorkin and Goh, 2009). Upon activation, EGFR is internalized into early endosomes where the cytoplasmic tail is still able to engage downstream signaling proteins. Maturation of early endosomes into late endosomes is accompanied by the formation of multivesicular bodies (MVBs) and the internalization of EGFR from the outer membrane into intraluminal vesicles and thus sequestration of EGFR from downstream signaling proteins. Subsequent fusion with lysosomes results in the ultimate destruction of EGFR. Rab GTPases are important mediators of endosome trafficking (Stenmark, 2009). The coordinated functions of the Rab5 and Rab7 GTPases regulate early to late endosome maturation and lysosomal fusion. Inhibition of Rab7 in mammalian cells results in accumulation of EGFR in MVBs and in *C. elegans* leads to increased signaling via the *C. elegans* EGFR, LET-23 (Skorobogata and Rocheleau, 2012; Vanlandingham and Ceresa, 2009). In addition to mediating late endosome fusion with lysosomes along with the HOPS complex, Rab7 couples with the dynein minus-end microtubule motor via the Rab7 interacting proteins, RILP and ORP1L, which tether to the dynactin complex, a regulator of Dynein (Johansson et al., 2007). Inhibition of dynactin by overexpression of the p50 subunit blocks endosome movement from the cell periphery, inhibits EGFR degradation and causes sustained Erk1/2 activation (Taub et al., 2007). However, dynein can be recruited by other Rab GTPases to mediate membrane trafficking in the endocytic and secretory pathways (Horgan and McCaffrey, 2011; Hunt and Stephens, 2011). In *Drosophila*, dynein promotes EGFR signaling during eye and wing development by promoting

secretion of the EGFR ligand, Spitz (Iyadurai et al., 2008). Thus, dynein has both positive and negative effects on EGFR signaling in the fruit fly and mammalian tissue culture cells, respectively.

C. elegans vulva development provides an *in vivo* model to study EGFR signaling in epithelial cells (Schmid and Hajnal, 2015; Sundaram, 2013). During larval development, six vulval precursor cells (VPCs), P3.p-P8.p, express LET-23 EGFR on both the apical and basolateral membranes. The anchor cell in the overlying gonad secretes an EGF-like ligand, LIN-3, that engages LET-23 EGFR on the basolateral membrane initiating a conserved Ras/mitogen activated protein kinase (MAPK) signaling pathway in the P6.p cell and specifying the primary vulval cell fate. Graded LIN-3 signaling and LIN-12 Notch signaling specify the neighboring P5.p and P7.p cells to adopt the secondary vulval fates. P5.p-P7.p cells undergo three rounds of cell division to generate the 22 cells of the mature vulva. The remaining un-induced VPCs (P3.p, P4.p and P8.p) divide once (P3.p does not divide 50% of the time) and fuse with the surrounding hypodermis. Mutations that decrease LET-23 EGFR signaling result in a vulvaless (Vul) phenotype in which less than 3 VPCs are induced. Mutations that increase LET-23 EGFR signaling result in a multivulva (Muv) phenotype in which greater than 3 VPCs are induced. The LIN-2 Cask/LIN-7 Veli/LIN-10 Mint (LIN-2/7/10) complex binds the C-terminal tail of LET-23 EGFR and is required for the basolateral localization of LET-23 EGFR in the VPCs and vulva induction. Mutations in the *lin-2/7/10* complex result in apical only localization of LET-23 EGFR and a strong Vul phenotype.

In a suppressor screen of the *lin-2* mutant Vul phenotype, we identified two suppressors with embryonic lethal phenotypes, *vh4* and *vh22* (Skorobogata et al., 2014). We previously reported that *vh4* is a mutation in the *agef-1* gene that partially restores basolateral membrane

localization of LET-23 EGFR. Here we report that *vh22* is a temperature sensitive mutation in *dhc-1*, the heavy chain of the dynein minus-end directed microtubule motor. We demonstrate that *dhc-1* is a strong negative regulator of LET-23 EGFR signaling that functions upstream of or in parallel to LET-23 EGFR. LET-23::GFP accumulates in foci in the P6.p descendants of *dhc-1(vh22)* animals consistent with a defect in endocytic trafficking of LET-23 EGFR. Unlike *rab-7* mutants, many of the LET-23::GFP foci in *dhc-1(vh22)* mutants remain adjacent to the plasma membrane, suggesting that *dhc-1* regulates an earlier step of LET-23 EGFR trafficking to the lysosome.

MATERIALS AND METHODS

Strains and alleles

General methods for the handling and culturing of *C. elegans* were as previously described (Brenner, 1974). *C. elegans* Bristol strain N2 is the wild-type parent for all the strains used in this study; *E. coli* strain HB101 was used as a food source. The Hawaiian strain CB4856 was used for SNP mapping. Unless otherwise noted, experiments were performed at 20°C. Information on the genes and alleles used in this work can be found on WormBase (www.wormbase.org) and are available through Caenorhabditis Genetics Center (www.cbs.umn.edu/cgc) unless otherwise noted in the strain list (Table S2).

Genetic mapping and cloning of *dhc-1(vh22)*

Single nucleotide polymorphism (SNP) mapping was used to place *vh22* to the middle region of chromosome I (Davis et al., 2005). Chromosome mapping showed linkage of *vh22* to SNPs at -6 (W03D8), -1(D1007), 5 (B0205), 13 (F58D5), 14 (T06G6) and 26 (Y105E8B) map units (m.u.). Interval mapping using two sets of recombinants, 127 animals in total, was conducted using the following SNPs: Y71G12A at -17 m.u. (RFLP DraI), W03D8 at -6 m.u. (RFLP DraI), D1007 at -1 m.u. (RFLP DraI), pkP1055 at 0 m.u. (RFLP AvaI), pkP1057 at 1 m.u. (RFLP NaeI), pkP1059 at 3 m.u. (RFLP DraI), B0205 at 5 m.u. (RFLP DraI), F58D5 at 13 m.u. (RFLP DraI), T06G6 at 14 m.u. (RFLP DraI) and Y105E8B at 25 m.u. (RFLP DraI). Genomic DNA from QR180 *agef-1(vh4)* (Skorobogata et al., 2014) and QR160 *dhc-1(vh22)* was isolated and submitted to Genome Quebec for Illumina sequencing. Within the defined map region, *dhc-1* (V3228D, D4344N), *elpc-1* (A629T) and *cpd-1* (T493I) carried homozygous non-synonymous mutations unique to QR160

dhc-1(vh22) strain.

RNA interference

RNAi feeding was performed essentially as previously described (Kamath et al., 2001) using the *dhc-1, elpc-1, cpd-1,* and *rab-7* clones from the Ahringer RNAi library (Geneservice, Cambridge, United Kingdom). Clones were verified by DNA sequencing. To avoid embryonic and larval lethal phenotypes, synchronized L1 larvae were placed on RNAi plates and scored for vulva induction when the animals reached L4 stage 36-48 hours later.

Microscopy and phenotype analysis

General methods for live animal imaging using Nomarski differential interference contrast (DIC) microscopy were as previously described (Sulston and Horvitz, 1977). Animals were analyzed on an Axio Zeiss A1 Imager compound microscope (Zeiss, Oberkochen, Germany), images were captured using an AxioCam MRm camera and AxioVision software (Zeiss, Oberkochen, Germany). Muv and Vul phenotypes were scored by counting the numbers of vulval and non-vulval descendants of P3.p-P8.p in L4 stage larvae as described previously (Skorobogata and Rocheleau, 2012). Fisher's exact test (www.graphpad.com/quickcalcs) was used for statistical analysis of the vulval phenotypes. Confocal analysis was performed using a Zeiss LSM-510 Meta laser scanning microscope with 63X oil immersion lens (Zeiss, Oberkochen, Germany) in a single-track mode using a 488 nm excitation for GFP. Images were captured using ZEN 2009 Image software (Zeiss, Oberkochen, Germany). *zhIs038* transgene-carrying animals were

visualized at early L3 larval stage. The number of punctae in the P6.p descendants was calculated manually in each animal.

The percent embryonic lethality was determined by plating adult hermaphrodites, one per plate, and allowing them to lay eggs for several hours after which hermaphrodites are removed and the total number of laid eggs is counted. Approximately 24 hours later, the unhatched eggs are counted. The number of unhatched eggs was divided by the total number of laid eggs to determine the percent embryonic lethality for each strain.

RESULTS

Identification of *vh22* as an essential suppressor of the *lin-2(-)* Vul phenotype

Mutations in the *lin-2*, *lin*-7 or *lin-10* genes result in a strong Vul phenotype that is easily suppressed by loss of a negative regulator of LET-23 EGFR signaling such as the SLI-1 Cbl E3 ubiquitin ligase homolog, the GAP-1 Ras GAP, or the LIP-1 MAPK Phosphatase (Berset et al., 2001; Hajnal et al., 1997; Jongeward et al., 1995; Yoon et al., 1995). We previously identified the *rab-7(ok511)* deletion as a strong suppressor of mutations in the *lin-2, lin-7*, and *lin-10* genes, reverting a strong Vul phenotype back to wild-type and Muv phenotypes (Skorobogata and Rocheleau, 2012). The maternal effect embryonic lethality of the *rab-7(ok511)* would preclude its identification in screens for viable suppressors. Therefore, we conducted a clonal forward genetic screen for essential suppressors of the *lin-2(e1309)* Vul phenotype to identify additional genes that might function with *rab-7* to antagonize LET-23 EGFR signaling (Skorobogata et al., 2014). We identified the *vh22* mutation as a strong suppressor of the *lin-2(e1309)* Vul phenotype. While *lin-2(e1309)* mutants are 100% Vul, the *vh22; lin-2(e1309)* double mutants are only 15% Vul at 20°C with 85% of the animals developing a wild-type vulva (Figure 18A-D and Table 4). Like mutations in other negative regulators, *vh22* single mutants have essentially normal vulva induction (Figure 18C and Table 4). In addition, *vh22* animals are ~80% embryonic lethal at 20°C and have a small body morphology phenotype (Table 5 and not shown). Embryos often arrest with undifferentiated multinucleate cells indicative of an early cell division defect (Figure 18 E and D). However, no cell division defects were observed in the vulval cell lineages. The embryonic lethality and the suppression of the *lin-2(e1309)* Vul phenotypes were temperature sensitive as both phenotypes were considerably less severe at 15°C and more severe at 25°C (Tables 4 and 5).

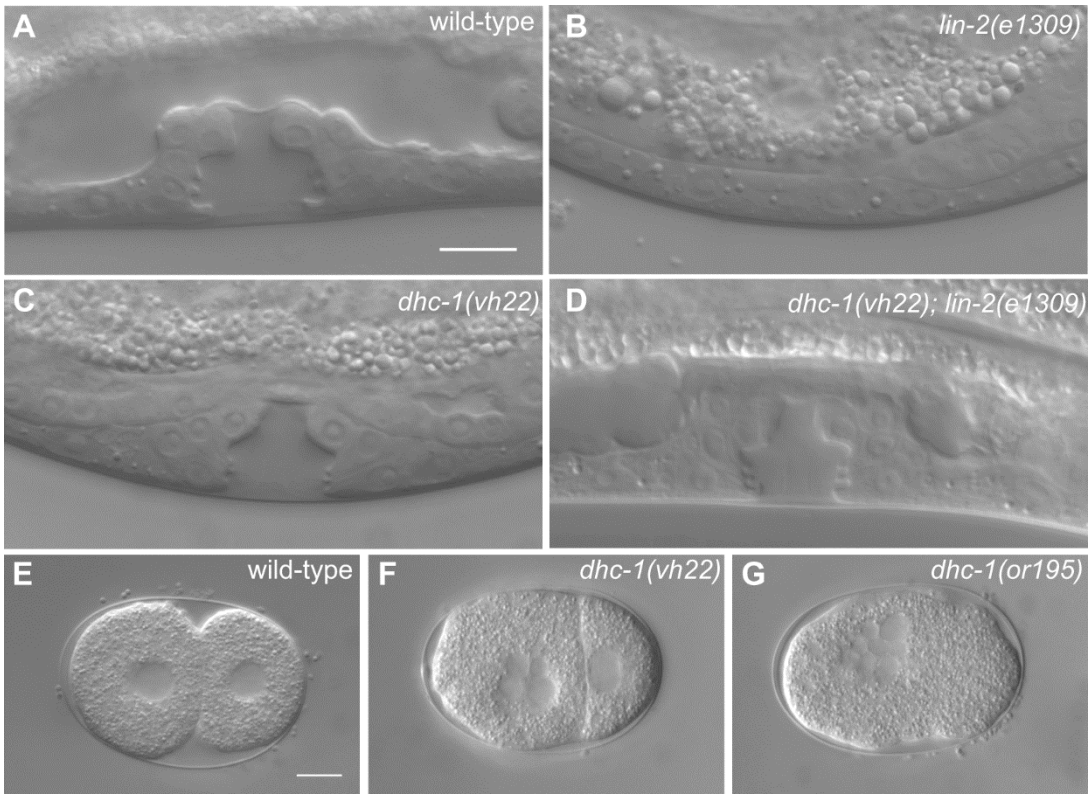

Figure 18. *dhc-1(vh22)* suppresses the *lin-2(e1309)* Vul phenotype.

(A-D) Representative Differential Interference Contrast (DIC) images of vulvas of wild-type, *lin-2(e1309)*, *dhc-1(vh22)* and *dhc-1(vh22); lin-2(e1309)* L4 stage larvae. The *lin-2(e1309)* larva lacks a vulva while in *dhc-1(vh22); lin-2(e1309)* the vulva is mostly restored. *dhc-1(vh22)* single mutants have a wild-type vulva. (E, F) DIC images of early embryos of wild-type, *dhc-1(vh22)* and *dhc-1(or195)*. Bars, 10 µm.

Table 4. Loss of *dhc-1* suppresses the *lin-2(-)* and *lin-7(-)* Vul phenotypes

Genotype	Temperature	Muv, %	Vul, %	Avg. # of VPCs induced	*n*
wild-type	all temps	0	0	3.0	many
dhc-1(vh22)	20°C	0	5	2.98	20
lin-2(e1309)	20°C	0	100	0.29	21
dhc-1(vh22); lin-2(e1309)	15°C	5	80**	1.5***	20
	20°C	0	15***	2.85***	20
	25°C	0	11***	2.98***	20
dhc-1(vh22); lin-2(e1309); orIs17[GFP::DHC-1]	15°C	0	100*	0.44	26
	20°C	12	58***	1.80****	33
dhc-1(or195); lin-2(e1309)	15°C	0	100	0.13	15
	20°C	0	96	0.78**	23
	25°C	0	89**	0.9**	29
dhc-1(or352); lin-2(e1309)	15°C	0	100	0.23	15
	20°C	0	88**	0.69**	18

	25°C	0	76**	1.53***	44
GFP(RNAi); lin-2(e1309)	20°C	0	100	0.32	31
dhc-1(RNAi); lin-2(e1309)	20°C	7	85*	1.59****	17
elpc-1(RNAi); lin-2(e1309)	20°C	0	95	0.36	40
cpd-1(RNAi); lin-2(e1309)	20°C	0	98	0.3	40

Statistical significance was determined using Fisher's exact test (www.graphpad.com/quickcalcs). **P<0.05, **P<0.01, ***P<0.001, ****P<0.0001. dhc-1; lin-2* mutants were compared to *lin-2* single mutants. *orIs17* carrying strains were compared to *dhc-1(vh22); lin-2(e1309)* at the same temperatures. *dhc-1(RNAi), elpc-1(RNAi)* and *cpd-1(RNAi)* were compared to *gfp(RNAi).* The penetrance of the *lin-2(e1309)* phenotype is similar at all temperatures. *n*, number of animals scored.

Table 5. *dhc-1(vh22)* is temperature sensitive embryonic lethal

Genotype	%, embryonic lethality (*n*)		
	15°C	**20°C**	**25°C**
dhc-1(vh22)	23 (211)	81 (274)	96 (126)
dhc-1(or195)	22 (369)	97 (514)	99 (304)
dhc-1(or352)	26 (507)	90 (460)	97 (934)
dhc-1(vh22)/dhc-1(or195)		96 (1218)	
dhc-1(vh22)/dhc-1(or352)		95 (1167)	
dhc-1(vh22); orIs17(DHC-1::GFP)	1.3 (382)****	0.5 (583)****	2.3 (264)****

Statistically analysis was performed as in Table 4. The *dhc-1(vh22); orIs17* strain has the *lin-2(e1309)* mutation in the background and was compared *dhc-1(vh22)* single mutants at the same temperature. *n*, number of embryos scored.

vh22 is an allele of *dhc-1*

To identify the gene mutated by *vh22* we used the associated small body morphology and embryonic lethal phenotypes to map *vh22.* First we found that *vh22* was balanced by the *hT2* balancer consisting of a translocation between chromosomes I and III (Zetka and Rose, 1992). Single nucleotide polymorphism mapping located *vh22* between SNPs *W03D8* at -6 map units (mu) and *pkP1057* at 1 mu on chromosome I (Figure 19A). The location was further delineated by complementation with chromosomal deficiencies: *vh22* complemented *qDf3* and *mnDf111*, but failed to complement *sDf4* and *hDf6* indicating that *vh22* was located between -2.21 and 0.1 mu (Figure 19A). Whole genome sequencing identified two missense mutations in the *dhc-1* gene, which has previously been reported to have early cell division defects (Figure 18G) (Gonczy et al., 1999; Schmidt et al., 2005), as well as homozygous non-synonymous mutations in the *elpc-1* and *cpd-1* genes (see Materials and Methods). We found that RNAi of *dhc-1,* but not *elpc-1* or *cpd-1,* significantly suppressed the *lin-2(e1309)* Vul phenotype (Table 4). Consistent with *vh22* being a mutation in *dhc-1*, two conditional alleles of *dhc-1, or195* and *or352,* suppressed the *lin-2(e1309)* Vul phenotype at non-permissive temperature (Table 4) (Hamill et al., 2002). Furthermore, *vh22* fails to complement *dhc-1(or195)* and *dhc-1(or352)* for the embryonic lethal phenotype (Table 5). Finally, we can rescue the *vh22* embryonic lethality and suppression of *lin-2(e1309)* Vul phenotype with a GFP::DHC-1 transgene, *orIs17* (Tables 4 and 5) (Gassmann et al., 2008). Therefore we conclude that *vh22* is a mutation in *dhc-1.*

DHC-1 is the *C. elegans* dynein Heavy Chain subunit of the cytoplasmic dynein complex, a minus-end directed microtubule motor (Lye et al., 1995). DHC-1 comprises the motor and microtubule binding domain (C-terminal half) and a stem (N-terminal) that is involved in dimerization and recruitment of numerous accessory chains and regulators (Figure 19B) (Allan, 2011). The

missense mutations in *dhc-1* change two amino acid residues that are identical among metazoans and conserved with fungi. The first mutation changes a Valine 3228 to an Aspartic Acid in the microtubule binding domain, the second, an Aspartic Acid 4344 to Asparagine in a metazoan specific C-terminal domain. We do not know which change, or if both changes contribute to the *dhc-1(vh22)* phenotypes, but *vh22* is a stronger suppressor of the *lin-2(-)* Vul phenotype than the *or195* or *or352* alleles, which have been deemed strong mutations with respect to embryonic phenotypes (Table 4).

dhc-1* functions upstream or in parallel to *let-23 EGFR

Suppression of the *lin-2(-)* Vul phenotype by *dhc-1* alleles suggests that DHC-1 is a negative regulator of LET-23 EGFR signaling. Consistent with this hypothesis, we find that *dhc-1(vh22)* enhances the Muv phenotype of a gain-of-function mutation in *let-60 Ras, n1046* (Table 6). The *let-23(sy1)* allele truncates the last six amino acids shown to be required for binding the LIN-2/7/10 complex, and thus has an identical vulval phenotype as mutations in *lin-2/7/10* (Aroian et al., 1994; Kaech et al., 1998). We find that *dhc-1(vh22)* strongly suppresses Vul phenotype of the *let-23(sy1)* and *lin-7(e1413)* mutations (Table 6). The *let-23(sy97)* mutation is a more severe truncation of LET-23 EGFR that blocks signaling to LET-60 Ras in multiple tissues (Aroian and Sternberg, 1991). We find that *dhc-1(vh22)* fails to suppress the Vul phenotype of *let-23(sy97)* consistent with *dhc-1* functioning upstream or in parallel to *let-23 EGFR* (Table 6). *lin-3(e1417)* is a strong hypomorphic mutation in the promoter of *lin-3 EGF* that specifically abrogates *lin-3 EGF* expression in the Anchor Cell (Hwang and Sternberg, 2004). We find that *dhc-1(vh22)* significantly suppresses the Vul phenotype of *lin-3(e1417)* suggesting that *dhc-1* functions downstream of, or in parallel to, *lin-3 EGF* (Table 6). Taken together, these data suggest that

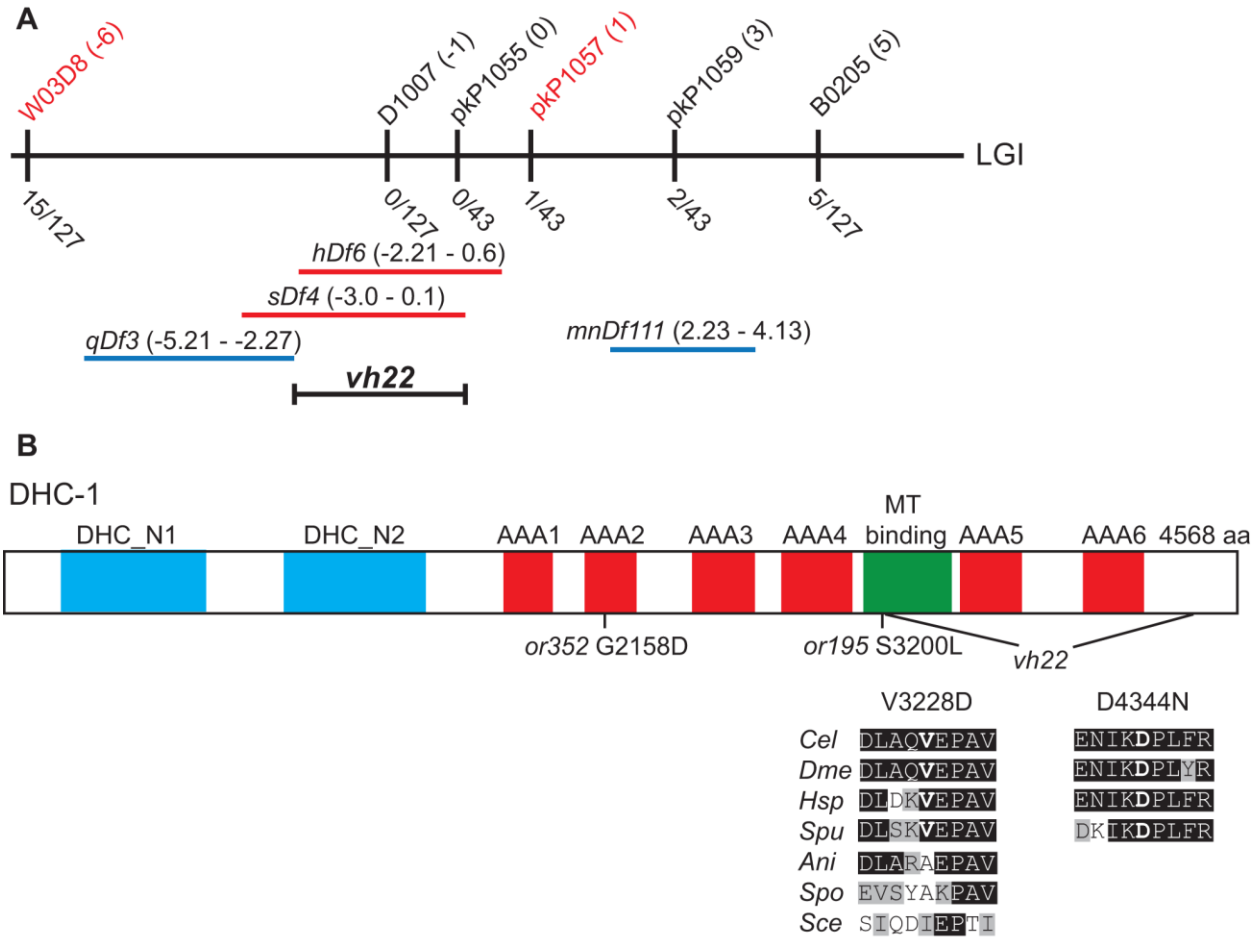

Figure 19. *dhc-1* mapping and the lesions.

(A) Schematic representation of the middle of chromosome I (LGI). The SNPs used for interval mapping are indicated on top with their chromosomal locations (map units). The number of recombinant animals positive for the Hawaiian SNP out of the total number of animals tested for each SNP is indicated below. The two chromosomal deficiencies that fail to complement *vh22, sDf4* and *hDf6* are shown in red and the complementing deficiencies, *qDf3* and *mnDf111*, are shown in blue. A bracket indicates the 2.1 map unit interval between the left end of *hDf6* and the right end of *sDf4* to which *vh22* maps. (B) Homology domains of the DHC-1 protein in common with the dynein Heavy Chains from other organisms: dimerization and accessory chain interaction domains (DHC_1 and DHC_2) in blue, AAA-type ATPase domains (AAA1-6) in red, and the microtubule binding stalk (MT binding) in green. The locations of the two missense mutations in

vh22, as well as the *or195* and *or352* alleles are shown below. Valine 3228 is in the microtubule binding stalk is changed to an Aspartic Acid. Valine 3228 in *C. elegans* (*Cel)* is conserved in *D. melanogaster (Dme)* NP_001261430.1, *H. sapiens (Hsp)* NP_0011367.2 and *S. purpuratus (Spu)* XP_797645.3, but not in the fungi *A. nidulans (Ani)* XP_657722.1, *S. pombe (Spo)* XP_001713108.1 or *S. cerevisiae (Sce)* GAA24775.1. Aspartic Acid 4344 resides in a C-terminal region is changed to an Asparagine. Aspartic Acid 4344 and the surrounding region are conserved amongst the metazoans analyzed, but not present in the fungi. Amino acid (aa) identities are highlighted in black and similarities in grey.

Table 6. DHC-1 negative regulates LET-23 EGFR signaling downstream or in parallel to LIN-3 EGF

Genotype	Muv, %	Vul, %	Avg. # of VPCs induced	*n*
let-60(n1046)[a]	65	0	3.55	20
dhc-1(vh22); let-60(n1046)	92	0	4.18**	24
lin-7(e1314)	0	92	0.278	36
dhc-1(vh22); lin-7(e1314)	5	38****	2.5****	42
let-23(sy1)	0	100	0.06	25
dhc-1(vh22); let-23(sy1)	3	57****	1.79****	35
let-23(sy97) [a]	0	93	0.4	29
dhc-1(vh22); let-23(sy97)	0	100	0.24	23
lin-3(e1417)	0	92	0.94	36
dhc-1(vh22); lin-3(e1417)	0	82	1.56***	50

Statistical analysis was done as in Table 4. Experiments were performed at 20°C.

[a]Control data was previously published as it was collected together with both *agef-1(vh4)* (Skorobogata et al., 2014) and *dhc-1(vh22)* double mutant strains. *n*, number of animals scored.

DHC-1 is genetically a negative regulator of LET-23 EGFR signaling and functions at the level of LET-23 EGFR.

DHC-1 functions in the VPCs to negatively regulate LET-23 EGFR signaling

If DHC-1 is regulating LET-23 EGFR, then we anticipated that DHC-1 would function in the VPCs, the signaling receiving cells. To determine if DHC-1 negatively regulates signaling in the signal receiving cells, we performed *dhc-1(RNAi)* specifically in the VPCs. We took advantage of the tissue-specific rescue of *rde-1(ne219)* mutant animals, which are deficient for RDE-1, an Argonaute required for exogenous RNAi (Qadota et al., 2007; Tabara et al., 1999). Expression of wild-type *rde-1(+)* under the VPC-specific promoter *lin-31* (*mfIs70)* in the *rde-1(ne219)* mutant confers sensitivity to RNAi specifically in the VPCs (Barkoulas et al., 2013; Tan et al., 1998). *rde-1(ne219); lin-2(e1309)* double-mutants expressing *rde-1(+)* in the VPCs were fed RNAi for *GFP*, *dhc-1* and *rab-7*. Consistent with our previous findings in the whole-animal RNAi experiments, depletion of either *dhc-1* or *rab-7* by RNAi specifically in the VPCs partially suppressed the *lin-2* Vul phenotype, while RNAi targeting GFP did not (Table 7). These data are consistent with both DHC-1 and RAB-7 functioning in the VPCs to negatively regulate EGFR signaling.

DHC-1 and RAB-7 regulate LET-23 EGFR trafficking

We previously found that RAB-7 regulates the localization of LET-23 EGFR in the VPCs (Skorobogata and Rocheleau, 2012). Specifically, the *rab-7(ok511)* deletion results in the accumulation of cytoplasmic LET-23::GFP foci in the VPCs of wild-type and *lin-2(e1309)* mutants expressing the *gaIs27* LET-23::GFP transgene. However, this transgene did not show the expected localization of LET-23::GFP at the basolateral membrane and precluded us from determining whether RAB-7 regulates apical versus basolateral localization. We reassessed the

Table7. DHC-1 functions in the VPCs

RNAi	Muv, %	Vul, %	Avg. # of VPCs induced	*n*
GFP	0	100	0.09	48
dhc-1	0	98	0.44***	50
rab-7	2	98	0.33**	46

The strain QR405: *rde-1(ne219); mfIs70[Plin-31::RDE-1]; lin-2(e1309)* was used for VPC-specific RNAi feeding. Statistical analysis was done as in Table 4. Experiments were performed at 20°C. *n*, number of animals scored.

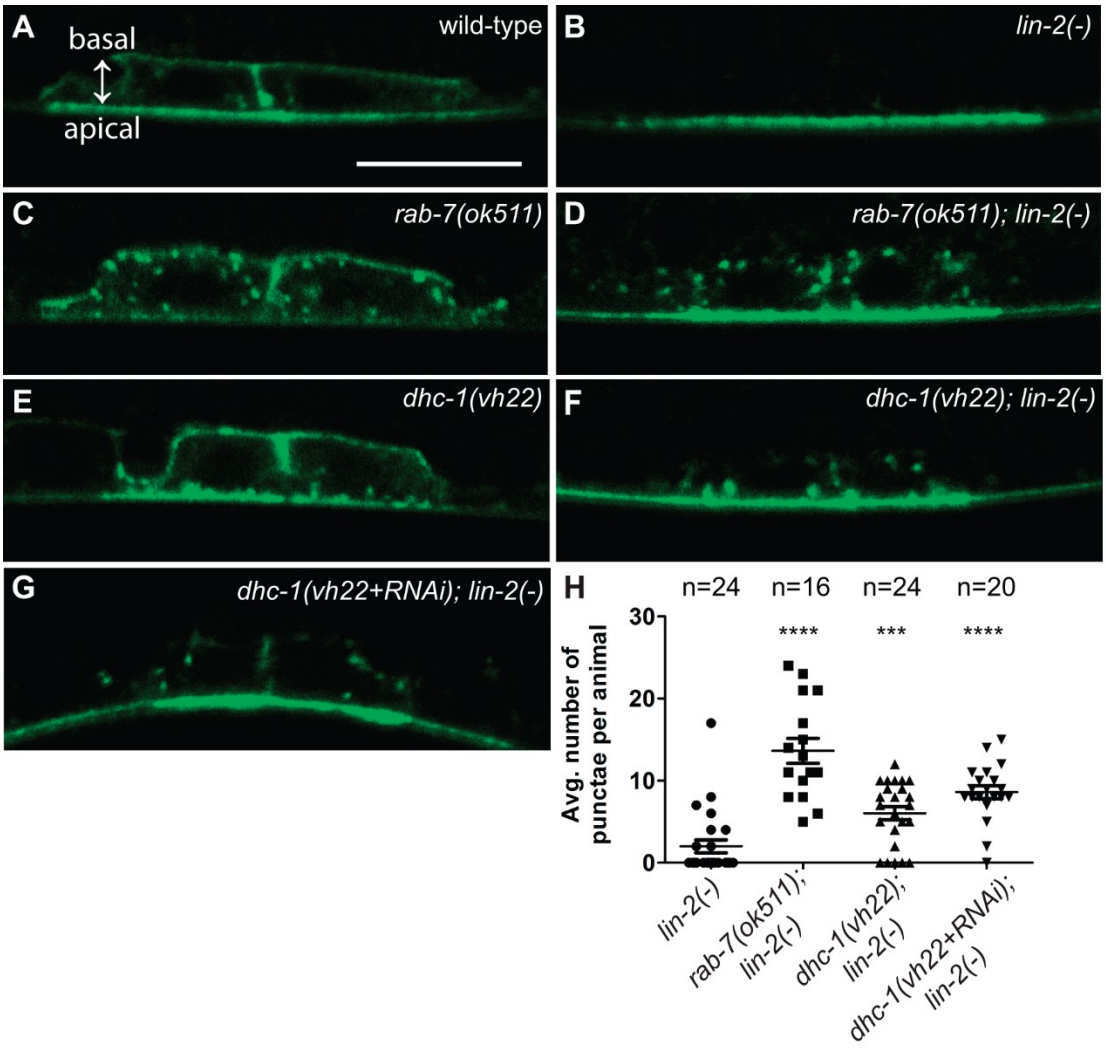

Figure 20. DHC-1 and RAB-7 differentially regulate LET-23 EGFR trafficking.

(A-G) Representative confocal images of LET-23::GFP localization in the P6.p daughter cells, P6.pa and P6.pp, of *zhIs038* transgene-carrying animals. The receptor is localized to both basolateral and apical membranes of wild-type animals (A), but is restricted to the apical membrane in *lin-2(e1309)* animals (B). *rab-7(ok511)* and *dhc-1(vh22)* mutants accumulate LET-23::GFP in the punctate structures within the vulval cells (C and D) and adjacent to the plasma membrane (E and F), respectively in both wild-type (C and E) and *lin-2(e1309)* backgrounds. (G) *dhc-1(RNAi)* does not significantly change the *dhc-1(vh22); lin-2(e1309)* phenotype. (H)

Quantification of the number of punctae in the P6.p descendants. All double-mutants were compared to *lin-2(-)*, a two-tailed t test was used to calculate statistical significance (*** - P=0.008, **** - P<0.0001). Basal and apical membranes are facing in the same direction in all the images and are indicated in (A). Bar, 5µm.

role of RAB-7 in the regulation of LET-23 EGFR trafficking in the VPCs of live animals using a new LET-23::GFP transgene, *zhIs038*, that expresses at levels comparable to endogenous LET-23 EGFR and shows clear localization at the basolateral membrane in wild-type VPCs, but not *lin-2(e1309)* mutants (Figure 20A and B) (Haag et al., 2014). The *rab-7(ok511)* mutation had little effect on LET-23::GFP localization in the P6.p cell. However, the daughter cells, P6.pa and P6.pp, showed a robust accumulation in cytoplasmic LET-23::GFP foci in *rab-7(ok511)* mutants (Figure 20C). This confirms our previous data with the *gaIs27* transgene and is consistent with RAB-7 being required for LET-23 EGFR trafficking to lysosomes (Skorobogata and Rocheleau, 2012).

In mammalian cell culture, Rab7 can recruit dynein to EGFR containing late endosomes to traffic them along microtubules toward lysosomes in the perinuclear region (Johansson et al., 2007). Therefore we tested if the VPCs of *dhc-1(vh22)* mutants also accumulated LET-23::GFP foci like *rab-7(ok511)* mutants. Similar to *rab-7(ok511)* animals, *dhc-1(vh22)* mutants have a more pronounced effect on LET-23::GFP localization in the P6.p daughter cells, P6.pa and P6.pp, with about 70% of the animals presenting accumulation of the LET-23::GFP in foci. Unlike the *rab-7(ok511)* mutants, the LET-23::GFP foci in *dhc-1(vh22)* accumulated adjacent to the plasma membrane (Figure 20E).

We also tested if loss of *rab-7* or *dhc-1* restored basolateral localization of LET-23::GFP in a *lin-2(e1309)* background. We found that neither loss of *rab-7* or *dhc-1* could restore basolateral localization of LET-23 EGFR in the *lin-2* mutant, but still accumulated LET-23::GFP foci; cytoplasmic in the *rab-7(ok511)* mutants and juxtamembrane in the *dhc-1(vh22)* mutants (Figure 20D, F, G and H). Therefore, the suppression of the *lin-2(e1309)* Vul phenotype by *rab-7(ok511)* and *dhc-1(vh22)* mutations is likely due to failure to downregulate LET-23 EGFR via

the endosome/lysosome trafficking rather than restoration of LET-23 EGFR localization on the basolateral membrane (Figure 21).

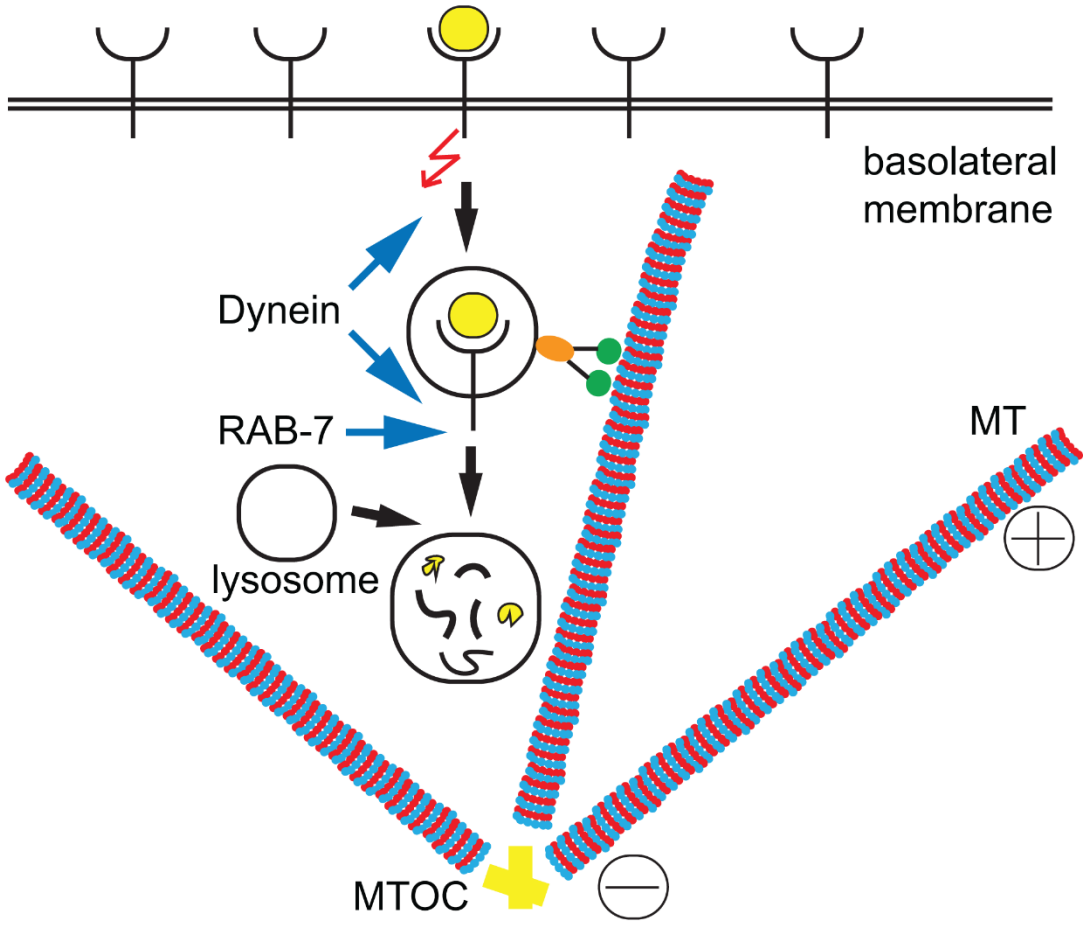

Figure 21. Model of LET-23 EGFR regulation by DHC-1 and RAB-7.

DHC-1 (dynein) and RAB-7 promote endocytic trafficking of LET-23 EGFR to the lysosome for degradation. Our data suggest that dynein functions at an early step of receptor trafficking moving endosomes along microtubules (MT) from the plasma membrane and toward the microtubule-organizing center (MTOC). Then RAB-7 facilitates lysosomal degradation of LET-23 EGFR, which could also involve dynein. Disruption of either dynein or RAB-7 would result in accumulation of active LET-23 EGFR on endosomes from which it can continue signaling.

DISCUSSION

Endosome trafficking and lysosome degradation of EGFR is an important mechanism for signal downregulation. The late endosomal Rab7 GTPase couples with the dynein minus-end directed microtubule motor to traffic late endosomes to lysosomes and facilitate EGFR degradation. We previously identified RAB-7 as a potent negative regulator of LET-23 EGFR signaling during *C. elegans* vulva induction. Here we have identified mutations in *dhc-1*, the dynein heavy chain, in a forward genetic screen for regulators of LET-23 EGFR signaling and intracellular trafficking. DHC-1 is a strong negative regulator of LET-23 EGFR signaling during *C. elegans* vulva induction. DHC-1 functions in the VPCs, the signal receiving cells, and genetically functions at the level of LET-23 EGFR. Consistent with a role in EGFR trafficking, RAB-7 and DHC-1 are required for the proper localization of LET-23 EGFR in the VPCs. However, LET-23::GFP foci accumulate adjacent to the plasma membrane in *dhc-1* mutant animals whereas in *rab-7* mutants, LET-23::GFP foci are distributed throughout the cytoplasm. Together these data suggest that DHC-1 is required for an early step in LET-23 EGFR trafficking to the lysosome in the VPCs and thus plays an important role in signal attenuation.

Cytoplasmic dynein is a heteromeric multiprotein minus-end directed microtubule motor, which is involved in a variety of cellular processes ranging from movement of a multitude of cargo towards the nucleus to mitotic spindle assembly during mitosis (Roberts et al., 2013). At the core of dynein complex is the DHC dimer, which contains a hexameric AAA+ (ATPase associated with various cellular activities) domain involved in ATP hydrolysis. Amongst the C-terminally located AAA+ domains lies the stalk and microtubule-binding domain. The N-terminal coiled-coil domains mediate dimerization, interactions with various intermediate, light, and light-intermediate chains as well we interactions with LIS1 and the dynactin complex which regulate cargo binding,

and motor activity (Allan, 2011). The *dhc-1(vh22)* allele has two missense mutations. One resides in the very C-terminus, a region specific to metazoan DHCs and is of unknown function. The other missense mutation is in the microtubule-binding stalk and thus might alter the conformation of the stalk and potentially its interaction with microtubules. The previously identified conditional alleles of *dhc-1, or195* and *or352*, have been deemed strong alleles of *dhc-1* with respect to several embryonic defects (Hamill et al., 2002; Schmidt et al., 2005). The *or195* allele also causes a defect in the microtubule binding stalk while the *or352* allele alters the second AAA+ domain (O'Rourke et al., 2007). Surprisingly, these *dhc-1* alleles were less effective suppressors of *lin-2(e1309).* The *lin-2(e1309)* allele has often been used to facilitate the identification of embryonic lethal mutations (Kemphues et al., 1988), and was in the background for genetic screens that identified the *or195* and *or352* alleles and thus there might have been a negative selection for alleles of *dhc-1* that suppress the *lin-2* Vul phenotype (Hamill et al., 2002).

Dynein and the dynactin complex promote EGFR trafficking to the lysosome in mammalian cell culture (Taub et al., 2007), however there is little data for dynein regulating EGFR signaling. In Hela cells, indirect inhibition of dynein via overexpression of the p50 dynamitin subunit of the dynactin complex inhibited EGFR degradation and caused sustained Erk1/2 activation (Taub et al., 2007). In *Drosophila melanogaster*, mutations in *dhc* and *p150 Glued* enhanced mutations in EGFR and Star, a regulator of Spitz ligand secretion, suggesting a positive role for dynein and the dynactin complex in Spitz-EGFR signaling (Iyadurai et al., 2008). Our findings may be the first to demonstrate an *in vivo* role for dynein negatively regulating EGFR signaling and are congruent with the p50 dynamitin overexpression studies in Hela cells. The differences between the Drosophila study and ours likely reflects the fact that dynein can regulate multiple trafficking pathways and its effects on cell signaling are likely to be context dependent.

Rab7 recruits the dynein-dynactin complex to late endosomes to drive microtubule-based movement toward lysosomes (Johansson et al., 2007). Since RAB-7 and DHC-1 both negatively regulate LET-23 EGFR signaling in the VPCs, we hypothesized that as in Hela cells, RAB-7 and DHC-1 function together to regulate LET-23 EGFR trafficking to the lysosome. We found that LET-23::GFP accumulated in foci adjacent to the plasma membrane of *dhc-1* mutants, which is again in line with EGFR localization in Hela cells overexpressing p50 dynamitin. In *rab-7* mutants, LET-23::GFP accumulated in foci that are distributed throughout the cytoplasm. Both phenotypes are consistent with defective endosome to lysosome trafficking of LET-23 EGFR in *rab-7* and *dhc-1* mutants, but are inconsistent with DHC-1 functioning exclusively with RAB-7. Rather, we propose that DHC-1/dynein is required at an earlier step of LET-23 EGFR trafficking, promoting movement of endosomes from the plasma membrane deeper into the cytoplasm, while RAB-7 is regulating later steps of endosome trafficking (Figure 21). Importantly, our data does not preclude DHC-1/dynein functioning both early and late in the endocytic pathway.

In summary, we identify DHC-1, the core component of the dynein minus-end directed microtubule motor, as a potent negative regulator of LET-23 EGFR signaling in *C. elegans.* DHC-1 functions in the VPCs to promote an early step in the endocytic trafficking of LET-23 EGFR to the lysosome. This study highlights how alterations to basic cellular machinery such vesicular trafficking and cytoskeletal transport can strongly impact signal transduction. In human cells, dynein could have a tumor suppressive function via its role in endosome trafficking and attenuating signaling by EGFR or other receptors that regulate growth control.

Table S 2. Strains used in this study

BC700 *sDf4/bli-4(e937) dpy-14(e188) I*

CB1309 *lin-2(e1309) X*

CB1413 *lin-7(e1413) II*

CB1415 (Hawaiian mapping strain)

CB1417 *lin-3(e1417) IV*

EU828 *dhc-1(or195) I*

EU1386 *dhc-1(or352ts) I*

EU1444 *unc-119(ed3) III*; *orIs17[Pdhc-1 ::GFP ::DHC-1; unc-119(+)]*

JK323 *qDf3/szT1[lon-2(e678)] I; +/szT1 X*

JU2039 *mfIs70[lin-31p::rde-1, myo2p::GFP] IV; rde-1(ne219) V*

KR1737 *hDf6 dpy-5(e61) unc-13(e450) I; hDp31(I;f)*

MT2124 *let-60(n1046) IV*

N2 (Bristol wild-type parent strain)

PS80 *let-23(sy1) unc-4(e120) II*

PS295 *let-23(sy97) unc-4(e120)/mnC1[dpy-10(e128) unc-152(e444)] II*

QR160 *dhc-1(vh22) I* (this study)

QR253 *dhc-1(vh22) I; lin-2(e1309) X* (this study)

QR298 *dhc-1(vh22) I; IV* (this study)

QR362 *dhc-1(vh22) I; orIs17[Pdhc-1 ::GFP ::DHC-1; unc-119(+)]; lin-2(e1309) X* (this study)

QR367 *dhc-1(vh22) I*; *let-23(sy1) unc-4 II* (this study)

QR371 *dhc-1(vh22) I; lin-3(e1314) IV* (this study)

QR405 *mfIs70[lin-31p::rde-1, myo2p::GFP] IV; rde-1(ne219) V; lin-2(e1309) X* (this study)

QR476 *zhIs038[Plet-23::LET-23::GFP; unc-119(+)] IV; lin-2(e1309) X* (Skorobogata et al)

QR509 *dhc-1(vh22) I; zhIs038[Plet-23::LET-23::GFP; unc-119(+)] IV* (this study)

QR522 *dhc-1(vh22*) *I; let-23(sy97) unc-43/mnC1[dpy-10(e128) unc-152(e444)] II* (this study)

QR548 *rab-7(ok511)/mIn1[mIs14 dpy-10(e128)] II; zhIs038[Plet-23::LET-23::GFP; unc-119(+)] IV* (this study)

QR632 *dhc-1(vh22) I; zhIs038[Plet-23::LET-23::GFP; unc-119(+)] IV; lin-2(e1309) X* (this study)

QR633 *rab-7(ok511)/mIn1[mIs14 dpy-10(e128)] II; zhIs08[Plet-23::LET-23::GFP; unc-119(+)] IV; lin-2(e1309) X* (this study)

QR634 *dhc-1(vh22) I; lin-7(e1413) II* (this study)

SP1540 *mnDf11/unc-13(e1091) lin-11(n566) I*

VC308 *rab-7(ok511)/mIn1[mIs14 dpy-10(e128)] II*

zhIs038[Plet-23::LET-23::GFP; unc-119(+)] IV (Alex Hajnal, University of Zurich)

CHAPTER 4: RAB-10 and ZEN-4 promote LET-23 EGFR signaling

PREFACE

Having identified AGEF-1 and DHC-1 as antagonizing LET-23 EGFR signaling during *C. elegans* vulva development by regulating the polarized distribution of LET-23 EGFR and endocytic trafficking of the internalized receptor in the VPCs, respectively, we have set out to determine genes functioning opposite AGEF-1 and DHC-1 in regulating the strength of *Ras* signaling in the VPCs. Identification of genes opposing the effects of AGEF-1 and DHC-1 could further our knowledge about the mechanisms linking various steps of receptor trafficking with modulations of signaling strength. Furthermore, understanding how these genes regulate EGFR signaling and trafficking in *C. elegans* will inform our understanding of EGFR signaling in human epithelial cells. This chapter contains unpublished and preliminary data.

MATERIALS AND METHODS

Stains and alleles

General methods for the handling and culturing of *C. elegans* were as previously described (Brenner, 1974). *C. elegans* Bristol strain N2 was used as a wild-type parent strain, *E. coli* strain HB101 was used as a food source. The majority of the experiments were carried at 20°C unless otherwise specified for stains carrying *zen-4(or153)* and/or *dhc-1(vh22)* in a homozygous form. Information on genes and alleles used in this work can be found on WormBase (www.wormbase.org). The following genes and alleles were used: *rab-10(q373) I*, *agef-1(vh4) I*, *zen-4(or153) IV, lin-2(e1309) X*. Transgenes used in this study: *zhIs038[Plet-23::LET-23::GFP; unc-119(+)] IV*, *bIs1[Pvit-2::VIT-2::GFP; rol-6(su1006)] X,* linkage group unknown: *pwIs50[Plmp-1::LMP-1::GFP + Cbr-unc-119(+)]*.

RNA interference

RNAi feeding was essentially performed as previously described (Kamath et al., 2001) using the *rab-11.1*, *rab-8*, *rab-10*, *rab-5*, *rab-7*, *unc-116, osm-3*, *zen-4*, *arf-6*, *klp-4* and *klp-8* clones from Ahringer RNAi library (Geneservice, Cambridge, United Kingdom). Clones were verified by DNA sequencing. To avoid embryonic and larval lethal phenotypes, synchronized L1 larvae were placed on RNAi plates and scored for vulva induction and/or size of LMP-1::GFP-positive vesicles when the animals reached L4 stage 36-48 hours later.

Microscopy and phenotype analysis

General methods for live animal imaging using Nomarski differential interference contrast (DIC) microscopy were as previously described (Sulston and Horvitz, 1977). Animals were

analyzed on an Axio Zeiss A1 Imager compound microscope (Zeiss, Oberkochen, Germany), images were captured using an Axio Cam MRm camera and AxioVision software (Zeiss, Oberkochen, Germany). Muv and Vul phenotypes were scored by counting the numbers of vulval and non-vulval descendants of P3.p-P8.p in L4 stage larvae as described previously (Skorobogata and Rocheleau, 2012). Fisher's exact test (www.graphpad.com/quickcalcs) was used for statistical analysis of the vulval phenotypes. To analyze early embryos (2 cell – early gastrula), gravid adult mothers were transferred on a microscope slide with 2% agarose pad and the embryos were released onto the agarose pad by puncturing mothers in the vulva region. To analyse later staged embryos (late gastrula – 3-fold), mothers were plated on fresh NGM plates and allowed to lay eggs for 3-4 hours, the eggs were then mounted on 2% agarose pads.

Confocal analysis was performed using a Zeiss LSM-510 Meta laser scanning microscope with 63X oil immersion lens (Zeiss, Oberkochen, Germany) in a single-track mode using a 488 nm excitation for GFP. Images were captured using ZEN 2009 Image software (Zeiss, Oberkochen, Germany). *zhIs038* transgene-carrying animals were visualized at early L3 larval stage. The number of punctae in the P6.p descendants was calculated manually in each animal.

RESULTS

rab-10 and *rab-8* RNAi partially reverts the suppression of the *lin-2(-)* Vul phenotype by *agef-1(vh4)*

In order to further understand the mechanisms underlying the antagonistic effect of AGEF-1 on LET-23 EGFR signaling during vulva induction; it would be informative to find genes involved in the endocytic trafficking that might oppose the function of AGEF-1. Mammalian BIG1/2 have been found on endosomes, in addition to being present on Golgi membranes, and double-knockdown of BIG1/2 led to mislocalization of some of the Golgi and recycling endosome resident proteins as well as defects in the retrograde trafficking to the Golgi (Ishizaki et al., 2008). Furthermore, loss of BIG2 results in tubulation of the recycling endosomal compartment (Boal and Stephens, 2010). Presence of enlarged late endosomes/lysosomes in the coelomocytes of *agef-1(vh4)* mutants may be a result of retrograde trafficking defect from endosomes. Thus, recycling and/or retrograde trafficking pathways could be involved in the antagonizing effect of AGEF-1 on LET-23 EGFR signaling.

If any of the small GTPases involved in recycling are required for the ability of *agef-1(vh4)* to suppress the *lin-2(-)* Vul phenotype, then RNAi-mediated knock down of these genes in the *agef-1(vh4); lin-2(-)* background will revert the phenotype back to Vul observed in *lin-2(-)* mutants. I have silenced the expression of four recycling GTPases in the *agef-1(vh4); lin-2(-)* double mutants and compared the level of Vul phenotype to GFP control RNAi (Table 8, lines 3-8). A small GTPase RAB-10 and a closely related RAB-8 are required for the ability of *agef-1(vh4)* to suppress the *lin-2(e1309)* Vul phenotype.

Table 8. *rab-10* and *rab-8* are required for the ability of *agef-1(vh4)* to suppress the *lin-2(-)* Vul phenotype.

	Genotype	Vul, %	Muv, %	Avg. # VPCs induced	*n*
1	*lin-2(e1309)*	100	0	0.31	35
2	*agef-1(vh4); lin-2(e1309)*	20	30	3.0	40
3	*agef-1(vh4); lin-2(-); GFP(RNAi)*	8	48	3.26	60
4	*rab-10(RNAi) agef-1(vh4); lin-2(-)*	38***	25**	2.83	60
5	*rab-8(RNAi) agef-1(vh4); lin-2(-)*	33**	30**	2.8	40
6	*rab-10+rab-8(RNAi) agef-1(vh4); lin-2(-)*	23	12***	2.87	26
7	*agef-1(vh4); arf-6(RNAi); lin-2(-)*	5	50	3.39	40
8	*rab-11.1(RNAi) agef-1(vh4); lin-2(-)*	13	52	3.33	40
9	*rab-10(q373)*	0	0	3.0	21
10	*rab-10(q373) agef-1(vh4)*	0	5	3.03	22
11	*rab-10(q373); lin-2(e1309)*	100	0	0.3	25
12	*rab-10(q373) agef-1(vh4); lin-2(e1309)*	86****	0	1.2****	22

Statistical analysis was performed using Fisher's exact test (www.graphpad.com/quickcalcs) comparing line 3 with lines 4-8, line 1 with line 11, and line 2 with line 12. **P<0.01; ***P<0.001; ****P<0.0001.

rab-10, but not *rab-8* is required for multiple *agef-1(vh4)* phenotypes

The ability of *rab-10* and *rab-8* knock down to increase the Vul phenotype in *agef-1(vh4); lin-2(-)* background may be due to positive roles of RAB-10 and RAB-8 on LET-23 EGFR signaling pathway. Thus, in order to verify whether the phenotype observed in the VPCs is due to antagonistic relationship between these small GTPases and *agef-1(vh4)*, I have examined another *agef-1(vh4)* phenotype following *rab-10* and *rab-8* knock down. Of the numerous phenotypes observed in *agef-1(vh4)* mutants, enlarged LMP-1::GFP-positive late endosomes/lysosomes in the coelomocytes, macrophage-like scavenger cells, are the most pronounced and easily detectable (described in Chapter 2). Knock down of *rab-10*, but not *rab-8* by RNAi led to significant decrease in the size of LMP-1::GFP-positive structures in *agef-1(vh4)* animals (Figure 22B, C). This effect is specific to *rab-10* since knocking down early and late endosomal GTPases, *rab-5* and *rab-7*, respectively, did not result in changes to the size of these LMP-1::GFP-positive vesicles in *agef-1(vh4)* mutant background (Figure 22D, E). Thus, *rab-10* functions closely with *agef-1(vh4)* in an antagonistic manner to regulate both the strength of LET-23 EGFR signaling during vulva induction and the size of LMP-1::GFP-positive late endosomes/lysosomes.

Moreover, the phenotypes observed with RNAi-mediated knockdown of *rab-10* are also present when a genetic mutant of *rab-10(q373)* is used. Notably, *rab-10(q373) agef-1(vh4); lin-2(e1309)* triple mutants were reverted to 86% Vul compared to 20% Vul observed in *agef-1(vh4); lin-2(e1309)* animals (Table 8, lines 2 and 12). Whereas *rab-10(q373)* single mutants do not show any vulval phenotypes and are not able to modify the *lin-2(-)* Vul phenotype (Table 8, lines 1, 9 and 11).

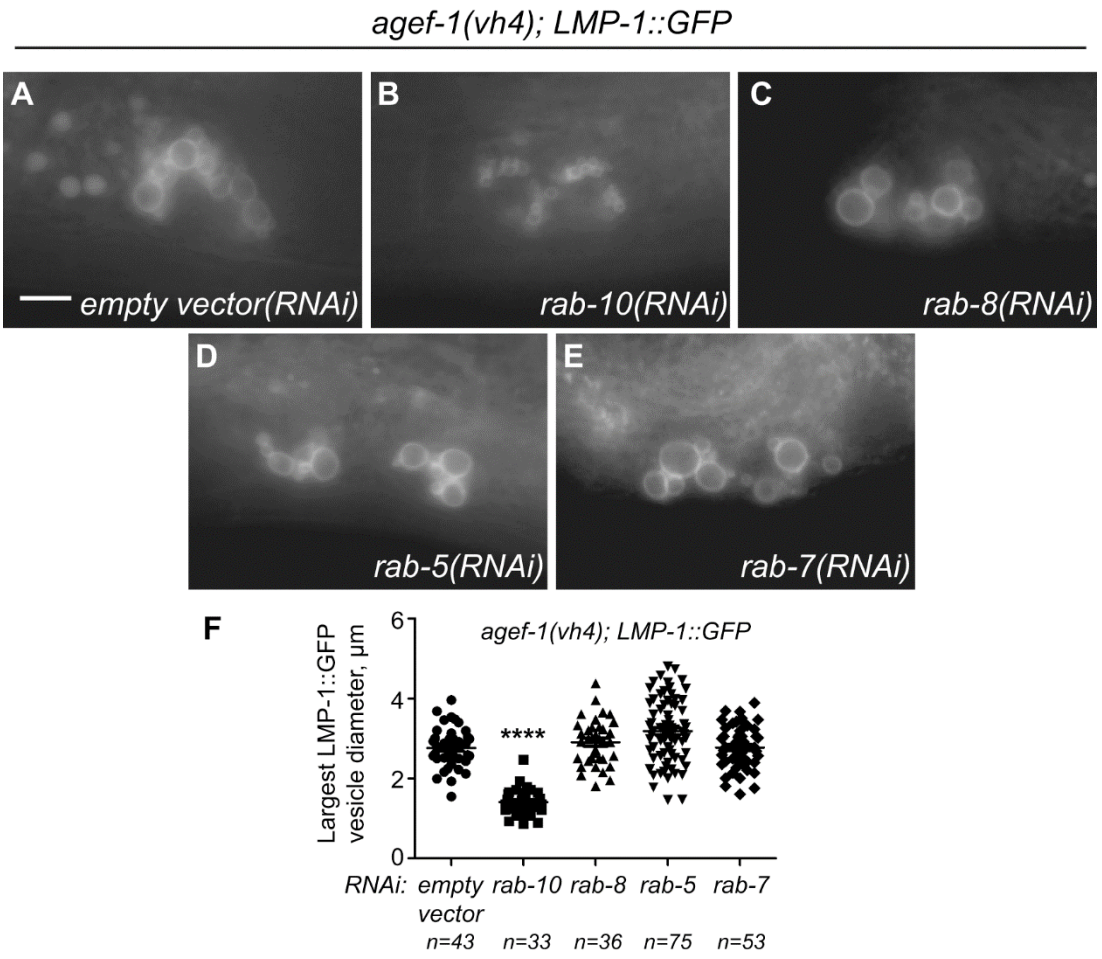

Figure 22. RAB-10 is required for the *agef-1(vh4)* enlarged late endosome/lysosome phenotype.

(A-E) Epifluorescent images of coelomocytes upon RNAi-mediated knock down of *rab-10*, *rab-8*, *rab-5* and *rab-7* in *agef-1(vh4)* animals expressing late endosomal/lysosomal marker LMP-1::GFP. Empty vector RNAi was performed as a negative control. (F) Quantification of the size of the largest LMP-1::GFP-positive vesicles. Size of the vesicles upon RNAi of Rab GTPases was compared to the empty vector control RNAi. **** P<0.001. An unpaired two-tailed t-test was performed to determine statistical significance. Bar, 5µm.

agef-1(vh4) embryos accumulate yolk blobs, which are *rab-10*-dependent

A trafficking assay using YP170::GFP, a yolk fusion protein, in *agef-1(vh4)* background has shown a normal uptake of the yolk protein by the mature oocytes (described in Chapter 2). However, *agef-1(vh4)* embryos accumulate large blobs positive for YP170::GFP, which increase in size with the progression in embryonic development. These blobs appear at the gastrula stage and persist through the 3-fold stage (Figures 23 and 24). They seem to be excluded from the embryonic tissue and accumulate under the eggshell (Figure 23D, J). In wild-type embryos, at the early stages of embryogenesis the yolk protein is uniformly distributed between the cells (Figure 23A'). As the embryogenesis progresses, gut primordium begins to accumulate yolk, whereas non-gut cells lose yolk (Figure 23E') (Bossinger and Schierenberg, 1996). It has been proposed that non-gut cells secrete yolk into the perivitelline space followed by its endocytosis by the developing intestine. The observation that newly hatched L1 larvae still have a high level of yolk in the intestine, which is lost upon starvation suggests that yolk serves as a food source (Bossinger and Schierenberg, 1996). The accumulation of the yolk blobs in the *agef-1(vh4)* embryos correlates with its reduced accumulation in the gut (preliminary data) implying that there is a defect during the process of yolk transfer from non-gut tissues to the developing intestine (Figure 23 G-J').

Since RAB-10 is required for multiple *agef-1(vh4)* phenotypes, I have checked for the presence of the blobs in the embryos of *rab-10(q373) agef-1(vh4)* animals. Double mutants lack blobs under the DIC optics (Figure 24, A'-E'), when YP170::GFP transgene was introduced into the double-mutant background, the GFP-positive blobs were still absent (Figure 25). Since RAB-10 is involved in both recycling and trafficking from the Golgi, we have confirmed that the lack of blobs in *rab-10(q373) agef-1(vh4)* embryos is not due to lack of YP170::GFP in the oocytes of these double-mutants as a result of *rab-10* loss. Both *rab-10(q373)* and *rab-10(q373) agef-1(vh4)*

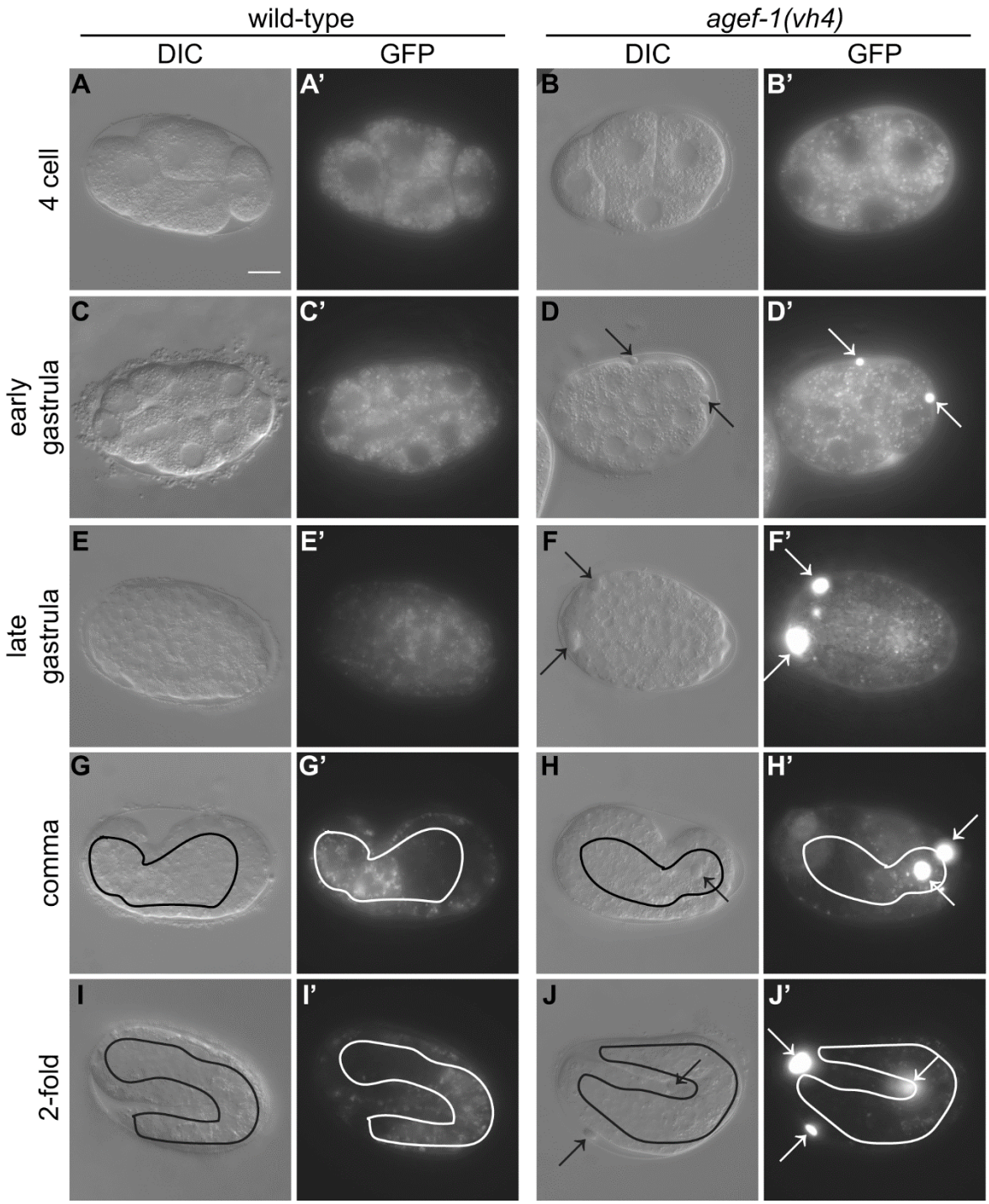

Figure 23. *agef-1(vh4)* mutant embryos accumulate YP170::GFP-positive blobs. (Figure legend is on the next page)

(A-J) Differential interference contrast (DIC) and epifluorescent (A'-J') images of the wild-type and *agef-1(vh4)* embryos at different stages of embryonic development. Accumulation of yolk blobs is first detectable at an early gastrulation stage in the mutants using both DIC and epifluorescence, the penetrance of the blob phenotype is 100%. Note that depending on the focal plane, some of the blobs are observed as exclusions from the embryonic tissue (D, J). Also of interest is the decreased YP170::GFP florescence in the gut primordium (outlined in G-J') of developing *agef-1(vh4)* embryos compared to wild-type (H' vs. G', J' vs. I', respectively) (preliminary data). Arrows indicate YP170::GFP-positive blobs. Exposure time, 50 ms. Bar, 10 μm.

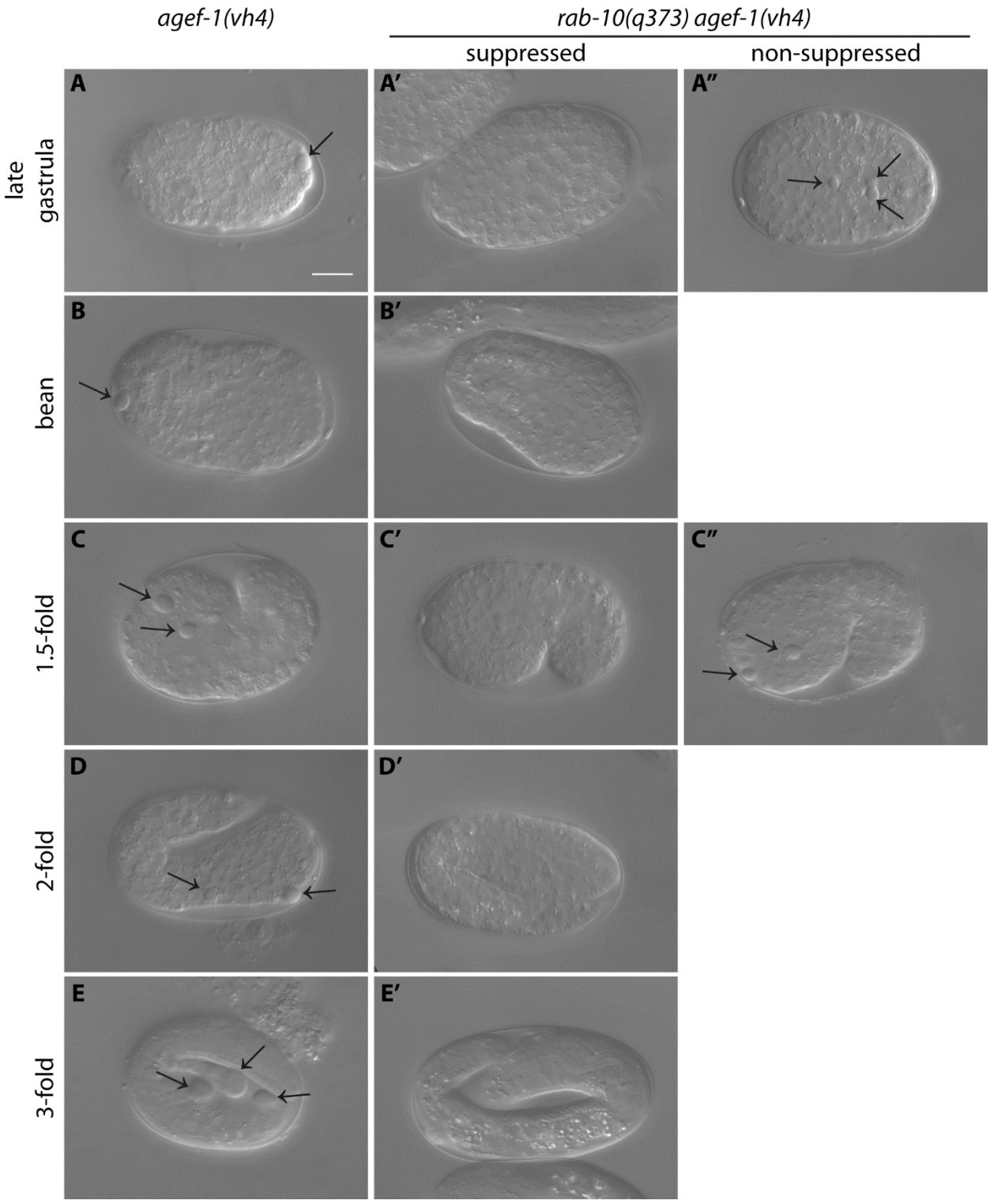

Figure 24. RAB-10 is required for the *agef-1(vh4)* embryonic yolk blob phenotype. (Figure legend is on the next page)

Differential interference contrast (DIC) images of *agef-1(vh4)* and *rab-10(q373) agef-1(vh4)* embryos at different stages of embryonic development. Blobs are clearly visible under the DIC optics in *agef-1(vh4)* mutants. Loss of *rab-10* suppresses this phenotype. Out of 49 *rab-10(q373) agef-1(vh4)* embryos scored, 47 lacked the blobs; the two non-suppressed embryos are shown in A'' and C''. Arrows indicate blobs. Bar, 10 μm.

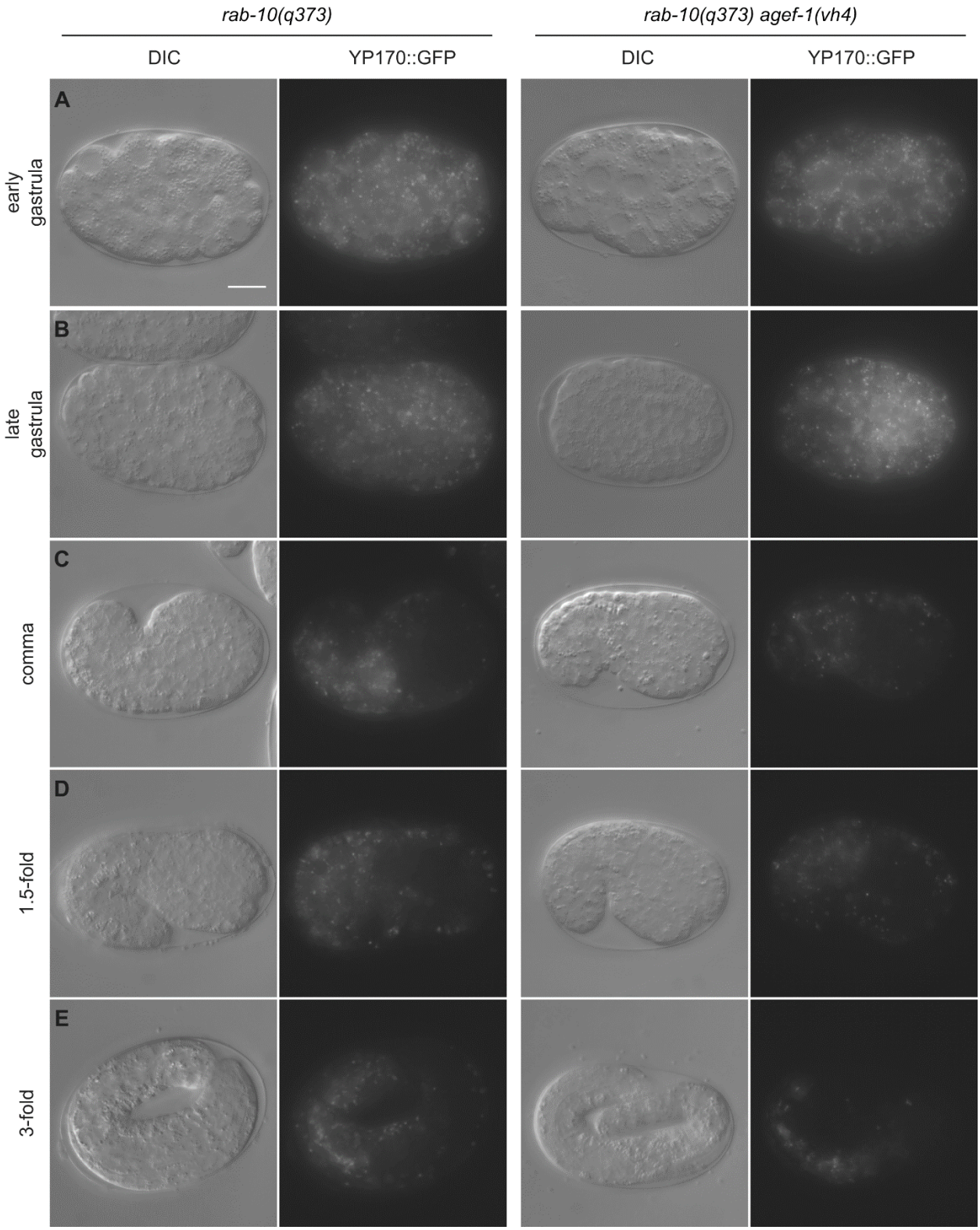

Figure 25. Loss of *rab-10* suppresses YP170::GFP-positive blobs in *agef-1(vh4)* mutant embryos. (Figure legend is on the next page)

Differential interference contrast (DIC) and epifluorescence images of *rab-10(q373)* and *rab-10(q373) agef-1(vh4)* embryos expressing YP170::GFP throughout embryogenesis. Note lack of YP170::GFP-positive blobs in *rab-10(q373) agef-1(vh4)* double-mutant embryos. Exposure time, 75 ms. Bar, 10 µm.

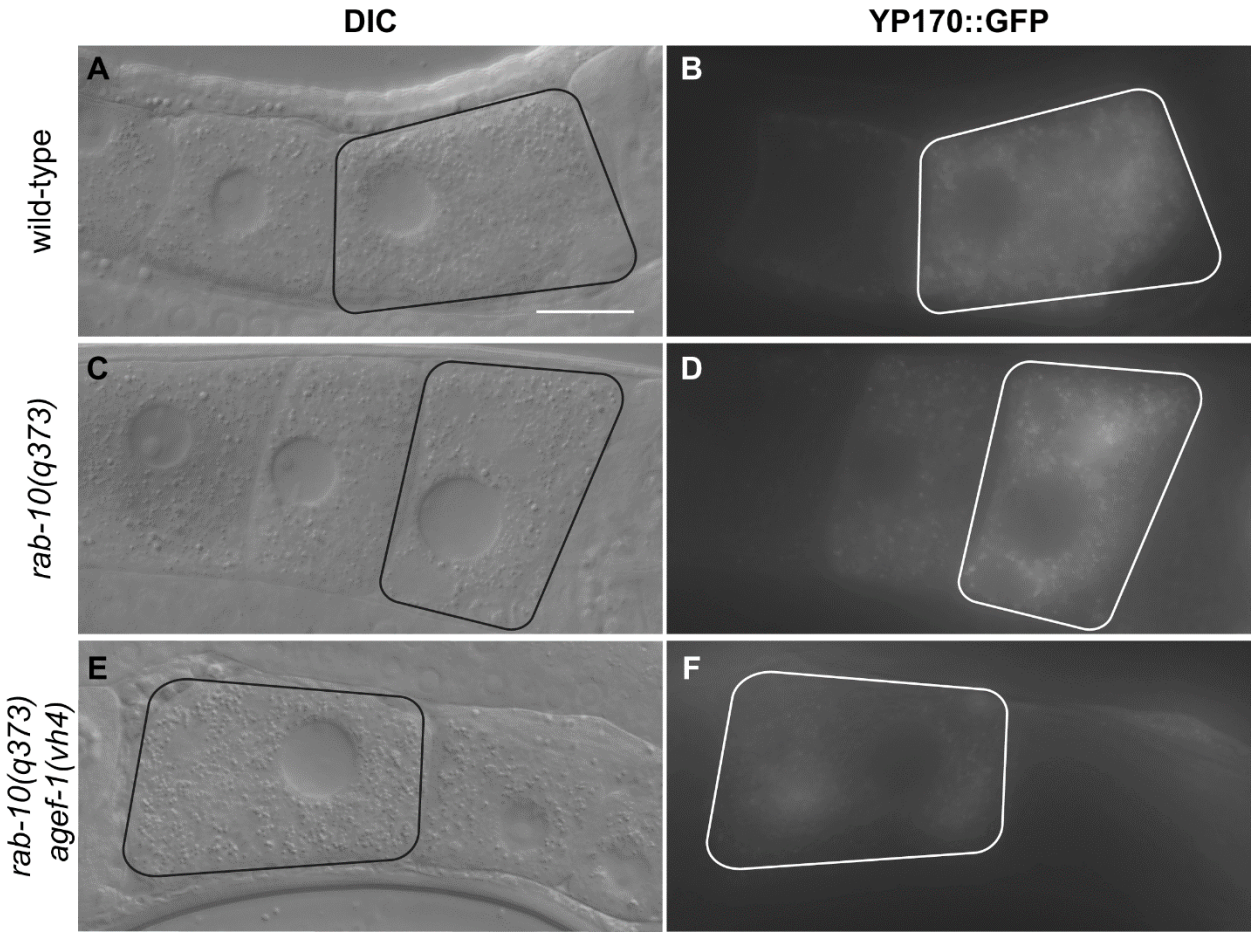

Figure 26. Yolk uptake by *rab-10(q373)* and *rab-10(q373) agef-1(vh4)* oocytes.

DIC (A, C, E) and epifluorescence (B, D, F) images of the mature oocytes. Both *rab-10(q373)* and *rab-10(q373) agef-1(vh4)* mutants are able to accumulate YP170::GFP in the proximal (most mature) oocyte (D and F). Outlines of the proximal oocytes are shown. Exposure time, 35 ms. Bar, 15 µm.

animals accumulate YP170::GFP in the oocytes and it is also present in the embryos throughout embryogenesis (Figures 26 and 25, respectively). One of the future avenues for studying this phenotype is to quantify the amount of the YP170::GFP accumulated in the developing intestines of the embryos in different genetic backgrounds since accumulation of the yolk in the blobs is expected to reduce its amount available for endocytosis into the intestinal cells or alternatively failure to endocytose the yolk by intestinal cells could result in the blob formation.

ZEN-4 kinesin promotes LET-23 EGFR signaling during vulva development

DHC-1 dynein, a minus-end directed microtubule motor, negatively regulates LET-23 EGFR signaling in the VPCs. We have asked the question of whether there is a kinesin, a plus-end directed motor that could oppose the function of DHC-1 in regulating the strength of LET-23 EGFR signaling during vulva induction. *C. elegans* has 21 genes predicted to express kinesin-like proteins, which have close homology to mammalian proteins (Siddiqui, 2002). Five kinesins were chosen based on the expression patterns and/or function to test for their ability to revert *dhc-1(vh22); lin-2(e1309)* back to Vul phenotype by RNAi. OSM-3 KIF17 expression is limited to neurons (Tabish et al., 1995), however mammalian studies have revealed that KIF17 interacts with mLin10 to direct the trafficking and localization of the 2B subunit of the NMDA receptor in hyppocampal neurons (Guillaud et al., 2003). Thus, I have tested the effect of *osm-3 kif17* knock-down on the strength of LET-23 EGFR signaling during vulva induction, since LIN-10 is part of the LIN-2/7/10 complex required for LET-23 EGFR basolateral localization in the *C. elegans* VPCs (Kaech et al., 1998). ZEN-4 MKLP1 is expressed in the VPCs and has been shown to regulate polarity of another epithelial tissue during the process of foregut formation in *C. elegans* (Portereiko et al., 2004). UNC-116 is the only kinesin heavy chain and, together with KLP-4 and KLP-8, is ubiquitously expressed, which could also include expression in the VPCs. Out of 5

kinesins tested, only one, ZEN-4 MKLP1, was able to make *dhc-1(vh22); lin-2(e1309)* more Vul when downregulated by RNAi (Table 9).

ZEN-4 MKLP-1 is a component of the centralspindlin complex involved in cytokinesis, it also plays a role in microtubule organization in neurites and is required for the polarity of arcade cells in the *C. elegans* foregut (del Castillo et al., 2015; Nislow et al., 1992; Portereiko et al., 2004; Raich et al., 1998). The genetic mutant of *zen-4(or153)* is temperature-sensitive, and has high embryonic lethality at the restrictive temperature of 20°C due to failure of cytokinesis. At the permissive temperature, 15°C, the animals develop normally. ZEN-4 has a positive effect on LET-23 EGFR signaling during vulva induction since *zen-4(or153)* mutants have a mild Vul phenotype at 20°C (Table 10). *zen-4(or153)* did not have an effect on the *lin-2(e1309)* Vul phenotype, but reverted *dhc-1(vh22); lin-2(e1309)* double-mutants to a more Vul phenotype at restrictive temperature (Table 10).

Cargo-containing vesicles have been found to carry simultaneously plus- and minus-end directed microtubule motors and it has been proposed that these motors work cooperatively to promote movement of the vesicle in the proper direction (Bryantseva and Zhapparova, 2012). Thus, one possible explanation for the increased Vul phenotype in *dhc-1(vh22); zen-4(or153); lin-2(e1309)* is due to opposing functions of DHC-1 and ZEN-4 motors in the movement of LET-23 EGFR-containing vesicles along the microtubule track. Loss of DHC-1 in the *lin-2(e1309)* background could have allowed for the increased trafficking of a portion of LET-23 EGFR-containing vesicles towards the plus end of the microtubules (cell periphery) by the kinesin motor leading to promotion of signaling and suppression of the Vul phenotype. Whereas simultaneous loss of DHC-1 and ZEN-4 in *lin-2(e1309)* animals, would block trafficking of the receptor-containing vesicles towards cell periphery. I have studied the VPCs of the *dhc-1(vh22); lin-2*

Table 9. RNAi-mediated knock-down of ZEN-4 kinesin reverts *dhc-1(vh22); lin-2(e1309)* to a more Vul phenotype

Genotype	Muv, %	Vul, %	Avg. # VPCs induced	*n*
GFP(RNAi)	4	48	2.16	79
zen-4(RNAi)	0	81***	1.28****	42
unc-116(RNAi)	0	60	2.04	42
osm-3(RNAi)	5	43	2.19	42
klp-4(RNAi)	7	48	2.11	42
klp-8(RNAi)	2	41	2.31	42

The strain QR253: *dhc-1(vh22); lin-2(e1309)* was used for RNAi feeding. Statistical analysis was performed as above, all experimental conditions were compared to a *GFP(RNAi)* control. ***P<0.001; ****P<0.0001.

Table 10. ZEN-4 has a positive effect on LET-23 EGFR signaling during *C. elegans* vulva induction

Genotype	Temp.	Vul, %	Muv, %	Avg. # VPCs induced	*n*
wild-type	All temps	0	0	3.0	many
zen-4(or153)	15°C	0	0	3.0	21
zen-4(or153)[1]	20°C	40****	0	2.45	20
zen-4(or153); lin-2(-)[1]	20°C	100	0	0.24	25
dhc-1(vh22); lin-2(-)	20°C	15	0	2.85	20
dhc-1(vh22); zen-4(or153); lin-2(-)[2]	20°C	86****	0	1.27****	28

Statistical analysis was performed as above, *zen-4(or153)* at 20°C was compared to wild-type; *dhc-1(vh22); zen-4(or153); lin-2(-)* strain was compared to *dhc-1(vh22); lin-2(-)*. ****P<0.0001.

[1] mothers grown at 15°C were allowed to have progeny, which were transferred to 20°C as L1 larvae and scored, when L4 larval stage was reached.

[2] *dhc-1(vh22); zen-4(or153)/nT1; lin-2(-)* animals were grown at 15°C due to 100% embryonic lethality at 20°C, allowed to have progeny, which were transferred to 20°C as L1 larvae and non-green animals homozygous for *zen-4(or153)* were scored at L4 larval stage.

(e1309) animals following RNAi-mediated knock down of *zen-4* for the localization pattern of LET-23 EGFR tagged with GFP. If ZEN-4 were to positively regulate LET-23 EGFR signaling by promoting the movement of the receptor-containing vesicles in the direction opposite to DHC-1, a change in the number or localization of LET-23::GFP-positive punctae in the VPCs of the *dhc-1(vh22); zen-4(RNAi); lin-2(e1309)* animals compared to *dhc-1(vh22); lin-2(e1309)* double-mutants would be expected. However, the number and localization of punctae positive for LET-23 EGFR remained the same following *zen-4* RNAi (Figure 27). Thus, ZEN-4 is likely to promote LET-23 EGFR signaling by an alternative mechanism. Since ZEN-4 is required for polarity in the arcade cells of the developing *C. elegans* foregut, it is possible that it also plays a role in the polarity of the VPCs and indirectly affects apical/basolateral distribution of LET-23 EGFR. In order to test this hypothesis, proteins known to be differentially localized between apical and basolateral membranes of the VPCs could be studied in *zen-4(or153)* background to determine whether their distribution is affected. Additionally, localization of GFP-tagged LET-23 EGFR should be studied in the *zen-4(or153)* mutant backgrounds to determine if the apical vs basolateral localization is altered.

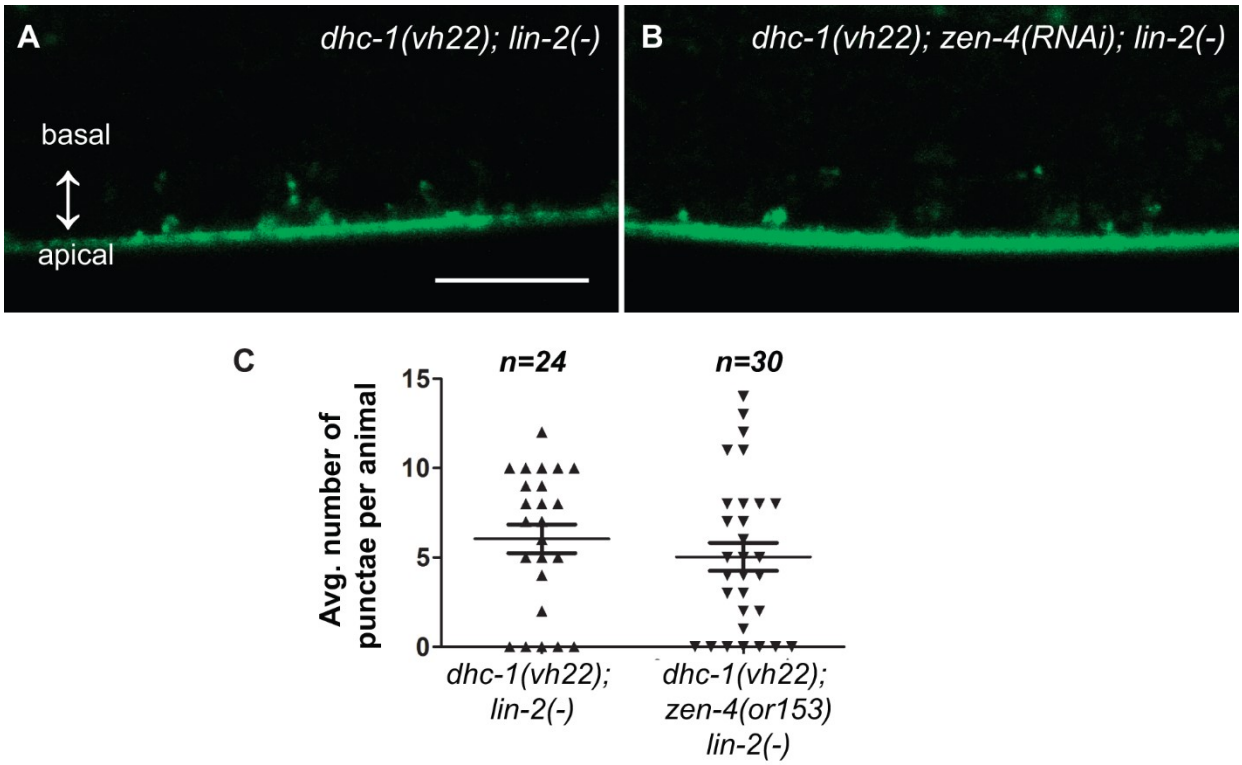

Figure 27. *zen-4* knock down by RNAi does not affect the amount of LET-23 EGFR punctae in the VPCs.

(A-B) Confocal images of the P6.p daughter cells, P6.pa and P6.pp, expressing LET-23 EGFR tagged with GFP. In both genetic backgrounds, the receptor is present on the apical membrane and in the cytoplasmic foci. (C) Quantification of the number of punctae present in the P6.pa and P6.pp. Apical and basal membranes are indicated with an arrow. Bar, 10 µm.

CHAPTER 5: DISCUSSION

5.1. Novel negative regulators of LET-23 EGFR signaling and trafficking

Activating mutations in the EGFR or other core components of the Ras/MAPK signaling cascade as well as their aberrant expression have been strongly linked to various types of malignancies, drug resistance and metastasis (McCubrey et al., 2015). This is not surprising due to the ability of the EGFR/Ras/MAPK signaling pathway to regulate cell proliferation, migration and apoptosis, which when dysregulated can directly contribute to the pathogenesis of cancer. Furthermore, a majority of tumors originate from epithelial cells and EGFR is frequently overexpressed in epithelial cancers (Scaltriti and Baselga, 2006). Thus, studies aimed at understanding the mechanisms regulating the levels and polarized distribution of the EGFR might uncover potential targets for the treatment of malignancies.

5.1.1. AGEF-1/Arfs/AP-1 complex and LET-23 EGFR localization in the VPCs

5.1.1.1. AGEF-1 is required for multiple phenotypes

Identification of a partially embryonic lethal allele of *agef-1* as a negative regulator of Ras signaling not only distinguished it from other previously identified negative regulators, but also suggested the involvement of this gene in other processes required for viability. Indeed, *agef-1(vh4)* mutants are defective in secretion from at least two tissues, intestine and body wall muscle cells as we have shown by expression of secreted GFP-tagged proteins. This phenotype is consistent with the role of mammalian homologs of AGEF-1, BIG1/2, in secretion from the TGN.

agef-1(vh4) carries a lesion that substitutes a conserved negatively charged glutamic acid for a positively charged lysine in the HDS2 domain of the protein. It is not clear what role this domain has in terms of protein function. Our genetic analysis supports a hypomorphic nature for this mutation since *agef-1(vh4)* placed in *trans*- to a deletion, *dxDf2*, that removes this gene, or to

strong lethal deletion alleles of *agef-1*, *tm1693* or *ok1736*, leads to 100% lethality, which would be consistent with the HDS2 domain promoting the function of the protein. It has been shown that in the yeast homolog of BIG1/2, Sec7, the C-terminal part of the protein containing HDS2, HDS3 and HDS4 domains has an inhibitory role on function, where removal of this region increases Sec7 GEF activity towards Arf1 (Richardson et al., 2012). Additionally, Sec7 is recruited to the TGN membranes via a positive feedback loop, where active GTP bound Arf1 recruits Sec7 to the TGN by interaction with the HDS1 domain (Richardson et al., 2012). Moreover, mammalian BIG1 and BIG2 have been shown to be recruited to the TGN membranes by Arf4 and Arf5 as well as Arl1 GTPases (Christis and Munro, 2012; Lowery et al., 2013). A further study by McDonold and Fromme has demonstrated that yeast Sec7 is an effector of four GTPases, Arf1, Arl1, Ypt1/Rab1 and Ypt31/Rab11 (McDonold and Fromme, 2014). This latest study suggests that Arl1, Ypt1/Rab1 and Arf1 are involved in membrane recruitment of Sec7 by interaction with the N-terminal DCB and HUS1, HDS2/3 and HDS1, respectively, whereas Ypt31/Rab11 functions later once Sec7 is at the TGN membrane to relieve autoinhibition by HDS4 domain and promote GEF activity of Sec7 towards Arf1 (McDonold and Fromme, 2014).

These findings support a role for HDS2 in recruitment to the TGN. Therefore, it is possible that the lesion found in *agef-1(vh4)* may disrupt the recruitment of the mutant AGEF-1 protein to the TGN. This hypothesis could be tested by studying the localization of the GFP-tagged wild-type and mutant (E1028K) AGEF-1 proteins with respect to the Golgi by co-expression of AGEF-1::GFP and one of the TGN markers, e.g. MANNS::mCherry (mannosidase). Moreover, it would be informative to investigate the degree of AGEF-1::GFP Golgi localization upon loss of ARF-1.2, ARL-1 and/or RAB-1. If these three *C. elegans* GTPases are involved in the AGEF-1 recruitment to the TGN membranes similar to yeast proteins, it would be expected that removing

ARF-1.2, ARL-1 and/or RAB-1 function will decrease the co-localization between AGEF-1::GFP and MANNS::mCherry. The role of Arf1 in a positive feedback loop involved in Sec7 TGN recruitment (Richardson et al., 2012) and a potential function of the HDS2 domain in AGEF-1 TGN localization are in accord with our data showing that overexpression of wild-type ARF-1.2 in the VPCs of *agef-1(vh4); lin-2(e1309)* animals was able to compensate for a partial loss-of-function of *agef-1* and to revert these double-mutants back to Vul phenotype. This effect could be achieved through increased recruitment of mutant AGEF-1 protein to the TGN by overexpressed ARF-1.2.

Since Arl1 has been shown both in mammalian studies and in yeast to recruit BIG1/2 and Sec7, respectively, to the Golgi (Christis and Munro, 2012; McDonold and Fromme, 2014), it is possible that this small GTPase is also involved in negative regulation of the strength of the EGFR signaling. Thus, it would be expected that loss of *arl-1* will be able to suppress the *lin-2* Vul and could be Muv with *agef-1* and *arf-1.2*.

The presence of the enlarged LMP-1::GFP-positive late endosomes/lysosomes in the coelomocytes of the *agef-1(vh4)* mutants could be suggestive of a defect in retrograde trafficking from the late endosomes to the Golgi since knock-down of mammalian BIG1, BIG2 or AP-1 have been shown to block the retrograde traffic of furin from late endosomes to the TGN (Ishizaki et al., 2008). Consistent with these findings, we show that simultaneous removal of multiple subunits of AP-1 also leads to enlarged LMP-1::GFP-positive structures being present in the coelomocytes. An independent study has proposed that AGEF-1 is involved in late endosome to lysosome trafficking due to partial AGEF-1 co-localization with late endosomal and lysosomal markers as well as presence of enlarged LMP-1::GFP-positive endosomes in the coelomocytes upon RNAi-mediated depletion of *agef-1* (Tang et al., 2012). However, Tang and colleagues did not observe a

defect in lysosomal acidification or degradation (Tang et al., 2012). In this study lysosomal acidification was tested with LysoTracker, which fluoresces in the compartments with pH below 6.5 and thus is not lysosome-specific, whereas a more precise measure of lysosomal acidity could be achieved by using LysoSensor, whose fluorescence increases in intensity upon acidification (Liu et al., 2008). It is possible that AGEF-1 contributes to the size of the late endosomes/lysosomes by multiple mechanisms, which could include both the retrograde trafficking to Golgi from the late endosomes as well as its role in promoting trafficking from late endosome to lysosome.

5.1.1.2. AGEF-1 and UNC-101 negatively regulate Ras signaling by antagonizing basolateral localization of the LET-23 EGFR

Our genetic findings indicate that AGEF-1 is a potent negative regulator of LET-23 EGFR signaling during *C. elegans* vulva induction. Consistent with mammalian findings that BIG1/2 proteins are involved in activation of Arf GTPases and recruitment of coat proteins such as AP-1, our data suggest that two Arf GTPases, ARF-1.2 and ARF-3, also antagonize LET-23 EGFR signaling. Additionally, AGEF-1 is likely to function through both ARF-1.2 and ARF-3 in regulating the strength of LET-23 EGFR signaling since removing the function of a single Arf GTPase in the *lin-2(e1309)* mutant background leads to a weaker level of suppression of the Vul phenotype compared to *arf-1.2(ok796); arf-3(RNAi); lin-2(e1309)* triple mutant, which is similar to *agef-1(vh4); lin-2(e1309)* in the level of suppression.

Previous studies have identified two AP-1μ subunits, UNC-101 and APM-1, as negative regulators of Ras signaling as well (Lee et al., 1994; Shim et al., 2000). Moreover, our data implicates AP-1γ subunit, APG-1, in antagonizing LET-23 EGFR signaling. Furthermore, double mutants between *arf-1.2(ok796)*, *agef-1(vh4)* and *unc-101(sy108) AP-1* have a synthetic Muv

phenotype, which is consistent with these genes functioning together, given that they are either non-null alleles or redundant with a paralog, to negatively regulate LET-23 EGFR signaling.

In mammals, AP-1 has been shown to regulate the basolateral localization of proteins in polarized epithelial cells (Bonifacino, 2014). Moreover, EGFR is localized to the basolateral membrane of polarized epithelial kidney cells via interaction of the di-leucine motif in the C-terminal of the receptor with the AP-1B adaptor (Ryan et al., 2010). *C. elegans* LET-23 EGFR has putative AP-1 binding sites in the cytoplasmic tail, however its interaction with the two AP-1μ subunits, UNC-101 and APM-1, have not been demonstrated biochemically. We showed that AGEF-1 and AP-1 prevent basolateral localization of LET-23 EGFR in the descendants of the primary VPC, P6.pa and P6.pp, since *agef-1(vh4)*, *unc-101(RNAi)* and *unc-101(RNAi) agef-1(vh4)* in the *lin-2(e1309)* mutant background led to partial restoration of LET-23::GFP basolateral localization. Even though we do not observe complete restoration of the basolateral LET-23::GFP localization in *lin-2(e1309)* background upon loss of AGEF-1 and UNC-101, this amount of receptor present basolaterally is sufficient to strongly suppress the *lin-2* Vul phenotype since we do not observe basolateral LET-23::GFP in *lin-2* single mutants yet the animals expressing the transgene are suppressed in terms of vulva induction. Moreover, *agef-1(vh4)* mutant animals have increased fluorescence intensity of LET-23::GFP on the basal membrane compared to apical suggesting that AGEF-1 either promotes apical or antagonizes basolateral LET-23 EGFR localization. If *C. elegans* LET-23 EGFR relies on interaction of its C-terminal with AP-1 on polarized distribution, then our *in vivo* data is in disaccord with mammalian studies on the role of AP-1 in basolateral cargo targeting. However, the role of AP-1 in cargo retention intracellularly by binding to a conventional di-leucine motif of chitin synthase III (Chs3p) has been demonstrated in yeast (Starr et al., 2012). The yeast integral plasma membrane protein Chs3p relies on the

exomer coat complex for the delivery from the TGN and RE to the cell surface (Wang et al., 2006). Whereas in the absence of exomer components, AP-1 promotes Chs3p intracellular retention either in the TGN or the RE (Valdivia et al., 2002). Thus, it is possible that AP-1 prevents basolateral localization of LET-23 EGFR by competing with the LIN-2/7/10 complex at the TGN or the RE for binding to the receptor, where loss of the components of the AGEF-1/Arf/AP-1 ensemble will lead to increased basolateral delivery of LET-23 EGFR.

Alternatively, AGEF-1 and AP-1 may regulate LET-23 EGFR localization by maintaining the polarity of the VPCs. Indeed, *in vivo* studies in the mouse and *C. elegans* intestine have demonstrated that AP-1 is required for the maintenance of polarity in epithelial cells since loss of AP-1 results in missorting of both basolateral and apical transmembrane and cytoskeletal proteins (Hase et al., 2013; Shafaq-Zadah et al., 2012; Zhang et al., 2012). Additionally, ectopic apical-like membranes or invaginations of the lateral membrane were present in both organisms upon AP-1 loss (Hase et al., 2013; Shafaq-Zadah et al., 2012; Zhang et al., 2012). Furthermore, Zhang and colleagues have observed similar phenotypes in the *C. elegans* intestine upon clathrin knock-down (Zhang et al., 2012). It has been proposed that defects observed upon loss of AP-1 might arise due to changes in the properties of the TGN and the CRE membranes, which would lead to missorting of both apical and basolateral cargo (Bonifacino, 2014). Similarly, we have discovered ectopic apical lumens and invaginations of the apical intestinal membranes in *agef-1(vh4)* mutants. Moreover, normally apical SID-2::GFP marker is mislocalized basolaterally in *agef-1(vh4)* intestines. These data taken together suggest that AGEF-1 and AP-1 have a role in the maintenance of polarity in the intestinal cells of the whole animals. Thus, analogous to polarized intestinal cells AGEF-1/Arfs/AP-1 might regulate polarity of the VPCs and control polarized distribution of LET-23 EGFR. In order to address this possibility, localization of basolateral (ERM-1::GFP ERM

(Ezrin, Radixin, Moesin) and LET-413::GFP ERBIN) and apical (PAR-3::GFP ASIP (atypical PKC isotype-specific interacting protein) and PAR-6::GFP Par6) markers should be investigated in the VPCs of singly or doubly mutant *agef-1(vh4)*, *arf-1.2* and *unc-101(sy1)* animals. If the AGEF-1/Arf/AGEF-1 ensemble is indeed involved in the maintenance of VPC polarity, then loss of polarized distribution of these markers is expected in the mutants. Even though the exact mechanism of AGEF-1 and AP-1 antagonizing EGFR signaling is not yet clear, our study provides a discovery of an exciting new role for these proteins in both the control of the signaling strength of an oncogene and in the maintenance of epithelial polarity, which is often lost at the early stages of tumorigenesis.

5.1.2. DHC-1 dynein and RAB-7 antagonize Ras signaling by regulating LET-23 EGFR trafficking

An important mechanism of the EGFR signal attenuation involves endocytic trafficking of the receptor followed by lysosomal degradation (Sorkin and Goh, 2008). However, whereas the role of the proteins involved in receptor internalization, ubiquitination and early steps of MVB formation in the control of signaling strength is accepted, it is not fully elucidated what effect the loss of late endocytic components has on signal strength (Wegner et al., 2011). The dynein microtubule motor and the small GTPase Rab7 have been shown to be involved in the trafficking of EGFR-containing late endosomes to the lysosome for degradation (Ceresa and Bahr, 2006; Taub et al., 2007). Overexpression of the p50 dynamitin subunit of dynactin complex leads to uncoupling of dynein from microtubules, clustering of late endosomes close to the cell periphery and sustained Erk1/2 activation, whereas overexpression of dominant-active Rab7 prevented fusion of late endosomes with lysosomes, caused perinuclear accumulation of EGFR-containing late endosomes and sustained MAPK signaling (Taub et al., 2007). Additionally, inactivating

mutations of Rab7 result in accumulation of EGF::EGFR complexes in late endosomes preventing the degradation of receptor-ligand complexes, however the effect on signaling is not clear (Ceresa and Bahr, 2006). Rab7 couples late endosomes to dynein allowing for their trafficking along microtubules towards the lysosome (Johansson et al., 2007), thus Rab-7 and dynein could function together to facilitate EGFR lysosomal degradation.

DHC-1 dynein heavy chain is a component of the heteromeric multiprotein cytoplasmic dynein complex, a minus-end directed microtubule motor. Dynein is driving a variety of cellular processes including cell division and cargo trafficking (Roberts et al., 2013). In non-polarized cells dynein is moving various cargo, which includes endosomes, lysosomes, lipid droplets and mitochondria, towards the microtubule-organizing center located near the nucleus (Roberts et al., 2013). Due to a unique nature of microtubule organization in the polarized cells, dynein is also involved in cargo delivery to the apical membrane (Rodriguez-Boulan and Macara, 2014). We have demonstrated that *dhc-1(vh22)* is a strong negative regulator of LET-23 EGFR signaling during *C. elegans* vulva development. Genetic analysis indicates that DHC-1 functions at the level of LET-23 EGFR in the signal-receiving cell. Consistent with mammalian findings that blocking dynein function by overexpression of p50 dynamitin leads to mislocalization of late endosomes containing EGFR to the cell periphery (Taub et al., 2007), we observe juxtamembrane accumulation of LET-23::GFP EGFR in the descendants of the primary VPC upon loss of DHC-1 function. Interestingly, in the animals mutant for *rab-7*, LET-23::GFP accumulates in the endosomal structures dispersed throughout the cell. These differences in the phenotypes are suggestive of DHC-1 dynein being involved in the earlier step of LET-23 EGFR trafficking. It still remains to be determined which endosomal compartments accumulate the receptor in the *dhc-1* and *rab-7* mutants, however we show evidence for LET-23 EGFR ability to signal from these

compartments in both mutants. It was technically challenging to assess co-localization of LET-23 EGFR and endocytic markers by immunostaining in the VPCs to identify which compartment accumulates LET-23::GFP in both *dhc-1(vh22)* and *rab-7(ok511)* mutants due to a small size of the VPCs, short window during development prior to divisions of P6.pa and P6.pp as well as low percentage of animals stained simultaneously against two proteins. I predict, based on mammalian data, that punctae observed in *dhc-1(vh22)* mutants are late endosomes that fail to fuse with the lysosome and accumulate LET-23 EGFR. The *rab-7(ok511)* allele is a deletion, thus it is possible that these animals accumulate LET-23 EGFR in the compartment positive for early endocytic markers such as RAB-5 since a defect in endosomal maturation is expected. To further address this question, transgenic lines expressing both LET-23::GFP and endocytic markers tagged with mCherry should be developed to study co-localization in live animals.

It has been previously demonstrated in Hela cells that activated Rab7 is able to couple late endosomes to the dynein-dynactin complex and that RILP bridges Rab7 and dynein, by functioning as a Rab7 effector and directly binding dynactin (Johansson et al., 2007). Our preliminary unpublished RNAi data indicate that *C. elegans* RILP-1 has a negative effect on LET-23 EGFR signaling, similar to RAB-7. This could be a point of overlap between LET-23 EGFR regulation by DHC-1 and RAB-7 in the VPCs, where the receptor endocytosed into the early endosome is transported along the microtubules by the dynein motor, and once the endosome undergoes maturation and accumulates activated RAB-7, trafficking of LET-23 EGFR destined for lysosomal degradation is further promoted and enhanced by linking late endosomes to the dynein-dynactin complex via RILP. Thus, further studies should address the role of RILP-1 on LET-23 EGFR localization in the VPCs. If the above hypothesis is correct, then it would be

expected that loss of RILP-1 will have a phenotype similar to *rab-7(ok511)* rather than that of *dhc-1(vh22)*.

It has been proposed that EGFR loses its ability to signal to downstream targets once it is entrapped in the ILVs of the MVBs and that degradation of the receptor is not required to terminate signaling (Bache et al., 2006). Our previous work suggests that *C. elegans* LET-23 EGFR does travel through the MVBs since RNAi-mediated knock down of the early ESCRT components, *hrs-1 Hrs* (ESCRT-0) and *tsg-101 Tsg101* (ESCRT-I), increases the LET-23 EGFR signaling output in the sensitized *lin-2(-)* background (Skorobogata and Rocheleau, 2012). Loss of Rab7 in Hela cells have been shown to block EGFR degradation and promote its accumulation in enlarged late endosomes/MVBs (Vanlandingham and Ceresa, 2009). We show that *rab-7* mutants have increased strength of LET-23 EGFR signaling *in vivo* in the *C. elegans* VPCs suggesting that LET-23 EGFR entrapped in the vesicular structures observed in the *rab-7* background is still able to transmit signal to downstream targets. Even though based on the studies in the mammalian tissue culture one could expect that loss of Rab7 function would not lead to increased EGFR signaling, our data is consistent with the *in vivo* findings in *Drosophila*, where loss of ESCRT-I, -II and –III components leads to decreased EGFR degradation and increased signaling (Vaccari et al., 2009). Moreover, it has been demonstrated that signaling complexes exist on the late endosomes, are required for proper Erk-mediated signal transduction and promote Erk1/2 nuclear entry (Teis et al., 2006). Thus, our *in vivo* data support these studies and show evidence that LET-23 EGFR is capable of signaling upon loss of components of endocytic machinery involved in the late stages of vesicular trafficking.

Since LET-23 EGFR accumulates in the vesicular structures adjacent to the plasma membrane in *dhc-1(vh22)* mutants, whereas *rab-7(ok511)* animals accumulate LET-23 EGFR-

positive punctae throughout the cytoplasm, it is suggestive of DHC-1 functioning at the early steps of LET-23 EGFR vesicular trafficking, however DHC-1 could still be involved with RAB-7 in the late endosome to lysosome transition. It would be expected that if DHC-1 functions upstream of RAB-7 in the LET-23 EGFR trafficking, then loss of DHC-1 function in the *rab-7(ok511)* background should resemble the *dhc-1* mutant phenotype rather than that of *rab-7*. Unfortunately, due to a high level of lethality upon loss of both DHC-1 and RAB-7, it was challenging to address this question. *dhc-1(RNAi)* in *rab-7(ok511)* led to lethality of progeny when L4 mothers were placed on RNAi. While placing *rab-7(ok511)* larvae at L1 stage on *dhc-1(RNAi)* resulted in viable L3 larvae, the localization of LET-23 EGFR in these mutants did not differ from *rab-7(ok511)*. This lack of effect could be due to the short amount of time the larvae were subjected to RNAi combined with our experience that RNAi is not very effective in the VPCs and potentially animals that do survive to be L3 larvae are those that are not strongly affected by the RNAi treatment. The above hypothesis is supported by no effect of *rab-5(RNAi)* on LET-23 EGFR localization in *rab-7(ok511)* animals, which was performed as a positive control in parallel with *dhc-1(RNAi)*. Since RAB-5 is an early endocytic Rab GTPase, it would be expected that its effect on LET-23 EGFR localization should be similar to that observed in *dhc-1(vh22)* mutants. Since available *rab-5(ok2605)* mutant animals die during early larval development and *dhc-1(vh22)* has a very high percentage of lethality at 20°C, it might be challenging if not impossible to obtain viable *dhc-1(vh22); rab-7(ok511)* and *rab-5(ok2605); rab-7(ok511)* double mutants to study the distribution of LET-23::GFP in the VPCs. To overcome this limitation, it would be informative to construct a double mutant between *rab-7(ok511)* and *dyn-1(ky51) dynamin*, which is a temperature-sensitive allele that loses dynamin function after 60 seconds of being upshifted to 25°C. Since dynamin is involved in early stages of endocytosis, the pinching off of the endocytic vesicles from the plasma

membrane, it is expected that it would have a phenotype similar to *dhc-1(vh22)* in terms of LET-23::GFP distribution in the VPCs, and *rab-7(ok511); dyn-1(ky51)* double-mutants should have LET-23::GFP localization similar to *dyn-1(ky51)*.

Future studies aimed at determining the identity of the compartments accumulating LET-23::GFP in *dhc-1(vh22)* and *rab-7(ok511)* as well as deciphering the relationship between DHC-1 and RAB-7 in the regulation of LET-23 EGFR signaling and trafficking would further our understanding of the mechanisms governing both endocytic trafficking and signaling of the EGFR.

5.1.3. Opposing roles of AGEF-1 and RAB-10

5.1.3.1. LET-23 EGFR signaling

Given the multiple phenotypes observed in *agef-1(vh4)* mutants, the possibility of AGEF-1 functioning in multiple ways to negatively regulate LET-23 EGFR signaling and localization exists. In order to be able to discern these various functions of AGEF-1 and their role on EGFR signaling and trafficking, finding genes acting opposite AGEF-1 is necessary. Discovery of a requirement for the small GTPase RAB-10 not only for the ability of *agef-1(vh4)* to suppress the *lin-2(-)* Vul phenotype, but also for other *agef-1(vh4)* phenotypes is suggestive of RAB-10 functioning closely with and opposite to AGEF-1.

In mammalian fibroblasts Rab10 has been shown to localize to the TGN (Chen et al., 1993). Furthermore, the differential role of Rab10 in MDCK cells during and after polarization has been demonstrated. During early polarization of MDCK cells, Rab10 is localized mostly to the TGN and simultaneous loss of Rab10 and Rab8 function or overexpression of dominant active Rab10 at this stage inhibits biosynthetic cargo transport and leads to missorting of basolateral cargo to the apical membrane (Schuck et al., 2007). In polarized MDCK cells Rab10 localizes to common

recycling endosome, not the TGN, and is involved in cargo transport from basolateral early endosomes to the CRE, which is a point of convergence of trafficking from both the apical and basolateral membranes (Babbey et al., 2006). Overexpression of either active or inactive Rab10 in polarized MDCK cells did not affect apical cargo recycling or later steps of basolateral recycling, but led to a defect in the early basolateral endocytic pathway (Babbey et al., 2006). In *C. elegans* polarized intestinal cells, RAB-10 is localized to both Golgi and endosomes, and has been proposed to function in a basolateral recycling pathway since *rab-10* mutants accumulate enormous GFP::RAB-5-positive endosomes that contain basolateral recycling cargo (Chen et al., 2006). Furthermore, RAB-10 has been shown to be involved in the recruitment of the RAB-5 GAP TBC-2 to endosomal membranes in order to inactivate RAB-5 and promote exit of the basolateral recycling cargo from early endosomes (Liu and Grant, 2015). Studies in a different type of polarized cells, *C. elegans* neurons, showed that RAB-10 functions in parallel to LIN-10 Mint in the recycling of AMPA-type glutamate receptor subunit GLR-1 from endosomes to synapses (Glodowski et al., 2007). Taken together these data suggest that Rab10 is involved in both the establishment of polarity by promoting basolateral biosynthetic cargo delivery and in the maintenance of polarity by control of the basolateral recycling pathway.

AGEF-1 prevents basolateral LET-23 EGFR localization in the VPCs, where loss of *agef-1* function leads to increased basolateral localization of the receptor. Since Rab10 is involved in basolateral endocytic trafficking, I hypothesize that loss of RAB-10 in *agef-1(vh4)* mutant backgrounds will block basolateral delivery of LET-23 EGFR, underlying the reason for *rab-10(q373) agef-1(vh4); lin-2(e1309)* being reverted back to a Vul phenotype. To test this hypothesis, LET-23::GFP localization should be studied in the *rab-10(q373)*, *rab-10(q373) agef-1(vh4)* and *rab-10(q373) agef-1(vh4); lin-2(e1309)* mutants. *rab-10(q373)* single mutants might

have a reduced basolateral LET-23::GFP in respect to apical receptor localization, since multiple pathways are likely to be involved in basolateral LET-23 EGFR localization (i.e. LIN-2/7/10 complex) and *rab-10(q373)* animals are wild type in terms of vulva induction. Whereas *rab-10(q373) agef-1(vh4)* might be wild-type for LET-23 EGFR localization if RAB-10 function is required for *agef-1*-induced increase in basolateral/apical LET-23::GFP intensity. Finally, if this hypothesis is true, then *rab-10(q373) agef-1(vh4); lin-2(e1309)* triple mutants will more closely resemble *lin-2(-)* single mutants. Additionally, if *C. elegans* RAB-10 is involved in the establishment of VPC polarity, then basolateral (ERM-1::GFP ERM and LET-413::GFP ERBIN) and apical (PAR-3::GFP ASIP and PAR-6::GFP Par6) markers will be mislocalized in the VPCs of *rab-10(q373)* mutants.

5.1.3.2. Other agef-1(vh4) phenotypes

As mentioned earlier, the mechanism by which AGEF-1 regulates the size of late endosomes/lysosomes is unclear. To further investigate the involvement of RAB-10 in the control of the size of the LMP-1::GFP-positive late endosomes/lysosomes in the coelomocytes, it should be assessed whether a decrease in the size of LMP-1::GFP-positive structures in *rab-10(q373) agef-1(vh4)* double mutants is direct or indirect. *rab-10* mutants have been shown to accumulate enormous RAB-5::GFP-positive early endosomes in the intestinal cells (Chen et al., 2006; Liu and Grant, 2015), thus this effect could be translated to coelomocytes as well. It is possible that enlargement of one endocytic compartment might lead to decrease in size of another compartment due to re-distribution of endomembranes. If this is the case in the *rab-10* background, then an increase in the size of early endosomes might cause a decrease is size of late endosomes/lysosomes leading to suppression of *agef-1(vh4)* late endosomal phenotypes in *rab-10(q373) agef-1(vh4)* doubles. Thus, the size of early endosomes and late endosomes in the coelomocytes of *rab-10*,

agef-1(vh4) and *rab-10(q373) agef-1(vh4)* mutants should be assessed and compared to wild-type. Moreover, the ratio of early/late endosomal size could be calculated to test this hypothesis if significant changes are found in the mutants.

agef-1(vh4) embryos accumulate YP170::GFP yolk blobs, which increase in size throughout embryonic development. The nature of this phenotype is unclear, however it appears that in *agef-1(vh4)* mutants yolk fails to be endocytosed by the cells of the developing gut following its secretion by non-gut cells into the perivitelline space (Bossinger and Schierenberg, 1996). Preliminary assessment of YP170::GFP accumulation by the gut of wild-type and *agef-1(vh4)* embryos using epifluorescence suggests lower fluorescence intensity in the *agef-1(vh4)* background. However, in order to have a precise quantification, confocal microscopy should be used since blobs positive for YP170::GFP, which are present in *agef-1(vh4)* mutants, produce background fluorescence that interferes with quantifications when epifluorescence microscopy is used. The same experiment should be performed in *rab-10(q373)* and *rab-10(q373) agef-1(vh4)* mutants.

In order for yolk to accumulate in the oocytes prior to fertilization, it has to be produced by the gut of the hermaphrodite and then be secreted into the pseudocoelom followed by an uptake of the yolk by maturing oocytes (Grant and Hirsh, 1999). Since yeast and *Drosophila* homologs of Rab10 are required for secretion (Lerner et al., 2013; Liu et al., 2005), yolk secretion by the intestinal cells of *rab-10(q373)* mutant animals should be assessed along with *agef-1(vh4)* and *rab-10(q373) agef-1(vh4)* by measuring YP170::GFP fluorescence in the intestinal cells of the above mutants and comparing it to wild-type. Additionally, a similar experiment should be performed for YP170::GFP intensity in the most proximal oocyte to exclude the possibility that the ability of

rab-10 to suppress the blob phenotype in *agef-1(vh4)* embryos is due to less yolk being present in the embryos at the time of fertilization.

Identification of RAB-10, a GTPase involved in basolateral cargo trafficking, to be required for multiple *agef-1(vh4)* phenotypes, represents a good start toward further understanding the mechanisms of AGEF-1 function as well as identifies a new modulator of EGFR signaling output. Further detailed studies aimed at elucidating the relationship between the two proteins should be conducted.

5.1.4. ZEN-4 kinesin vs. DHC-1 dynein in LET-23 EGFR signaling

The dynein complex and the kinesins are the minus and plus end directed microtubule motors, respectively. Vesicles carrying cargo have been shown to contain motors of opposite polarity on their surface thus enabling the movement of organelles in both directions determined by stochastic binding of the motors (Bryantseva and Zhapparova, 2012). Having identified ZEN-4 MKLP1 kinesin as required for *dhc-1(vh22)* suppression of the *lin-2(-)* Vul phenotype, we have hypothesized that ZEN-4 kinesin might be involved in the movement of LET-23 EGFR-containing vesicles in the direction opposite DHC-1 dynein along the microtubules. However, when *zen-4 MKLP1* was depleted by RNAi in *dhc-1(vh22); lin-2(-)* mutants, no effect on the punctate distribution of LET-23::GFP was observed suggesting that ZEN-4 MKLP1 is likely to regulate LET-23 EGFR signaling independently of DHC-1 dynein.

zen-4(or153) mutant animals have a partial Vul phenotype at the restrictive temperature of 20°C, which suggests that ZEN-4 promotes LET-23 EGFR signaling in the VPCs, however whether this effect is direct or indirect has to be determined. Since ZEN-4 is a microtubule motor, it is still possible that it could affect signaling by regulating the localization of the LET-23 EGFR.

To test whether this is the case, LET-23::GFP localization/distribution in the VPCs of *zen-4(or153)* mutants should be assessed and compared to wild-type animals. If there is a difference, then the role of ZEN-4 in LET-23::GFP localization in the *dhc-1(vh22); lin-2(-)* background should be re-assessed. *zen-4(RNAi)* in *dhc-1(vh22); lin-2(-)* did not result in changes in LET-23::GFP localization, thus *dhc-1(vh22); zen-4(or153)* and *dhc-1(vh22); zen-4(or153); lin-2(-)* mutants expressing LET-23::GFP should be constructed. However, this could be challenging due to high lethality of animals doubly homozygous for *dhc-1(vh22)* and *zen-4(or153)* coming from mothers heterozygous for *zen-4(or153)* even at permissive temperature of 15°C. If a redistribution of LET-23::GFP subcellular localization is present in both mutants compared to *dhc-1(vh22)* alone, then it is possible that ZEN-4 directly regulates trafficking of the LET-23 EGFR-containing vesicles in the VPCs.

One of the functions of *C. elegans* ZEN-4 MKLP1 is to control the polarization of the arcade cells of the developing foregut during pharyngeal tubulogenesis (Portereiko et al., 2004). *zen-4* mutants failed to generate adherens junctions (CeAJ), the sole type of junctions separating apical and basolateral domains in the polarized cells of *C. elegans*, and apical membranes in the arcade cells (Portereiko et al., 2004). Thus, possible changes in LET-23::GFP localization in *zen-4(or153)* mutants might be caused indirectly by an effect on VPC polarity. *zen-4(or153)* mutants could have defects in the establishment of VPC polarity, which could be tested by studying the morphology of CeAJ in the VPCs using GFP-tagged components of the apical junction, such as coiled coil protein AJM-1 or VAB-9 Claudin (Koppen et al., 2001; Simske et al., 2003). As has been described above for RAB-10, the distribution of apical and basolateral markers could be assessed in *zen-4(or153)* background.

Alternatively, ZEN-4 MKLP1 might be causing a Vul phenotype without affecting LET-23 EGFR signaling in the VPCs. ZEN-4 MKLP1 has been shown to be required for cytokinesis (Raich et al., 1998), thus it is possible that *zen-4* Vul phenotype is due to failure of the VPCs to divide. My preliminary analysis did not detect undivided multinucleated VPCs in *zen-4(or153)* mutant backgrounds. In order to further address lack of VPC divisions in these mutants, a plasma membrane marker, fluorescently tagged pleckstrin-homology domain of phospholipase C gamma (PH::mCherry) (Kachur et al., 2008), expressed in the VPCs could be used to see the boundaries of the individual daughter VPCs. Additionally, this hypothesis could be tested by genetic epistasis between *lin-1(n304)* and *zen-4(or153)*. LIN-1 is an ETS domain-containing transcription factor that is an effector of MAPK signaling (Beitel et al., 1995). When MAPK is inactive, it is present as a dimer with LIN-31 winged helix (WH)-like transcription factor in an active form to inhibit vulva induction; whereas upon MAPK activation, LIN-1 is phosphorylated, dissociates from LIN-31 and becomes inactive allowing for vulval cell fate specification (Jacobs et al., 1998). *lin-1(n304)* is a null allele and the animals have a Muv phenotypes, which does not depend on the presence of inductive LIN-3 EGF signal (Beitel et al., 1995). Thus, if the Vul phenotype of *zen-4(or153)* mutants is due to a failure in VPC division, then *zen-4(or153)* will be able to suppress the *lin-1(n304)* Muv phenotype.

Given the various roles of ZEN-4 MKLP1 described in the literature, it is likely that it functions independently of DHC-1 dynein in the regulation of the LET-23 EGFR signaling during vulva induction, however the evidence of its role in the control of epithelial polarity in *C. elegans* makes it an interesting candidate for extending the studies of this role of ZEN-4 MKLP1 into mammalian systems. Furthermore, there still could be other kinesins among the ones that have not

yet been tested by us, which are acting opposite DHC-1 dynein in the transport of LET-23 EGFR-containing vesicles along microtubules.

5.2. Contribution of the presented research to our scientific understanding

EGFR and RTK family members are overexpressed and/or activated in a large number of cancers of different origins, i.e. lung, breast, colon (Normanno et al., 2006). Moreover, high EGFR expression levels correlate with a poor prognosis for cancer survivors (Nicholson et al., 2001). Thus, development of anti-EGFR therapies has been one of the priorities for pharmaceutical companies. In *C. elegans*, loss of negative regulators of EGFR/Ras/MAPK pathway, such as AGEF-1 BIG1/2 and DHC-1 dynein, leads to increased signaling suggesting that these proteins could function as tumor suppressors in humans and could represent potential targets for anti-EGFR directed therapies.

A large number of cancers originate from epithelial cells with strongly established and maintained polarity. *C. elegans* vulva provides an excellent *in vivo* model to study EGFR signaling in polarized cells, which is difficult to achieve using other experimental systems. A lot of effort has been put into investigating the role of BIG1/2 Arf GEFs on cellular trafficking; however their function is still not fully understood especially in the context of a whole organism. *agef-1(vh4)* is a partial loss-of-function allele, the only viable *C. elegans agef-1* mutant available, which allowed me to study the requirement for an Arf GEF during development *in vivo*. Work presented in this thesis demonstrates that AGEF-1 antagonizes EGFR signaling by regulating the polarized localization of the receptor in the VPCs. A human homolog of AGEF-1 is mutated in numerous cancer cell lines supporting a tumor suppressive function in humans (Barretina et al., 2012). This

corroborates our findings and emphasizes the importance of the presented studies in determining the cellular mechanisms by which AGEF-1 BIG1/2 regulates EGFR signaling and cellular polarity.

Mutations in BIG2 Arf GEF have been linked to autosomal recessive periventricular heterotopia, a disorder characterized by failure in neuronal migration during development due to defects in vesicular trafficking (Bui et al., 2009). In addition, BIG2 has been proposed as a biomarker for Huntington's disease (Lovrecic et al., 2010). Even though the morphology of the neurons is quite distinct from that of polarized epithelial cells, both cell types have similarities in polarity with the axon and somatodendritic surfaces being equivalent to apical and basolateral membrane domains of polarized epithelial cells, respectively (Muth and Caplan, 2003). Thus, our findings might not only be relevant to EGFR signaling and cancer but also be important for understanding of neural development and disease.

Evidence for DHC-1 dynein attenuating the strength of EGFR signaling *in vivo* by promoting endocytic trafficking of the receptor towards the lysosome for degradation is presented in this thesis. It has been demonstrated in mammalian cell culture that inhibiting the function of cytoplasmic dynein indirectly could promote sustained EGFR signaling, however the direct role of dynein on signaling has not been investigated. To the best of our knowledge, this work is the first to provide evidence for an *in vivo* role for dynein in negatively regulating EGFR signaling. This study demonstrates how basic cellular processes such as vesicular trafficking and cytoskeletal transport can have profound effects on cell signaling and cell fate specification. It provides new knowledge about the regulation of EGFR signaling that may have broader impacts on other signal transduction pathways. Our data are consistent with mammalian studies and indicate that DHC-1 promotes both early and then, together with a small GTPase RAB-7, later steps of endocytic trafficking of EGFR destined for degradation. These findings could be translated to humans, where

dynein might function in the role of tumor suppressor to prevent malignancy.

REFERENCES

Abdus-Saboor, I., V.P. Mancuso, J.I. Murray, K. Palozola, C. Norris, D.H. Hall, K. Howell, K. Huang, and M.V. Sundaram. 2011. Notch and Ras promote sequential steps of excretory tube development in C. elegans. *Development*. 138:3545-3555.

Ackema, K.B., U. Sauder, J.A. Solinger, and A. Spang. 2013. The ArfGEF GBF-1 Is Required for ER Structure, Secretion and Endocytic Transport in. *PLoS One*. 8:e67076.

Allan, V.J. 2011. Cytoplasmic dynein. *Biochem Soc Trans*. 39:1169-1178.

Anderson, J.M., and C.M. Van Itallie. 2009. Physiology and function of the tight junction. *Cold Spring Harb Perspect Biol*. 1:a002584.

Apodaca, G., L.A. Katz, and K.E. Mostov. 1994. Receptor-Mediated Transcytosis of Iga in Mdck Cells Is Via Apical Recycling Endosomes. *Journal of Cell Biology*. 125:67-86.

Aroian, R.V., G.M. Lesa, and P.W. Sternberg. 1994. Mutations in the Caenorhabditis elegans let-23 EGFR-like gene define elements important for cell-type specificity and function. *EMBO J*. 13:360-366.

Aroian, R.V., and P.W. Sternberg. 1991. Multiple functions of let-23, a Caenorhabditis elegans receptor tyrosine kinase gene required for vulval induction. *Genetics*. 128:251-267.

Au, J.S., C. Puri, G. Ihrke, J. Kendrick-Jones, and F. Buss. 2007. Myosin VI is required for sorting of AP-1B-dependent cargo to the basolateral domain in polarized MDCK cells. *J Cell Biol*. 177:103-114.

Babbey, C.M., N. Ahktar, E. Wang, C.C. Chen, B.D. Grant, and K.W. Dunn. 2006. Rab10 regulates membrane transport through early endosomes of polarized Madin-Darby canine kidney cells. *Mol Biol Cell*. 17:3156-3175.

Bacallao, R., C. Antony, C. Dotti, E. Karsenti, E.H. Stelzer, and K. Simons. 1989. The subcellular organization of Madin-Darby canine kidney cells during the formation of a polarized epithelium. *J Cell Biol*. 109:2817-2832.

Bache, K.G., T. Slagsvold, and H. Stenmark. 2004. Defective downregulation of receptor tyrosine kinases in cancer. *EMBO J*. 23:2707-2712.

Bache, K.G., S. Stuffers, L. Malerod, T. Slagsvold, C. Raiborg, D. Lechardeur, S. Walchli, G.L. Lukacs, A. Brech, and H. Stenmark. 2006. The ESCRT-III subunit hVps24 is required for degradation but not silencing of the epidermal growth factor receptor. *Mol Biol Cell*. 17:2513-2523.

Barbieri, M.A., R.L. Roberts, A. Gumusboga, H. Highfield, C. Alvarez-Dominguez, A. Wells, and P.D. Stahl. 2000. Epidermal growth factor and membrane trafficking. EGF receptor activation of endocytosis requires Rab5a. *J Cell Biol*. 151:539-550.

Barfield, R.M., J.C. Fromme, and R. Schekman. 2009. The exomer coat complex transports Fus1p to the plasma membrane via a novel plasma membrane sorting signal in yeast. *Mol Biol Cell*. 20:4985-4996.

Barkoulas, M., J.S. van Zon, J. Milloz, A. van Oudenaarden, and M.A. Felix. 2013. Robustness and epistasis in the C. elegans vulval signaling network revealed by pathway dosage modulation. *Dev Cell*. 24:64-75.

Barman, S., and D.P. Nayak. 2000. Analysis of the transmembrane domain of influenza virus neuraminidase, a type II transmembrane glycoprotein, for apical sorting and raft association. *J Virol*. 74:6538-6545.

Barretina, J., G. Caponigro, N. Stransky, K. Venkatesan, A.A. Margolin, S. Kim, C.J. Wilson, J. Lehar, G.V. Kryukov, D. Sonkin, A. Reddy, M. Liu, L. Murray, M.F. Berger, J.E.

Monahan, P. Morais, J. Meltzer, A. Korejwa, J. Jane-Valbuena, F.A. Mapa, J. Thibault, E. Bric-Furlong, P. Raman, A. Shipway, I.H. Engels, J. Cheng, G.K. Yu, J. Yu, P. Aspesi, Jr., M. de Silva, K. Jagtap, M.D. Jones, L. Wang, C. Hatton, E. Palescandolo, S. Gupta, S. Mahan, C. Sougnez, R.C. Onofrio, T. Liefeld, L. MacConaill, W. Winckler, M. Reich, N. Li, J.P. Mesirov, S.B. Gabriel, G. Getz, K. Ardlie, V. Chan, V.E. Myer, B.L. Weber, J. Porter, M. Warmuth, P. Finan, J.L. Harris, M. Meyerson, T.R. Golub, M.P. Morrissey, W.R. Sellers, R. Schlegel, and L.A. Garraway. 2012. The Cancer Cell Line Encyclopedia enables predictive modelling of anticancer drug sensitivity. *Nature*. 483:603-607.

Batzer, A.G., D. Rotin, J.M. Urena, E.Y. Skolnik, and J. Schlessinger. 1994. Hierarchy of binding sites for Grb2 and Shc on the epidermal growth factor receptor. *Mol Cell Biol*. 14:5192-5201.

Beitel, G.J., S. Tuck, I. Greenwald, and H.R. Horvitz. 1995. The Caenorhabditis elegans gene lin-1 encodes an ETS-domain protein and defines a branch of the vulval induction pathway. *Genes Dev*. 9:3149-3162.

Berkowitz, L.A., A.L. Knight, G.A. Caldwell, and K.A. Caldwell. 2008. Generation of stable transgenic C. elegans using microinjection. *J Vis Exp*.

Berset, T., E.F. Hoier, G. Battu, S. Canevascini, and A. Hajnal. 2001. Notch inhibition of RAS signaling through MAP kinase phosphatase LIP-1 during C. elegans vulval development. *Science*. 291:1055-1058.

Berset, T.A., E.F. Hoier, and A. Hajnal. 2005. The C. elegans homolog of the mammalian tumor suppressor Dep-1/Scc1 inhibits EGFR signaling to regulate binary cell fate decisions. *Genes Dev*. 19:1328-1340.

Boal, F., and D.J. Stephens. 2010. Specific functions of BIG1 and BIG2 in endomembrane organization. *PLoS One*. 5:e9898.

Bonifacino, J.S. 2014. Adaptor proteins involved in polarized sorting. *J Cell Biol*. 204:7-17.

Bonifacino, J.S., and J. Lippincott-Schwartz. 2003. Coat proteins: shaping membrane transport. *Nat Rev Mol Cell Biol*. 4:409-414.

Bossinger, O., and E. Schierenberg. 1996. The use of fluorescent marker dyes for studying intercellular communication in nematode embryos. *Int J Dev Biol*. 40:431-439.

Brankatschk, B., S.P. Wichert, S.D. Johnson, O. Schaad, M.J. Rossner, and J. Gruenberg. 2012. Regulation of the EGF transcriptional response by endocytic sorting. *Sci Signal*. 5:ra21.

Braulke, T., and J.S. Bonifacino. 2009. Sorting of lysosomal proteins. *Biochim Biophys Acta*. 1793:605-614.

Brenner, S. 1974. The genetics of Caenorhabditis elegans. *Genetics*. 77:71-94.

Brown, D.A., and J.K. Rose. 1992. Sorting of GPI-anchored proteins to glycolipid-enriched membrane subdomains during transport to the apical cell surface. *Cell*. 68:533-544.

Brown, P.S., E. Wang, B. Aroeti, S.J. Chapin, K.E. Mostov, and K.W. Dunn. 2000. Definition of distinct compartments in polarized Madin-Darby canine kidney (MDCK) cells for membrane-volume sorting, polarized sorting and apical recycling. *Traffic*. 1:124-140.

Bryant, D.M., and K.E. Mostov. 2008. From cells to organs: building polarized tissue. *Nat Rev Mol Cell Biol*. 9:887-901.

Bryantseva, S.A., and O.N. Zhapparova. 2012. Bidirectional transport of organelles: unity and struggle of opposing motors. *Cell Biol Int*. 36:1-6.

Bui, Q.T., M.P. Golinelli-Cohen, and C.L. Jackson. 2009. Large Arf1 guanine nucleotide exchange factors: evolution, domain structure, and roles in membrane trafficking and human disease. *Mol Genet Genomics*. 282:329-350.

Butz, S., M. Okamoto, and T.C. Sudhof. 1998. A tripartite protein complex with the potential to couple synaptic vesicle exocytosis to cell adhesion in brain. *Cell*. 94:773-782.

Cantalupo, G., P. Alifano, V. Roberti, C.B. Bruni, and C. Bucci. 2001. Rab-interacting lysosomal protein (RILP): the Rab7 effector required for transport to lysosomes. *EMBO J*. 20:683-693.

Cao, X., M.A. Surma, and K. Simons. 2012. Polarized sorting and trafficking in epithelial cells. *Cell Res*. 22:793-805.

Caplan, M.J. 1997. Membrane polarity in epithelial cells: protein sorting and establishment of polarized domains. *Am J Physiol*. 272:F425-429.

Carpenter, G., and S. Cohen. 1979. Epidermal growth factor. *Annu Rev Biochem*. 48:193-216.

Carvajal-Gonzalez, J.M., D. Gravotta, R. Mattera, F. Diaz, A. Perez Bay, A.C. Roman, R.P. Schreiner, R. Thuenauer, J.S. Bonifacino, and E. Rodriguez-Boulan. 2012. Basolateral sorting of the coxsackie and adenovirus receptor through interaction of a canonical YXXPhi motif with the clathrin adaptors AP-1A and AP-1B. *Proc Natl Acad Sci U S A*. 109:3820-3825.

Casanova, J.E. 2007. Regulation of Arf activation: the Sec7 family of guanine nucleotide exchange factors. *Traffic*. 8:1476-1485.

Ceol, C.J., and H.R. Horvitz. 2004. A new class of C. elegans synMuv genes implicates a Tip60/NuA4-like HAT complex as a negative regulator of Ras signaling. *Dev Cell*. 6:563-576.

Ceresa, B.P., and S.J. Bahr. 2006. rab7 activity affects epidermal growth factor:epidermal growth factor receptor degradation by regulating endocytic trafficking from the late endosome. *J Biol Chem*. 281:1099-1106.

Chang, C., N.A. Hopper, and P.W. Sternberg. 2000. Caenorhabditis elegans SOS-1 is necessary for multiple RAS-mediated developmental signals. *Embo Journal*. 19:3283-3294.

Chang, C., and P.W. Sternberg. 1999. C. elegans vulval development as a model system to study the cancer biology of EGFR signaling. *Cancer Metastasis Rev*. 18:203-213.

Chen, C.C., P.J. Schweinsberg, S. Vashist, D.P. Mareiniss, E.J. Lambie, and B.D. Grant. 2006. RAB-10 is required for endocytic recycling in the Caenorhabditis elegans intestine. *Mol Biol Cell*. 17:1286-1297.

Chen, M.K., and M.C. Hung. 2015. Proteolytic cleavage, trafficking, and functions of nuclear receptor tyrosine kinases. *FEBS J*. 282:3693-3721.

Chen, N., and I. Greenwald. 2004. The lateral signal for LIN-12/Notch in C. elegans vulval development comprises redundant secreted and transmembrane DSL proteins. *Dev Cell*. 6:183-192.

Chen, Y.T., C. Holcomb, and H.P. Moore. 1993. Expression and localization of two low molecular weight GTP-binding proteins, Rab8 and Rab10, by epitope tag. *Proc Natl Acad Sci U S A*. 90:6508-6512.

Cherfils, J., and M. Zeghouf. 2013. Regulation of small GTPases by GEFs, GAPs, and GDIs. *Physiol Rev*. 93:269-309.

Chi, S., H. Cao, Y. Wang, and M.A. McNiven. 2011. Recycling of the epidermal growth factor receptor is mediated by a novel form of the clathrin adaptor protein Eps15. *J Biol Chem*. 286:35196-35208.

Christis, C., and S. Munro. 2012. The small G protein Arl1 directs the trans-Golgi-specific targeting of the Arf1 exchange factors BIG1 and BIG2. *J Cell Biol*. 196:327-335.
Cohen, A.R., D.F. Woods, S.M. Marfatia, Z. Walther, A.H. Chishti, and J.M. Anderson. 1998. Human CASK/LIN-2 binds syndecan-2 and protein 4.1 and localizes to the basolateral membrane of epithelial cells. *J Cell Biol*. 142:129-138.
Cohen, D., A. Musch, and E. Rodriguez-Boulan. 2001. Selective control of basolateral membrane protein polarity by cdc42. *Traffic*. 2:556-564.
Cohen, S., and R.A. Fava. 1985. Internalization of functional epidermal growth factor:receptor/kinase complexes in A-431 cells. *J Biol Chem*. 260:12351-12358.
Cotton, C.U., M.E. Hobert, S. Ryan, and C.R. Carlin. 2013. Basolateral EGF receptor sorting regulated by functionally distinct mechanisms in renal epithelial cells. *Traffic*. 14:337-354.
Cresawn, K.O., B.A. Potter, A. Oztan, C.J. Guerriero, G. Ihrke, J.R. Goldenring, G. Apodaca, and O.A. Weisz. 2007. Differential involvement of endocytic compartments in the biosynthetic traffic of apical proteins. *EMBO J*. 26:3737-3748.
Cui, M., J. Chen, T.R. Myers, B.J. Hwang, P.W. Sternberg, I. Greenwald, and M. Han. 2006. SynMuv genes redundantly inhibit lin-3/EGF expression to prevent inappropriate vulval induction in C. elegans. *Dev Cell*. 10:667-672.
Davies, G.C., P.E. Ryan, L. Rahman, M. Zajac-Kaye, and S. Lipkowitz. 2006. EGFRvIII undergoes activation-dependent downregulation mediated by the Cbl proteins. *Oncogene*. 25:6497-6509.
Davis, M.W., M. Hammarlund, T. Harrach, P. Hullett, S. Olsen, and E.M. Jorgensen. 2005. Rapid single nucleotide polymorphism mapping in C. elegans. *BMC Genomics*. 6:118.
Davison, E.M., M.M. Harrison, A.J. Walhout, M. Vidal, and H.R. Horvitz. 2005. lin-8, which antagonizes Caenorhabditis elegans Ras-mediated vulval induction, encodes a novel nuclear protein that interacts with the LIN-35 Rb protein. *Genetics*. 171:1017-1031.
Davison, E.M., A.M. Saffer, L.S. Huang, J. DeModena, P.W. Sternberg, and H.R. Horvitz. 2011. The LIN-15A and LIN-56 transcriptional regulators interact to negatively regulate EGF/Ras signaling in Caenorhabditis elegans vulval cell-fate determination. *Genetics*. 187:803-815.
Deborde, S., E. Perret, D. Gravotta, A. Deora, S. Salvarezza, R. Schreiner, and E. Rodriguez-Boulan. 2008. Clathrin is a key regulator of basolateral polarity. *Nature*. 452:719-723.
del Castillo, U., W. Lu, M. Winding, M. Lakonishok, and V.I. Gelfand. 2015. Pavarotti/MKLP1 regulates microtubule sliding and neurite outgrowth in Drosophila neurons. *Curr Biol*. 25:200-205.
Delacour, D., A. Koch, and R. Jacob. 2009. The role of galectins in protein trafficking. *Traffic*. 10:1405-1413.
Deora, A.A., D. Gravotta, G. Kreitzer, J. Hu, D. Bok, and E. Rodriguez-Boulan. 2004. The basolateral targeting signal of CD147 (EMMPRIN) consists of a single leucine and is not recognized by retinal pigment epithelium. *Mol Biol Cell*. 15:4148-4165.
DeVore, D.L., H.R. Horvitz, and M.J. Stern. 1995. An FGF receptor signaling pathway is required for the normal cell migrations of the sex myoblasts in C. elegans hermaphrodites. *Cell*. 83:611-620.
Donaldson, J.G., A. Honda, and R. Weigert. 2005. Multiple activities for Arf1 at the Golgi complex. *Biochim Biophys Acta*. 1744:364-373.

Dong, J., W. Chen, A. Welford, and A. Wandinger-Ness. 2004. The proteasome alpha-subunit XAPC7 interacts specifically with Rab7 and late endosomes. *J Biol Chem*. 279:21334-21342.

Doyotte, A., M.R. Russell, C.R. Hopkins, and P.G. Woodman. 2005. Depletion of TSG101 forms a mammalian "Class E" compartment: a multicisternal early endosome with multiple sorting defects. *J Cell Sci*. 118:3003-3017.

Dunbar, L.A., P. Aronson, and M.J. Caplan. 2000. A transmembrane segment determines the steady-state localization of an ion-transporting adenosine triphosphatase. *J Cell Biol*. 148:769-778.

Durrbach, A., G. Raposo, D. Tenza, D. Louvard, and E. Coudrier. 2000. Truncated brush border myosin I affects membrane traffic in polarized epithelial cells. *Traffic*. 1:411-424.

Dutt, A., S. Canevascini, E. Froehli-Hoier, and A. Hajnal. 2004. EGF signal propagation during C. elegans vulval development mediated by ROM-1 rhomboid. *PLoS Biol*. 2:e334.

Ebner, R., and R. Derynck. 1991. Epidermal growth factor and transforming growth factor-alpha: differential intracellular routing and processing of ligand-receptor complexes. *Cell Regul*. 2:599-612.

Fares, H., and I. Greenwald. 2001. Regulation of endocytosis by CUP-5, the Caenorhabditis elegans mucolipin-1 homolog. *Nat Genet*. 28:64-68.

Fay, D.S., and J. Yochem. 2007. The SynMuv genes of Caenorhabditis elegans in vulval development and beyond. *Dev Biol*. 306:1-9.

Ferguson, E.L., and H.R. Horvitz. 1985. Identification and characterization of 22 genes that affect the vulval cell lineages of the nematode Caenorhabditis elegans. *Genetics*. 110:17-72.

Fiedler, K., and K. Simons. 1995. The role of N-glycans in the secretory pathway. *Cell*. 81:309-312.

Fisher, R.D., B. Wang, S.L. Alam, D.S. Higginson, H. Robinson, W.I. Sundquist, and C.P. Hill. 2003. Structure and ubiquitin binding of the ubiquitin-interacting motif. *J Biol Chem*. 278:28976-28984.

Folsch, H., P.E. Mattila, and O.A. Weisz. 2009. Taking the scenic route: biosynthetic traffic to the plasma membrane in polarized epithelial cells. *Traffic*. 10:972-981.

Folsch, H., H. Ohno, J.S. Bonifacino, and I. Mellman. 1999. A novel clathrin adaptor complex mediates basolateral targeting in polarized epithelial cells. *Cell*. 99:189-198.

Gaestel, M. 2006. MAPKAP kinases - MKs - two's company, three's a crowd. *Nat Rev Mol Cell Biol*. 7:120-130.

Galperin, E., V.V. Verkhusha, and A. Sorkin. 2004. Three-chromophore FRET microscopy to analyze multiprotein interactions in living cells. *Nat Methods*. 1:209-217.

Garrett, T.P., N.M. McKern, M. Lou, T.C. Elleman, T.E. Adams, G.O. Lovrecz, H.J. Zhu, F. Walker, M.J. Frenkel, P.A. Hoyne, R.N. Jorissen, E.C. Nice, A.W. Burgess, and C.W. Ward. 2002. Crystal structure of a truncated epidermal growth factor receptor extracellular domain bound to transforming growth factor alpha. *Cell*. 110:763-773.

Gassmann, R., A. Essex, J.S. Hu, P.S. Maddox, F. Motegi, A. Sugimoto, S.M. O'Rourke, B. Bowerman, I. McLeod, J.R. Yates, 3rd, K. Oegema, I.M. Cheeseman, and A. Desai. 2008. A new mechanism controlling kinetochore-microtubule interactions revealed by comparison of two dynein-targeting components: SPDL-1 and the Rod/Zwilch/Zw10 complex. *Genes Dev*. 22:2385-2399.

Gazdar, A.F. 2009. Activating and resistance mutations of EGFR in non-small-cell lung cancer: role in clinical response to EGFR tyrosine kinase inhibitors. *Oncogene*. 28:S24-S31.
Ge, H., X. Gong, and C.K. Tang. 2002. Evidence of high incidence of EGFRvIII expression and coexpression with EGFR in human invasive breast cancer by laser capture microdissection and immunohistochemical analysis. *Int J Cancer*. 98:357-361.
Gilbert, T., A. Le Bivic, A. Quaroni, and E. Rodriguez-Boulan. 1991. Microtubular organization and its involvement in the biogenetic pathways of plasma membrane proteins in Caco-2 intestinal epithelial cells. *J Cell Biol*. 113:275-288.
Glodowski, D.R., C.C. Chen, H. Schaefer, B.D. Grant, and C. Rongo. 2007. RAB-10 regulates glutamate receptor recycling in a cholesterol-dependent endocytosis pathway. *Mol Biol Cell*. 18:4387-4396.
Goffin, J.R., and K. Zbuk. 2013. Epidermal growth factor receptor: pathway, therapies, and pipeline. *Clin Ther*. 35:1282-1303.
Goldstein, N.S., and M. Armin. 2001. Epidermal growth factor receptor immunohistochemical reactivity in patients with American Joint Committee on Cancer Stage IV colon adenocarcinoma - Implications for a standardized scoring system. *Cancer*. 92:1331-1346.
Gonczy, P., S. Pichler, M. Kirkham, and A.A. Hyman. 1999. Cytoplasmic dynein is required for distinct aspects of MTOC positioning, including centrosome separation, in the one cell stage Caenorhabditis elegans embryo. *J Cell Biol*. 147:135-150.
Gonzalez, A., and E. Rodriguez-Boulan. 2009. Clathrin and AP1B: key roles in basolateral trafficking through trans-endosomal routes. *FEBS Lett*. 583:3784-3795.
Grandal, M.V., R. Zandi, M.W. Pedersen, B.M. Willumsen, B. van Deurs, and H.S. Poulsen. 2007. EGFRvIII escapes down-regulation due to impaired internalization and sorting to lysosomes. *Carcinogenesis*. 28:1408-1417.
Grant, B., and D. Hirsh. 1999. Receptor-mediated endocytosis in the Caenorhabditis elegans oocyte. *Mol Biol Cell*. 10:4311-4326.
Guillaud, L., M. Setou, and N. Hirokawa. 2003. KIF17 dynamics and regulation of NR2B trafficking in hippocampal neurons. *J Neurosci*. 23:131-140.
Guo, X., R. Mattera, X. Ren, Y. Chen, C. Retamal, A. Gonzalez, and J.S. Bonifacino. 2013. The adaptor protein-1 mu1B subunit expands the repertoire of basolateral sorting signal recognition in epithelial cells. *Dev Cell*. 27:353-366.
Haag, A., P. Gutierrez, A. Buhler, M. Walser, Q. Yang, M. Langouet, D. Kradolfer, E. Frohli, C.J. Herrmann, A. Hajnal, and J.M. Escobar-Restrepo. 2014. An In Vivo EGF Receptor Localization Screen in C. elegans Identifies the Ezrin Homolog ERM-1 as a Temporal Regulator of Signaling. *PLoS Genet*. 10:e1004341.
Hajnal, A., C.W. Whitfield, and S.K. Kim. 1997. Inhibition of Caenorhabditis elegans vulval induction by gap-1 and by let-23 receptor tyrosine kinase. *Genes Dev*. 11:2715-2728.
Hamill, D.R., A.F. Severson, J.C. Carter, and B. Bowerman. 2002. Centrosome maturation and mitotic spindle assembly in C. elegans require SPD-5, a protein with multiple coiled-coil domains. *Dev Cell*. 3:673-684.
Han, M.V., and C.M. Zmasek. 2009. phyloXML: XML for evolutionary biology and comparative genomics. *BMC Bioinformatics*. 10:356.
Han, W., T. Zhang, H. Yu, J.G. Foulke, and C.K. Tang. 2006. Hypophosphorylation of residue Y1045 leads to defective Downregulation of EGFRvIII. *Cancer Biol Ther*. 5:1361-1368.

Harrison, M.M., C.J. Ceol, X. Lu, and H.R. Horvitz. 2006. Some C. elegans class B synthetic multivulva proteins encode a conserved LIN-35 Rb-containing complex distinct from a NuRD-like complex. *Proc Natl Acad Sci U S A*. 103:16782-16787.

Hase, K., F. Nakatsu, M. Ohmae, K. Sugihara, N. Shioda, D. Takahashi, Y. Obata, Y. Furusawa, Y. Fujimura, T. Yamashita, S. Fukuda, H. Okamoto, M. Asano, S. Yonemura, and H. Ohno. 2013. AP-1B-mediated protein sorting regulates polarity and proliferation of intestinal epithelial cells in mice. *Gastroenterology*. 145:625-635.

Hatanpaa, K.J., S. Burma, D.W. Zhao, and A.A. Habib. 2010. Epidermal Growth Factor Receptor in Glioma: Signal Transduction, Neuropathology, Imaging, and Radioresistance. *Neoplasia*. 12:675-684.

Haura, E.B., J. Turkson, and R. Jove. 2005. Mechanisms of disease: Insights into the emerging role of signal transducers and activators of transcription in cancer. *Nat Clin Pract Oncol*. 2:315-324.

He, C., M. Hobert, L. Friend, and C. Carlin. 2002. The epidermal growth factor receptor juxtamembrane domain has multiple basolateral plasma membrane localization determinants, including a dominant signal with a polyproline core. *Journal of Biological Chemistry*. 277:38284-38293.

Hill, R.J., and P.W. Sternberg. 1992. The gene lin-3 encodes an inductive signal for vulval development in C. elegans. *Nature*. 358:470-476.

Hopper, N.A., J. Lee, and P.W. Sternberg. 2000. ARK-1 inhibits EGFR signaling in C. elegans. *Mol Cell*. 6:65-75.

Horgan, C.P., and M.W. McCaffrey. 2011. Rab GTPases and microtubule motors. *Biochem Soc Trans*. 39:1202-1206.

Horvitz, H.R., S. Brenner, J. Hodgkin, and R.K. Herman. 1979. A uniform genetic nomenclature for the nematode Caenorhabditis elegans. *Mol Gen Genet*. 175:129-133.

Huang, F., D. Kirkpatrick, X. Jiang, S. Gygi, and A. Sorkin. 2006. Differential regulation of EGF receptor internalization and degradation by multiubiquitination within the kinase domain. *Mol Cell*. 21:737-748.

Huang, F., X. Zeng, W. Kim, M. Balasubramani, A. Fortian, S.P. Gygi, N.A. Yates, and A. Sorkin. 2013. Lysine 63-linked polyubiquitination is required for EGF receptor degradation. *Proc Natl Acad Sci U S A*. 110:15722-15727.

Hubbard, S.R. 2004. Juxtamembrane autoinhibition in receptor tyrosine kinases. *Nat Rev Mol Cell Biol*. 5:464-471.

Hunt, S.D., and D.J. Stephens. 2011. The role of motor proteins in endosomal sorting. *Biochem Soc Trans*. 39:1179-1184.

Hunziker, W., and C. Fumey. 1994. A di-leucine motif mediates endocytosis and basolateral sorting of macrophage IgG Fc receptors in MDCK cells. *EMBO J*. 13:2963-2969.

Hunziker, W., C. Harter, K. Matter, and I. Mellman. 1991. Basolateral Sorting in Mdck Cells Requires a Distinct Cytoplasmic Domain Determinant. *Cell*. 66:907-920.

Hurley, J.H., and S.D. Emr. 2006. The ESCRT complexes: structure and mechanism of a membrane-trafficking network. *Annu Rev Biophys Biomol Struct*. 35:277-298.

Hwang, B.J., and P.W. Sternberg. 2004. A cell-specific enhancer that specifies lin-3 expression in the C. elegans anchor cell for vulval development. *Development*. 131:143-151.

Hynes, N.E., K. Horsch, M.A. Olayioye, and A. Badache. 2001a. The ErbB receptor tyrosine family as signal integrators. *Endocr Relat Cancer*. 8:151-159.

Hynes, N.E., K. Horsch, M.A. Olayioye, and A. Badache. 2001b. The ErbB receptor tyrosine family as signal integrators. *Endocr-Relat Cancer*. 8:151-159.
Ishizaki, R., H.W. Shin, H. Mitsuhashi, and K. Nakayama. 2008. Redundant roles of BIG2 and BIG1, guanine-nucleotide exchange factors for ADP-ribosylation factors in membrane traffic between the trans-Golgi network and endosomes. *Mol Biol Cell*. 19:2650-2660.
Iwakura, Y., and H. Nawa. 2013. ErbB1-4-dependent EGF/neuregulin signals and their cross talk in the central nervous system: pathological implications in schizophrenia and Parkinson's disease. *Front Cell Neurosci*. 7:4.
Iyadurai, S.J., J.T. Robinson, L. Ma, Y. He, S. Mische, M.G. Li, W. Brown, A. Guichard, E. Bier, and T.S. Hays. 2008. Dynein and Star interact in EGFR signaling and ligand trafficking. *J Cell Sci*. 121:2643-2651.
Jacobs, D., G.J. Beitel, S.G. Clark, H.R. Horvitz, and K. Kornfeld. 1998. Gain-of-function mutations in the Caenorhabditis elegans lin-1 ETS gene identify a C-terminal regulatory domain phosphorylated by ERK MAP kinase. *Genetics*. 149:1809-1822.
Jiang, L.I., and P.W. Sternberg. 1998. Interactions of EGF, Wnt and HOM-C genes specify the P12 neuroectoblast fate in C. elegans. *Development*. 125:2337-2347.
Jiang, X., F. Huang, A. Marusyk, and A. Sorkin. 2003. Grb2 regulates internalization of EGF receptors through clathrin-coated pits. *Mol Biol Cell*. 14:858-870.
Johannessen, L.E., N.M. Pedersen, K.W. Pedersen, I.H. Madshus, and E. Stang. 2006. Activation of the epidermal growth factor (EGF) receptor induces formation of EGF receptor- and Grb2-containing clathrin-coated pits. *Mol Cell Biol*. 26:389-401.
Johansson, M., N. Rocha, W. Zwart, I. Jordens, L. Janssen, C. Kuijl, V.M. Olkkonen, and J. Neefjes. 2007. Activation of endosomal dynein motors by stepwise assembly of Rab7-RILP-p150Glued, ORP1L, and the receptor betalll spectrin. *J Cell Biol*. 176:459-471.
Johnson, S.M., H. Grosshans, J. Shingara, M. Byrom, R. Jarvis, A. Cheng, E. Labourier, K.L. Reinert, D. Brown, and F.J. Slack. 2005. RAS is regulated by the let-7 microRNA family. *Cell*. 120:635-647.
Jongeward, G.D., T.R. Clandinin, and P.W. Sternberg. 1995. sli-1, a negative regulator of let-23-mediated signaling in C. elegans. *Genetics*. 139:1553-1566.
Kachur, T.M., A. Audhya, and D.B. Pilgrim. 2008. UNC-45 is required for NMY-2 contractile function in early embryonic polarity establishment and germline cellularization in C. elegans. *Dev Biol*. 314:287-299.
Kaech, S.M., C.W. Whitfield, and S.K. Kim. 1998. The LIN-2/LIN-7/LIN-10 complex mediates basolateral membrane localization of the C. elegans EGF receptor LET-23 in vulval epithelial cells. *Cell*. 94:761-771.
Kahn, R.A., J. Cherfils, M. Elias, R.C. Lovering, S. Munro, and A. Schurmann. 2006. Nomenclature for the human Arf family of GTP-binding proteins: ARF, ARL, and SAR proteins. *J Cell Biol*. 172:645-650.
Kamath, R.S., M. Martinez-Campos, P. Zipperlen, A.G. Fraser, and J. Ahringer. 2001. Effectiveness of specific RNA-mediated interference through ingested double-stranded RNA in Caenorhabditis elegans. *Genome Biol*. 2:RESEARCH0002.
Karnoub, A.E., and R.A. Weinberg. 2008. Ras oncogenes: split personalities. *Nat Rev Mol Cell Biol*. 9:517-531.
Katoh, K., K. Misawa, K. Kuma, and T. Miyata. 2002. MAFFT: a novel method for rapid multiple sequence alignment based on fast Fourier transform. *Nucleic Acids Res*. 30:3059-3066.

Kemphues, K.J., J.R. Priess, D.G. Morton, and N.S. Cheng. 1988. Identification of genes required for cytoplasmic localization in early C. elegans embryos. *Cell*. 52:311-320.
Kim, S.K. 1997. Polarized signaling: basolateral receptor localization in epithelial cells by PDZ-containing proteins. *Current Opinion in Cell Biology*. 9:853-859.
Kimble, J. 1981. Alterations in cell lineage following laser ablation of cells in the somatic gonad of Caenorhabditis elegans. *Dev Biol*. 87:286-300.
Kitagawa, Y., Y. Sano, M. Ueda, K. Higashio, H. Narita, M. Okano, S. Matsumoto, and R. Sasaki. 1994. N-glycosylation of erythropoietin is critical for apical secretion by Madin-Darby canine kidney cells. *Exp Cell Res*. 213:449-457.
Klapper, L.N., S. Glathe, N. Vaisman, N.E. Hynes, G.C. Andrews, M. Sela, and Y. Yarden. 1999. The ErbB-2/HER2 oncoprotein of human carcinomas may function solely as a shared coreceptor for multiple stroma-derived growth factors. *Proc Natl Acad Sci U S A*. 96:4995-5000.
Koivisto, U.M., A.L. Hubbard, and I. Mellman. 2001. A novel cellular phenotype for familial hypercholesterolemia due to a defect in polarized targeting of LDL receptor. *Cell*. 105:575-585.
Koppen, M., J.S. Simske, P.A. Sims, B.L. Firestein, D.H. Hall, A.D. Radice, C. Rongo, and J.D. Hardin. 2001. Cooperative regulation of AJM-1 controls junctional integrity in Caenorhabditis elegans epithelia. *Nat Cell Biol*. 3:983-991.
Kreitzer, G., J. Schmoranzer, S.H. Low, X. Li, Y. Gan, T. Weimbs, S.M. Simon, and E. Rodriguez-Boulan. 2003. Three-dimensional analysis of post-Golgi carrier exocytosis in epithelial cells. *Nat Cell Biol*. 5:126-136.
Kritikou, E.A., S. Milstein, P.O. Vidalain, G. Lettre, E. Bogan, K. Doukoumetzidis, P. Gray, T.G. Chappell, M. Vidal, and M.O. Hengartner. 2006. C. elegans GLA-3 is a novel component of the MAP kinase MPK-1 signaling pathway required for germ cell survival. *Genes Dev*. 20:2279-2292.
Kroschewski, R., A. Hall, and I. Mellman. 1999. Cdc42 controls secretory and endocytic transport to the basolateral plasma membrane of MDCK cells. *Nat Cell Biol*. 1:8-13.
Kuan, C.T., C.J. Wikstrand, and D.D. Bigner. 2001. EGF mutant receptor vIII as a molecular target in cancer therapy. *Endocr Relat Cancer*. 8:83-96.
LaConte, L., and K. Mukherjee. 2013. Structural constraints and functional divergences in CASK evolution. *Biochem Soc Trans*. 41:1017-1022.
Lafky, J.M., J.A. Wilken, A.T. Baron, and N.J. Maihle. 2008. Clinical implications of the ErbB/epidermal growth factor (EGF) receptor family and its ligands in ovarian cancer. *Biochim Biophys Acta*. 1785:232-265.
Lakkaraju, A., and E. Rodriguez-Boulan. 2008. Itinerant exosomes: emerging roles in cell and tissue polarity. *Trends Cell Biol*. 18:199-209.
Lapierre, L.A., M.C. Dorn, C.F. Zimmerman, J. Navarre, J.O. Burnette, and J.R. Goldenring. 2003. Rab11b resides in a vesicular compartment distinct from Rab11a in parietal cells and other epithelial cells. *Exp Cell Res*. 290:322-331.
Lapierre, L.A., R. Kumar, C.M. Hales, J. Navarre, S.G. Bhartur, J.O. Burnette, D.W. Provance, Jr., J.A. Mercer, M. Bahler, and J.R. Goldenring. 2001. Myosin vb is associated with plasma membrane recycling systems. *Mol Biol Cell*. 12:1843-1857.
Lee, J., G.D. Jongeward, and P.W. Sternberg. 1994. unc-101, a gene required for many aspects of Caenorhabditis elegans development and behavior, encodes a clathrin-associated protein. *Genes Dev*. 8:60-73.

Lee, J.C., I. Vivanco, R. Beroukhim, J.H.Y. Huang, W.L. Feng, R.M. DeBiasi, K. Yoshimoto, J.C. King, P. Nghiemphu, Y. Yuza, Q. Xu, H. Greulich, R.K. Thomas, J.G. Paez, T.C. Peck, D.J. Linhart, K.A. Glatt, G. Getz, R. Onofrio, L. Ziaugra, R.L. Levine, S. Gabriel, T. Kawaguchi, K. O'Neill, H. Khan, L.M. Liau, S.F. Nelson, P.N. Rao, P. Mischel, R.O. Pieper, T. Cloughesy, D.J. Leahy, W.R. Sellers, C.L. Sawyers, M. Meyerson, and I.K. Mellinghoff. 2006a. Epidermal growth factor receptor activation in glioblastoma through novel missense mutations in the extracellular domain. *Plos Med*. 3:2264-2273.

Lee, M.H., B. Hook, L.B. Lamont, M. Wickens, and J. Kimble. 2006b. LIP-1 phosphatase controls the extent of germline proliferation in Caenorhabditis elegans. *EMBO J*. 25:88-96.

Lee, M.H., M. Ohmachi, S. Arur, S. Nayak, R. Francis, D. Church, E. Lambie, and T. Schedl. 2007. Multiple functions and dynamic activation of MPK-1 extracellular signal-regulated kinase signaling in Caenorhabditis elegans germline development. *Genetics*. 177:2039-2062.

Lemmon, M.A., and J. Schlessinger. 2010. Cell signaling by receptor tyrosine kinases. *Cell*. 141:1117-1134.

Leonoudakis, D., L.R. Conti, C.M. Radeke, L.M. McGuire, and C.A. Vandenberg. 2004. A multiprotein trafficking complex composed of SAP97, CASK, Veli, and Mint1 is associated with inward rectifier Kir2 potassium channels. *J Biol Chem*. 279:19051-19063.

Lerner, D.W., D. McCoy, A.J. Isabella, A.P. Mahowald, G.F. Gerlach, T.A. Chaudhry, and S. Horne-Badovinac. 2013. A Rab10-dependent mechanism for polarized basement membrane secretion during organ morphogenesis. *Dev Cell*. 24:159-168.

Levkowitz, G., H. Waterman, S.A. Ettenberg, M. Katz, A.Y. Tsygankov, I. Alroy, S. Lavi, K. Iwai, Y. Reiss, A. Ciechanover, S. Lipkowitz, and Y. Yarden. 1999. Ubiquitin ligase activity and tyrosine phosphorylation underlie suppression of growth factor signaling by c-Cbl/Sli-1. *Mol Cell*. 4:1029-1040.

Li, R., and G.G. Gundersen. 2008. Beyond polymer polarity: how the cytoskeleton builds a polarized cell. *Nat Rev Mol Cell Biol*. 9:860-873.

Li, W., M. Han, and K.L. Guan. 2000. The leucine-rich repeat protein SUR-8 enhances MAP kinase activation and forms a complex with Ras and Raf. *Genes Dev*. 14:895-900.

Lin, S., H.Y. Naim, A.C. Rodriguez, and M.G. Roth. 1998. Mutations in the middle of the transmembrane domain reverse the polarity of transport of the influenza virus hemagglutinin in MDCK epithelial cells. *J Cell Biol*. 142:51-57.

Lipardi, C., L. Nitsch, and C. Zurzolo. 2000. Detergent-insoluble GPI-anchored proteins are apically sorted in fischer rat thyroid cells, but interference with cholesterol or sphingolipids differentially affects detergent insolubility and apical sorting. *Mol Biol Cell*. 11:531-542.

Lisanti, M.P., I.W. Caras, M.A. Davitz, and E. Rodriguez-Boulan. 1989. A glycophospholipid membrane anchor acts as an apical targeting signal in polarized epithelial cells. *J Cell Biol*. 109:2145-2156.

Lisanti, M.P., M. Sargiacomo, L. Graeve, A.R. Saltiel, and E. Rodriguez-Boulan. 1988. Polarized apical distribution of glycosyl-phosphatidylinositol-anchored proteins in a renal epithelial cell line. *Proc Natl Acad Sci U S A*. 85:9557-9561.

Liu, J., W. Lu, D. Reigada, J. Nguyen, A.M. Laties, and C.H. Mitchell. 2008. Restoration of lysosomal pH in RPE cells from cultured human and ABCA4(-/-) mice: Pharmacologic approaches and functional recovery. *Invest Ophth Vis Sci*. 49:772-780.

Liu, O., and B.D. Grant. 2015. Basolateral Endocytic Recycling Requires RAB-10 and AMPH-1 Mediated Recruitment of RAB-5 GAP TBC-2 to Endosomes. *PLoS Genet*. 11:e1005514.

Liu, S.H., W.I. Chou, S.C. Lin, C.C. Sheu, and M.D. Chang. 2005. Molecular genetic manipulation of Pichia pastoris SEC4 governs cell growth and glucoamylase secretion. *Biochem Biophys Res Commun*. 336:1172-1180.

Lock, J.G., and J.L. Stow. 2005. Rab11 in recycling endosomes regulates the sorting and basolateral transport of E-cadherin. *Mol Biol Cell*. 16:1744-1755.

Lovrecic, L., I. Slavkov, S. Dzeroski, and B. Peterlin. 2010. ADP-ribosylation factor guanine nucleotide-exchange factor 2 (ARFGEF2): a new potential biomarker in Huntington's disease. *J Int Med Res*. 38:1653-1662.

Lowery, J., T. Szul, M. Styers, Z. Holloway, V. Oorschot, J. Klumperman, and E. Sztul. 2013. The Sec7 guanine nucleotide exchange factor GBF1 regulates membrane recruitment of BIG1 and BIG2 guanine nucleotide exchange factors to the trans-Golgi network (TGN). *J Biol Chem*. 288:11532-11545.

Lu, A., F. Tebar, B. Alvarez-Moya, C. Lopez-Alcala, M. Calvo, C. Enrich, N. Agell, T. Nakamura, M. Matsuda, and O. Bachs. 2009. A clathrin-dependent pathway leads to KRas signaling on late endosomes en route to lysosomes. *J Cell Biol*. 184:863-879.

Lu, X., and H.R. Horvitz. 1998. lin-35 and lin-53, two genes that antagonize a C. elegans Ras pathway, encode proteins similar to Rb and its binding protein RbAp48. *Cell*. 95:981-991.

Lye, R.J., R.K. Wilson, and R.H. Waterston. 1995. Genomic structure of a cytoplasmic dynein heavy chain gene from the nematode Caenorhabditis elegans. *Cell motility and the cytoskeleton*. 32:26-36.

Maday, S., E. Anderson, H.C. Chang, J. Shorter, A. Satoh, J. Sfakianos, H. Folsch, J.M. Anderson, Z. Walther, and I. Mellman. 2008. A PDZ-binding motif controls basolateral targeting of syndecan-1 along the biosynthetic pathway in polarized epithelial cells. *Traffic*. 9:1915-1924.

Malerod, L., S. Stuffers, A. Brech, and H. Stenmark. 2007. Vps22/EAP30 in ESCRT-II mediates endosomal sorting of growth factor and chemokine receptors destined for lysosomal degradation. *Traffic*. 8:1617-1629.

Manolea, F., A. Claude, J. Chun, J. Rosas, and P. Melancon. 2008. Distinct functions for Arf guanine nucleotide exchange factors at the Golgi complex: GBF1 and BIGs are required for assembly and maintenance of the Golgi stack and trans-Golgi network, respectively. *Mol Biol Cell*. 19:523-535.

Matter, K., W. Hunziker, and I. Mellman. 1992. Basolateral Sorting of Ldl Receptor in Mdck Cells - the Cytoplasmic Domain Contains 2 Tyrosine-Dependent Targeting Determinants. *Cell*. 71:741-753.

Mattila, P.E., C.L. Kinlough, J.R. Bruns, O.A. Weisz, and R.P. Hughey. 2009. MUC1 traverses apical recycling endosomes along the biosynthetic pathway in polarized MDCK cells. *Biol Chem*. 390:551-556.

Mattoon, D.R., B. Lamothe, I. Lax, and J. Schlessinger. 2004. The docking protein Gab1 is the primary mediator of EGF-stimulated activation of the PI-3K/Akt cell survival pathway. *BMC Biol*. 2:24.

Mayor, S., J.F. Presley, and F.R. Maxfield. 1993. Sorting of membrane components from endosomes and subsequent recycling to the cell surface occurs by a bulk flow process. *J Cell Biol*. 121:1257-1269.
McCubrey, J.A., S.L. Abrams, T.L. Fitzgerald, L. Cocco, A.M. Martelli, G. Montalto, M. Cervello, A. Scalisi, S. Candido, M. Libra, and L.S. Steelman. 2015. Roles of signaling pathways in drug resistance, cancer initiating cells and cancer progression and metastasis. *Adv Biol Regul*. 57:75-101.
McDonold, C.M., and J.C. Fromme. 2014. Four GTPases differentially regulate the Sec7 Arf-GEF to direct traffic at the trans-golgi network. *Dev Cell*. 30:759-767.
Miaczynska, M., S. Christoforidis, A. Giner, A. Shevchenko, S. Uttenweiler-Joseph, B. Habermann, M. Wilm, R.G. Parton, and M. Zerial. 2004. APPL proteins link Rab5 to nuclear signal transduction via an endosomal compartment. *Cell*. 116:445-456.
Miaczynska, M., and M. Zerial. 2002. Mosaic organization of the endocytic pathway. *Exp Cell Res*. 272:8-14.
Morinaga, N., S.C. Tsai, J. Moss, and M. Vaughan. 1996. Isolation of a brefeldin A-inhibited guanine nucleotide-exchange protein for ADP ribosylation factor (ARF) 1 and ARF3 that contains a Sec7-like domain. *Proc Natl Acad Sci U S A*. 93:12856-12860.
Muller, J., S. Ory, T. Copeland, H. Piwnica-Worms, and D.K. Morrison. 2001. C-TAK1 regulates Ras signaling by phosphorylating the MAPK scaffold, KSR1. *Mol Cell*. 8:983-993.
Musch, A. 2004. Microtubule organization and function in epithelial cells. *Traffic*. 5:1-9.
Musch, A., D. Cohen, and E. Rodriguez-Boulan. 1997. Myosin II is involved in the production of constitutive transport vesicles from the TGN. *J Cell Biol*. 138:291-306.
Muth, T.R., and M.J. Caplan. 2003. Transport protein trafficking in polarized cells. *Annu Rev Cell Dev Biol*. 19:333-366.
Myers, T.R., and I. Greenwald. 2005. lin-35 Rb acts in the major hypodermis to oppose ras-mediated vulval induction in C. elegans. *Dev Cell*. 8:117-123.
Nelson, F.K., P.S. Albert, and D.L. Riddle. 1983. Fine structure of the Caenorhabditis elegans secretory-excretory system. *J Ultrastruct Res*. 82:156-171.
Nelson, F.K., and D.L. Riddle. 1984. Functional study of the Caenorhabditis elegans secretory-excretory system using laser microsurgery. *J Exp Zool*. 231:45-56.
Nicholson, R.I., J.M. Gee, and M.E. Harper. 2001. EGFR and cancer prognosis. *Eur J Cancer*. 37 Suppl 4:S9-15.
Nickerson, D.P., M.R. Russell, and G. Odorizzi. 2007. A concentric circle model of multivesicular body cargo sorting. *EMBO Rep*. 8:644-650.
Nishimura, Y., B. Bereczky, and M. Ono. 2007. The EGFR inhibitor gefitinib suppresses ligand-stimulated endocytosis of EGFR via the early/late endocytic pathway in non-small cell lung cancer cell lines. *Histochemistry and Cell Biology*. 127:541-553.
Nislow, C., V.A. Lombillo, R. Kuriyama, and J.R. McIntosh. 1992. A plus-end-directed motor enzyme that moves antiparallel microtubules in vitro localizes to the interzone of mitotic spindles. *Nature*. 359:543-547.
Noda, Y., Y. Okada, N. Saito, M. Setou, Y. Xu, Z. Zhang, and N. Hirokawa. 2001. KIFC3, a microtubule minus end-directed motor for the apical transport of annexin XIIIb-associated Triton-insoluble membranes. *J Cell Biol*. 155:77-88.

Normanno, N., A. De Luca, C. Bianco, L. Strizzi, M. Mancino, M.R. Maiello, A. Carotenuto, G. De Feo, F. Caponigro, and D.S. Salomon. 2006. Epidermal growth factor receptor (EGFR) signaling in cancer. *Gene*. 366:2-16.

O'Rourke, S.M., M.D. Dorfman, J.C. Carter, and B. Bowerman. 2007. Dynein modifiers in C. elegans: light chains suppress conditional heavy chain mutants. *PLoS Genet*. 3:e128.

Ohmachi, M., C.E. Rocheleau, D. Church, E. Lambie, T. Schedl, and M.V. Sundaram. 2002. C. elegans ksr-1 and ksr-2 have both unique and redundant functions and are required for MPK-1 ERK phosphorylation. *Curr Biol*. 12:427-433.

Okamoto, I., L.C. Kenyon, D.R. Emlet, T. Mori, J. Sasaki, S. Hirosako, Y. Ichikawa, H. Kishi, A.K. Godwin, M. Yoshioka, M. Suga, M. Matsumoto, and A.J. Wong. 2003. Expression of constitutively activated EGFRvIII in non-small cell lung cancer. *Cancer Sci*. 94:50-56.

Olapade-Olaopa, E.O., D.K. Moscatello, E.H. MacKay, T. Horsburgh, D.P. Sandhu, T.R. Terry, A.J. Wong, and F.K. Habib. 2000. Evidence for the differential expression of a variant EGF receptor protein in human prostate cancer. *Br J Cancer*. 82:186-194.

Olayioye, M.A., R.M. Neve, H.A. Lane, and N.E. Hynes. 2000. The ErbB signaling network: receptor heterodimerization in development and cancer. *EMBO J*. 19:3159-3167.

Olsen, O., J.B. Wade, N. Morin, D.S. Bredt, and P.A. Welling. 2005. Differential localization of mammalian Lin-7 (MALS/Veli) PDZ proteins in the kidney. *Am J Physiol Renal Physiol*. 288:F345-352.

Orlando, K., and W. Guo. 2009. Membrane organization and dynamics in cell polarity. *Cold Spring Harb Perspect Biol*. 1:a001321.

Paez, J.G., P.A. Janne, J.C. Lee, S. Tracy, H. Greulich, S. Gabriel, P. Herman, F.J. Kaye, N. Lindeman, T.J. Boggon, K. Naoki, H. Sasaki, Y. Fujii, M.J. Eck, W.R. Sellers, B.E. Johnson, and M. Meyerson. 2004. EGFR mutations in lung cancer: Correlation with clinical response to gefitinib therapy. *Science*. 304:1497-1500.

Paladino, S., D. Sarnataro, R. Pillich, S. Tivodar, L. Nitsch, and C. Zurzolo. 2004. Protein oligomerization modulates raft partitioning and apical sorting of GPI-anchored proteins. *J Cell Biol*. 167:699-709.

Peschard, P., and M. Park. 2003. Escape from Cbl-mediated downregulation: a recurrent theme for oncogenic deregulation of receptor tyrosine kinases. *Cancer Cell*. 3:519-523.

Platta, H.W., and H. Stenmark. 2011. Endocytosis and signaling. *Curr Opin Cell Biol*. 23:393-403.

Polo, S., S. Pece, and P.P. Di Fiore. 2004. Endocytosis and cancer. *Curr Opin Cell Biol*. 16:156-161.

Portereiko, M.F., J. Saam, and S.E. Mango. 2004. ZEN-4/MKLP1 is required to polarize the foregut epithelium. *Curr Biol*. 14:932-941.

Prigent, S.A., and W.J. Gullick. 1994. Identification of c-erbB-3 binding sites for phosphatidylinositol 3'-kinase and SHC using an EGF receptor/c-erbB-3 chimera. *EMBO J*. 13:2831-2841.

Qadota, H., M. Inoue, T. Hikita, M. Koppen, J.D. Hardin, M. Amano, D.G. Moerman, and K. Kaibuchi. 2007. Establishment of a tissue-specific RNAi system in C. elegans. *Gene*. 400:166-173.

Rafael, J.A., T.L. Hutchinson, C.N. Lumeng, S.M. Marfatia, A.H. Chishti, and J.S. Chamberlain. 1998. Localization of Dlg at the mammalian neuromuscular junction. *Neuroreport*. 9:2121-2125.

Raiborg, C., L. Malerod, N.M. Pedersen, and H. Stenmark. 2008. Differential functions of Hrs and ESCRT proteins in endocytic membrane trafficking. *Exp Cell Res*. 314:801-813.
Raich, W.B., A.N. Moran, J.H. Rothman, and J. Hardin. 1998. Cytokinesis and midzone microtubule organization in Caenorhabditis elegans require the kinesin-like protein ZEN-4. *Mol Biol Cell*. 9:2037-2049.
Real, P.J., A. Sierra, A. De Juan, J.C. Segovia, J.M. Lopez-Vega, and J.L. Fernandez-Luna. 2002. Resistance to chemotherapy via Stat3-dependent overexpression of Bcl-2 in metastatic breast cancer cells. *Oncogene*. 21:7611-7618.
Regad, T. 2015. Targeting RTK Signaling Pathways in Cancer. *Cancers (Basel)*. 7:1758-1784.
Richardson, B.C., C.M. McDonold, and J.C. Fromme. 2012. The Sec7 Arf-GEF is recruited to the trans-Golgi network by positive feedback. *Dev Cell*. 22:799-810.
Riddle, D.L., T. Blumenthal, B.J. Meyer, and J.R. Priess. 1997. Introduction to C. elegans. *In* C. elegans II. D.L. Riddle, T. Blumenthal, B.J. Meyer, and J.R. Priess, editors, Cold Spring Harbor (NY).
Rink, J., E. Ghigo, Y. Kalaidzidis, and M. Zerial. 2005. Rab conversion as a mechanism of progression from early to late endosomes. *Cell*. 122:735-749.
Roberts, A.J., T. Kon, P.J. Knight, K. Sutoh, and S.A. Burgess. 2013. Functions and mechanics of dynein motor proteins. *Nat Rev Mol Cell Biol*. 14:713-726.
Robinson, M.S. 2004. Adaptable adaptors for coated vesicles. *Trends Cell Biol*. 14:167-174.
Rocheleau, C.E., A. Ronnlund, S. Tuck, and M.V. Sundaram. 2005. Caenorhabditis elegans CNK-1 promotes Raf activation but is not essential for Ras/Raf signaling. *Proc Natl Acad Sci U S A*. 102:11757-11762.
Rodriguez-Boulan, E., and A. Gonzalez. 1999. Glycans in post-Golgi apical targeting: sorting signals or structural props? *Trends Cell Biol*. 9:291-294.
Rodriguez-Boulan, E., G. Kreitzer, and A. Musch. 2005. Organization of vesicular trafficking in epithelia. *Nat Rev Mol Cell Biol*. 6:233-247.
Rodriguez-Boulan, E., and I.G. Macara. 2014. Organization and execution of the epithelial polarity programme. *Nat Rev Mol Cell Biol*. 15:225-242.
Roepstorff, K., M.V. Grandal, L. Henriksen, S.L. Knudsen, M. Lerdrup, L. Grovdal, B.M. Willumsen, and B. van Deurs. 2009. Differential effects of EGFR ligands on endocytic sorting of the receptor. *Traffic*. 10:1115-1127.
Roepstorff, K., L. Grovdal, M. Grandal, M. Lerdrup, and B. van Deurs. 2008. Endocytic downregulation of ErbB receptors: mechanisms and relevance in cancer. *Histochem Cell Biol*. 129:563-578.
Ruemmele, F.M., T. Muller, N. Schiefermeier, H.L. Ebner, S. Lechner, K. Pfaller, C.E. Thoni, O. Goulet, F. Lacaille, J. Schmitz, V. Colomb, F. Sauvat, Y. Revillon, D. Canioni, N. Brousse, G. de Saint-Basile, J. Lefebvre, P. Heinz-Erian, A. Enninger, G. Utermann, M.W. Hess, A.R. Janecke, and L.A. Huber. 2010. Loss-of-function of MYO5B is the main cause of microvillus inclusion disease: 15 novel mutations and a CaCo-2 RNAi cell model. *Hum Mutat*. 31:544-551.
Ryan, S., S. Verghese, N.L. Cianciola, C.U. Cotton, and C.R. Carlin. 2010. Autosomal Recessive Polycystic Kidney Disease Epithelial Cell Model Reveals Multiple Basolateral Epidermal Growth Factor Receptor Sorting Pathways. *Molecular Biology of the Cell*. 21:2732-2745.
Saftig, P., and J. Klumperman. 2009. Lysosome biogenesis and lysosomal membrane proteins: trafficking meets function. *Nat Rev Mol Cell Biol*. 10:623-635.

Sato, K., M. Sato, A. Audhya, K. Oegema, P. Schweinsberg, and B.D. Grant. 2006. Dynamic regulation of caveolin-1 trafficking in the germ line and embryo of Caenorhabditis elegans. *Mol Biol Cell*. 17:3085-3094.

Scaltriti, M., and J. Baselga. 2006. The epidermal growth factor receptor pathway: a model for targeted therapy. *Clin Cancer Res*. 12:5268-5272.

Scheiffele, P., J. Peranen, and K. Simons. 1995. N-glycans as apical sorting signals in epithelial cells. *Nature*. 378:96-98.

Schenck, A., L. Goto-Silva, C. Collinet, M. Rhinn, A. Giner, B. Habermann, M. Brand, and M. Zerial. 2008. The endosomal protein Appl1 mediates Akt substrate specificity and cell survival in vertebrate development. *Cell*. 133:486-497.

Schindelin, J., I. Arganda-Carreras, E. Frise, V. Kaynig, M. Longair, T. Pietzsch, S. Preibisch, C. Rueden, S. Saalfeld, B. Schmid, J.Y. Tinevez, D.J. White, V. Hartenstein, K. Eliceiri, P. Tomancak, and A. Cardona. 2012. Fiji: an open-source platform for biological-image analysis. *Nat Methods*. 9:676-682.

Schlessinger, J. 2000. Cell signaling by receptor tyrosine kinases. *Cell*. 103:211-225.

Schmid, T., and A. Hajnal. 2015. Signal transduction during C. elegans vulval development: a NeverEnding story. *Curr Opin Genet Dev*. 32:1-9.

Schmidt, D.J., D.J. Rose, W.M. Saxton, and S. Strome. 2005. Functional analysis of cytoplasmic dynein heavy chain in Caenorhabditis elegans with fast-acting temperature-sensitive mutations. *Mol Biol Cell*. 16:1200-1212.

Schouest, K.R., Y. Kurasawa, T. Furuta, N. Hisamoto, K. Matsumoto, and J.M. Schumacher. 2009. The germinal center kinase GCK-1 is a negative regulator of MAP kinase activation and apoptosis in the C. elegans germline. *PLoS One*. 4:e7450.

Schuck, S., M.J. Gerl, A. Ang, A. Manninen, P. Keller, I. Mellman, and K. Simons. 2007. Rab10 is involved in basolateral transport in polarized Madin-Darby canine kidney cells. *Traffic*. 8:47-60.

Setou, M., T. Nakagawa, D.H. Seog, and N. Hirokawa. 2000. Kinesin superfamily motor protein KIF17 and mLin-10 in NMDA receptor-containing vesicle transport. *Science*. 288:1796-1802.

Shafaq-Zadah, M., L. Brocard, F. Solari, and G. Michaux. 2012. AP-1 is required for the maintenance of apico-basal polarity in the C. elegans intestine. *Development*. 139:2061-2070.

Shan, Y., M.P. Eastwood, X. Zhang, E.T. Kim, A. Arkhipov, R.O. Dror, J. Jumper, J. Kuriyan, and D.E. Shaw. 2012. Oncogenic mutations counteract intrinsic disorder in the EGFR kinase and promote receptor dimerization. *Cell*. 149:860-870.

Shaye, D.D., and I. Greenwald. 2002. Endocytosis-mediated downregulation of LIN-12/Notch upon Ras activation in Caenorhabditis elegans. *Nature*. 420:686-690.

Sheff, D.R., E.A. Daro, M. Hull, and I. Mellman. 1999. The receptor recycling pathway contains two distinct populations of early endosomes with different sorting functions. *Journal of Cell Biology*. 145:123-139.

Sheff, D.R., R. Kroschewski, and I. Mellman. 2002. Actin dependence of polarized receptor recycling in Madin-Darby canine kidney cell endosomes. *Mol Biol Cell*. 13:262-275.

Shelly, M., Y. Mosesson, A. Citri, S. Lavi, Y. Zwang, N. Melamed-Book, B. Aroeti, and Y. Yarden. 2003. Polar expression of ErbB-2/HER2 in epithelia. Bimodal regulation by Lin-7. *Dev Cell*. 5:475-486.

Sheng, M. 1996. PDZs and receptor/channel clustering: rounding up the latest suspects. *Neuron*. 17:575-578.
Shibatohge, M., K. Kariya, Y. Liao, C.D. Hu, Y. Watari, M. Goshima, F. Shima, and T. Kataoka. 1998. Identification of PLC210, a Caenorhabditis elegans phospholipase C, as a putative effector of Ras. *J Biol Chem*. 273:6218-6222.
Shim, J., P.W. Sternberg, and J. Lee. 2000. Distinct and redundant functions of mu1 medium chains of the AP-1 clathrin-associated protein complex in the nematode Caenorhabditis elegans. *Mol Biol Cell*. 11:2743-2756.
Siddiqui, S.S. 2002. Metazoan motor models: kinesin superfamily in C. elegans. *Traffic*. 3:20-28.
Sieburth, D.S., Q. Sun, and M. Han. 1998. SUR-8, a conserved Ras-binding protein with leucine-rich repeats, positively regulates Ras-mediated signaling in C. elegans. *Cell*. 94:119-130.
Sigismund, S., E. Argenzio, D. Tosoni, E. Cavallaro, S. Polo, and P.P. Di Fiore. 2008. Clathrin-mediated internalization is essential for sustained EGFR signaling but dispensable for degradation. *Dev Cell*. 15:209-219.
Sigismund, S., T. Woelk, C. Puri, E. Maspero, C. Tacchetti, P. Transidico, P.P. Di Fiore, and S. Polo. 2005. Clathrin-independent endocytosis of ubiquitinated cargos. *Proc Natl Acad Sci U S A*. 102:2760-2765.
Simons, K., and G. van Meer. 1988. Lipid sorting in epithelial cells. *Biochemistry*. 27:6197-6202.
Simske, J.S., S.M. Kaech, S.A. Harp, and S.K. Kim. 1996. LET-23 receptor localization by the cell junction protein LIN-7 during C-elegans vulval induction. *Cell*. 85:195-204.
Simske, J.S., and S.K. Kim. 1995. Sequential signalling during Caenorhabditis elegans vulval induction. *Nature*. 375:142-146.
Simske, J.S., M. Koppen, P. Sims, J. Hodgkin, A. Yonkof, and J. Hardin. 2003. The cell junction protein VAB-9 regulates adhesion and epidermal morphology in C. elegans. *Nat Cell Biol*. 5:619-625.
Singh, B., G. Bogatcheva, M.K. Washington, and R.J. Coffey. 2013. Transformation of polarized epithelial cells by apical mistrafficking of epiregulin. *Proc Natl Acad Sci U S A*. 110:8960-8965.
Skorobogata, O., J.M. Escobar-Restrepo, and C.E. Rocheleau. 2014. An AGEF-1/Arf GTPase/AP-1 ensemble antagonizes LET-23 EGFR basolateral localization and signaling during C. elegans vulva induction. *PLoS Genet*. 10:e1004728.
Skorobogata, O., and C.E. Rocheleau. 2012. RAB-7 antagonizes LET-23 EGFR signaling during vulva development in Caenorhabditis elegans. *PLoS One*. 7:e36489.
Sonnichsen, B., S. De Renzis, E. Nielsen, J. Rietdorf, and M. Zerial. 2000. Distinct membrane domains on endosomes in the recycling pathway visualized by multicolor imaging of Rab4, Rab5, and Rab11. *J Cell Biol*. 149:901-914.
Sorkin, A., and G. Carpenter. 1991. Dimerization of internalized epidermal growth factor receptors. *J Biol Chem*. 266:23453-23460.
Sorkin, A., and L.K. Goh. 2008. Endocytosis and intracellular trafficking of ErbBs. *Exp Cell Res*. 314:3093-3106.
Sorkin, A., and L.K. Goh. 2009. Endocytosis and intracellular trafficking of ErbBs. *Exp Cell Res*. 315:683-696.
Sorkin, A., S. Krolenko, N. Kudrjavtceva, J. Lazebnik, L. Teslenko, A.M. Soderquist, and N. Nikolsky. 1991. Recycling of epidermal growth factor-receptor complexes in A431 cells: identification of dual pathways. *J Cell Biol*. 112:55-63.

Sorkin, A., and M. von Zastrow. 2009. Endocytosis and signalling: intertwining molecular networks. *Nat Rev Mol Cell Biol*. 10:609-622.
Sorkin, A.D., L.V. Teslenko, and N.N. Nikolsky. 1988. The endocytosis of epidermal growth factor in A431 cells: a pH of microenvironment and the dynamics of receptor complex dissociation. *Exp Cell Res*. 175:192-205.
Sousa, L.P., I. Lax, H. Shen, S.M. Ferguson, P. De Camilli, and J. Schlessinger. 2012. Suppression of EGFR endocytosis by dynamin depletion reveals that EGFR signaling occurs primarily at the plasma membrane. *Proc Natl Acad Sci U S A*. 109:4419-4424.
Stamnes, M.A., and J.E. Rothman. 1993. The binding of AP-1 clathrin adaptor particles to Golgi membranes requires ADP-ribosylation factor, a small GTP-binding protein. *Cell*. 73:999-1005.
Stang, E., F.D. Blystad, M. Kazazic, V. Bertelsen, T. Brodahl, C. Raiborg, H. Stenmark, and I.H. Madshus. 2004. Cbl-dependent ubiquitination is required for progression of EGF receptors into clathrin-coated pits. *Mol Biol Cell*. 15:3591-3604.
Starr, T.L., S. Pagant, C.W. Wang, and R. Schekman. 2012. Sorting signals that mediate traffic of chitin synthase III between the TGN/endosomes and to the plasma membrane in yeast. *PLoS One*. 7:e46386.
Stenmark, H. 2009. Rab GTPases as coordinators of vesicle traffic. *Nat Rev Mol Cell Biol*. 10:513-525.
Sternberg, P.W. 2005. Vulval development. *WormBook*:1-28.
Sternberg, P.W., and H.R. Horvitz. 1982. Postembryonic nongonadal cell lineages of the nematode Panagrellus redivivus: description and comparison with those of Caenorhabditis elegans. *Dev Biol*. 93:181-205.
Stetak, A., P. Gutierrez, and A. Hajnal. 2008. Tissue-specific functions of the Caenorhabditis elegans p120 Ras GTPase activating protein GAP-3. *Dev Biol*. 323:166-176.
Stetak, A., E.F. Hoier, A. Croce, G. Cassata, P.P. Di Fiore, and A. Hajnal. 2006. Cell fate-specific regulation of EGF receptor trafficking during Caenorhabditis elegans vulval development. *EMBO J*. 25:2347-2357.
Stoops, E.H., and M.J. Caplan. 2014. Trafficking to the apical and basolateral membranes in polarized epithelial cells. *J Am Soc Nephrol*. 25:1375-1386.
Sugawa, N., A.J. Ekstrand, C.D. James, and V.P. Collins. 1990. Identical splicing of aberrant epidermal growth factor receptor transcripts from amplified rearranged genes in human glioblastomas. *Proc Natl Acad Sci U S A*. 87:8602-8606.
Sulston, J.E., and H.R. Horvitz. 1977. Post-embryonic cell lineages of the nematode, Caenorhabditis elegans. *Dev Biol*. 56:110-156.
Sulston, J.E., and J.G. White. 1980. Regulation and cell autonomy during postembryonic development of Caenorhabditis elegans. *Dev Biol*. 78:577-597.
Sundaram, M., and M. Han. 1995. The C. elegans ksr-1 gene encodes a novel Raf-related kinase involved in Ras-mediated signal transduction. *Cell*. 83:889-901.
Sundaram, M.V. 2013. Canonical RTK-Ras-ERK signaling and related alternative pathways. *WormBook*:1-38.
Tabara, H., M. Sarkissian, W.G. Kelly, J. Fleenor, A. Grishok, L. Timmons, A. Fire, and C.C. Mello. 1999. The rde-1 gene, RNA interference, and transposon silencing in C. elegans. *Cell*. 99:123-132.

Tabish, M., Z.K. Siddiqui, K. Nishikawa, and S.S. Siddiqui. 1995. Exclusive expression of C. elegans osm-3 kinesin gene in chemosensory neurons open to the external environment. *J Mol Biol*. 247:377-389.

Taguchi, T. 2013. Emerging roles of recycling endosomes. *J Biochem*. 153:505-510.

Tai, A.W., J.Z. Chuang, C. Bode, U. Wolfrum, and C.H. Sung. 1999. Rhodopsin's carboxy-terminal cytoplasmic tail acts as a membrane receptor for cytoplasmic dynein by binding to the dynein light chain Tctex-1. *Cell*. 97:877-887.

Tall, R.D., M.A. Alonso, and M.G. Roth. 2003. Features of influenza HA required for apical sorting differ from those required for association with DRMs or MAL. *Traffic*. 4:838-849.

Tan, P.B., M.R. Lackner, and S.K. Kim. 1998. MAP kinase signaling specificity mediated by the LIN-1 Ets/LIN-31 WH transcription factor complex during C. elegans vulval induction. *Cell*. 93:569-580.

Tang, L., H. Fares, X. Zhao, W. Du, and B.F. Liu. 2012. Different endocytic functions of AGEF-1 in C. elegans coelomocytes. *Biochim Biophys Acta*. 1820:829-840.

Taub, N., D. Teis, H.L. Ebner, M.W. Hess, and L.A. Huber. 2007. Late endosomal traffic of the epidermal growth factor receptor ensures spatial and temporal fidelity of mitogen-activated protein kinase signaling. *Mol Biol Cell*. 18:4698-4710.

Teis, D., N. Taub, R. Kurzbauer, D. Hilber, M.E. de Araujo, M. Erlacher, M. Offterdinger, A. Villunger, S. Geley, G. Bohn, C. Klein, M.W. Hess, and L.A. Huber. 2006. p14-MP1-MEK1 signaling regulates endosomal traffic and cellular proliferation during tissue homeostasis. *J Cell Biol*. 175:861-868.

Tejedor, F.J., A. Bokhari, O. Rogero, M. Gorczyca, J. Zhang, E. Kim, M. Sheng, and V. Budnik. 1997. Essential role for dlg in synaptic clustering of Shaker K+ channels in vivo. *J Neurosci*. 17:152-159.

Thalappilly, S., P. Soubeyran, J.L. Iovanna, and N.J. Dusetti. 2010. VAV2 regulates epidermal growth factor receptor endocytosis and degradation. *Oncogene*. 29:2528-2539.

Togawa, A., N. Morinaga, M. Ogasawara, J. Moss, and M. Vaughan. 1999. Purification and cloning of a brefeldin A-inhibited guanine nucleotide-exchange protein for ADP-ribosylation factors. *J Biol Chem*. 274:12308-12315.

Tomas, A., C.E. Futter, and E.R. Eden. 2014a. EGF receptor trafficking: consequences for signaling and cancer. *Trends Cell Biol*. 24:26-34.

Tomas, A., C.E. Futter, and E.R. Eden. 2014b. EGF receptor trafficking: consequences for signaling and cancer. *Trends in Cell Biology*. 24:26-34.

Traub, L.M., and J.S. Bonifacino. 2013. Cargo recognition in clathrin-mediated endocytosis. *Cold Spring Harb Perspect Biol*. 5:a016790.

Traub, L.M., J.A. Ostrom, and S. Kornfeld. 1993. Biochemical dissection of AP-1 recruitment onto Golgi membranes. *J Cell Biol*. 123:561-573.

Udell, C.M., T. Rajakulendran, F. Sicheri, and M. Therrien. 2011. Mechanistic principles of RAF kinase signaling. *Cell Mol Life Sci*. 68:553-565.

Umebayashi, K., H. Stenmark, and T. Yoshimori. 2008. Ubc4/5 and c-Cbl continue to ubiquitinate EGF receptor after internalization to facilitate polyubiquitination and degradation. *Mol Biol Cell*. 19:3454-3462.

Vaccari, T., T.E. Rusten, L. Menut, I.P. Nezis, A. Brech, H. Stenmark, and D. Bilder. 2009. Comparative analysis of ESCRT-I, ESCRT-II and ESCRT-III function in Drosophila by efficient isolation of ESCRT mutants. *J Cell Sci*. 122:2413-2423.

Valdivia, R.H., D. Baggott, J.S. Chuang, and R.W. Schekman. 2002. The yeast clathrin adaptor protein complex 1 is required for the efficient retention of a subset of late Golgi membrane proteins. *Dev Cell*. 2:283-294.

Van Buskirk, C., and P.W. Sternberg. 2007. Epidermal growth factor signaling induces behavioral quiescence in Caenorhabditis elegans. *Nat Neurosci*. 10:1300-1307.

van Meer, G., and K. Simons. 1988. Lipid polarity and sorting in epithelial cells. *J Cell Biochem*. 36:51-58.

Vanlandingham, P.A., and B.P. Ceresa. 2009. Rab7 regulates late endocytic trafficking downstream of multivesicular body biogenesis and cargo sequestration. *J Biol Chem*. 284:12110-12124.

Vivanco, I., and C.L. Sawyers. 2002. The phosphatidylinositol 3-Kinase AKT pathway in human cancer. *Nat Rev Cancer*. 2:489-501.

Wang, C.W., S. Hamamoto, L. Orci, and R. Schekman. 2006. Exomer: A coat complex for transport of select membrane proteins from the trans-Golgi network to the plasma membrane in yeast. *J Cell Biol*. 174:973-983.

Watari, Y., K. Kariya, M. Shibatohge, Y. Liao, C.D. Hu, M. Goshima, M. Tamada, A. Kikuchi, and T. Kataoka. 1998. Identification of Ce-AF-6, a novel Caenorhabditis elegans protein, as a putative Ras effector. *Gene*. 224:53-58.

Wegner, C.S., L.M. Rodahl, and H. Stenmark. 2011. ESCRT proteins and cell signalling. *Traffic*. 12:1291-1297.

Wehrle-Haller, B., and B.A. Imhof. 2001. Stem cell factor presentation to c-Kit. Identification of a basolateral targeting domain. *J Biol Chem*. 276:12667-12674.

Whitfield, C.W., C. Benard, T. Barnes, S. Hekimi, and S.K. Kim. 1999. Basolateral localization of the Caenorhabditis elegans epidermal growth factor receptor in epithelial cells by the PDZ protein LIN-10. *Mol Biol Cell*. 10:2087-2100.

Wilson, P.D. 2011. Apico-basal polarity in polycystic kidney disease epithelia. *Biochim Biophys Acta*. 1812:1239-1248.

Winston, W.M., M. Sutherlin, A.J. Wright, E.H. Feinberg, and C.P. Hunter. 2007. Caenorhabditis elegans SID-2 is required for environmental RNA interference. *Proc Natl Acad Sci U S A*. 104:10565-10570.

Winter, J.F., S. Hopfner, K. Korn, B.O. Farnung, C.R. Bradshaw, G. Marsico, M. Volkmer, B. Habermann, and M. Zerial. 2012. Caenorhabditis elegans screen reveals role of PAR-5 in RAB-11-recycling endosome positioning and apicobasal cell polarity. *Nat Cell Biol*. 14:666-676.

Wittinger, M., P. Vanhara, A. El-Gazzar, B. Savarese-Brenner, D. Pils, M. Anees, T.W. Grunt, M. Sibilia, M. Holcmann, R. Horvat, M. Schemper, R. Zeillinger, C. Schofer, H. Dolznig, P. Horak, and M. Krainer. 2011. hVps37A Status affects prognosis and cetuximab sensitivity in ovarian cancer. *Clin Cancer Res*. 17:7816-7827.

Wortzel, I., and R. Seger. 2011. The ERK Cascade: Distinct Functions within Various Subcellular Organelles. *Genes Cancer*. 2:195-209.

Xue, X., F. Jaulin, C. Espenel, and G. Kreitzer. 2010. PH-domain-dependent selective transport of p75 by kinesin-3 family motors in non-polarized MDCK cells. *J Cell Sci*. 123:1732-1741.

Yao, I., T. Ohtsuka, H. Kawabe, Y. Matsuura, Y. Takai, and Y. Hata. 2000. Association of membrane-associated guanylate kinase-interacting protein-1 with Raf-1. *Biochem Biophys Res Commun*. 270:538-542.

Yarden, Y., and B.Z. Shilo. 2007. SnapShot: EGFR signaling pathway. *Cell*. 131:1018.
Yeaman, C., A.H. Le Gall, A.N. Baldwin, L. Monlauzeur, A. Le Bivic, and E. Rodriguez-Boulan. 1997. The O-glycosylated stalk domain is required for apical sorting of neurotrophin receptors in polarized MDCK cells. *J Cell Biol*. 139:929-940.
Yochem, J., M. Sundaram, and M. Han. 1997. Ras is required for a limited number of cell fates and not for general proliferation in Caenorhabditis elegans. *Mol Cell Biol*. 17:2716-2722.
Yoder, J.H., H. Chong, K.L. Guan, and M. Han. 2004. Modulation of KSR activity in Caenorhabditis elegans by Zn ions, PAR-1 kinase and PP2A phosphatase. *EMBO J*. 23:111-119.
Yoo, A.S., C. Bais, and I. Greenwald. 2004. Crosstalk between the EGFR and LIN-12/Notch pathways in C-elegans vulval development. *Science*. 303:663-666.
Yoon, C.H., J. Lee, G.D. Jongeward, and P.W. Sternberg. 1995. Similarity of sli-1, a regulator of vulval development in C. elegans, to the mammalian proto-oncogene c-cbl. *Science*. 269:1102-1105.
Zand, T.P., D.J. Reiner, and C.J. Der. 2011. Ras effector switching promotes divergent cell fates in C. elegans vulval patterning. *Dev Cell*. 20:84-96.
Zetka, M.C., and A.M. Rose. 1992. The meiotic behavior of an inversion in Caenorhabditis elegans. *Genetics*. 131:321-332.
Zhang, H., A. Kim, N. Abraham, L.A. Khan, D.H. Hall, J.T. Fleming, and V. Gobel. 2012. Clathrin and AP-1 regulate apical polarity and lumen formation during C. elegans tubulogenesis. *Development*. 139:2071-2083.
Zhang, X., J. Gureasko, K. Shen, P.A. Cole, and J. Kuriyan. 2006. An allosteric mechanism for activation of the kinase domain of epidermal growth factor receptor. *Cell*. 125:1137-1149.
Zmasek, C.M., and S.R. Eddy. 2001. ATV: display and manipulation of annotated phylogenetic trees. *Bioinformatics*. 17:383-384.
Zoncu, R., R.M. Perera, D.M. Balkin, M. Pirruccello, D. Toomre, and P. De Camilli. 2009. A phosphoinositide switch controls the maturation and signaling properties of APPL endosomes. *Cell*. 136:1110-1121.